Terms and Conditions of Use of Digitised Theses from Trinity College Library Dublin

Copyright statement

All material supplied by Trinity College Library is protected by copyright (under the Copyright and Related Rights Act, 2000 as amended) and other relevant Intellectual Property Rights. By accessing and using a Digitised Thesis from Trinity College Library you acknowledge that all Intellectual Property Rights in any Works supplied are the sole and exclusive property of the copyright and/or other IPR holder. Specific copyright holders may not be explicitly identified. Use of materials from other sources within a thesis should not be construed as a claim over them.

A non-exclusive, non-transferable licence is hereby granted to those using or reproducing, in whole or in part, the material for valid purposes, providing the copyright owners are acknowledged using the normal conventions. Where specific permission to use material is required, this is identified and such permission must be sought from the copyright holder or agency cited.

Liability statement

By using a Digitised Thesis, I accept that Trinity College Dublin bears no legal responsibility for the accuracy, legality or comprehensiveness of materials contained within the thesis, and that Trinity College Dublin accepts no liability for indirect, consequential, or incidental, damages or losses arising from use of the thesis for whatever reason. Information located in a thesis may be subject to specific use constraints, details of which may not be explicitly described. It is the responsibility of potential and actual users to be aware of such constraints and to abide by them. By making use of material from a digitised thesis, you accept these copyright and disclaimer provisions. Where it is brought to the attention of Trinity College Library that there may be a breach of copyright or other restraint, it is the policy to withdraw or take down access to a thesis while the issue is being resolved.

Access Agreement

By using a Digitised Thesis from Trinity College Library you are bound by the following Terms & Conditions. Please read them carefully.

I have read and I understand the following statement: All material supplied via a Digitised Thesis from Trinity College Library is protected by copyright and other intellectual property rights, and duplication or sale of all or part of any of a thesis is not permitted, except that material may be duplicated by you for your research use or for educational purposes in electronic or print form providing the copyright owners are acknowledged using the normal conventions. You must obtain permission for any other use. Electronic or print copies may not be offered, whether for sale or otherwise to anyone. This copy has been supplied on the understanding that it is copyright material and that no quotation from the thesis may be published without proper acknowledgement.

The impact of age and neuroinflammation on the blood-brain barrier and neurovascular unit

Lorraine Murray

Thesis submitted for the degree of Doctorate of Philosophy at the University of Dublin, Trinity College

Thesis submitted September 2012

School of Nursing and Midwifery

Trinity College Institute of Neuroscience

Trinity College

Dublin 2

I Declaration

I declare that this thesis has not been submitted as an exercise for a degree at this or any other university and it is entirely my own work.

I agree to deposit this thesis in the University's open access institutional repository or allow the library to do so on my behalf, subject to Irish Copyright Legislation and Trinity College Library conditions of use and acknowledgement.

Lorraine Murray

II Summary

The barrier function of the blood-brain barrier (BBB) occurs primarily due to the presence of tight junctions (TJ) between endothelial cells of brain capillaries. Neurons, astrocytes, pericytes, basal lamina and extracellular matrix, collectively referred to as the "neurovascular unit" (NVU) are in close anatomical proximity to the endothelial cells and contribute to the establishment and maintenance of the BBB. With increasing age, there is a progressive decline in cognitive function (Anderton, 2002) and shift of the innate immune system towards a pro-inflammatory profile (Licastro *et al.*, 2005). It has been hypothesised that the BBB may become altered in the senescent brain (Ueno *et al.*, 2001; Farrall & Wardlaw, 2009) where an impaired BBB would facilitate the entry of neurotoxins into brain parenchyma and exacerbate any age-related tissue degeneration. Inflammatory cytokines, particularly IL-1β cause increased paracellular permeability in many peripheral tissues. Considering that the TJ proteins are essential in regulating BBB permeability, it is possible that the age-related increase in pro-inflammatory cytokines may disrupt TJ and contribute to BBB dysfunction with age.

In this study, we report a functional disruption of the ageing BBB which facilitated the extravasation of exogenous sodium fluorescein and endogenous plasma albumin into the brain parenchyma, with a concomitant decrease in TJ protein expression. Structurally, the basal lamina of the NVU was fragmented and the expression of pericyte-specific proteins was reduced.

The elderly human population is more susceptible to bacterial infections which correlates with increased mortality and increased susceptibility to other morbidities (Butcher *et al.*, 2001; Goldstein, 2010). Many studies document the disruptive effect of LPS (a potent stimulator of systemic inflammation) on the barrier properties in multiple tissue types. We set out to establish if an additional inflammatory insult could further exacerbate damage to an already fragile ageing BBB. Young and aged rats received an intraperitoneal injection of a low-dose of LPS which did not disrupt either the young or aged BBB. This muted response highlights the plasticity of the cerebral endothelial cells and their ability to mount an appropriate response (or not) to an inflammatory stimulus.

That the pro-inflammatory cytokine IL-1β underlies the age-related disruption of the BBB is supported in our research by a number of factors; TJ protein concentration in aged IL-1R1$^{-/-}$ mice was significantly increased when compared with aged wildtype mice and TJ were decreased in IL-1β treated organotypic hippocampal slices. It is well documented that MMP activity is increased with neuroinflammation in many models and leads to TJ disruption and increased BBB permeability (Yong *et al.*, 2001; McColl *et al.*, 2008). Here we report an increase in both the expression and activity level of MMP-2 and MMP-9 in serum from aged rats and patients with Alzheimer's Disease (AD). We hypothesised that IL-1β-mediated increases in MMP activity was the underlying cause of BBB disruption and this was confirmed when a broad-scale MMP inhibitor rescued the IL-1β-mediated decrease in TJ expression in organotypic hippocampal slices.

In summary our findings provide evidence of a structurally and functionally disrupted BBB with age. IL-1β signalling mediated the TJ disruption, as evidenced by the increased TJ expression in aged IL-1R1$^{-/-}$ mice. We hypothesise that the IL-1β-mediated tight junction disruption is partially facilitated by its action on MMP, via signalling through the ERK-MAPK pathway. The age-related BBB disruption would facilitate the entry of potential toxins into the brain, probably exacerbating neuronal damage in an already fragile tissue and conceivably contributing to the decline in cognitive function apparent with increasing age.

III Acknowledgements

I'd like to thank my supervisor, Dr. Aileen Lynch, who is without a doubt the best supervisor, mentor, and most genuine person I've met during my 7 years in Trinity. I hope that, in a supervisory role, I would be as approachable, conscientious and diligent as you. Aileen, you are wonderful and I hope we'll always stay in contact, both professionally and personally. This has been a journey I think we both embarked upon together and I'll always remember it, thank you. To Prof. Marina Lynch, whose resources made it possible to carry out the research and for allowing me to engage as a member of the MAL lab. A huge thanks to the MAL lab post-docs, for their help and explanations, especially Dr. Aedin Minogue. Aedin, thank you so much for all your help and always answering " just one quick question". The girlies, Suzie, Tara and Steph, you're genuinely the best group of friends/roomie I could have ever wished for. We made it!! The boys, Doney and Jimmy for tea and biscuits, vital in research I think. Anto, for the chats, the endless lab help and Napoli pastries. Thank-you for always being there for me. I'd like to thank my family, who each in their own way made my PhD journey bearable for so many reasons. Mum, your words of encouragement and little messages always have and always will make me feel better. Thankyou so much for encouraging me to stick with it during the dark days. Peter, the best little brother anyone could ever wish for. I loved coming home at weekends to see your little face. You won't understand until you're older that you are the reason I stayed. Jody, my fairy godmother, I'd be lost without you, simple as that.

And finally, to Dad- you helped me, in your own words, gain "the Serenity to accept the things I cannot change, Courage to change the things I can, and the Wisdom to know the difference".

Thank-you all so much.

IV Table of Contents

Chapter 2: Methods

Chapter 4: Does inflammation exacerbate age-related changes at the blood-brain barrier?

Chapter 5: Investigating the impact of inflammatory stimuli on aspects of the neurovascular unit *in vitro*.

V List of Figures

VI List of Tables

VII Abbreviations

ΔCt	change in cycle time
ΔΔCt	change in cycle time (relative to control)
Ω/cm^2	Ohm per centimeter squared (Electrical resistance measurement)
°C	degrees celcius
α-SMA	Alpha smooth muscle actin
β-actin	Beta -actin
β-Me	Beta-mercaptoethanol
aCSF	Artificial cerebrospinal fluid
Aβ	Amyloid beta
AEBSF	4-(2-Aminoethyl) benzenesulfonyl fluoride hydrochloride (serine proteinase inhibitor)
AD	Alzheimer's disease
ANOVA	Analysis of variance
APS	Ammonium persulfate
BBB	Blood-brain barrier
BCA	Bicinchonininc assay
BRB	Blood-retinal barrier
BSA	Bovine serum albumin
bEnd.3	Brain endothelial cell (cortical)
C57	C57 lab mouse strain
C57BL/6	C57 black6 lab mouse strain
$CaCl_2$	Calcium chloride
Caco2	epithelial colorectal adenocarcinoma cells
CD-14	Cluster of differentiation 14
cDNA	Complimentary deoxyribonucleic acid
CDR	Clinical dementia rating
CH_3COOH	Acetic acid
Cld5	Claudin-5
CNS	Central nervous system
CO_2	Carbon dioxide
COOH-	Carboxy terminus of amino acid)

CSF	Cerebrospinal fluid
Ct	Cycle time
Da	Dalton (Molecular weight measurement)
DAPI	4', 6-diamidino-2-phenylindole (nuclear stain)
DEPC	Diethylpyrocarbonate
dH_2O	Distilled water
DIV	Days *in vitro*
DMEM	Dulbecco's modified eagle medium
DMSO	Dimethyl sulfoxide
DNA	Deoxyribonucleic acid
E-64[N-]	Cysteine proteinase inhibitor
EBSS	Earle's balanced salt solution
ECL	Enhanced chemiluminescence
ECM	Extracellular matrix
EGTA	Ethylene glycol tetra-acetic acid
ELISA	Enzyme-linked immunosorbent assay
ERK	Extracellular signal-related kinase
EtOH	Ethanol
FACS	Fluorescence-activated cell sorting
FBS	Fetal bovine serum
g	Gravitational force
GAPDH	Glyceraldehyde-3 phosphate dehydrogenase
H_2O_2	Hydrogen peroxide
H_2SO_4	Sulphuric acid
HCl	Hydrogen chloride
HEPES	Hydroxyethyl -piperazineethanesulfonic acid
HUVEC	Human vascular endothelial cells
HRP	Horse-radish peroxidase
i.c.v.	Intracerebroventricular
IFN-γ	Interferon gamma
IgG	Imunoglobulin G
IkB	Interleukin kappa kinase B

IKK	Interleukin kappa kinase
IL	Interleukin
IL-1α	Iterleukin-1 alpha
IL-1β	Interleukin-1 beta
IL-1R1	Interleukin-1 receptor type I
IL-1RII	Interleukin-1 receptor type II
IL-1ra	Interleukin-1 receptor antagonist
IL-1RAcp	Interleukin-1 accessory protein
IRAK	Il-1 receptor associated kinase
i.p.	Intraperitoneally
JNK	c-Jun N-terminal kinase
KCL	Potassium chloride
kDa	Kilodalton
KH_2PO_4	Potassium dihydrogen phosphate
LBP	Lipoploysaccharide binding protien
LPS	Lipopolysaccharide
MAGUK	Membrane associated guanylkinase
MAPK	Mitogen-activated protein kinase
MCAO	Middle cerebral artery occlusion
MCI	Mild cognitive impaired
MD2	adaptor protein
MDB	Membrane desalting buffer
MDCK	Madin-darby canine kidney (epithelial cell line)
MEM-42360	Modified Eagle's Media
MeOH	Methanol
$MgCl_2$	Magnesium chloride
MHCII	Major histocompatibility complex II
MLC	Myosin light chain
MLCK	Myosin light chain kinase
MMP	Matrix metalloproteinase
MMSE	Mini-mental state exam
MRI	Magnetic resonance imaging

mRNA	Messenger ribonucleic acid
MS	Multiple sclerosis
MyD88	Myeloid differentiation factor-88
NaCl	Sodium chloride
Na-F	Sodium fluorescein
NaF	Sodium fluoride
$NaHCO_3$	Sodium bicarbonate
Na_2HPO_4	Sodium hydrophosphate
NaN_3	Sodium azide
NaOH	Sodium hydroxide
$Na_4P_2O_7$:	Sodium pyrophosphate
NFκB	Nuclear factor kappa B
NGS	Normal goat serum
NHS	Normal horse serum
NINCDS/ADRDA	National Institute of Neurological and Communicative Disorders/ Alzheimer's Disease and Related Disorders Association
NP-40	Detergent
NRS	Normal rabbit serum
NVU	Neurovascular unit
O_2	Oxygen
OCT	Tissue mounting media
OSC	Organotypic slice culture
OHSC	Organotypic hippocampal slice culture
P38	Type of mitogen-activated protein kinase
PN	Post-natal
PAMP	Pathogen associated molecular pattern
PBS	Phosphate buffered saline
PCR	Polymerase chain reaction
PD	Parkinsons' disease
PDGF	Platelet-derived growth factor
PDGFR-β	Platelet derived growth factor receptor beta
PECAM	Platelet endothelial cell adhesion molecule

pH	$-[\log H^+]$
PHEM	(buffer)
PIPES	(buffer)
PKC	Protein kinase C
PNS	Peripheral nervous system
PO_3^{2-}	Phosphorylation
PRR	Pattern recognition receptor
RNA	Ribonucleic acid
rpm	Revs per minute
RT-PCR	Real-time polymerase chain reaction
RQ	Relative quantity
SDS	Sodium dodecylsulfate
SEM	Standard error of the mean
SH3	SRC homology-3 domain
siRNA	Small interfering ribonucleic acid
Strep-HRP	Streptavidin horse-radish peroxidase
TBS	Tris buffered saline
TBS-T	Tris buffered saline plus tween
TER	Transepithelial electrical resistance
TEER	Transendothelial electrical resistance
TEMED	Tetamethylethlyenediamine
TGF	Transformng growth factor
TIMP	Tissue inhibitor of metalloproteinase
TIR	Toll-IL-1 receptor domain
TJ	Tight Junction
TLR	Toll-like receptor
TMR	Tetramethylrhodamine
TNF-α	Tumor necrosis factor-alpha
µg	microgram
µl	microlitre
µm	micrometer
UV	Ultraviolet light

VEGF	Vascular endothelial growth factor
WT	Wildtype
ZO-1	Zonula occludens-1

Chapter 1

Introduction

1. Introduction

1.1 The blood-brain barrier

When one considers the complexity of neural signalling in the brain, coupled with the fragile nature of neurons and their limited regenerative capacity, it is vital that the microenvironment within the brain is highly regulated to maintain proper brain function. In order to maintain this homeostasis the brain must be free from potentially damaging endogenous and exogenous substances. Taking into account that (a) the brain receives up to 20% of cardiac output, (b) there is approximately $20m^2$ of capillary surface area available for exchange in the brain and (c) on average, any given brain cell is less than 25μm from a capillary (Zlokovic, 2008; Abbott *et al.*, 2010), there is huge potential for changes in plasma constituents to rapidly and profoundly disturb the cerebral microenvironment. Fluctuations in plasma constituents including ions, amino acids, proteins or potentially harmful neurotoxins occur under normal physiological conditions, during illness, after exercise or following food intake and it is essential that the brain microenvironment is unaffected by these changes. The endothelial cells lining the cerebral capillaries are physically and functionally distinct from peripheral capillaries (see Figure 1.1). This cell specialisation of brain capillaries forms the "blood-brain barrier" (BBB) and contributes to maintaining brain homeostasis by decreasing capillary permeability to blood components. Cerebral capillary endothelial specialisations (Weiss *et al.*, 2009) include:

i. A lack of fenestrations and increased occurrence of tight junctions (TJ) – this limits hydrophilic substance movement via the paracellular pathway between adjacent endothelial cells,
ii. High transendothelial electrical resistance, which repels ionic substances,
iii. Low levels of pinocytosis, which decreases non-specific transcytosis of macromolecules,
iv. High expression of various transporters, allowing specificity of substance movement via the transcellular pathway through endothelial cells,
v. Increased mitochondrial numbers to facilitate higher energy expenditure by cerebral endothelial cells due to the maintenance of transporters.

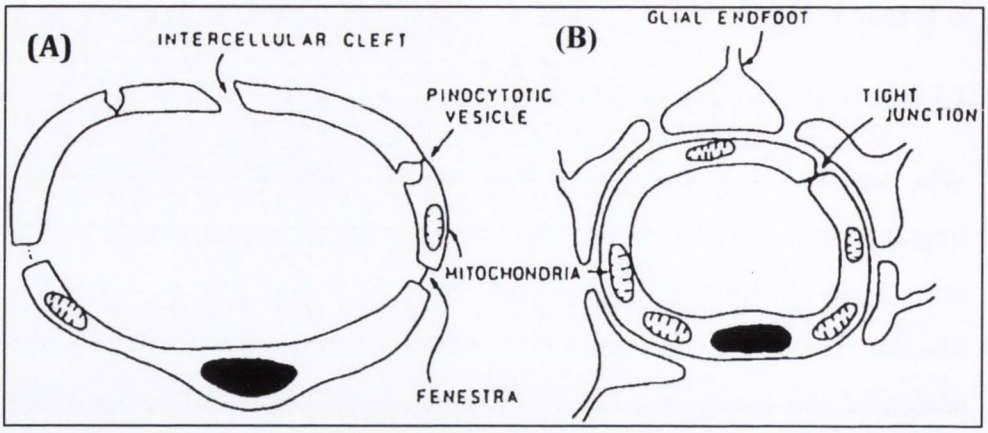

Figure 1.1: Schematic diagram comparing the morphological differences between endothelial cells of peripheral capillaries (A) and endothelial cells composing the blood-brain barrier (B). The fenestrations between endothelial cells in peripheral capillaries **(A)** are replaced by the presence of TJ in BBB capillaries. The blood brain-barrier capillaries are also characterised by decreased pinocytosis, and increased numbers of mitochondria. Image adapted from (de Vries *et al.*, 1997).

It was first observed in the late 1800s that water-soluble dyes injected into the circulatory system did not stain brain tissue, a result that was attributed to the neural tissue having low affinity for the dye, rather than the presence of a barrier (Ehrlich, 1885). In the early 1900s Goldmaan injected trypan blue to the central nervous system (CNS) and noted that it did not stain peripheral tissue. He suggested the presence of a physical barrier between the blood and the brain (Hawkins & Davis, 2005). Though the physical "barrier" function of the BBB (due to the presence of tight junctions), is the main factor limiting brain penetration of blood-borne substances, the BBB also has transport capacity due to the presence of transendothelial transporters. The BBB also functions as a metabolic barrier due to the presence of enzymes on the plasma membrane (aminopeptidases, endopeptidases, cholinesterases) that modify substances as they enter and exit the brain (Zlokovic, 2008; Abbott *et al.*, 2010) Certain regions of the brain lack a BBB due to their need to communicate rapidly and directly with the peripheral circulation in order to regulate autonomic control of bodily function. These areas are collectively referred to as "circumventricular organs" and include the pineal gland (involved in circadian rhythms), the area postrema (vomiting centre), the posterior pituitary (detects hormone levels, stores anti-diuretic hormone and oxytocin),

the lamina terminalis and subfrontal organ (involved in fluid and electrolyte balance; (Weiss *et al.*, 2009).

1.2 The neurovascular unit

The barrier function of the BBB occurs primarily due to the presence of TJ between endothelial cells of brain capillaries, however a number of other cell types in close anatomical proximity to the endothelial cells contribute to the establishment and maintenance of the BBB. These include neurons, astrocytes, pericytes, basal lamina and extracellular matrix; all collectively referred to as the "neurovascular unit" (NVU); see Figure 1.2. It is now widely accepted that there is dynamic signalling between vascular endothelial cells and the cells of the NVU. Research on the BBB must take into account these interactions in order to fully comprehend BBB regulation. The research presented in this thesis includes data on basal lamina and pericytes of the NVU. These particular cells were chosen as their contribution to BBB functioning is much less documented than astrocytes and neurons. An extensive review of the literature pertaining to the other cells of NVU and their contribution to the BBB can be sought in (Hawkins & Davis, 2005; Zlokovic, 2008; Weiss *et al.*, 2009; Abbott *et al.*, 2010). For consistency purposes, and in keeping with the terminology of the literature, when referring to the cellular milieu of the BBB in this thesis, it will be referred to as the NVU.

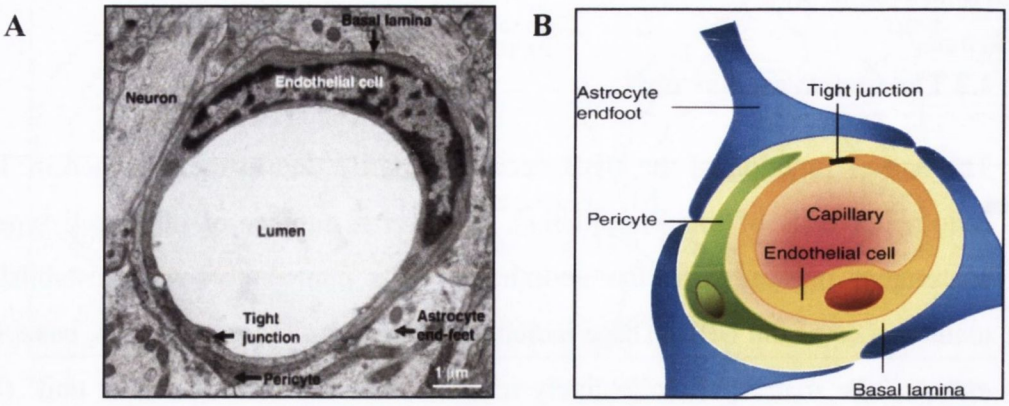

Figure 1.2: The neurovascular unit. (A) Electron micrograph of rat brain showing a microvascular endothelial cell, surrounded by basal lamina within which the pericytes are embedded. Astrocyte end-feet and neurons are closely associated. Image adapted from (Weiss *et al.*, 2009). **(B)** Schematic diagram depicting the cells of the neurovascular unit. Image adapted from (Abbott *et al.*, 2010).

1.2.1 The basal lamina

Basement membranes are tissue sheets of extracellular matrix (ECM), and they underlie all epithelia, muscles and vascular endothelium. Although primarily a structural support for the overlying tissue, the function of the basement membrane now incorporate roles in cell motility, differentiation and angiogenesis (Kitajewski, 2011). One of the major functional and structural components of basement membranes is the laminin family of large glycoproteins, of which there are many isoforms (Aumailley *et al.*, 2005). The basal lamina, a component of the ECM in basement membranes, is a 30-40nm thick membrane ensheathing cerebral endothelial cells and pericytes (Yurchenco & Schittny, 1990; Farkas & Luiten, 2001). The basal lamina is generated and maintained by endothelial cells, pericytes and astrocytes, and contains structural proteins like collagen and laminin (Zlokovic, 2008). Endothelial cells bind to ECM proteins like laminin via their integrin receptors and are anchored in place to maintain stability and allow correct intracellular signalling (Hawkins & Davis, 2005). Basal lamina disruption in the periphery is known to contribute to disease states like muscular dystrophy and cardiac myopathy (Durbeej, 2010). Disruption of the basal lamina surrounding brain capillaries could lead to physical disruption of the endothelial cells and other NVU components, thus interfering with signalling and leading to a dysfunctional BBB. In fact it has been

shown that disrupting the basal lamina via bacterial collagenase causes increased BBB permeability in the rat (Rosenberg *et al.*, 1993) and injecting mice intraperitoneally with lipopolysaccharide causes disintegration of the basal lamina, also leading to increased BBB paracellular permeability (Nishioku *et al.*, 2009). In addition, the particular isoform of laminin in any given tissue plays a considerable role in the function of that tissue. Laminin isoforms, as well as being developmentally regulated (Beck *et al.*, 1990), are influenced by pro-inflammatory signalling molecules (Sixt *et al.*, 2001) The distribution of particular isoforms is noted to be differentially expressed in brain tissue of Alzheimer's patients when compared with controls (Palu & Liesi, 2002).

1.2.2 Pericytes

Pericytes were first identified in the 1870s as perivascular cells that encircle capillaries, larger arterioles and venules in many tissues in a variety of species including bovine, rodent and human (Shepro & Morel, 1993; Hirschi & D'Amore, 1996). They have a large cell body and long primary processes which run parallel along the length of the capillary, and secondary and tertiary processes, which encircle the capillary (Shepro & Morel, 1993) see Figure 1.3. They are morphologically, biochemically and physiologically heterogeneous depending on their tissue location, species and *in vitro* culture conditions (Armulik *et al.*, 2005), rendering the development of a pericyte-specific marker extremely difficult.

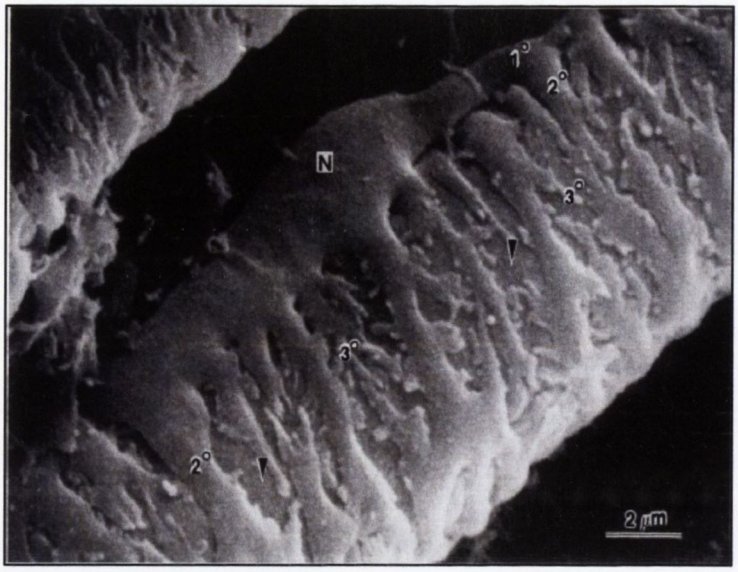

Figure 1.3 Electron micrograph of a pericyte encircling a capillary. N= nucleus of pericyte; 1°, 2° and 3° refer to the primary secondary and tertiary cell processes of the pericyte. Image taken from (Shepro & Morel, 1993).

Functionally pericytes are important cellular constituents of the BBB as they have important regulatory roles including angiogenesis, vascular remodelling, capillary stabilisation, TJ formation, perfusion regulation and phagocytic activity (Hirschi & D'Amore, 1996; Balabanov & Dore-Duffy, 1998; Guillemin & Brew, 2004). Support for the macrophage activity of brain pericytes is based on evidence that they express an abundance of lysosomes (Rucker *et al.*, 2000), can ingest polystyrene beads by phagocytosis and exhibit antigen presentation and macrophage markers e.g. major-histocompatability complex class II (Bergers & Song, 2005). The observed expression of α-smooth muscle actin within pericytes led to the finding that pericytes are capable of contraction and thus regulate capillary blood flow (Peppiatt *et al.*, 2006).

The cytoplasmic projections of pericytes pierce the surrounding basal lamina and make direct contact with the underlying endothelial cells (Shepro & Morel, 1993). Pericyte processes make contact with more than one endothelial cell on multiple capillaries, indicating that signal integration between capillaries occurs (Bergers & Song, 2005). As well as mechanically stabilising the capillaries, there is dynamic regulation of the capillary by intercellular signalling between endothelial cells and pericytes involving vascular-endothelial growth factor (VEGF), platelet-derived growth factor (PDGF) and

transforming growth factor (TGF) pathways (Shimizu *et al.*, 2008). Secreted PDGF from endothelial cells binds to the PDGF receptor-β (PDGFR-β) on pericytes and is responsible for proliferation, migration and recruitment of pericytes along the capillary (Armulik *et al.*, 2005).

Pericytes are differentially distributed in various tissues and the ratio of pericytes to endothelial cells is as follows; retina (1:3), BBB (1:5) and skeletal muscle (1:100). The highest ratios occur in neural tissue and correlates with the degree of "tightness" of these vessels, suggesting that pericytes have an active role in BBB maintenance (Shepro & Morel, 1993) rather than vessel stabilisation alone. Pericytes in the rat brain cover approximately 25% of the abluminal surface of capillaries (Sims, 1991). Pericytes may be involved in TJ regulation at the BBB because pericyte derived angiopoietin-1 induces occludin gene expression in brain capillary cells *in vivo* (Hori *et al.*, 2004).

1.3 Crossing the blood-brain barrier

Whilst the presence of the BBB is beneficial to protect the brain from harmful substances it also acts as a barrier to many essential nutrients like glucose. It is imperative that there are mechanisms for essential substances to circumvent the BBB and gain access to the brain. In the same manner, it is vital that brain-derived metabolic waste products and any neurotoxins that may have gained access to the brain under pathophysiological conditions are not allowed to accumulate in the brain, but are excreted into the circulatory system for disposal. There are two main routes of movement across the BBB (summarised in Figure 1.4): the transcellular pathway i.e. through the plasma membrane of endothelial cells, and the paracellular pathway i.e. between adjacent endothelial cells. Our research focuses on the paracellular pathway across the BBB (1.3.2), but outlined below is a brief summary of the transport systems of the transcellular pathway (detailed in (Bernacki *et al.*, 2008; Zlokovic, 2008)).

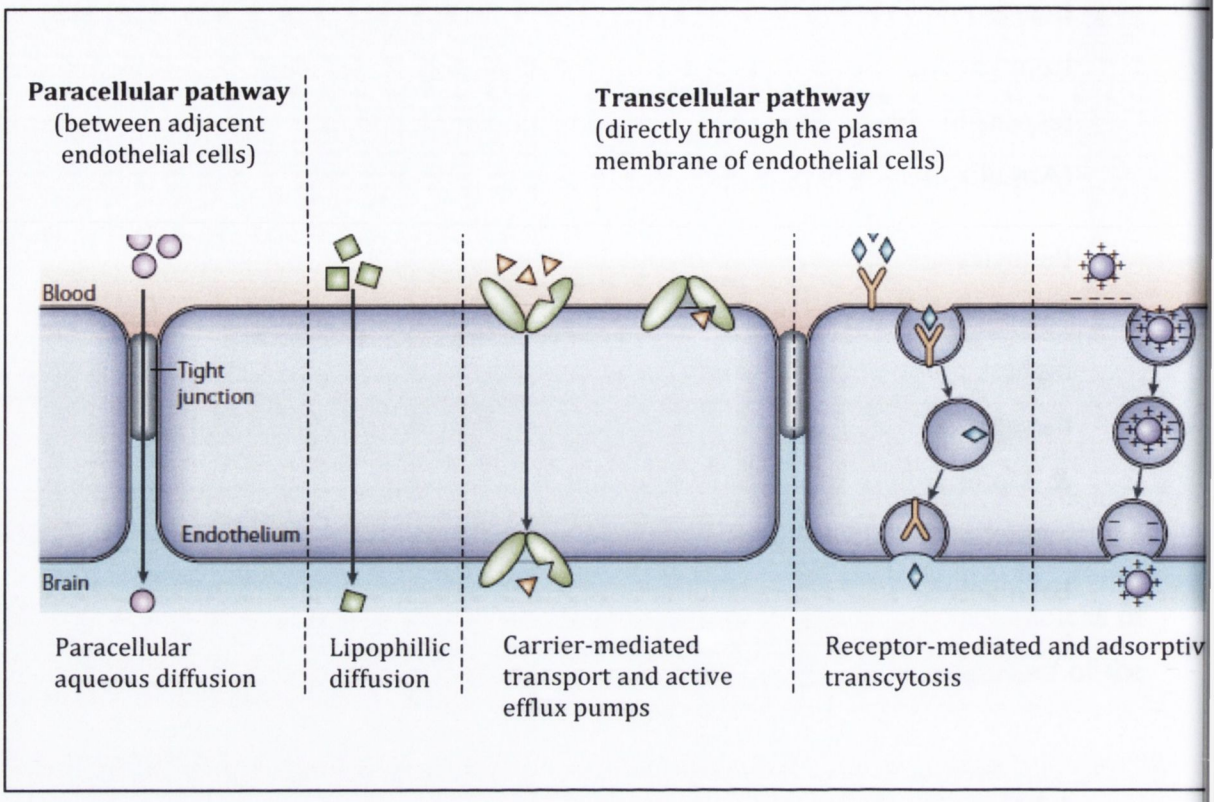

Figure 1.4. Diagram illustrating the routes across the blood-brain barrier. Substances can move via the paracellular route, between adjacent endothelial cells, or they can move directly through endothelial cells via the transcellular route. Image adapted from (Abbott *et al.*, 2006).

1.3.1 The transcellular pathway

Substances can move through endothelial cells via the transcellular pathway, either via passive diffusion, facilitated diffusion, active transport, or endocytosis (see Figure 1.4). Lipophilic substances and those with a molecular weight less than 450Da, can passively diffuse through the plasma membrane of endothelial cells (Liu *et al.*, 2004). Carrier-mediated transport is another route by which many essential polar molecules e.g. glucose and amino acids, gain access to the brain (Ueno *et al.*, 2001) and the route by which potentially harmful neurotoxins are disposed via active efflux pumps e.g. p-glycoprotein (Dallas *et al.*, 2006). Transport across the BBB can be bi-directional with certain transporters located on the abluminal, luminal or both sides of endothelial cells. Though beneficial in removing toxins from the brain, the transporters are the main reason that nearly 98% of potentially therapeutic drugs cannot gain access to the CNS

(Pardridge, 2007). The focus of this research is substance movement across the BBB via the paracellular route, between adjacent endothelial cells.

1.3.2 The paracellular pathway

The BBB is characterized by low paracellular permeability (size < 180Da) between endothelial cells (Kozler & Pokorny, 2003) and high transendothelial electrical resistance (TEER). This is a measure of the electrical resistance across a membrane and it is primarily responsible for expelling ions away from the paracellular pathway (Gonzalez-Mariscal *et al.*, 2008). A high TEER correlates with a "tight" barrier (Balda *et al.*, 1996). The low paracellular permeability of the BBB is attributed to the presence of junctional complexes between adjacent endothelial cells. These inter-endothelial junctional complexes form the structural basis of the BBB (see Figure 1.5). The protein complexes include adherens junctions and TJs that restrict paracellular diffusion and desmosomes that mediate intercellular communication (Hawkins & Davis, 2005). The TJs are the most apically located group of proteins which are found at the luminal end of capillaries and so are the primary barriers to the paracellular movement of substances into the brain (Schneeberger & Lynch, 2004).

(A) (B)

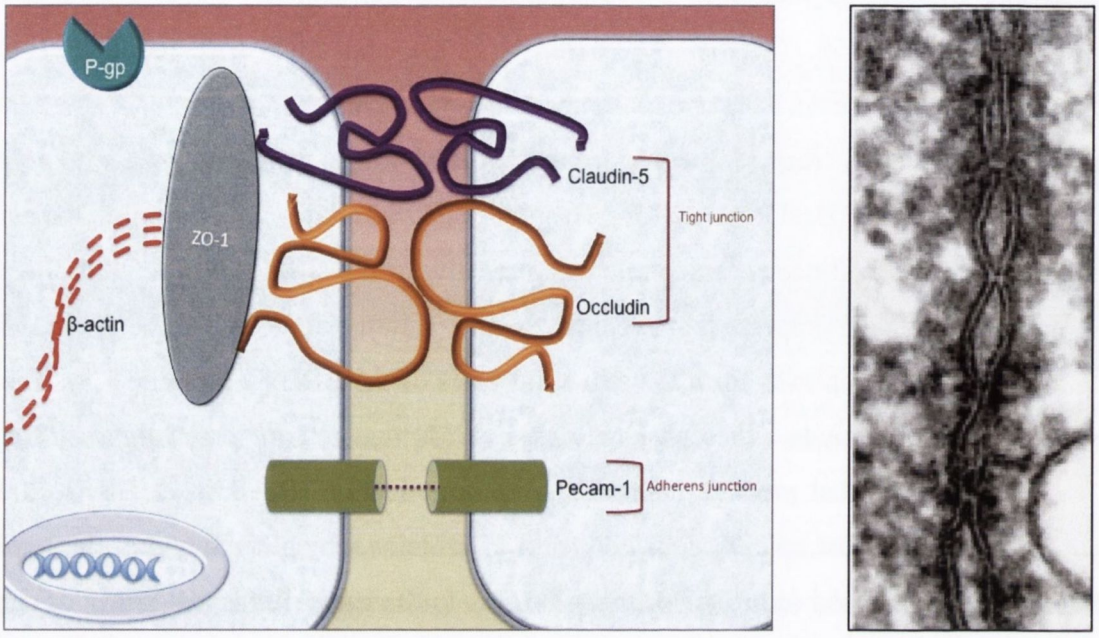

Figure 1.5. The blood-brain barrier proteins. Substance movement between adjacent endothelial cells is limited by the presence of TJ proteins claudin-5, and occludin. These proteins are anchored at their apical location by binding to the plaque protein ZO-1, which itself is anchored to the actin cytoskeleton. The expression of glucose-transporters and drug efflux pumps ensure nutrient influx to brain and toxic compound efflux. (B) An ultrathin section of TJ proteins between epithelial cells of the intestine. The intercellular space is almost obliterated where the TJ are located, thus limiting paracellular substance flux. Image adapted from (Tsukita *et al.*, 2001).

1.4 Tight junctions

Tight junctions (TJ) are a form of cell-cell adhesion molecule (Saitou *et al.*, 2000) and are found in all endothelial and epithelial tissues including those lining the kidney, bladder, skin, lungs and in the case of the BBB, the endothelial cells of brain capillaries (Hawkins & Davis, 2005). There are an ever-increasing number of proteins associated with the TJ complex and they are often divided into the following groups:

i. *Integral membrane proteins* e.g. claudin and occludin, which bridge the intercellular space between adjacent endothelial cells to form a regulated paracellular permeability barrier,
ii. *Tight junction plaque proteins* e.g. zonula occludens -1, -2, -3 are accessory proteins that act as physical links between the integral membrane proteins and the actin cytoskeleton. They also act as recruitment proteins for molecules involved in signalling with the TJ,
iii. *Cytosolic and nuclear proteins* interact both directly and indirectly with TJ plaque proteins to regulate cell functions such as solute permeability (Schneeberger & Lynch, 2004).

The categories of TJ proteins, specifically the claudins and occludin, which form the basis of this research, will be discussed in further detail below.

1.4.1 Integral membrane proteins

Claudin and occludin are the most apically located proteins on endothelial cells and the barrier function of the BBB is primarily attributed to their physical presence and correct signalling regulation (Abbott *et al.*, 2010). TJ proteins in the plasma membrane of one capillary endothelial cell joins with a TJ protein in the adjacent cell forming "paired TJ strands" where the intercellular space is obliterated (see Figure 1.5 (B)). The TJ is not simply an impenetrable barrier but shows ion and size selectivity, and can vary in their degree of tightness depending on the isoform e.g. claudin (Tsukita *et al.*, 2001; Nitta *et al.*, 2003). Caution is required when one is comparing the research regarding TJ proteins, as much of the early literature concerning TJ regulation has been carried out on epithelial tissues. In more recent times, the use of co-culture systems, primary endothelial cells and cell lines has yielded a range of different results due to the molecular components of TJ varying with tissue-type, species, cell line and *in vitro* culture conditions (Deli *et al.*, 2005).

1.4.2 Occludin

Occludin is a 60-65kDa protein and was the first integral membrane protein to be localised at the TJ in chicken liver cells (Furuse *et al.*, 1993). This protein was later confirmed to be expressed in mammalian TJ (Ando-Akatsuka *et al.*, 1996) and in human brain endothelial TJ (Vorbrodt & Dobrogowska, 2004). Furuse *et al.* (1993) used light and electron microscopy to confirm its exclusive localisation to the TJ, and cDNA sequencing to reveal the molecular structure of occludin; it has 4 hydrophobic transmembrane domains, creating two extracellular loops that span the intercellular space. The amino acid sequence of occludin varies in different species but there are some structural aspects that are phylogenetically conserved (Ando-Akatsuka *et al.*, 1996; Saitou *et al.*, 1998). The carboxyl terminal of occludin is rich in serine-threonine and tyrosine amino acid residues that are targets for multiple protein kinases (Schneeberger & Lynch, 2004). The phosphorylation state of occludin is important for the regulation of occludin assembly at the TJ (Gonzalez-Mariscal *et al.*, 2008).

The precise functional role of occludin at the TJ has been, and is still a topic of much debate. A high TEER reflects a "tight" barrier and it has been claimed that the second extracellular loop of occludin is responsible for conferring the TEER to endothelial cells. Evidence for this came from a combined electrophysiological and immunofluorescent study where Madin-Darby Canine Kidney Cells (MDCK) over expressing C-terminally-truncated occludin had decreased TEER, whereas wildtype cells and cells over expressing full-length occludin had greater TEER (Balda *et al.*, 1996). In contrast to this, a study involving occludin knockout mice has shown that although the mice have a complex phenotype (growth retardation, altered sexual and nursing behaviours, and brain calcifications), the TJ of their intestinal epithelium appeared morphologically and electrophysiologically normal (Saitou *et al.*, 2000).

The role of occludin in TJ formation has been investigated in insect Sf9 cells, which do not normally express occludin. Over expression of occludin in these cells resulted in the formation of cytoplasmic lamellar bodies with fused membranes, although they did not resemble actual TJ strands. This study indicated that although occludin plays a role in membrane fusion, occludin alone could not form TJ strands at the plasma membrane (Furuse *et al.*, 1998). Further support comes from a study where occludin deficient embryonic stem cells could fully differentiate into polarised epithelial cells which bore

TJ, and formed a functional barrier as assessed by TEER experiments (Saitou *et al.*, 2000). This study did not find significant differences in TJ morphology or the number of TJ strands between the knockout and wildtype cells, providing evidence that there were unidentified integral TJ proteins that functioned as the main TJ barrier. Clearly occludin has been localised to TJ but considering the numerous conflicting studies outlined above, a clear physiological role has yet to be definitively established. Taking the literature into account, it seems plausible that occludin has a major regulatory role rather than a structural function of the TJ at the BBB (Wolburg & Lippoldt, 2002). A comprehensive review documenting the structure, function and regulation of occludin has been provided by (Feldman *et al.*, 2005).

1.4.3 Claudin

Following on from the research indicating that occludin alone is not sufficient to form the TJ, the Furuse group (who first identified occludin) re-examined the junctional fraction of chicken livers to identify the integral membrane proteins constituting the TJ. They identified the first two members of the claudin family (Furuse *et al.*, 1998). To date, 24 claudin isoforms have been identified in mammals (Hawkins & Davis, 2005) with molecular weights ranging from 20-27kDa (Turksen & Troy, 2004). The claudin proteins appear to be expressed in a tissue-specific manner, with claudin-3, -5, and 12 located predominantly in TJ strands in the capillary endothelial cells of the murine BBB (Morita *et al.*, 1999; Wolburg & Lippoldt, 2002; Nitta *et al.*, 2003; Sandoval & Witt, 2008). The expression of claudin-1 in brain capillary endothelial cells remains controversial, as there are conflicting results from *in vivo* and *in vitro* studies (Sandoval & Witt, 2008). Immunogold experiments were carried out on "healthy" human autopsied cortex to verify the nature of BBB TJ proteins. This study reported that occludin was the most abundant TJ protein and that although claudin-5 had similar distribution patterns to occludin in that it was exclusively located at the junctional clefts between cells, its expression was approximately half as dense (Vorbrodt & Dobrogowska, 2004).

Most epithelial/endothelial cell types express more than two claudin isoforms, with each claudin regulating the paracellular diffusion of molecules based on different charges and molecular weights (Forster, 2008; Zlokovic, 2008). It has been hypothesised that the heterogeneity of barrier "tightness" in different tissues, is due to different claudin

isoform expression and interactions (Turksen & Troy, 2004). BBB claudin proteins, claudin-3, -5, and -12, collectively exclude substances of molecular weights greater than ~180Da through the paracellular pathway (Kozler & Pokorny, 2003). A groundbreaking study by Nitta *et al.* (2003) highlighted the complex nature of claudin-5 at the BBB. Claudin-5 knockout mice showed a size-selective loosening of the BBB (up to 800Da) rather than widespread dysfunction, as might be expected. This was partially attributed to the compensatory upregulation of claudin-12, and the authors also suggested that claudins can size-selectively regulate the BBB, perhaps by pore formation (Nitta *et al.*, 2003).

1.4.4 Tight junction plaque proteins

The TJ cytoplasmic plaque proteins are a group of over 30 cytoplasmic proteins that assemble within the cytoplasm at the TJ (Forster, 2008). They act to (i) regulate the assembly of TJ proteins, (ii) to stabilise the TJ by anchoring the proteins to the cytoskeleton and (iii) facilitate signal transduction (Balda & Matter, 2008; Forster, 2008). The plaque proteins are subdivided into two functional sub-groups:

i. *Peripherally associated scaffolding proteins* e.g. the zonula occludens proteins (ZO-1, -2, -3) that couple and stabilise the integral membrane proteins claudin and occludin, to the actin cytoskeleton (Paris *et al.*, 2008).
ii. *Signalling proteins* that are involved in TJ assembly and regulation e.g. kinases and phosphatases.

The zonula occludens (ZO) scaffold proteins belong to a family of 'membrane associated guanylate kinase' (MAGUK) proteins. They have conserved domains including a SH3-domain and a PDZ domain. The SH3 binds to both cytoskeletal and signalling proteins whilst the PDZ domains are sequences of 80-100 amino acids which form a hydrophobic loop facilitating the binding of the C-terminal of cytoplasmic proteins (Wolburg & Lippoldt, 2002; Schneeberger & Lynch, 2004). ZO-1, a 225kDa phosphoprotein was the first TJ associated protein to be identified (Stevenson *et al.*, 1986). It interacts with claudin by its PDZ domain (Balda & Matter, 2008) and with occludin by its guanylate cyclase domain (Schneeberger & Lynch, 2004), and anchors both proteins to the actin cytoskeleton (Fanning *et al.*, 1998). ZO proteins can bind to each other and actin directly and indirectly via adaptor proteins e.g. α-catenin (Paris *et al.*, 2008). Plaque proteins function to stabilise the TJ as dissociation of ZO-1 was

correlated with an increased permeability of the junction (Mark & Davis, 2002; Fischer *et al.*, 2005)

1.5 Modelling the blood-brain barrier

Experimental systems used in BBB research include *in vivo*, *ex vivo*, *in vitro* and now *in silico* approaches; the ultimate model depending on (i) the nature of the research question and (ii) the availability of resources.

In vivo studies obviously provide the most accurate representation of the BBB and the use of animals (particularly rodents and sometimes primates) and human subjects, has many advantages. The key advantage is that any assessments are made whilst all cells of the NVU are intact and are in their natural microenvironment. One assesses BBB functionality *in vivo* by contrast imaging, MRI or extravasation of dyes, and can correlate these results with biochemical and molecular pathways post-mortem, in the case of animal studies. In addition, results obtained from *in vivo* studies can be used as a reference guide for validating *in vitro* BBB models (Cardoso *et al.*, 2010). Despite the recognised benefits, research studies which assess the BBB *in vivo* are demanding resource-wise in that they are expensive to run and it takes a long time to both execute the studies and time for the final results to be obtained. For these reasons, many laboratories use *in vitro* BBB models as alternative approaches to studying the BBB.

Mimicking the *in vivo* BBB environment is extremely challenging as one strives to capture the following *in vivo* characteristics; high TEER, low paracellular permeability, functional nutrient/drug transporters, similar cellular phenotypes etc. This is an exceedingly complex task and no one fully representative *in vitro* BBB model exists. The TEER varies immensely between cultured endothelial cells and cell lines (Deli *et al.*, 2005) and the *in vivo* TEER measurements are consistently ten-fold higher (~1800Ωcm^2) than *in vitro* TEER measurements (Butt *et al.*, 1990; Abbott *et al.*, 2010).

The use of monocultures of endothelial cells (either from primary cell cultures or cell lines) has often been used to study the BBB. Although primary cell cultures more closely resemble the *in vivo* endothelial cell phenotype compared to cell lines (Cardoso *et al.*, 2010), there are marked species-specific differences in primary endothelial cells (Alanne *et al.*, 2009). Many studies now encompass multi-celled "co-culture" BBB

models, including not only endothelial cells, but also astrocytes and pericytes, or at the very least, conditioned media from these cells. However, there are complexities associated with co-culture models, which differ depending on whether mono or co-cultures are being used, and also whether or not the co-cultured cells are in direct contact (Cohen-Kashi Malina *et al.*, 2009). Despite the concerns with *in vitro* BBB models, they still provide a relatively inexpensive way to study the BBB; allowing for complete control and manipulation of the external experimental environment and making possible the investigation of biochemical/molecular signalling cascades etc. Given the wealth of literature regarding BBB permeability studies *in vitro*, the reader is directed to an excellent, fully comprehensive review comparing such BBB studies (Deli *et al.*, 2005).

Ex vivo tissue is a promising approach to studying the BBB, particularly the use of organotypic slice cultures (OSC). The advantage of using OSC is that the vessels remain *in situ,* under both the physical and biochemical influence of the surrounding NVU. Whilst it may be challenging to study the "barrier" function of the BBB in OSC, they are invaluable for studying the TJ proteins and cells of the NVU. However, one must ensure the OSC are given sufficient time to recover from the trauma of explantation, before treating. It was previously thought that capillaries had to be perfused in order to maintain endothelial cell survival (Carmeliet & Storkebaum, 2002), however it has since been shown that vessels in slices from rat cortex could survive in the absence of intraluminal flow for up to 3 weeks and the authors postulated that the cellular and trophic environment of OSC was sufficient to maintain vessels in culture (Moser *et al.*, 2003). That the TJ proteins claudin-5, occludin and ZO-1 and were preserved in OSC from neonatal mice brains has been confirmed (Bendfeldt *et al.*, 2007). In addition, Glut-1 and p-glycoprotein transporter proteins and the basal lamina were not only present/intact, but retained functionality in slice cultures (Camenzind *et al.*, 2010).

1.6 Inflammation

Inflammation is a complex physiological reaction to any 'insult' which could arise downstream of any traumatic, infectious, ischemic, toxic, or autoimmune event. The inflammatory process is a defence system involving immune cells and their secreted

soluble factors e.g. cytokines, which act to prevent tissue damage and to return the body to a state of physiological homeostasis.

The immune system is categorised into two distinct branches; the "innate" and the "acquired" systems, though both communicate in the immune response. The innate system is the initial, rapid response for immediate action against pathogens and in evolutionary terms, appeared earlier than the acquired immune system (Medzhitov & Janeway, 2000). The main distinction between the two systems being (i) their response time to insult and (ii) the mechanisms they employ for antigen recognition (Medzhitov & Janeway, 2000).

The cells of the innate system; monocytes, macrophages, dendritic cells and natural killer cells recognise harmful antigens by highly conserved structural motifs on microorganisms called "pathogen-associated molecular patterns" (PAMPs). Innate immune cells recognise these PAMPs via their pattern-recognition receptors (PRR) e.g. toll-like receptors (TLR) (Becher *et al.*, 2000; Bhat & Steinman, 2009; Colton, 2009). When activated, a combination of these cells act to target the pathogen for destruction, or they phagocytose and destroy the pathogen directly using antimicrobial peptides. The brain has its own resident macrophages called microglia.

The acquired immune system is a specific response against a specific pathogen; its onset is slower than the innate system due to the activation and recruitment of T and B lymphocytes and the release of cytokines. The acquired immune system cells produce specific antibodies against specific pathogens, ensuring a robust inflammatory response, particularly if there is a second encounter with the pathogen (Bhat & Steinman, 2009).

The innate immune system responds rapidly, in a similar manner to all pathogens, whereas the acquired immune response has a slower onset and results in a specific response against a given pathogen. Cross talk occurs between both the innate and acquired immune systems via cytokines and their associated signalling pathways, ensuring that the immune response is appropriate to manage the initial insult.

If the immune system becomes dysregulated, as occurs with age and in various disease states, chronic inflammation can ensue. This is thought to be detrimental to the tissue, resulting in even more tissue damage than the initial insult may have caused (Nathan, 2002). With regard to the brain, inflammatory tissue damage can be asymptomatic for

years, accumulating slowly, but eventually leading to severe neural tissue damage and loss of function (Licastro *et al.*, 2005).

Communication between cells of the immune system can occur by direct cell-cell contact, or indirectly by soluble signalling molecules called "cytokines". On a very basic level, most cytokines can be categorised as either "pro" or "anti" inflammatory proteins. Cytokines in the CNS can originate from peripheral immune cells which cross the BBB in diseased states (e.g. multiple sclerosis; MS) or they can originate in the CNS itself, having been produced by microglia and other glial cells (Szelenyi, 2001; Steinman, 2008). Altered expression of cytokines is implicated in CNS neurodegenerative diseases like Alzheimer's disease (AD) (Szelenyi, 2001). Cytokines are constitutively expressed at basal levels in the "normal" brain, not just during the inflammatory response. They are known to have broad neuromodulatory roles in the CNS under physiologic conditions such as metabolism, sleep and thermoregulation (Krueger & Bechmann, 2010) as well as co-coordinating inflammatory responses following an insult.

Outlined below (section 1.6.1- 1.6.3) is a brief background on some key modulators of inflammation, namely IL-1β, Lipopolysaccharide (LPS) and matrix metalloproteinases (MMP). These molecules are key modulators of inate inflammation and have distinct disruptive effects on the BBB, as will be discussed in section 1.8.

1.6.1 Interleukin-1

Charles Dinarello was the first to clone interleukin (IL)-1 in the 1980s (Dinarello, 1998) and since then the IL-1 family of cytokines have been extensively studied in the context of CNS inflammation. IL-1 cytokine (IL-1α) is secreted in a biologically active form however IL-1β is secreted in its "proprotein" form, becoming biologically active when enzymatically cleaved by caspase-1 (Dinarello, 1998; Vitkovic *et al.*, 2000). IL-1β is secreted and is responsible for the initiation and amplification of a robust pro-inflammatory response (Al-Sadi & Ma, 2007). IL-1 cytokines are secreted predominantly by microglia; in fact this is believed to be the earliest and primary source of CNS IL-1 in brain inflammation although it is now known that astrocytes and endothelial cells can also secrete IL-1 (Stanimirovic & Satoh, 2000; Vitkovic *et al.*, 2000).

There are two IL-1 receptors; IL-1R1 and IL-1RII, present on the surface of many cells, including cerebral endothelial cells (Ching *et al.*, 2007). IL-1R1 is a cell-surface receptor and binding of the ligand produces a signal transduction cascade leading to a pro-inflammatory state within the cell (O'Neill & Greene, 1998). In contrast the IL-1RII is a cytosolic receptor that upon ligand binding does not lead to an inflammatory cascade; rather it acts as a "decoy" receptor because it lacks the crucial signalling domain within the cytoplasm (O'Neill & Greene, 1998). Like the endogenous IL-1R antagonist (IL-1Ra), the IL-1RII counteracts the pro-inflammatory effects of IL-1β binding to IL-1R1 (Vitkovic *et al.*, 2000; Basu *et al.*, 2004). IL-1ra binds to the IL-1R1 with the same affinity as IL-1α and IL-1β, but does not initiate signal transduction (Granowitz *et al.*, 1992).

To initiate signal transduction within the cell, IL-1 must not only bind to the IL-1R1 but the additional binding of IL-1 receptor accessory protein (IL-1RAcp) to IL-R1 is also essential (Greenfeder *et al.*, 1995; O'Neill & Greene, 1998). The binding of IL-1 ligands causes a signal transduction cascade involving myeloid differentiation factor 88 (MyD88), a critical adaptor protein for IL-1 signalling as it acts as an adaptor protein to recruit IL-1 receptor-associated kinase (IRAK) (Takeuchi *et al.*, 2000).

Following receptor activation, there is a signalling cascade, involving many adaptor molecules and kinase, for full review see (Allan & Rothwell, 2001). However, activation of the IL-1R ultimately leads to activation of the mitogen-associated protein kinases (MAPK) that initiate activation of the nuclear transcription factor kappa-B (NFκB). In the resting cell, NFκB is located in the cytoplasm where it is bound to an inhibitory molecule, interleukin kappa kinase B (IκB), and this sequestration inhibits the ability of NFκB to translocate to the nucleus and bind to nuclear DNA. Phosphorylation of IκB by interleukin kappa kinase (IKK) leads to IκB degradation (Takeda & Akira, 2005), releasing NFκB, allowing it to translocate to the nucleus (Karin & Ben-Neriah, 2000). Within the nucleus, NFκB binds to the promotor region of genes involved in inflammation, including including TNF-α and more IL-1β in a positive feedback loop (Vitkovic *et al.*, 2000; Basu *et al.*, 2004). Over 90 genes upregulated by IL-1β are involved in the inflammatory processes (O'Neill & Greene, 1998), and IL-1 signalling is a primary component in the initiation and regulation of the innate immune response in the brain. This is highlighted in the case of IL-1RI knockout mice that have reductions

in the numbers of activated microglia and decreased pro-inflammatory cytokine mRNA and protein expression (Basu *et al.*, 2002).

1.6.2 Lipopolysaccharide

Lipopolysaccharide (LPS) is a component of the outer membrane of gram-negative bacteria and as it is a potent stimulator of the innate inflammatory response in the CNS it is commonly used as a research tool to stimulate the immune system. As mentioned earlier, mammalian endothelial and immune cells possess PRR which recognise PAMPs on foreign bacteria. One particular PRR family is the toll-like receptor (TLR) family. There are 10 TLR recognised in humans (Bowie, 2007) and TLR4 is the primary receptor that recognises LPS and more specifically, its lipid A domain (O'Neill *et al.*, 2009). Due to the different adaptor proteins recruited in varying combinations to the different TLR, there is huge scope for the innate immune system to respond to a variety of insults, and tailor specific inflammatory responses.

The TLR family is actually part of a larger superfamily of receptors known as the IL-1R/TLR superfamily. This is because although IL-1 and TLR express different extracellular domains, they share a highly conserved domain (TIR domain) in the cytoplasmic region of the receptor (O'Neill & Dinarello, 2000). As with binding of IL-1β to IL-1R1, the binding of bacterial LPS to TLR4 initiates a signalling cascade that ultimately leads to activation of common signalling pathways due to this conserved TIR-domain (see Figure 1.6).

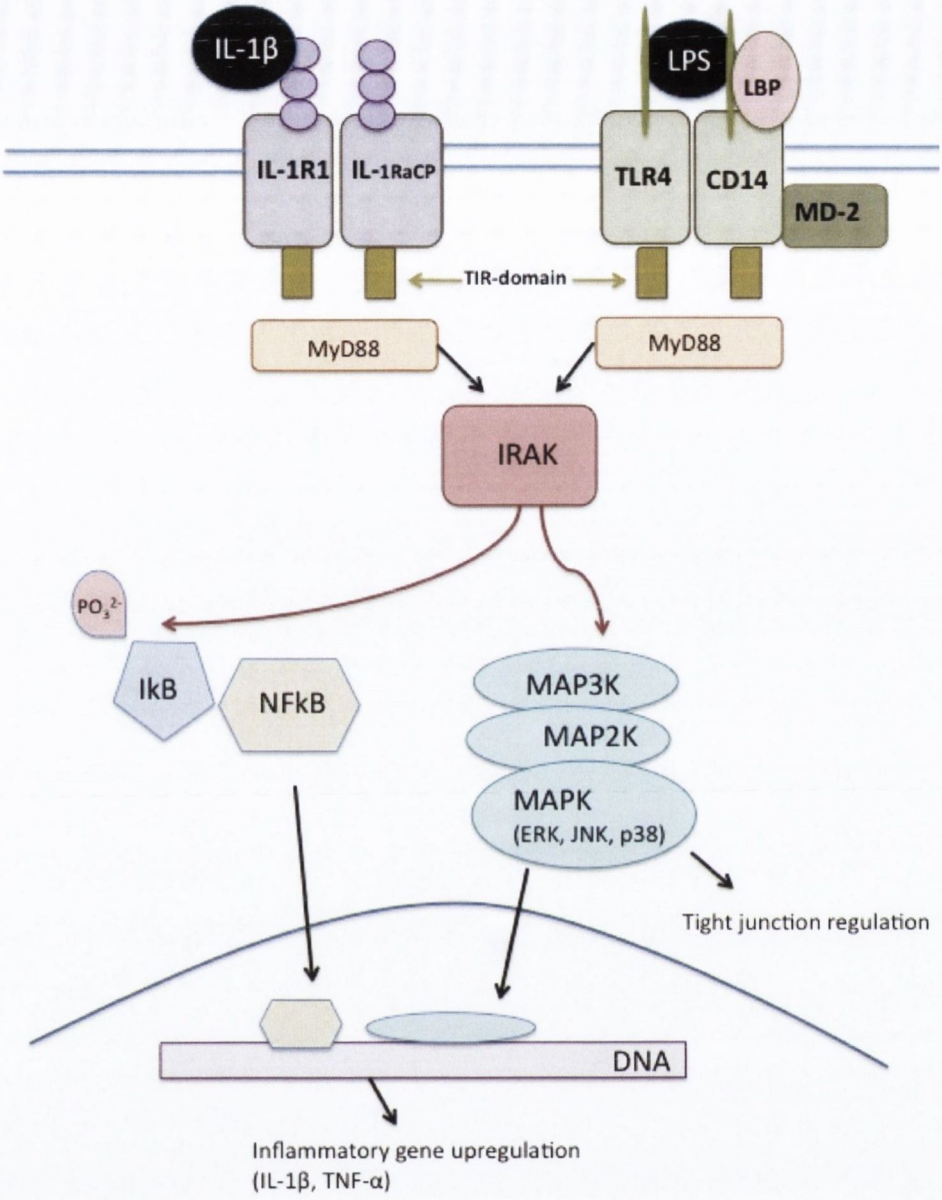

Figure 1.6: IL-1β and LPS share common signalling pathways.

The binding of IL-1 to its receptor, IL-1R1 is facilitated by the accessory protein IL-1RacP and the binding of LPS to its receptor, TLR4, is facilitated by the LPS binding protein (LBP) and accessory proteins CD14 and MD-2. The formation of both IL-1R1 and TLR4 complexes facilitates the binding of MyD88 to the TIR-domain, a motif conserved in both receptors. MyD88 binding initiates a series of signalling cascades unique to each receptor, but ultimately resulting in activation of IRAK. This kinase phosphorylates IκB, a protein involved in sequestering NFκB in the cytosol. Phosphorylation of IκB signals for its degradation and allows for NFκB to migrate to the nucleus, where it is involved in the regulation of genes involved in inflammation. In addition, activation of IRAK induces signalling via the MAPK pathway, leading to ERK, JNK and p38 activation; kinases involved in TJ regulation.

Binding of the LPS ligand to TLR4, with the help of LPS binding protein (LBP) induces the formation of a TLR4-MD2-LPS complex that along with the recruitment of the adaptor protein CD14, initiates signal transduction (Hennessy *et al.*, 2010). LPS signalling engages adaptor proteins and triggers activation of two signalling cascades: the myeloid differentiation factor 88 (MyD88)-dependent or MyD88-independent pathway. As with the IL-R1 signalling, a variety of adaptor molecules are recruited in TLR4 signalling see (Dauphinee & Karsan, 2006) for full review, but ultimately, the signalling of both LPS via TLR4 and IL-1β via IL-R1 leads to the activation of the mitogen-activated protein kinases and transcription factor NFκB and (Dauphinee & Karsan, 2006). This leads to the upregulation and activation of protein kinases and pro-inflammatory cytokines.

1.6.3 Matrix metalloproteinases

Matrix metalloproteinases (MMP) are a large family of structurally related, zinc-dependent proteases, first observed mediating collagenase activity in the developing tadpole tail (Brinckerhoff & Matrisian, 2002), and now known to collectively degrade all aspects of the extracellular matrix (Yang *et al.*, 2007). They are often grouped within the MMP family according to structure and substrate specificity, although there is much overlap (Candelario-Jalil *et al.*, 2009). Of particular interest to our research are the gelatinases A and B commonly referred to as MMP-2 and MMP-9, respectively.

Due to their potent proteolytic activity MMP are tightly regulated at many levels. Firstly, aside from MMP-2, they are generally not constitutively expressed and cells must be activated to release them, usually by an insult e.g. cytokines (Yong *et al.*, 2001; Rosenberg, 2002). When released, it is usually as an inactive zymogen and the pro-MMP must be cleaved at the pro-domain to expose the catalytic site (Sternlicht & Werb, 2001). In addition, MMP are inhibited by endogenous tissue inhibitors of MMP, (TIMP), of which there are four. All TIMPs are capable of inhibiting MMP (Lo *et al.*, 2002) certain TIMP having preferential MMP substrates (Brew *et al.*, 2000) and a tight balance between TIMP and MMP activity is essential to proper cellular regulation.

Despite MMP being traditionally regarded in the context of normal tissue-remodelling processes including regulation of the ECM, wound healing and angiogenesis (Lo *et al.*, 2002) they have now been implicated as major proteins involved in pathological processes including cancer metastasis (Yong *et al.*, 2001) and neuroinflammation

(Candelario-Jalil *et al.*, 2009). During the inflammatory process MMP (especially MMP-2 and MMP-9) are upregulated with a simultaneous downregulation of TIMPs, thus contributing to CNS damage (Rosenberg, 2002; Gurney *et al.*, 2006).

1.7 The ageing brain

The brain, like all other tissues in the body, is subject to change during the ageing process (Is *et al.*, 2008). The molecules and mechanisms underlying the ageing process have been intensely debated and researched over the last century. Many theories have been suggested in an attempt to explain the ageing process at the cellular level. Some researchers have postulated that cellular senescence is pre-programmed and ageing is simply the final stage of the developmental process (Beckman & Ames, 1998). The "free radical theory of ageing", first hypothesised in the 1950s (Harman, 1956) attributed damage of cellular constituents (fats, proteins, DNA) to the reactive oxygen species, which are produced as a by-product of aerobic respiration. Mitochondria are the primary source of reactive oxygen species and mitochondrial dysfunction is evident in the ageing brain as well as in age-related neurodegenerative disorders like Alzheimer's disease (Floyd *et al.*, 2001; Lin & Beal, 2006).

With increasing age, there is a progressive decline in cognitive function (Anderton, 2002). The hippocampus is an area of the brain particularly susceptible to damage during normal ageing (Is *et al.*, 2008), and is the basis of impaired learning and memory in both elderly humans and in animal models of senescence (Ueno *et al.*, 2001). Morphological and biochemical changes occur during normal ageing. It is generally accepted that there is not mass neuronal loss but rather other changes e.g. neuronal shrinkage, loss and retraction of dendritic spines, loss of synapses and changes in neurotransmitters and their receptors which all lead to altered neuronal signalling and result in an overall decrease in brain function (Anderton, 2002).

There is a gradual and progressive loss of anatomically and functionally related neuronal circuits in neurodegenerative diseases e.g. AD and Parkinson's disease (PD) which result in comprised cognitive status in the affected individual (Farkas & Luiten, 2001). The greatest risk factor of developing a neurodegenerative disease like AD is age (Lin & Beal, 2006). In contrast to the "minor" cognitive impairments in the "normal"

ageing brain where neuronal loss is limited, autopsied brain tissue from AD patients exhibited significant neuronal and synaptic loss with significant reductions in brain weight, particularly in the hippocampus and frontal cortex (Dickstein *et al.*, 2007).

The ageing brain is associated with a shift of the innate immune system towards a pro-inflammatory profile (Licastro *et al.*, 2005). In fact, gene expression analysis of brain tissue from young and aged rodents revealed that 50% of the genes that are upregulated with age are related to inflammation (Lee *et al.*, 2000; Prolla, 2002). The physiological mechanisms underlying the shift to a pro-inflammatory status is unclear. Some current theories include: (i) that certain individuals have a "pro" inflammatory genotype, (ii) that increased stimulation of the immune system in early life may impact on the system as it ages, or (iii) that age-related immune cell dysfunction with increasing age causes a gradual decline in the functionality of all cells (Licastro *et al.*, 2005).

It is widely accepted that the activation state of microglia is switched to an activated "primed" state in the aged "healthy" brains of humans, primates and rodents (Godbout *et al.*, 2005). There is an abundance of evidence that shows that there is an age-related increase in pro-inflammatory cytokine levels, in particular IL-1β, in the aged brain (Gelinas *et al.*, 2005; Loane *et al.*, 2009; Lynch, 2010) and a concomitant decrease in levels of anti-inflammatory cytokines such as IL-4 (Lynch, 2008) and IL-10 (Ye & Johnson, 2001). Microglial senescence and the functional changes in expression of inflammatory cytokines is thought to be a major contributing factor in driving the age-related shift in the brain to a pro-inflammatory phenotype. The resulting neuroinflammation is thought to contribute to the normal ageing of the brain and also to the pathogenesis of age-related neurodegenerative diseases like AD (Basu *et al.*, 2002; Blasko *et al.*, 2004; Godbout *et al.*, 2005; Lynch, 2010) as increased levels of IL-18 (Ojala *et al.*, 2009) and IL-1β (Licastro *et al.*, 2005) have been found in post-mortem brain tissue of AD patients.

1.8 Blood-brain barrier disruption

As discussed in 1.1, the BBB is a vital component of the CNS and the BBB TJ proteins are dynamically regulated as part of normal physiological functioning to adapt to the changing permeability needs of neural tissue (Turksen & Troy, 2004). Any factors that

disrupt the BBB and more specifically the proteins of the TJ complex, lead to increased paracellular permeability and could result in subsequent neuronal damage. Cells of the NVU act to maintain and regulate the BBB and similarly, any alterations to the NVU or intercellular signalling might also result in an impaired BBB.

1.8.1 Age-related disruption of the blood-brain barrier

As mentioned previously, the aged brain is associated with a progressive decline in cognitive function and it has been hypothesised that the BBB may become altered in the senescent brain, thus augmenting neuronal damage (Ueno *et al.*, 2001; Farrall & Wardlaw, 2009). An impaired BBB would facilitate the entry of neurotoxins into brain parenchyma and exacerbate any age-related tissue degeneration. Such neurotoxins might act in a causative or secondary role in the pathogenesis of age-related neurodegenerative disorders like AD. In support of this hypothesis include the evidence of circulating plasma components e.g. serum albumin, in the cerebral parenchyma of aged animals (Shah & Mooradian, 1997; Pelegri *et al.*, 2007) and hence provide good evidence for an age-related disruption of the BBB.

There are age-related changes in the cerebral capillaries which include: (i) decreased numbers of brain capillary endothelial cells, (ii) decreased capillary cross section (Shah & Mooradian, 1997) and (iii) decreased blood flow leading to reduced glucose and nutrient supply to the brain and slower waste removal from the brain (Farkas & Luiten, 2001). As previously noted, mitochondrially-generated reactive oxygen species damage cellular constituents and considering that brain capillary endothelial cells have especially high numbers of mitochondria, these cells may be particularly susceptible to oxidative damage. The CNS endothelial cells are vital to the BBB and any age-related changes impairing their function might affect BBB integrity and compromise overall brain function.

Considering the structural and functional age-related changes at the BBB, it is possible that the TJ proteins themselves (claudins, occludin, and TJ plaque proteins) are altered with age. A study comparing the expression levels of occludin and ZO-1 in young and aged rats aged 3-, 12- and 24-months revealed age-related changes. There was a significant decrease in occludin protein but not mRNA expression in aged animals. There was no significant difference in ZO-1 protein expression between young and aged animals but a significant age-related increase in ZO-1 mRNA expression was reported

(Mooradian *et al.*, 2003). Considering the important role that the claudin proteins play in establishing and maintaining the BBB, this is an area of research worth investigating.

1.8.2 Cytokine- and LPS-induced disruption of the blood-brain barrier

It is well-documented that cytokines, particularly IL-1β cause increased paracellular permeability in many tissues including the gastrointestinal epithelium (Al-Sadi *et al.*, 2010), respiratory epithelium (Holgate, 2007), and the brain capillaries (Capaldo & Nusrat, 2009). Cytokine-induced increases in paracellular permeability is a significant contributor to the cause and/or pathogenesis of different diseases in a variety of tissues e.g. inflammatory bowel disease and asthma (Capaldo & Nusrat, 2009). Much of the research concerning cytokine regulation of vascular permeability has been carried out on epithelial tissues from the periphery. Permeability studies in patients with chronic irritable bowel disease show significant correlations between increased expression levels of IL-1β and increased disease severity (Al-Sadi & Ma, 2007). The anatomical location of brain capillary endothelial cells between the blood and the brain tissue is interesting, considering that they are both targets of IL-1β and that they are also capable of producing IL-1β (Stanimirovic & Satoh, 2000).

Assessment of the literature regarding cytokine regulation of TJ at the BBB indicates that they are generally disruptive (Cardoso *et al.*, 2010). Human brain endothelial cells from autopsy cerebral cortex treated with IL-1β, TNF-α and IFN-γ displayed significantly decreased electrical resistance (TEER) across the endothelial monolayer as early as 4 hours post-treatment, indicating cytokine-induced increased permeability (Wong *et al.*, 2004). Assessing the movement of horseradish peroxidase tracer (40-45 kDa) confirmed that there was increased permeability across the paracellular pathway. Although it was hypothesised, the authors did not investigate if there were TJ protein changes with cytokine treatment. An intracerebrally administered IL-1β injection to the striatum of juvenile rats caused BBB disruption, assessed with magnetic resonance imaging (MRI), and this was apparent as early as 5 hours post treatment, although the changes were attenuated by 27 hours (Blamire *et al.*, 2000).

Considering that the TJ proteins are essential in regulating BBB permeability, it is possible that the age-related increase in pro-inflammatory cytokines may disrupt TJ and contributes to BBB dysfunction with age.

As the cerebral endothelia are at a key interface between the periphery and the brain, they are vulnerable to systemic inflammation resulting in BBB disruption, for example in the case of bacterial meningitis (Tunkel & Scheld, 1993). LPS, a potent stimulator of inflammation has also been shown to increase BBB permeability. Nishioku *et al.* (2009) showed that an acute intraperitoneal injection of LPS was capable of (i) increasing BBB permeability to small molecules e.g. sodium fluorescein (376Da) and (ii) also fragmenting the basal lamina of the NVU. They postulated that these LPS-induced barrier disruptions were caused by activation of microglia, as evidenced by a shift in the morphology of microglial processes from a ramified "resting" state to an amoeboid-like morphology, consistent with "activated" microglia. In addition, the LPS-induced microglial activation correlated with the time-course of cerebrovascular disruption.

There are many studies documenting the disruptive effects of LPS on the *in vivo* BBB (Xaio *et al.*, 2001; Erickson *et al.*, 2012) and *in vitro* models of the BBB (Xiaolu *et al.*, 2011; Cardoso *et al.*, 2012). Chronic systemic inflammation, induced by an intraperitoneal injection of LPS to neonate rodents resulted in increased BBB permeability for weeks following the insult (Stolp *et al.*, 2005). LPS was capable of disrupting the proteins of the transcellular pathway, such as the saturable insulin-carrier protein (Xaio *et al.*, 2001). LPS was shown to cause increased influx and decreased efflux of amyloid-beta (Aβ) across the BBB (Jaeger *et al.*, 2009), thus supporting the idea that inflammation contributes to the pathology of AD and other neurodegenerative diseases (Holmes *et al.*, 2009; Murray *et al.*, 2011). In addition, systemic administration of LPS to pregnant mice resulted in decreased TJ protein expression in the amniotic barriers (Kobayashi *et al.*, 2010). TLR4, the primary innate immune receptor for LPS, is located on brain endothelium (Dauphinee & Karsan, 2006) so it is not surprising that LPS activation of cerebral endothelium may be underlying the BBB disruption observed during systemic inflammation.

Following LPS-mediated activation of cerebral endothelia *in vitro,* many studies have reported disruptions to the subcellular localisation of claudin, occludin and ZO-1, where they were internalised away from the cell membrane (Yi *et al.*, 2000; Schlegel *et al.*, 2009; Xiaolu *et al.*, 2011; Cardoso *et al.*, 2012), or there was overall degradation of the TJ proteins (Yi *et al.*, 2000; Sheth *et al.*, 2007).

It is thought that LPS might mediate its disruptive effect on the BBB through the upregulation of pro-inflammatory cytokines. Systemic LPS acting on endothelial TLR4, results in the release of pro-inflammatory cytokines e.g. IL-1β, TNF-α from cerebral endothelia, that can in turn then act in an autocrine manner to disrupt the endothelial barrier properties (Gaillard *et al.*, 2003). Alternatively, CNS-administered LPS may lead to cytokine release from activated microglia (Nishioku *et al.*, 2009). Regardless of the cellular source of pro-inflammatory cytokines, this thesis will be concerned with establishing the molecular mechanisms underling the cytokine-mediated disruption of the aged BBB.

1.8.3 MMP-induced disruption of the blood-brain barrier

It is well documented that MMP activity increases wherever neuroinflammation features (Yong *et al.*, 2001; McColl *et al.*, 2008) particularly following infection (Gurney *et al.*, 2006) and ischemia (Yang *et al.*, 2007), and BBB disruption often follows. Endothelial cells, microglia, astrocytes and neutrophils all secrete MMP (Rosenberg, 2002). MMP have also been shown to disrupt TJ directly *in vivo*; decreased claudin-5 and occludin expression was attributed to increased MMP activity in LPS-injected mice, a result that was not apparent in MMP-3 knockout mice (Gurney *et al.*, 2006), indicating that MMP may be damaging the substrate for which endothelial cells are anchored, which could in turn, lead to disrupted TJ. Also, cerebral ischemia induced in MMP-9 knockout and wildtype mice, led to degradation of ZO-1 protein and more profound disturbances to BBB permeability in the wildtype animals (Asahi *et al.*, 2001).

MMP-2 and -9 in particular, directly led to decreased claudin-5 and occludin expression following middle cerebral artery occlusion in rats (Yang *et al.*, 2007) that resulted in increased BBB permeability. A number of other *in vitro* studies support the *in vivo* observations above, where MMP were implicated in signalling events involving the degradation of TJ protein (Reijerkerk *et al.*, 2006; Lischper *et al.*, 2010).

The balance of MMP and TIMP is responsible for maintaining basal lamina stability (Yang *et al.*, 2007). MMP-2 and -9 are also known modulators of the NVU. MMP-9 mediated the disruption of laminin following focal ischemia in mice (Gu *et al.*, 2005). It has been postulated that (i) MMP-mediated proteolysis of the basal lamina loosens the

base on which the TJ proteins are anchored and/or (ii) MMP-mediated proteolysis of components of the extracellular matrix exposes the endothelial TJ proteins, rendering them susceptible to damage (Gurney *et al.*, 2006). MMP-9 inhibitors rescued laminin proteolysis in the brain following cerebral ischemia in mice (Gu *et al.*, 2005) and additionally, in cultured human brain endothelial cells (Haorah *et al.*, 2007).

Up-regulation of MMP-2 and -9 activity has been implicated in a multitude of vascular diseases including vascular dementia and stroke, in addition to AD (Candiello *et al.*, 2010). Increased levels of MMP-9 activity in ischemic areas of post-mortem stroke brains have been observed with a concomitant increase in BBB permeability in those areas (Rosell *et al.*, 2008). Increased MMP-2 and -9 activity levels have been observed in CSF and plasma of MCI and AD patients compared with control (Lorenzl *et al.*, 2003; Lim *et al.*, 2011). Basal levels of MMP-2 and MMP-9 have been shown to be greater in the aged murine brain (Lee *et al.*, 2012) and their increase following cortical impact injury was postulated to be responsible for disrupting the BBB to a greater extent in the aged animals (Lee *et al.*, 2012).

1.8.4 Disrupting neurovascular unit components alters the blood-brain barrier

Though many studies have investigated the role of pericytes in vascular development, maintenance and blood flow, few have looked at the role of pericytes in the context of BBB permeability and more specifically, in the ageing brain. Mice with mutated or absent pericytes die, due to increased vascular permeability. Mice with disrupted PDGFβ-PDGFRβ signalling due to PDGFβ mutations, had decreased pericyte numbers in brain capillaries, increased BBB permeability and subsequently died from vascular haemorrhage. In a similar study, PDGFRβ knockout mice lacking CNS pericytes died at the embryonic stage as a result of vascular haemorrhage (Daneman *et al.*, 2010). These studies demonstrate the importance of pericytes in both neovascularisation and vessel maintenance *in vivo.*

Pericyte degeneration with age could lead to BBB disruption, increased permeability and contribute to age-associated neurodegenerative diseases like AD, which are associated with increased BBB permeability (Balabanov & Dore-Duffy, 1998). A very comprehensive study on age-related pericyte changes was recently carried out by Bell and colleagues (2010). They showed that PDGFRβ $^{+/-}$ mice had disrupted PDGFRβ signalling and were compared to PDGFRβ $^{+/+}$ (wildtype) mice at various ages: 1, 6-8

and 14-16 months old. There were significant age-related decreases in pericyte numbers in the PDGFRβ $^{+/-}$ mice (up to 60% by 14-16 months) compared to wildtype mice. The mutant mice had increased plasma IgG in their brains, indicating profound BBB breakdown with increasing age. There was evidence of neuroinflammation and neurodegeneration in the mutant mice; activated microglia, increased cytokine production, dendrite loss and neuronal loss (Bell *et al.*, 2010). That particular study highlighted the important contribution pericytes make to the neurovascular unit, especially considering that BBB compromise is associated with age-related neurodegenerative disorders like AD. Cultured human brain pericytes from autopsy tissue are rapidly degenerated following incubation with $A\beta_{1-42}$ peptides (Verbeek *et al.*, 1997). Although mutant animals were used in the Bell (2010) study, it is possible that a loss of pericytes occurs during the normal physiological ageing process. The loss of pericytes with age during the normal ageing process is something that will be investigated in this thesis.

It was shown that LPS-induced disruption of the basal lamina correlated with pericyte detachment and increased BBB permeability (Nishioku *et al.*, 2009) as the laminin-pericyte disruption correlated with the timepoints at which the LPS was administered. The authors hypothesised that LPS led to a destabilisation of the laminin-pericyte unit, ultimately exposing the endothelial cells, leading to TJ disruption and the subsequent alteration in BBB function.

1.8.5 Molecular pathways that dysregulate tight junction proteins

Tight junction proteins of the BBB are not merely static proteins, but are highly dynamic structures, that possess the capability of assembly/disassembly in response to their local microenvironment (Deli, 2009).

It was first demonstrated in the 1980s that a relationship between the degree of TJ phosphorylation and TJ function existed; ZO-1 was hyperphosphorylated in epithelial monolayers that exhibited low TEER (Stevenson *et al.*, 1986). The area of TJ phosphorylation is a complex field, due to the vast number of kinases involved in TJ phosphorylation on a large number of residues of a given TJ protein. TJ are known to be phosphorylated by the PKC family, G-proteins and MAPK, all of which are reviewed in a comprehensive manner by Gonzalez-Mariscal (2008). Of particular interest to our research is the MAPK regulation of TJ. LPS is a known activator of IL-1β, which itself

upregulates MMP-9 and all three molecules are capable of profoundly disrupting the *in vivo* BBB as well as disrupting TJ *in vitro*. In addition, both LPS and IL-1β share common signalling pathways that upregulate the MAPK.

MAPK are ubiquitous serine/threonine kinases that are activated in response to stressful stimuli e.g. LPS, IL-1β and comprise the p42/p44 extracellular signal-related kinase (ERK1/2), the c-Jun N-terminal kinase (JNK) and p38 kinases. Downstream signalling involves a sequential cascade of 3 kinases (MAPKKK, MAPKK, MAPK), ultimately leading to phosphorylation and subsequent activation of the MAPK (see Figure 1.7) which themselves are capable of phosphorylating a large number of proteins (Cross *et al.*, 2000).

Although the literature is conflicted regarding ERK regulation of TJ the majority of studies have found that activation of the ERK-MAPK pathway disrupts TJ, leading to barrier dysfunction (Gonzalez-Mariscal *et al.*, 2008). ERK phosphorylation has been indicated in BBB disruption in LPS-injected ethanol-drinking rats (Singh *et al.*, 2007) and following H_2O_2 mediated ZO-1 and occludin disruption in primary endothelial cells (Fischer *et al.*, 2005). However, barrier disruption in mouse/rat endothelial cell lines were unaffected by MAP kinase inhibitors, indicating that changes in barrier function were independent of any of the MAPK signalling cascades (Thornton *et al.*, 2010). It is likely that MAPK signalling may be capable of carrying out opposing effects on TJ proteins, depending on the cell type under investigation and the nature of the insult.

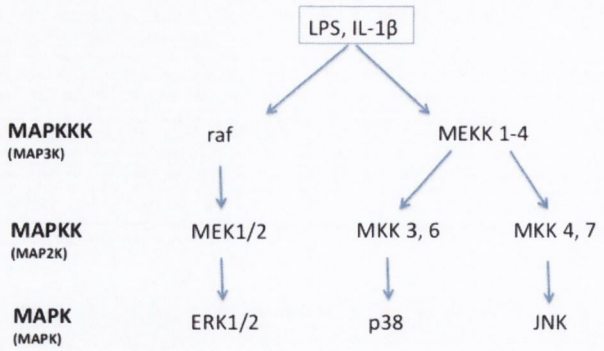

Figure 1.7: MAPK signalling cascade. Activation of the MAPK occurs when a stimulus, usually stressful e.g. LPS or IL-1β, initiates signal transduction causing a phosphorylation cascade involving serine/threonine kinases, leading to the ultimate activation of MAPK. This MAPK (ERK, p38, JNK) are capable of phosphorylating a myriad of cytosolic and nuclear proteins, thus changing the functional state of the cell (Image adapted from Gonzalez-Mariscal *et al.*, 2008).

1.9 Summary

A tightly regulated microenvironment is key to proper CNS function and the delicate CNS must be protected from potential neurotoxins in the circulatory system. This is achieved by specialisations of brain capillaries in the form of the BBB, which regulates capillary permeability to soluble blood components, thus maintaining homeostasis. The TJ proteins, claudin-3, -5, -12 and occludin, between adjacent endothelial cells form a tight seal and prevent paracellular flux of blood-borne substances into the brain. The TJ proteins are the primary protein components responsible for protecting the brain, although cells/components of the NVU (basal lamina, pericytes, astrocytes, neurons) also regulate and maintain the BBB.

CNS cellular dysfunction occurs during the ageing process, which results in the cognitive impairments often observed with "normal" ageing, and also in age-related neurodegenerative diseases. In particular, there is a shift in the aged brain to a pro-inflammatory phenotype where there is a significant increase in pro-inflammatory cytokines such as IL-1β. IL-1β is a known modulator of the paracellular permeability pathway between epithelial and endothelial cells, disrupting the barrier properties of these cells and leading to increases in paracellular substance flux. In addition, the

elderly, a demographic group particularly susceptible to bacterial infection may have a poorer outcome following injury.

It is our hypothesis that the age-related increases in IL-1β, due to the normal increase of these cytokines with age, or due to bacterial insult from LPS, leading to subsequent downstream signalling may cause disruption of the BBB via modulation of TJ proteins and NVU components, possibly via MMP and MAPK signalling. This BBB disruption would facilitate the entry of plasma components into an already fragile ageing brain, leading to stimulation of an immune response. Any additional inflammatory insult to an already fragile ageing BBB would exacerbate cellular damage.

1.10 Research aims

The aims of this research were to compare the functional and morphological differences in the BBB of young and aged rats and more specifically to:

- assess BBB paracellular permeability to substances of varying molecular weights in young and aged rats,
- investigate mRNA and protein expression levels of TJ proteins (claudin-5, occludin, ZO-1) in young and aged rats,
- investigate the disruption, if any, of the NVU; particularly the basal lamina and pericytes surrounding the endothelial cells,
- investigate if an additional systemic infection exacerbated BBB damage in the aged brain,
- investigate the key molecular pathways underlying TJ modulation using a combination of genetic knockout mice, cultured endothelial cells and *ex vivo* slice cultures.

Chapter 2

Methods

2. Methods

2.1. Animal samples

All animals and tissue samples were acquired as a result of a collaboration with Prof. Marina Lynch (Trinity College Institute of Neuroscience, Dept. Physiology, Trinity College Dublin) unless otherwise stated. All animals were housed in the BioResources Unit, Trinity College, Dublin, under 12-hour light-dark cycles and received food/water *ad libitum*. All procedures were carried out with ethical approval from the College Ethical Review Group and under license from the Department of Health and Children. Brain and plasma samples from a number of different animal experimental groups were assessed in the course of this work, and each group will be discussed below.

2.1.1. Animal study one: young and aged Wistar rats

This study included 8 young (4- to 6-month-old) and 9 aged (22- to 24- month-old) male Wistar rats (BioResources Unit, Trinity College, Dublin, Ireland). The animals were disease-free and did not receive a supplemental treatment. This cohort of animals was used to investigate any age-related differences in BBB permeability (see below) and to correlate these functional results with biochemical or molecular measurements.

Saline solution (0.9%) containing 2mg/ml sodium fluorescein (376 Da; Sigma Aldrich, UK) was filtered before injecting 1ml into the tail veins of young and aged rats. The control group received a saline-only injection. All procedures were performed under continuous tail vein anaesthesia (propofol or 1-2% isoflurane in 100% oxygen; Rapinovet, Schering-plough). Two animals from each age-group did not receive a sodium fluorescein injection and were used as negative controls. Animals injected with sodium fluorescein were sacrificed 10 min after the tail vein injection. According to the datasheet for Na-F, following administration to the systemic circulation, Na-F reaches central arteries in approximately 7-14 seconds and will gradually become bound to plasma albumin (80% one hour post injection). In addition, it gets rapidly metabolised to fluorescein monoglucoronide, a metabolite that exhibits half to one third the fluorescent capacity as non-metabolised Na-F. Based on this, 10 mins was chosen as an appropriate time to allow thorough systemic circulation of Na-F, but not so long as to allow Na-F metabolism or undue anaesthesia-related stress to the animals.

Rats were sacrificed by decapitation; their brains were rapidly removed, placed on ice and the meninges discarded. The brain was bisected sagittally, the right hemisphere was bisected again and the more medial section was coated in OCT (TissueTek®Sakura®, USA) and mounted onto cork discs before being placed in liquid nitrogen. Sagittal cryosections (15μm thick) were cut using a cryostat and were mounted onto gelatin-coated microscope slides. The slides were stored at -20 °C until required for immunostaining. The hippocampus, frontal cortex, and parietal cortex were dissected free from the remaining left and right hemispheres, snap frozen in liquid nitrogen (Cryoproducts, Ireland) and stored at -80 °C for later RNA and protein analysis. Trunk blood was also collected from each animal and centrifuged at 3000 rpm for 5 min at 20 °C. The serum was collected and stored at -20 °C.

2.1.2. Animal study two: C57BL/6 wildtype and IL-1R1$^{-/-}$ mice

The IL-1R1$^{-/-}$ mice and corresponding C57BL/6 wildtype controls were acquired from Prof. Kingston Mill's research group (School of Biochemistry and Immunology, Trinity College Dublin). This mouse strain (B6.12957-IL1R1^{tm1Imx}J) was generated by the Jackson Laboratory, USA.

In response to activation by the cytokine IL-1β, IL-1R1 activation is involved in mediating downstream immune, endocrine and behavioural responses associated with an inflammatory insult, including disrupted appetite, temperature, sleep-wake cycles and sickness-behaviour (Shaftel *et al.*, 2008). Mice homozygous for the IL-1RI targeted mutation fail to respond to IL-1 and exhibit an altered immune response to many different inflammatory stimuli (Glaccum *et al.*, 1997, Basu *et al.*, 2002). Of particular interest to our research is their resistance to the IL-1β – induced sickness response, when injected i.c.v or i.p with IL-1β, although they continue to respond to LPS (Bluthe *et al.*, 2000). In addition to an altered inate immune response, these mice also exhibit altered glucose metabolism, behavioural, cardiovascular and skeletal changes, to name but a few. Please refer to the Jackson website (http://jaxmice.jax.org/strain/003245.html) for a full list of references pertaining to the altered phenotype of these mice.

All mice were further divided into either young (2-month) or middle-aged (14-18-month) groups. Therefore the four experimental groups were as follows: young wildtypes (n=5), middle-aged wildtypes (n=6), young IL-1R1$^{-/-}$ (n=5) and middle-aged IL-1R1$^{-/-}$ (n=7) male mice. The animals did not receive a supplemental treatment and the tissue was used to assess the role of IL-1 signalling (or absence thereof) on a number of biochemical readouts relating to the BBB. Animals were sacrificed by cervical disconnection, their brains were removed rapidly, placed on ice and the meninges discarded. The hippocampus was dissected free, snap frozen in liquid nitrogen (Cryoproducts, Ireland) and stored at -80 °C for later protein analysis.

2.1.3. Animal study three: young and aged Wistar rats ± LPS treatment

This study consisted of young (3-month old) and aged (26-month old) Wistar rats (Bantham & Kingman, UK). Animals were randomly assigned to either saline-treated (controls) or LPS-treated groups (n=6 per group). Animals received an intraperitoneal (i.p.) injection of sterile, nonpyrogenic isotonic saline (referred to as 'saline' hereafter; 0.9% saline solution, B. Braun, Ireland) or LPS (100μg/kg; LPS from E. coli, Serotype R515 (Re), Alexis, Switzerland). Animals were sacrificed by decapitation 4 hours after injection; their brains were rapidly removed, placed on ice and the meninges discarded. The hippocampus, frontal cortex and striatum were dissected free from the left and right hemispheres, snap frozen in liquid nitrogen (Cryoproducts, Ireland) and stored at -80 °C for later RNA and protein analysis.

Given that the downstream consequences of LPS signalling i.e. release of pro-inflammatory cytokines peaks in the 3-6 hour timeframe post i.p. injection (Nadeau & Rivest, 1999), 4 hours was chosen as an appropriate time to sacrifice the animals, to assess the initial effect inflammation has on the BBB. Much of the literature that utilise LPS as a tool to cause an immune response use doses of approximately 1-3mg/kg (Xaio *et al.*, 2001; Jaeger *et al.*, 2009; Erickson *et al.*, 2012). For the purposes of our research, we decided to use a lower dose (100μg/kg), to assess if a moderate immune challenge could alter the BBB.

2.1.4. Animal study four: young and aged Wistar rats (serum)

This study consisted of 5 young (6-month-old) and 9 aged (25-29-month-old) male Wistar rats. Rats were anesthetised by intraperitoneal injection of urethane (1.5 g/kg). A

heparin-coated syringe was used to collect approximately 10 ml blood via cardiac puncture to the left ventricle. Whole blood was diluted (1:1) with phosphate buffered saline (PBS; 137mM NaCl, 2.7mM KCl, 8.1mM Na_2HPO_4, 1.5mM KH_2PO_4, pH 7.3) and centrifuged (1500 rpm for 30 min at 4 °C). The serum was removed and stored at -80 °C until required for gelatin zymography, as outlined in section 2.9 below.

2.2 Serum samples from human subjects

2.2.1. Serum from young, middle-aged and aged healthy human subjects

Whole blood was acquired from participants ranging in age from 21 to 70 years old. The male subjects were sub-categorised into young (21-23 years; N=6), middle-aged (52-57 years; N=6) and aged (64-70 years; N=6) groups. Whole blood was centrifuged (1500 rpm for 30 min at 4 °C) and the serum was removed and stored at -80 °C until required for gelatin zymography, as outlined in section 2.9. All subjects provided informed consent prior to their participation in the study and they were recruited under the supervision of Dr. Mikel Egana (Department of Physiology, Trinity College Dublin). Ethical approval for the study was granted by the Faculty of Health Sciences Ethics Committee, Trinity College Dublin and the study was conducted in accordance with the Declaration of Helsinki (2008).

2.2.2. Serum from Alzheimer's disease patients and their carers

Whole blood acquired from participants was centrifuged (1500 rpm for 30 min at 4 °C). The serum was removed and stored at -80 °C until required for gelatin zymography, as outlined in section 2.9. In brief, patients were recruited from the Memory Clinic, Psychiatry for the Elderly Services in St. James's Hospital, Dublin 8 (PI: Professor Brian Lawlor, Department of Psychiatry, School of Medicine, Trinity College Dublin). All participants (and carers in the case of AD patients) were given written information (by post or in person) regarding the objectives and methods of the study and were asked to indicate their preference to either participate or not in the study. Participants gave informed consent when they had the capacity to do so, or otherwise, caregivers gave informed consent by proxy. Potential participants were also informed that refusal to participate in the study would in no way compromise their care. The inclusion criteria

for the AD patients were (i) age (between 55-80 years), (ii) that they met the National Institute of Neurological and communicative Disorders/ Alzheimer's Disease and related Disorders Association (NINCDS/ADRDA) criteria for possible and probable AD, (iii) that they had a Mini-Mental State Examination (MMSE) score of <24 and (iv) that they had a Clinical Dementia Rating (CDR) status of <0.5. The inclusion criteria for the control group were as follows: (i) aged between 65-80 years, (ii) that symptoms of cognitive impairment were absent, (iii) that they had no history of dementia or mild cognitive impairment and (iv) that they had a MMSE score of 27 or higher. Patients with active medical disease or active psychiatric illness or with alcohol/drug abuse/dependency were excluded. The assessments were completed by a research nurse and carer in the patient's home, outpatient clinic or nursing home.

2.3. Bicinchoninic acid (BCA) protein assay

All samples from animal and cell culture experiments were sonicated in lysis buffer (10mM Tris-HCl; 50mM NaCl; 10mM $Na_4P_2O_7.10H_2O$; 50mM NaF; 1% NP-40; protease inhibitor cocktail containing proteinase inhibitor cocktail I, proteinase inhibitor cocktail II, phosphatase inhibitor cocktail; 1:100, all Sigma Aldrich, UK) using a sonicator (Soniprep-150, at 4 micron for 15 s). Protein concentrations of samples were measured using the bicinchoninic acid (BCA) protein assay kit (Pierce, USA). Briefly: standards (0-2000 µg/ml) were prepared with bovine serum albumin (BSA; Sigma Aldrich, UK) diluted with lysis buffer. Triplicates of standards and samples (25 µl) were added to a 96-well plate, to which the working reagent (200 µl) was also added. The plate was incubated at 37 °C for 30 min. The absorbance was read at 560nm on a plate-reader (SynergyHT, Biotek®). The standard curve was calculated by plotting protein concentration of known standards against their corresponding absorbance read-out. The protein concentration of samples was then calculated from this standard curve. Samples were equalised for protein concentration using lysis buffer.

2.4. Capillary separation from brain homogenate

Cortical tissue from young and aged Wistar rats (animal group one, see section 2.1.1) was homogenized in DMEM (Dulbeco's Modified Eagle Medium, +4.5g/L glucose, minus L-glutamine; Biowhitaker, UK). Capillary separation was attempted using a density centrifugation technique adapted from Dr. Matthew Campbell, Smurfit Institute of Genetics, Trinity College, as follows: cortical homogenate was centrifuged (3000 rpm for 5 min at 20 °C) and supernatant removed. Capillaries were enzymatically dissociated from the brain pellet with 0.005% (wt/vol) dispase (Sigma Aldrich, UK) in DMEM for 2 hours at 37°C. The homogenate was centrifuged (3000 rpm for 5 min at 20 °C) and the pellet re-suspended in dextran solution (10% wt/vol in PBS; Mw 70,000 Da; Sigma Aldrich, UK) and this homogenate was then centrifuged (3000 *g* for 10 min at 4 °C). This resulted in the neuronal fraction floating on top of the dextran solution, leaving the blood vessel fraction pelleted at the bottom of the falcon tube. Both neuronal and blood vessel fractions were separated, re-suspended in PBS, and centrifuged (800 *g* for 5 min at 20 °C). Pellets were then lysed in lysis buffer and stored at -20 °C until required for Western immunoblotting. Confirmation that capillaries had successfully been separated from brain homogenate was assessed by Western immunoblotting and probing for endothelial cell- specific markers e.g. claudin-5 or PECAM. Positive staining for endothelial-specific markers in the "capillary" fraction but not the brain homogenate was taken to indicate adequate capillary separation.

2.5. Sodium fluorescein permeability

Microscope slides containing cryosections from sodium fluorescein-injected and saline-injected Wistar rats (animal group one, see section 2.1.1) were removed from storage at -20°C and allowed to adapt to room temperature. Slides were mounted with glass coverslips using mounting medium containing the nuclear stain DAPI (Vectashield® Hard Set™; Vector Laboratories Inc, CA) and fixed with clear varnish. Slides were stored at 4 °C until required for analysis by confocal microscopy. Prior to analysis, slides were re-coded and relabelled by the PI so the slides could be analysed in blinded manner to minimise subjectivity. Three saggittal brain slices, at intervals of 180 μm apart were taken from each young and aged animal. The fluorescence from these 3 slices, for any given anatomical area, was measured, and the mean score was calculated.

Slides were visualised with a Zeiss 510 Meta-Confocal Laser Microscope using an Axiovert 200M inverted microscope. The fluorescent microscope setting was initially used to visualise the DAPI nuclear stain at 10X in order to locate the following brain regions (dentate gyrus, hippocampus, parietal cortex, frontal cortex) on each slide. The same brain regions were examined on every slide. When the region of interest was located (with DAPI), the microscope filter was switched to the confocal laser scanning setting to visualise sodium fluorescein (excitation wavelength, 494nm; emission wavelength 518nm). Image analysis was carried out using Zeiss software which calculated mean fluorescence intensity, measured in pixels, for each image.

In summary there were (8 young + 9 aged rats) x 4 anatomical areas (dentate gyrus, hippocampus, frontal cortex, parietal cortex) x (3 fluorescent readings per anatomical area). The mean of the three fluorescent readings for any given anatomical area was taken as the *mean fluorescent score* for that animal, in that particular region. Thus in comparing the overall Na-F fluorescence in the dentate gyrus of young versus aged rats, the *mean fluorescent scores* of the dentate gyrus for each group, either young or aged, was combined to give an overall "mean fluorescent pixel", and these values are reported in the relevant results sections.

2.6. Immunohistochemistry

Slides were taken from -20 °C and allowed to adapt to room temperature. A pap pen (Dako, UK) was used to enclose sections in a hydrophobic well, preventing antibody loss and slice dehydration. Sections were fixed in either 4% paraformaldehyde in PBS for 5 min or ice-cold methanol for 10 min, followed by 3 x 5 min washes with PHEM buffer (25mM HEPES, 10mM EGTA, 60mM PIPES, 2mM $MgCl_2$, pH 6.9). Where necessary, sections were permeabilised with 0.1% Triton-X-100 (Sigma Aldrich, UK), again followed by 3 x 5 min PHEM washes. Non-specific binding of antibodies was prevented by blocking sections in 10% serum in 4% BSA in PBS for 30 min at room temperature. The serum used in the blocking stage depended on the species in which the appropriate secondary antibody was raised. Primary and secondary antibodies were diluted 1% serum in PBS. Primary antibodies (1:200 dilution for all primary antibodies except a-smooth muscle actin (1:400) Abcam, UK; or laminin (1:1000), Sigma, UK) were incubated overnight at 4 °C. Secondary antibodies conjugated to specific

fluorophores (goat anti-mouse AlexaFluor® 546™ or chicken anti-rabbit AlexaFluor® 488™; Invitrogen, UK) were used at 1:500 dilution in 1% serum in PBS containing Hoechst stain (1:1000; Hoechst33342, Invitrogen™, UK). Negative controls were incubated in diluent alone where the primary antibody was omitted, however the secondary antibody was applied as per the experimental slides. Slides were removed from 4 °C and washed 3 x 5 min in PHEM. All subsequent stages were carried out in the dark to prevent photobleaching of the fluorophores. Secondary antibodies were applied for 90 min followed by 12 x 10 min washes in PHEM. Slides were mounted with glass coverslips using mounting medium containing DAPI (Vectashield®, Hard Set™, Vector Laboratories, UK) and fixed with clear varnish. Slides were stored at 4 °C until required for analysis by confocal microscopy.

For double immunostaining of slides, the procedure above was followed i.e. one primary antibody was incubated at 4 °C overnight, followed by 3 x 5 min PHEM washes the next day. The slides were then incubated on the subsequent night with the second primary antibody of interest. On the third day, the slides were washed 3 x 5 min PHEM washes and incubated in a mixture of the relevant secondary antibodies for 2 h. Slides were then washed 12 x 10 min washes in PHEM, mounted and visualised as described above.

2.7. Polyacrylamide gel electrophoresis and Western immunoblotting

2.7.1. Sample preparation

Sample buffer (4X; 150mM Tris-HCl, pH 6.8; glycerol 10% w/v; sodium dodecylsulfate 4% w/v; β-mercaptoethanol (β-Me), 5% w/v; bromophenol blue, pinch) was added to tissue samples, equalised for protein concentration (see methods section 2.3). Aliquots of tissue samples were heated at 80°C for 5 min before loading onto separating acrylamide gels (tris-glycine) of varying percentages (see Table 2.1). The molecular weight protein markers Sea blue (Precision Plus Protein™ Standards, BioRad, UK) and Dual Colour Marker (MagicMark™ XP, Invitrogen, UK) were loaded (5 µl) into the end lanes of each gel.

Ingredients for one gel	Percentage gel			
	7%	**10%**	**12%**	**15%**
30% acrylamide	2.3ml	3.3ml	4ml	5ml
d.H_2O	5.1ml	4.1ml	3.4ml	2.4ml
Separating gel buffer	2.5ml	2.5ml	2.5ml	2.5ml
10% APS	100µl	100µl	100µl	100µl
TEMED	5µl	5µl	5µl	5µl

APS – ammonium persulfate (facillitates polymerisation and cross linking of acrylamide

TEMED- tetramethylethylenediamene (catalyses the polymerisation of acrylamide by the ammonium persulfate)

Separating gel buffer- ingredients listed in appendix

Table 2.1: Recipe for the varying the percentage acrylamide gels used for polyacrylamide gel electrophoresis.

2.7.2. Gel electrophoresis

Proteins were separated according to their molecular weight by application of 80-110V across the acrylamide gel for 90-120min in a tank, containing electrode-running buffer (25mM Tris-Base, 192mM glycine, 0.1% SDS; BioRad PowerPack™system). Gels were subsequently transferred to 0.2µm or 0.45µm nitrocellulose membranes (Whatman®, Protran®, Germany) using a transfer buffer (dH_2O, 25mM Tris-base, 192mM glycine, 20% v/v methanol) at 70 V for 70 min or 25 V overnight (detailed in Table 2.2). Efficiency of protein transfer was confirmed by washing the nitrocellulose membrane in ponceau-S for 5 min (Sigma Aldrich, UK).

2.7.3. Protein immunoblotting

After transfer, non-specific binding sites were blocked in BSA or 5% non-fat milk in TBS containing 0.05% Tween (TBS-T). Nitrocellulose membranes were incubated in primary antibody in 1% non-fat milk in TBS-T, overnight at 4 °C. Primary antibody was washed in TBS-T (3 x 5 min) followed by incubation in the appropriate secondary antibody (Jackson ImmunoResearch, USA) at a dilution of 1:5000 in 1% milk for 2hr at room temperature. Secondary antibody was washed off with TBS-T (5 x 5 min) and immunoreactive bands were detected with enhanced chemiluminescence using ECL substrate (Imobilon™ Western Chemiluminescence Substrate, Milipore, USA).

To account for equal protein loading, membranes were normalised to either β-actin or GAPDH. Membranes were stripped (Re-Blot Plus Strong Solution, Chemicon, USA) for 10 min, washed in TBS-T (3 x 5 min) and re-probed with anti-β-actin antibody (1:5000; Sigma Aldrich, UK) or GAPDH (1:2500; Abcam) in 1% non-fat milk/TBS-T for 2 h at room temperature. Membranes were washed in TBS-T (3 x 5 min) and incubated in the appropriate secondary antibody. Again, immunoreactive bands were detected using ECL as outlined above. Following ECL detection of immunoreactive bands, densitometric analysis was carried out using Image J software (ImageJ-64). Statistical analysis and graphing of the data was carried out using GraphPad Prism 5. The specific details pertaining to each target is outlined below, in Table 2.2.

Target	**MW (kDa)**	**% gel**	**Transfer conditions**	**Nitrocellulose pore size (μm)**	**Antibody Dilution**	**Source; catalogue number**
α-smooth muscle actin	37	12	70V 70min	0.2	1:400	Abcam; Ab-7817
Albumin	65	10	30V o/n	0.2	1:5000 (cortex) 1:10000 (plasma)	Alpha Diagnostic International; ALBR-12-A
β-actin	42	-	-	-	1:5000	Sigma Aldrich; A5441
Claudin-5	25	12	70V 70min	0.2	1:500	Invitrogen; 35-2500
ERK (pan)	45	10	70V 70min	0.2	1:1000	Santa Cruz; sc-1647
ERK (phospho)	42-46	10	70V 70min	0.2	1:500	Santa Cruz; sc-7383
GAPDH	36	-	-	-	1:2500	Abcam; Ab8245
JNK1, 2/3 (pan)	46, 54	10	70V 70min	0.2	1:500	Cell Signaling; 9252
JNK1, 2/3 (phospho)	46, 54	10	70V 70min	0.2	1:500	Cell Signaling; 9251
IL-1R1	80	7	30V o/n	0.45	1:1000	Santa Cruz; sc-689
Laminin	220	7	30V o/n	0.45	1:5000	Sigma Aldrich; L9393
MMP-9	92	10	70V 70min	0.2	1:250	Santa Cruz; sc-6840

Target	MW (kDa)	% gel	Transfer conditions	Nitrocellulose pore size (μm)	Antibody Dilution	Source; catalogue number
Occludin	65	10	70V 70min	0.45	1:1000	Invitrogen; 71-1500
PDGFRβ	180	7	30V o/n	0.45	1:1000	Santa Cruz; sc-1627
PECAM	135	-	-	-	1:500	Santa Cruz; sc-28188
TIMP-1	28-30	12	70 V 70min	0.2	1:250	Millipore; Ab770
TLR-4	93	7	30V o/n	0.45	1:200 (1%BSA)	Abcam; Ab22048
ZO-1	220	7	30V o/n	0.45	1:1000	Millipore; MAB-T11
V = VOLTS; o/n = over night						

Table 2.2 List of primary antibodies used in Western immunoblotting

2.8. Polymerase chain reaction

2.8.1. RNA extraction

The RNA extraction hood and all pipettes were sterilised under UV light for 15 min prior to use, wiped with RNAse away™ and tissue samples were placed into RNase free tubes. RNA was isolated from tissue/cells using a commercial kit (Total RNA isolation, NucleoSpin®, RNA II, Machary-Nagel, GmbH & Co.) and procedures were followed according to the manufacturer's instructions. Briefly, tissue samples were homogenised using a sonicator (350 μl RA1 buffer, 3.5 μl β-Me). The lysate was added to NucleoSpin® filter units within collecting tubes and centrifuged (11000 *g* for 1 min). The lysate was collected and placed in a NucleoSpin® RNA II column containing 350 μl ethanol (70%) and was triturated to mix evenly. The column was placed in a 2 ml centrifuge tube and centrifuged (8000 *g* x 30 s) to bind RNA to the membrane, To dry the membrane, the flow-through was discarded, and 350μl membrane desalting buffer was added to the column, which was placed in a new collecting tube and centrifuged (11000 *g* for 1 min). Again flow-through was discarded and the column was placed in a

new collecting tube. Ninety-five microlitres of the DNase reaction mixture (10 µl DNase I, 90 µl DNAse reaction buffer) was added to the column and left for 15 min at room temperature to digest any DNA present, followed by addition of 200 µl RA2 buffer to the column and further centrifugation (8000 *g* for 30 s). The flow-through was discarded and the column placed in a new collecting tube before adding 600 µl RA3 buffer to the column and centrifuging (8000 *g* for 30 s). Again, flow-through was discarded and the column placed in a new collecting tube before adding 250 µl RA3 buffer to the column and centrifuging (11000 *g* for 2 min). The column was placed in a nuclease free 1.5 ml eppendorph tube before adding 60µl H_2O (RNAse-free) and centrifuging (11000 *g* x 1 min) to elute the RNA into the eppendorph tube. The resultant RNA was stored at -80 ^{o}C until required for quantification and cDNA synthesis.

2.8.2. Quantifying and equalising RNA

Total RNA concentrations were determined using a Nanodrop Spectrophotometer (Thermo Scientific, Inc). Briefly, 1 µl of RNase-free H_2O was added to the pedastal of the Nanodrop and the machine's readings were blanked. Following thorough mixing of RNA samples, individual samples (1 µl) were applied to the pedestal and RNA concentration was determined (ng/ml). The pedestal was cleaned with RNase-free H_2O in-between the reading of each sample in order to minimise cross-contamination. Samples were equalised to a concentration of 1mg/ml using RNase-free H_2O, in preparation for cDNA synthesis.

2.8.3. cDNA synthesis

Total RNA (1 mg) was reverse transcribed into cDNA using a high-capacity cDNA kit (Applied BioSystems) and a thermocycler (BioSciences, PTC-200). Briefly, a Mastermix (2X) was made (10x reverse transcription buffer, 25X dNTPs, 10X random primers, reverse transcriptase (50U/µl), nuclease free H_2O), and added to RNA samples in a 1:1 ratio, followed by trituration and a brief mini-centrifuge for 10 s. The samples were placed in the thermocycler at the following settings (25 °C for 10 min, 37 °C for 120 min). cDNA was stored at -20 °C until required for real- time polymerase chain reaction (next section).

2.8.4. Real- time polymerase chain reaction (RT-PCR)

Gene expression was carried out using Taqman gene expression assay kit (Applied Biosystems). Equalised cDNA samples were diluted 1:4 with nuclease-free H_2O, and samples (10 µl) were added to a 96-well plate. Fifteen microlitres of PCR mastermix (12.5 µl Taqman® universal PCR MasterMix, 1.25 µl primer of interest, 1.25µl endogenous control β-actin) was added to each well. The primers used in our study are detailed further in Table 2.3 below.

The PCR plate was covered with an adhesive cover and the plate was centrifuged (800 x rpm, 1 min). The RT-PCR amplification was carried out on a PCR plate-reader (7300 Real time PCR system, Applied BioSciences) using the appropriate software (7500 Fast System V1.3.1). Briefly the RT-PCR cycling conditions were as follows; stage 1: 50 °C for 2 min; stage 2: 95 °C for 10 min; stage 3: 95 °C for 15 s; stage 4: 60 °C for 1 min. Following a minimum of 40 cycles, along with an extension of 20 cycles where necessary, the plate was removed and the resultant data was analysed.

Target Name	**Primer code**
β-actin (rat)	4352340E
β-actin (mouse)	4352341E
Claudin-5 (rat)	Rn01753146_s1
Occludin (rat)	Rn00580064_m1
ZO-1 (rat)	Rn02116071_s1
PDGFR-β (rat)	Rn00709573_m1
α-smooth muscle actin (rat)	Rn01759928_g1

Table 2.3. List of primers used in RT-PCR

2.8.5. RT-PCR data analysis

Data was analysed using 7500 Fast System V1.1.1 software. The ΔΔCt method was used to assess gene expression for all RT-PCR analysis. This is a method whereby relative gene expression of a target in a treated group is compared to gene expression in the control group (young animals in this study). This allows for observation of "fold-changes" in expression of the target gene, rather than quantifying the gene expression itself. This "fold-change" in gene expression is assessed using the cycle time (Ct) difference between samples i.e. based on the principal that samples in which the target gene amplifies at an earlier cycle time compared with another given sample, have greater quantities of the target gene to begin with. A cycle difference of 1 (ΔCt=1) between 2 samples means a two-fold difference in gene expression. Cycle times are visualised in a linear amplification plot, and from this, an optimal baseline Ct is established i.e. when the RT-PCR reaction is in the exponential phase and optimal for efficiency.

Each sample acts as its own control, thus each samples own endogenous β-actin Ct value is subtracted from its Ct value for the given target gene. This accounts for discrepancies in cDNA quantity on the plate and is referred to as the ΔCt value. The average difference in cycle time (mean ΔCt) of control values is subtracted from the ΔCt value and this is referred to as the ΔΔCt value (i.e. the cycle time difference, corrected for β-actin and relative to the control group). To get the fold-difference in gene expression from control, the following formula is applied to all samples (2^(-ΔΔCt)), giving the fold-difference as a relative quantity (RQ). Data (RQ values) were statistically analysed and graphed using GraphPad Prism 5.

2.9 Gelatin Zymography

2.9.1. Tissue preparation

Plasma or supernatant from in vitro studies were prepared as follows: sample buffer (4x; 150mM Tris-HCL, pH6.8; glycerol 10% w/v; sodium dodecylsulfate 4% w/v; 5%w/v; bromophenol blue, pinch) were added to samples of plasma or supernatant before being loaded (10 μl) onto gelatin separating gels (see Table 2.4). The molecular weight protein markers Sea blue (Precision Plus Protein™ Standards, BioRad, UK) and

Dual Colour Marker (MagicMark™ XP, Invitrogen, UK) were loaded (5 µl) into the end lanes of each gel.

With regard to the gel electrophoresis, enzymes were separated according to their molecular weight by application of 125 V across the gelatin gel for 90-120 min in a tank containing electrode-running buffer (25mM Tris-Base, 192mM glycine, 0.1%SDS; BioRad PowerPack™system). Next the gels were digested where the gelatin gel was washed with 2.5% Triton-X 100 buffer (3 x 20 min) followed by washing with digestion buffer (2M Tris-HCl, 0.9% NaCl, 0.074% $CaCl_2$, 0.05% NaN_3, pH 7.4; 2 x 20 min). Gels were incubated overnight in digestion buffer at 37 °C and then the gel was incubated for 3 h in staining solution (25% methanol, 10% CH_3COOH, 0.025% Coomassie Blue, 65% dH_2O), which was followed by regular washes in de-staining solution (4% methanol, 8% CH_3COOH, 88% dH_2O) for 2-3 h, as required. Areas of enzymatic activity appear as clear bands of digested gel against a dark blue background. Gels are visualised using an imaging system (Odyssey Infrared Imaging system, CLx, Li-Cor) and following image acquisition, densitometric analysis was carried out using Image J software (Image-J-64).

Ingredients (one gel)	8% separating gel	Stacking gel
30% acrylamide	2ml	325µl
1.5M Tris-HCl	1.875ml	-
0.5M Tris-HCl	-	625µl
d.H_2O	2.875ml	1.5ml
Gelatin (20mg/ml containing 1% SDS)	750µl	-
10% APS	25µl	12.5µl
TEMED	5µl	2.5µl

Table 2.4 Recipe for gelatin gels used for gelatin zymography.

2.10. Enzyme-linked immunosorbent assay (ELISA)

2.10.1. Rat IL-1β ELISA

The commercially available ELISA kit for rat IL-β was used (R&D, UK) and the following protocol was followed according to manufacturer's instructions. Anti-rat IL-1β capture antibody (144 µg/ml) was diluted in PBS to a working concentration of 0.8 µg/ml, added (100 µl) to each well of a 96-well plate and incubated overnight at room temperature. Wells were washed 4 times with wash buffer (Tween-20 (0.05%) in TBS) followed by a blocking step for 2 h with block buffer (200 µl; 1% BSA in PBS, 0.05% Tween). Wells were washed 4 times with wash buffer. IL-1β standards (0-2000 pg/ml) were prepared in DMEM and duplicates (100 µl/ well) of standards and tissue samples (rat cortex, hippocampus) were added for 2 h at room temperature before washing 4 times with wash buffer. Detection antibody (biotinylated anti-rat IL-1β (63 µg/ml)) was diluted in assay diluent containing 2% normal goat serum (NGS) to give a working concentration of 350 ng/ml. Detection antibody (100 µl) was added to wells and incubated for 2 h at room temperature before washing 4 times with wash buffer. Diluted strep-HRP (2% in assay diluent) was added (100 µl) to wells and incubated for approximately 20 min in the dark before washing 4 times with wash buffer. Substrate solution (100 µl; supplied in kit) was added to wells for approximately 30 min or until colour developed, followed by addition of stop solution (50 µl; 980 µl 2M H_2SO_4, 9.02 ml dH_2O). Absorbance was read at 450 nm on a plate-reader (SynergyHT, Biotek®). The standard curve was calculated by plotting cytokine concentration of known standards against their corresponding absorbance read-out. The cytokine concentration of relevant tissue samples was then calculated from this standard curve and expressed as pg/ml on graphs.

2.10.2. Mouse pro-MMP-9 ELISA

The commercially available ELISA kit for mouse pro-MMP-9 was used (R&D systems, UK) and the following protocol was followed according to manufacturer's instructions. Anti-mouse pro-MMP-9 capture antibody (720 µg/ml) was diluted in PBS to a working concentration of 4 µg/ml and added (100 µl) to a 96-well and incubated overnight at room temperature. Wells were washed 4 times with wash buffer (Tween-20 (0.05%) in TBS) followed by a 2 h blocking step (200 µl) with blocking buffer (1% BSA in PBS, 0.05% Tween). Wells were washed 4 times with wash buffer. Pro-MMP-9 standards (0-

20 000 pg/ml) were prepared with DMEM and duplicates (100 µl/ well) of standards and samples (organotypic hippocampal slices) were added for 2 h at room temperature before washing 4 times with wash buffer. Detection antibody (biotinylated rat anti-mouse pro-MMP-9 (45 µg/ml)) was diluted in assay diluent (50mM Tris HCl, 10mM $CaCl_2$, 0.15M NaCl, 0.05% Tween, pH 7.45) to give a working concentration of 250 ng/ml. Detection antibody (100 µl) was added to wells and incubated for 2 h at room temperature before washing 4 times with wash buffer. Diluted strep-HRP (2% in assay diluent) was added (100 µl) to wells and incubated for approximately 20 min in the dark before washing 4 times with wash buffer. Substrate solution (100 µl; supplied in kit) was added to wells for approximately 30 mins or until colour developed followed by addition of stop solution (50 µl; 980 µl 2M H_2SO_4, 9.02 ml dH_2O). Absorbance was read at 450 nm on a plate-reader (SynergyHT, Biotek®). The standard curve was calculated by plotting cytokine concentration of known standards against their corresponding absorbance read-out. The cytokine concentration of samples was then calculated from this standard curve and expressed as pg/ml on graphs.

2.10.3. Rat pro-TIMP-1 ELISA

The commercially available ELISA kit for rat pro-TIMP-1 was used (R&D systems, UK) and the following protocol was followed according to manufacturer's instructions. Anti-rat pro-TIMP-1 capture antibody (360 µg/ml) was diluted in PBS to a working concentration of 2 µg/ml and added (100 µl) to a 96-well plate and incubated overnight at room temperature. Wells were washed 4 times with wash buffer (Tween-20 (0.05%) in TBS) followed by a blocking step for 2 h with blocking buffer (200µl; 1% BSA in PBS, 0.05% Tween). Wells were washed 4 times with wash buffer. Pro-TIMP-1 standards (0-2000 pg/ml) were prepared with 1% BSA in PBS and duplicates of standards and samples (serum, diluted 1:5 with PBS) were added (100 µl) for 2 h at room temperature before washing 4 times with wash buffer. Detection antibody (biotinylated goat anti-rat pro-TIMP-1 (9 µg/ml)) was diluted in assay diluent (1% BSA in PBS, pH 7.2-7.4) to give a working concentration of 50 ng/ml. Detection antibody (100 µl) was added to wells and incubated for 2 h at room temperature before washing 4 times with wash buffer. Diluted strep-HRP (2% in assay diluent) was added (100 µl) to wells and incubated for approximately 20 min in the dark before washing 4 times with wash buffer. Substrate solution (100 µl; supplied in kit) was added to wells for approximately 30 min or until colour developed, followed by addition of stop solution

(50 µl; 980µl 2M H_2SO_4, 9.02ml dH_2O). Absorbance was read at 450nm on a plate-reader (SynergyHT, Biotek®). The standard curve was calculated by plotting cytokine concentration of known standards against their corresponding absorbance read-out. The enzyme concentration of samples was then calculated from this standard curve and expressed as pg/ml on graphs.

2.11. Cell culture

The following procedures were carried out under sterile conditions using the aseptic technique. The culture hoods and equipment were sterilised under UV light prior to spraying with 70% ethanol and the dissecting tools were sterilised by oven-baking them at 200 °C prior to use. The distilled water was autoclaved and all solutions were filter sterilised prior to use.

Note: The following cell culture methods (2.11.1 and 2.11.2) describe the general procedures undertaken for all *in vitro* experiments carried out using the bEnd.3 cell line. Specific information with regard to individual experiments will be detailed separately due to the progressive characterisation of treating bEnd.3 that occurred during the course of this research.

2.11.1. Seeding and re-plating the bEnd.3 cell line

Aliquots of mouse-brain derived cortical endothelial cell line (bEnd.3; American Type Culture Collection; USA) were removed from liquid nitrogen storage where they had been stored in cell freezing media (50% Dulbeco's Modified Eagle Media, (DMEM), Sigma Aldrich, UK; 40% fetal bovine serum, (FBS), Gibco, UK; and 10% dimethyl sulfoxide, (DMSO), Sigma, UK). Cells (passage 3-5) were rapidly thawed in a 37 °C water bath and placed into 50 ml ice-cold sterilised DMEM, supplemented with penicillin (100 µl/ml; Gibco, UK), streptomycin (100 µl/ml; Gibco, UK), FBS (10% w/v), and GlutaMAX (100 µl/ml; Gibco, UK). Cells were centrifuged (1200 rpm for 5 min at 4 °C) to remove DMSO before the cell pellet was re-suspended in warm DMEM, which was again centrifuged (1200 rpm for 5 min at 20 °C). This media was removed before addition of 6 ml of warm DMEM. The cell pellet was gently triturated to ensure a homogeneous cell suspension, before adding 2 ml of the suspension to each well of a 6-well plate. Cells were maintained in a humidified incubator (37°C, 95 % O_2, 5 %

CO_2). Culture media was replaced every 2 days and cells were re-plated into sequentially larger flasks (T25 cm^2, T75cm^2, T175cm^2; Sarstedt, Germany) when confluent to achieve sufficient cell quantities for subsequent experiments.

The following procedures were undertaken when confluence was reached and re-plating became necessary. Culture flasks were removed from the incubator and rinsed in sterile filtered PBS (Dulbeco's phosphate buffered saline, 1X, Sigma, UK) to remove traces of culture media. Trypsin-EDTA (Invitrogen, UK) was added and incubated at 37 °C for 10-15 min before the flask was gently tapped to remove adherent cells from the surface. A light microscope (Olympus, IX-51) was used to verify that cells had been removed before the cell/trypsin suspension was added to 50 ml DMEM to stop the reaction. The cell suspension was centrifuged (1200 rpm for 5 min at 20 °C) and the media was removed, and fresh DMEM was added to the pellet, which was triturated. The cell density was determined (below) and the cells were replated in new flasks. As before, flasks were topped up with warmed DMEM culture media.

2.11.2. Cell count and plating density verification prior to treatment

Cells were collected via trypsinisation, as outlined above and a cell count was carried out when the cell pellet was re-suspended in 1ml DMEM. 20 µl of this cell suspension was added to 180 µl of trypan blue (Sigma, UK). The solution was triturated to ensure homogenization before placing into a haemocytometer (Bright-line, Hausser scientific, USA) and visualized under a light microscope. Cells were counted and equalized to a final density of either 2 x 10^5 cells/ml or 1.5 x 10^5 cells/ml. 50 µl of this suspension was plated into each well of a 24-well plate. Wells were immediately topped up with DMEM and cells were maintained in the incubator for 1-2 days, or until they had established a confluent monolayer, prior to treatment.

2.11.3. Treatment of bEnd.3 cells with either IL-1β or LPS (Figures 5.1 - 5.3).

Confluent bEnd.3 cells (passage 3-4) were plated at a density of 2 x 10^5 cells/ml in a 6-well plate (see above) and allowed to adhere for 1-2 days. On treatment day, media was removed and replaced with fresh media containing either IL-1β (10ng/ml; R&D Systems, UK) or LPS (100ng/ml; Alexis® Biochemical, Enzo Life Sciences, Switzerland) which was added to cells for 1, 3, 6, 12 and 24 hours before harvesting.

Reproducing the initial IL-1β- and LPS-mediated effects proved to be challenging and as such, the subsequent *in vitro* experiments on bEnd.3 cells evolved into a characterisation of the treatment conditions that might affect results. In our initial attempt to replicate the timecourse experiments (IL-1β and LPS decrease TJ concentration, see results section 5.3), the Western immunoblotting results varied tremendously at each time point, so much so that we carried out parallel experiments with IL-1β from 2 different companies – but the cellular response to both reagents was comparable (see Appendix 8). We then set out to establish the optimal culturing parameters that would guarantee reproducible IL-1β- or LPS-mediated effects on tight junction protein expression as observed in section 5.3. Outlined in the following sections are the treatment conditions employed when treating bEnd.3 with IL-1β and the effect the impact they had on the outcome of an experiment, particularly the effect of a media change on TJ. Results from these experiments are outlined in Chapter 5.

2.11.4. Treatment of bEnd.3 cells with Il-1β following media disruption (Figure 5.4)

bEnd.3 cells (passage 12-14) were plated at a density of 1 x 10^5 cells/ml in a 24-well plate and allowed to adhere until a confluent monolayer was formed. On treatment day, all media was removed and untreated control wells had fresh media added. Treatment wells had fresh media containing IL-1β (10ng/ml). Cells were treated for 6 hours before harvesting.

2.11.5. Treatment of bEnd.3 cells with IL-1β and minimal media disruption (Figure 5.5)

bEnd.3 cells (passage 8-10) were plated at a density of 1 x 10^5 cells/ml in a 24-well plate and allowed to adhere until a confluent monolayer was formed. On treatment day, a fraction of media was removed and this was used to prepare the IL-1β treatment. IL-1β was applied to wells as a 10X treatment, to a final concentration of 10ng/ml in the well. Untreated cells (controls) had the same volume removed as the treated cells, but fresh media (rather than IL-1β treatment) was added instead. Cells were treated for 3- 6 hours before harvesting.

2.11.6. Treatment of bEnd.3 cells with IL-1β following media disruption (Figures 5.6, 5.7)

Twenty-four well plates were coated with fibronectin from bovine plasma (4μg/ml in PBS, 37 °C, Sigma, UK) for a minimum of 2 h prior to cell plating. Fibronectin was removed and wells were rinsed with sterile PBS and allowed to air-dry. bEnd.3 cells (passage 5-7) were plated at a density of 1 x 10^5 cells/ml in a 24-well plate and allowed to adhere until a confluent monolayer was formed. On treatment day, a fraction of media was removed and this was used to make up the IL-1β treatment mix. IL-1β was applied to wells as a 10X treatment to a final concentration of 10ng/ml in the well. Untreated cells (controls) had the same volume removed as the treated cells, but fresh media (rather than IL-1β treatment) was added instead. Cells were treated for up to 48 hours before harvesting.

2.11.7. Treatment of bEnd.3 cells with IL-1β in serum-starved cells (Figure 5.8)

24-wells plates were coated with fibronectin from bovine plasma (4μg/ml in PBS, 37°C, Sigma) for a minimum of 2 h prior to cell plating. Fibronectin was removed and wells were rinsed with sterile PBS and allowed to air-dry. bEnd.3 cells (passage 14-17) were plated at a density of 1 x 10^5 cells/ml in a 24-well plate and allowed to adhere until a confluent monolayer was formed. On treatment day, all media was removed from wells and cells were serum-starved for 3-4 hrs by application of serum-free culture media. IL-1β was made up as a 10X treatment in either serum-free or serum-containing fresh media to a final concentration of 10ng/ml. Untreated control wells either had serum-free or serum-containing media applied.

2.11.8. Harvesting bEnd.3 cells for analysis

When harvesting bEnd.3, culture media (supernatant) was retained from individual wells and the bEnd.3 cells were rinsed in ice-cold sterile-filtered PBS. Lysis buffer or RA1 buffer (Machery-Nagel, Germany) was added to wells for either protein or mRNA analysis, respectively. Cells were manually removed with a cell scraper and the resultant cell suspension was either collected for protein quantification (cells suspended in lysis buffer; see Section 2.3) or mRNA analysis (cells suspended in RA1 buffer and stored in RNAse-free tubes; Biosphere® Safeseal tubes, Sarstedt, Germany). All samples were stored at -20 °C until required for further analysis.

In some cases, sub-fractionation steps were carried out on cell lysate, depending on whether or not the cytosolic or membrane fractions of lysates were required. In this case, the cells were initially harvested in PBS plus inhibitors (PBS, Proteinase inhibitor cocktail I, Proteinase inhibitor cocktail II, Phosphatase inhibitor cocktail; all 1:100; Sigma). The cell suspension was centrifuged (14000 rpm, 4 °C, 5 min) to yield a supernatant containing the "cytosolic fraction" and a pellet. The pellet was then lysed in modified RIPA buffer (10mM sodium phosphate buffer, 150mM NaCl, 50mM NaF, 0.1% SDS, 1% Triton-X-100, 0.5% sodium deoxycholate, dH_2O; proteinase inhibitor cocktail I, proteinase inhibitor cocktail II, phosphatase inhibitor cocktail, all 1:100, all Sigma) and was considered the "membrane fraction".

2.12. Organotypic hippocampal slices in culture

Postnatal day 10 mice pups (C57/Bl6) were sprayed with 70% ethanol before bringing into culture hood. Mice were decapitated and brains were rapidly removed. The hippocampi from left and right hemispheres were dissected free in ice-cold slicing medium (Earle's balanced salt solution (EBSS, Gibco, UK) supplemented with 1M HEPES (2.5%)). Hippocampal slices (450μm) were prepared using a McIlwain tissue chopper. Optimal slices were chosen based on visualisation under a dissection microscope. Slices were placed on culture inserts (0.4 μm pore; 30 mm or 12mm diameter, Millicell® cell culture inserts, Millipore) where 3 slices were placed on the 30mm inserts and 1 slice was placed on the 12mm inserts, and all inserts were placed into 6- or 24-well plates, respectively. Culture inserts were placed into wells containing organotypic culture media (50% Modified eagle media ((MEM-42360) plus GlutaMax™, 25mM HEPES, Gibco, UK), 18% EBSS (Gibco, UK), 5% EBSS plus glucose (12%), 25% horse serum, penicillin (100μl/ml; Gibco, UK), streptomycin (100 μl/ml; Gibco, UK). Slices were maintained in a humidified incubator (37°C, 95% O_2, 5% CO_2) and media was replaced initially on the second day after slice preparation, and subsequently every 2 days for 10 days, until ready for treatment. When examined under the microscope, any slices with tears or excessive glial scarring were discarded and not used in any further experiments.

2.12.1. Harvesting organotypic hippocampal slices

Inserts containing organotypic hippocampal slices were removed from wells with a pipette tip and placed into eppendorf tubes containing ice-cold lysis buffer (10mM Tris-HCl; 50mM NaCl; 10mM $Na_4P_2O_7.10H_2O$; 50mM NaF; 1% NP-40; protease inhibitor cocktail containing proteinase inhibitor cocktail I, proteinase inhibitor cocktail II, phosphatase inhibitor cocktail; 1:100, all Sigma Aldrich, UK). Slices were homogenised using a sonicator (Soniprep-150, at 4 micron for 15 s). Protein concentrations of samples were measured using the BCA protein assay kit (Pierce, USA; Section 2.3).

2.12.2 Treatment of organotypic hippocampal slices

Media on organotypic hippocampal slices was changed the night before the treatment day. On the treatment day, all reagents were added as a 10X solution whereas untreated control slices received media only. Slices were treated with IL-1β (10ng/ml; RnD Systems, UK) for either 6 or 24 hours. These timepoints were chosen in an attempt to maintain consistency with other *in vitro* experiments in our research; results from a timecourse using IL-1β treated bEnd.3 cells showed that TJ protein concentration was maximally reduced at 6 hours, and had recovered by 24 hours (see Chapter 5, figure 5.1A).

In some experiments, slices were pre-treated for 1 hour with either IL-1ra (250ng/ml) or the broad spectrum MMP inhibitor, ONO-4817 (10 μM or 20 μM; Tocris Biosciences, UK) before harvesting. IL-1ra is the endogenous antagonist for the IL-1R1 and binds competitively to the receptor to prevent downstream signalling from the binding of both IL-1 ligands (IL-1α and IL-1β) (Hannum *et al.*, 1990).

The MMP inhibitor ONO-4817 is abroad spectrum MMP inhibitor and is most selective at inhibiting MMP-2 and MMP-9 (Ki = 0.73 and 2.1 nM, respectively), it is also specific for MMP-8, -12 and -13, and less so for MMP-3 and -7. It displays no action at other proteases up to a concentration of 100μM. Though there has been no research published on the treatment of endothelial cell with ONO-4817 (Tocris, UK) this broad spectrum MMP inhibitor has been used extensively on other cells types. MMP-2 and MMP-9 activities in PC14PE6 cells (highly metastatic lung tumour cells) were inhibited by a 1 hour treatment with ONO-4817 at 10uM (Shiraga *et al.*, 2002). In assessing the role of MMP activity on human fibroblasts and epithelial cells, ONO-4817 did not

affect cell proliferation at 20uM and inhibited fibroblast released MMP-2 and epithelial released MMP-9 following incubation with *P. gingivalis* (Yoshioka *et al.*, 2003). ONO-4817 (1 hour treatment) inhibited the enzymatic activity of MMP-2 produced by murine renal cell carcinoma cells in a concentration-dependent manner up to 10uM (Muraishi *et al.*, 2001). Additional information on the role of MMP and their associated inhibitors has been summarised by Medina &Radomski (2006).

Following treatements of organotypic slices, the protein concentration was determined and equalised (Section 2.3) and protein expression was determined by western immunoblotting (Section 2.7). In addition, MMP activity in supernatant from organotypic slices was assessed by gelatin zymography (Section 2.9).

2.13 Statistical Analysis

All data is expressed as mean ± standard error of the means (SEM). A student's *t*-test (two-tailed) for independent means, or a one-way or two-way analysis of variance (ANOVA) was performed as appropriate. When one- or two-way ANOVA analysis indicated that significant differences existed ($p<0.05$), Newman-Keuls or Bonferroni *post-hoc* tests were applied, respectively, to the data to establish between which groups the significance lay. All statistical analyses were performed using GraphPad Prism software, version 5.0c (GraphPad software Inc., USA).

Chapter 3

Age-related changes in blood-brain barrier permeability and neurovascular unit integrity.

3.1 Introduction

The occurrence of the tight-junction proteins claudin-5, occludin and ZO-1 between adjacent endothelial cells of cerebral capillaries forms the primary barrier to the paracellular movement of blood-borne substances into the brain. Other cell types in close anatomical proximity to the endothelial cells contribute to BBB functionality and these include astrocytes, neurons, pericytes, basal lamina and extracellular matrix; collectively referred to as the "neurovascular unit" (NVU).

This blood-brain barrier (BBB) is vital to keep potentially harmful plasma substances out of the brain and maintain homeostasis. The ageing brain is associated with a progressive decline in cognitive function and it has been hypothesised that the BBB may become altered in the senescent brain, thus augmenting neuronal damage and contributing to age-related cognitive deficits (Ueno *et al.*, 2001; Farrall & Wardlaw, 2009). An impaired BBB would likely facilitate the entry of neurotoxins into brain parenchyma and primarily cause or potentially exacerbate age-related tissue damage. Incoming neurotoxins in turn might act in a causative or secondary role in the pathogenesis of age-related neurodegenerative disorders e.g. AD. In support of this hypothesis evidence of circulating plasma components e.g. serum albumin, has been reported in the cerebral parenchyma of aged animals (Shah & Mooradian, 1997; Pelegri *et al.*, 2007) thus providing evidence for an age-related disruption of the BBB. It is possible that the TJ proteins themselves (claudins, occludin, and TJ plaque proteins) are altered with age. One particular study comparing the expression levels of occludin and ZO-1 in young and aged rats aged 3-, 12- and 24-months revealed age-related changes at the protein and mRNA level in these crucial BBB proteins (Mooradian *et al.*, 2003). It has also been shown that disrupting the basal lamina via bacterial collagenase causes increased BBB permeability in the rat (Rosenberg *et al.*, 1993) and injecting mice intraperitoneally with lipopolysaccharide (LPS) causes disintegration of the basal lamina, also leading to increased paracellular permeability at the BBB (Nishioku *et al.*, 2009). Matrix metalloproteinases -2 and-9 are known modulators of the NVU; MMP-9 mediated the disruption of laminin following focal ischemia in mice (Gu *et al.*, 2005). They are also capable of degrading tight junctions themselves as demonstrated when a broad scale MMP inhibitor prevented the TJ degradation caused by middle cerebral artery occlusion (Yang *et al.*, 2007). They have also been implicated in altering BBB permeability in AD (Candiello *et al.*, 2010). Considering the critical role that the tight

junction proteins and the NVU play in establishing and maintaining BBB functionality, and the limited amount of research on these proteins in the context of normal physiological ageing, further investigation was merited.

The aims of this chapter were:

1. To assess the functional integrity of the ageing blood-brain barrier.
2. To assess the structural integrity of tight junction proteins and the neurovascular unit at the ageing blood-brain barrier.
3. To assess matrix metalloproteinase activity with age.

3.2 Methods

3.2.1 Tissue samples

Rat brain tissue was acquired from:

- Eight young (4-6 month) and 9 aged (22-24 month) male Wistar rats which were anaesthetized with propofol or isofluorane, and administered a tail vein injection of 0.9% saline solution containing 0.02g/ml sodium fluorescein (MW 376 Da) 10 min before being sacrificed. Two animals from each age group did not receive an injection of sodium fluorescein and represented negative controls (see section 2.1.1).

Serum was acquired from:

- young (6 month) and aged (25-29 month) male Wistar rats (see section 2.1.4),
- young (21-23 years), middle-aged (52-57 years) and aged (64-70 years) healthy human subjects (see section 2.2.1),
- young (21-23 years), subjects with Alzheimer's disease (55-80 years) and their carers (65-80 years) (see section 2.2.2).

3.2.2 Experimental procedures

The experimental procedures carried out in this chapter are detailed in Chapter 2 where the following techniques are further described: protein assay (section 2.3), brain capillary separation (section 2.4), sodium fluorescein permeability (section 2.5), immunohistochemistry (section 2.6), Western immunoblotting (section 2.7), polymerase chain reaction (section 2.8), gelatin zymography (section 2.9) and ELISA (section 2.10).

All data is presented as mean ± SEM. Western immunoblotting data is presented as arbitrary values, not actual pixel values. For consistency, the mean data for control groups was normalised to a value of one, and relevant comparison groups are presented relative to this. Data was analysed by Student's *t*-test (two-tailed), and one-way ANOVA followed by *post-hoc* Newman Keuls tests to determine significance.

3.3 Localising the anatomical areas of interest of the rat brain with the nuclear stain, DAPI

For all immunohistochemical analyses, slides were mounted using medium containing DAPI (Vectashield®, Hard Set™, H-1500, Vector Laboratories, Inc. CA). This nuclear stain was used to locate anatomical regions of interest; dentate gyrus, hippocampus, parietal cortex and frontal cortex [Figure 3.1]. Examining the pattern of DAPI staining with a confocal microscope ensured that the same four anatomical areas were assessed in every slide, for all animals.

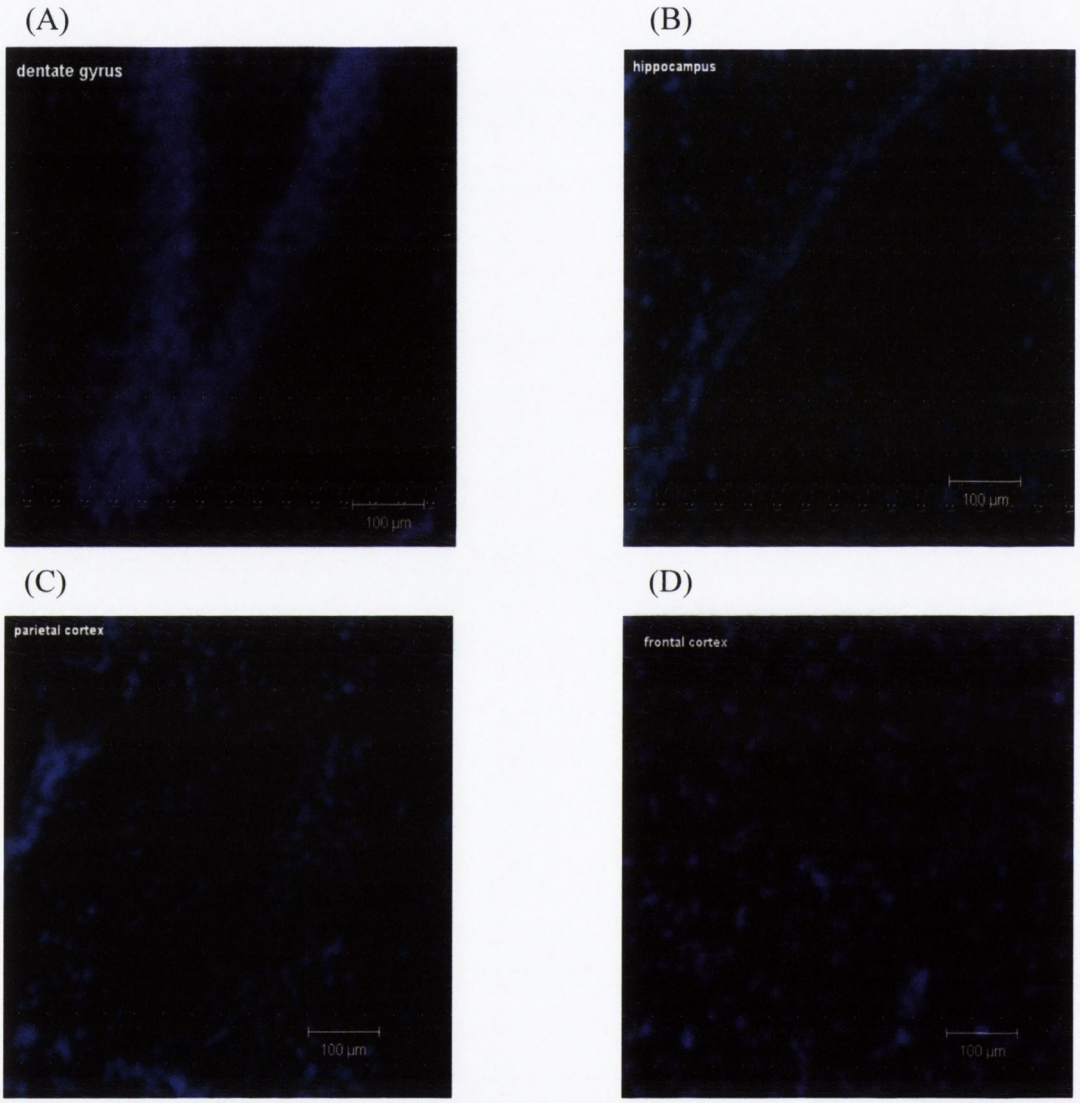

Figure 3.1: Illustration of anatomical brain regions examined in immunohistochemical studies.

The nuclear stain DAPI was used to locate the dentate gyrus (A), hippocampus (B), parietal cortex (C) and frontal cortex (D).

3.4 Capillary separation from brain parenchyma

When assessing extravasation of blood-borne substances into brain parenchyma, it is desirable to have capillaries separated from the brain parenchyma to ensure any blood-borne substance found in parenchyma is due to its extravasation from the capillaries, and not due to the substances remaining within. The young and aged Wistar rats used in this study were not perfused with saline before sacrifice, so capillary isolation from brain homogenate was attempted using enzymatic dissociation and density centrifugation (see section 2.4). Claudin-5 and PECAM are endothelial-cell specific markers and positive staining for these in the "capillary fraction" but not the "homogenate" via Western immunoblotting, indicates adequate capillary separation. Separated capillary and cortical fractions from previously frozen tissue from both young and aged rats were loaded alternately and western immunoblotting was carried out. The resulting immunoblot [see appendix 1.A] clearly shows that claudin-5 was observed predominantly in cortical rather than capillary fractions indicating inadequate capillary separation. However, when the capillary separation technique was repeated on fresh brain homogenate from mice, rather than frozen tissue, successful capillary separation was achieved [see appendix 1.B] indicating the technique is best applied to fresh rather than frozen tissue. This result precluded the use of the capillary separation technique on the frozen young and aged rat tissue.

3.5 Investigating blood-brain barrier integrity by assessing paracellular permeability

The ability of exogenous and endogenous compounds of varying molecular weights to cross the blood-brain barrier (BBB) was used as a measure of BBB permeability. Both exogenous sodium fluorescein (376 Da) and endogenous plasma albumin (65 kDa) are too large to cross the BBB and should not normally be detectable in the brain parenchyma of animals with a functionally intact BBB. The extravasation of exogenous sodium fluorescein and endogenous albumin to the brain parenchyma was assessed below.

3.5.1 Basal background fluorescence in untreated animals

Two young and two aged Wistar rats did not receive a sodium fluorescein injection and were used as negative controls. Figure 3.2 shows micrographs representing the negative controls for young (A) and aged (B) frontal cortices in those animals. Some unexpected

background fluorescence was observed in micrographs from aged (B) compared to young (A) rats (see orange circles on micrograph).

(A)

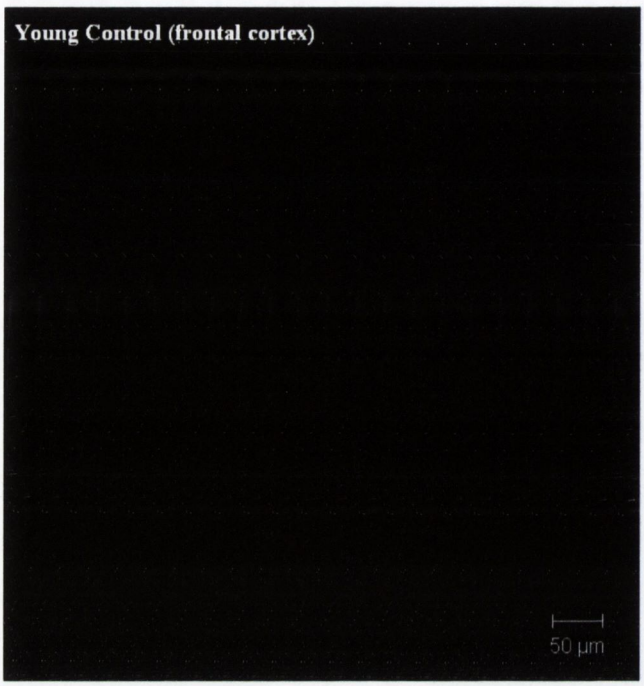

(B)

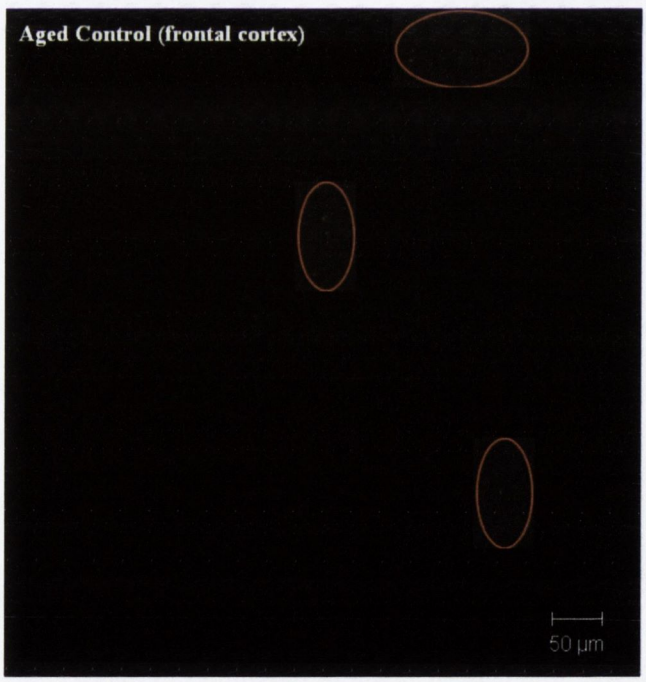

Figure 3.2: Micrographs representing the frontal cortices from young (A) and aged (B) rats that did not receive a sodium fluorescein injection (negative controls).

The orange circles (B) indicate unexpected fluorescence observed in aged animals.

3.5.2 Sodium fluorescein extravasation in young and aged animals

There was no observable fluorescence in the brain parenchyma of young animals in any of the four anatomical brain regions examined (dentate gyrus, hippocampus, parietal cortex, frontal cortex). Figure 3.3 shows a micrograph from the hippocampus of a young animal (A), which is representative of the absence of any fluorescence in the young cohort. Micrographs B to F are representative of the increased fluorescence observed in the brain parenchyma of all aged animals, in all four anatomical regions. Sodium fluorescein clearly extravasated into the brain parenchyma of the aged brains when compared to the young brains (B-F versus A). Of the aged rats, one animal in particular was older (28 month) than the other animals in that group (22-24 month) and the fluorescence was further increased in the parenchyma of this 28-month old aged rat (F).

Cryosections from sodium fluorescein injected young and aged animals were assessed by confocal microscopy. Semi-quantitative analyses of the mean fluorescence intensity from four anatomical areas was measured from three slides from each young and aged animal. There was a significant increase in the mean fluorescence intensity in all anatomical areas of aged compared to young brains [Figure 3.4, A-D]. More specifically the mean fluorescence intensity was increased in aged versus young animals in the dentate gyrus (323.60 ± 25.58 vs 1116 ± 141; *** $p<0.001$; Student's *t*-test; n=7), hippocampus (325.70 ± 24.31 vs 1104 ± 122.5; ***$p<0.001$; Student's *t*-test, n=7), parietal cortex (293.20 ± 15.12 vs 1096 ± 129.1; ***$p<0.001$; Student's *t*-test, n=7), frontal cortex (451.80 ± 50.75 vs 1059 ± 173.4; **$p<0.01$; Student's *t*-test, n=6).

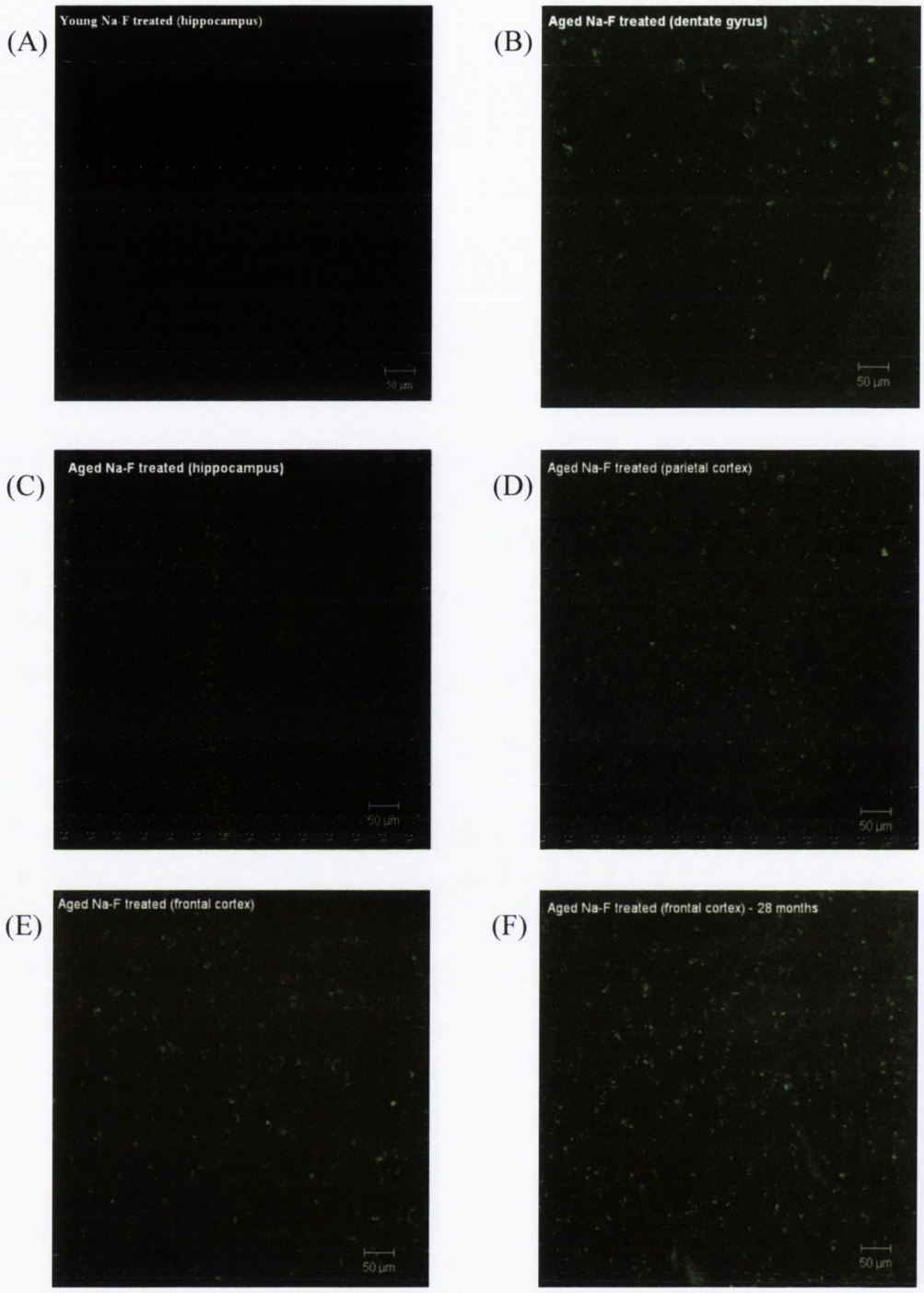

Figure 3.3: Micrographs from young and aged rats injected with sodium fluorescein.

Micrograph A illustrates the hippocampus from a sodium fluorescein (Na-F) injected young animal and is representative of all anatomical areas examined from the Na-F injected young animals. Micrographs B-F are representative of the increased fluorescence observed all anatomical areas in aged animals which was further increased in the 28-month old rat brain (F).

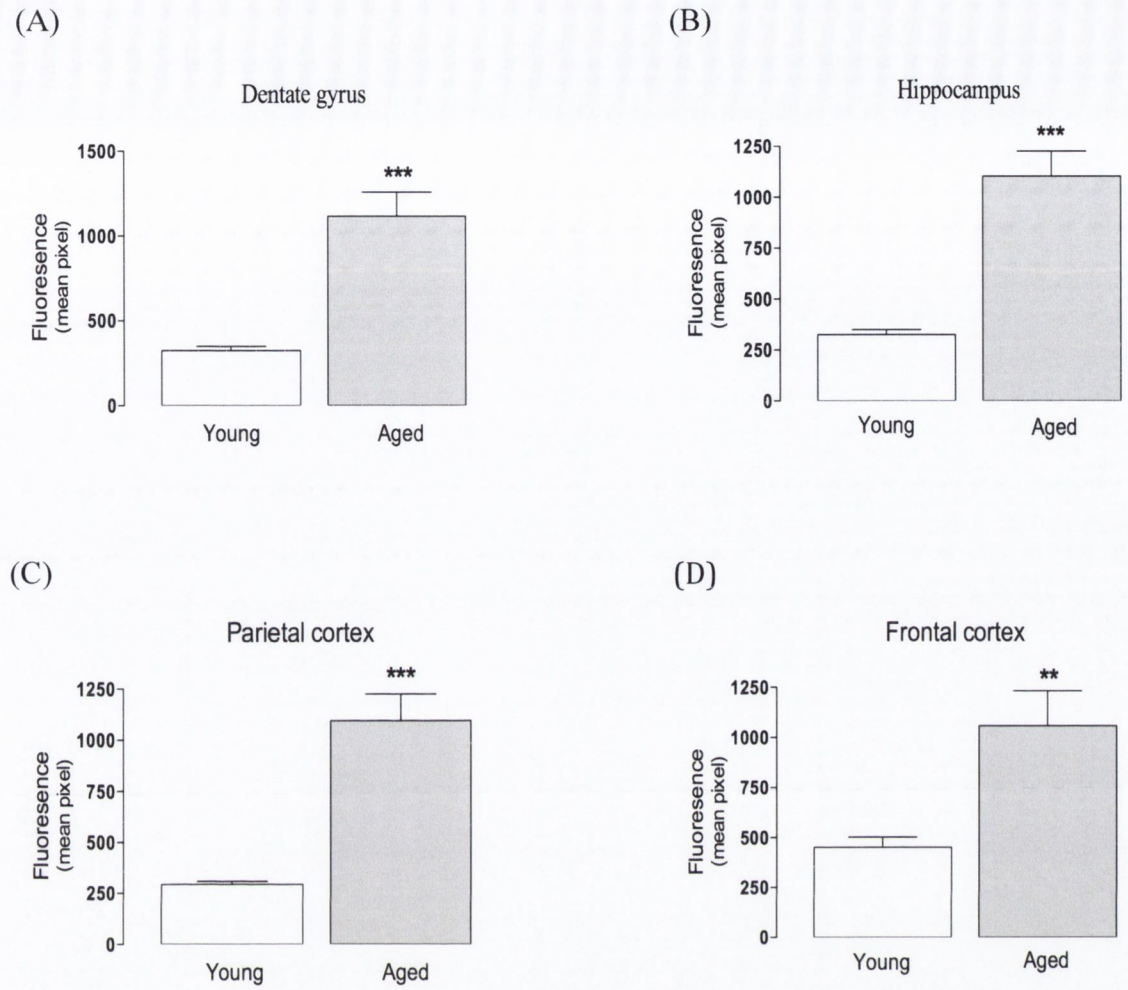

Figure 3.4: Sodium fluorescein extravasation in young and aged rats.

Semi-quantitative analysis of brain micrographs revealed a significant increase in the mean fluorescence intensity in all anatomical regions (A-D) in aged compared to young animals. Data expressed as mean ± SEM, n=6-7; ***$p<0.001$, **$p<0.01$; Student's *t*-test.

The micrograph (F) in Figure 3.3 indicated that there was considerably increased sodium fluorescein extravasation across the BBB of the oldest animal, aged 28 months. Quantitative analysis of images acquired from this animal indicated that this animal had the highest fluorescence values of all the aged animals for each brain region examined (see table 3.1, animal A4).

Animal Identity	Dentate gyrus	Hippocampus	Parietal cortex	Frontal cortex
A3	1024.16	1077.23	887.47	1025.98
A4	**1562.22**	**1477.65**	**1611.68**	**1742.83**
A5	1137.70	1205.85	1312.44	882.84
A6	1516.18	1414.85	1368.23	1620.75
A7	1276.16	1182.93	1024.37	756.57
A8	601.34	575.47	708.76	484.39
A9	696.54	792.16	757.47	898.51

Table 3.1*:* Mean fluorescent intensity values for aged animals administered sodium fluorescein. Of the aged cohort, animals A3 and A5 to A9 ranged in age between 22-24 months whereas animal A4 was 28 months old (red) and had the highest mean fluorescence intensity values in all four anatomical areas.

3.5.3 Albumin protein concentration in young and aged rat plasma and brain tissue

Endogenous albumin (65 kDa) protein concentration was assessed in serum, hippocampal and cortical tissue by Western immunoblotting [Figure 3.5]. There was no difference in the albumin protein concentration when the serum from young and aged rats was compared (A; 1 ± 0.092 vs 1.085 ± 0.051; Student's *t*-test; n=6-7). There was a significant increase in albumin protein concentration in the aged, compared to young cortex (B; 1 ± 0.089 vs 1.381 ± 0.123; *$p<0.05$; Student's *t*-test, n=6) though there was no age-related increase in the hippocampus (C; 1 ± 0.066 vs 0.920 ± 0.054; Student's *t*-test; n=6-8).

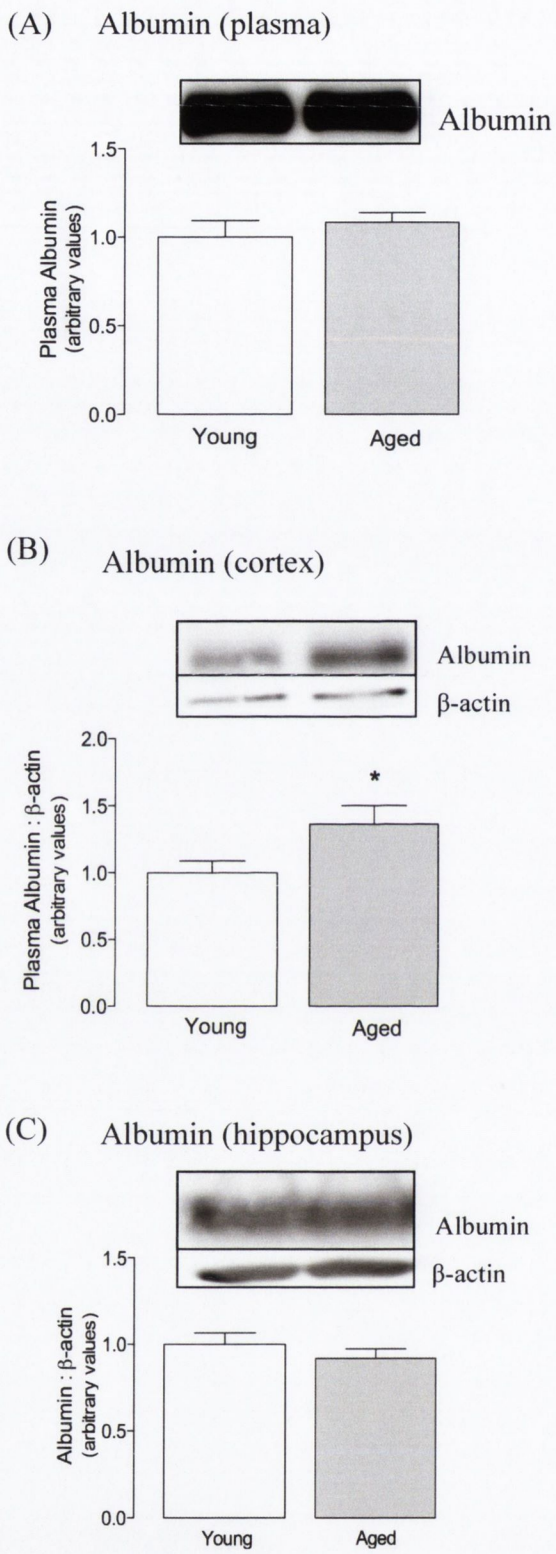

Figure 3.5: Albumin protein concentration was significantly increased in the aged rat cortex.

Albumin protein concentration was significantly increased in the aged, compared to young cortex (B) though there were no aged-related differences in serum (A) or hippocampus (C). Data expressed as mean ± SEM, n=6-8; *$p<0.05$; Student's *t*-test.

3.6 Assessment of tight junction integrity at the ageing blood-brain barrier

The tight junction proteins claudin-5 and occludin and the scaffolding protein ZO-1 are the main proteins involved in forming a tight seal between adjacent endothelial cells of brain capillaries. This "barrier" property of the BBB, which limits paracellular substance flux between adjacent endothelial cells, acts to protect the brain from potential neurotoxins. Changes in tight junction expression, particularly with age, could lead to increases in BBB permeability and may be the underlying cause of the age-related BBB dysfunction, as evidenced by extravasation of sodium fluorescein and albumin in the aged brain. As such, both protein concentration and mRNA expression of tight junctions were assessed in order to establish if disruption to TJ was occurring as a result of degradation (protein level) or due to downregulation of expression (mRNA level).

3.6.1 PECAM concentration in cortex and hippocampus of young and aged animals

It was important to first establish if there were any age-related differences in endothelial cell number before tight junction protein concentration levels were assessed. The endothelial cell marker, platelet endothelial cell adhesion molecule (PECAM, CD31) was quantified in cortical and hippocampal tissue from young and aged rats [Figure 3.6]. There were no significant differences in PECAM protein concentration in cortex (A; 1 ± 0.162 vs 0.905 ± 0.108; Student's *t*-test; n=7) or hippocampus (B; 1 ± 0.088 vs 1.089 ± 0.098; Student's *t*-test; n=7) from both age groups.

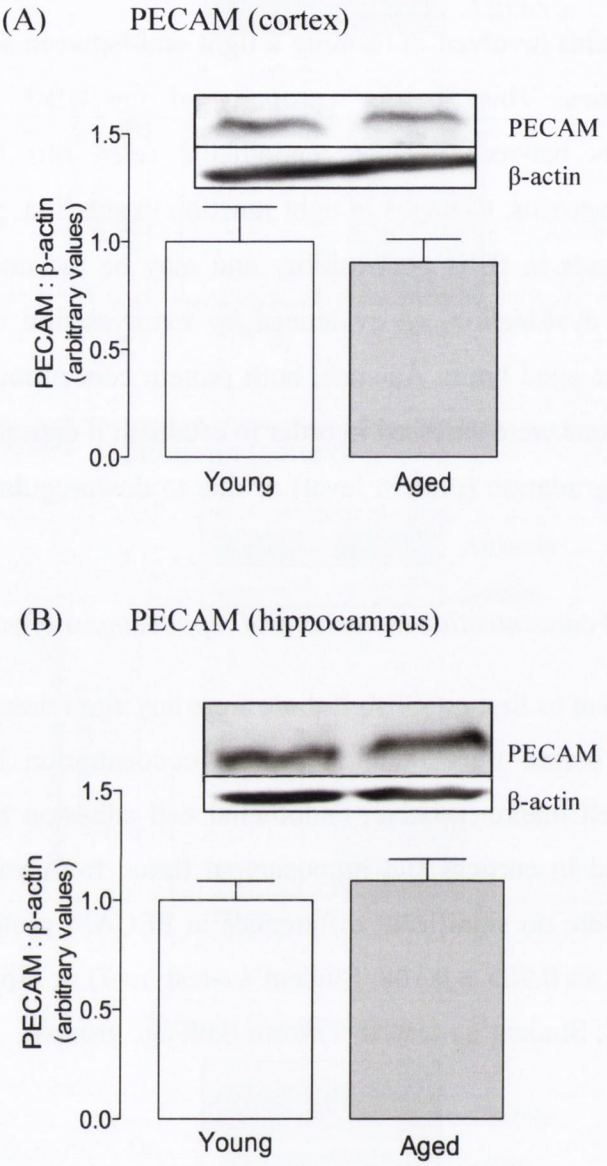

Figure 3.6: PECAM concentration was unchanged in cortex and hippocampus of young and aged rats.

There were no significant differences in concentration levels of PECAM between young and aged rats in cortex (A) or hippocampus (B). Data expressed as mean ± SEM, n=7; Student's *t*-test.

3.6.2 Claudin-5 changes in cortex and hippocampus of young and aged animals

Claudin-5 protein concentration and mRNA expression in cortical and hippocampal tissue was quantified by Western immunoblotting and qPCR respectively [Figure 3.7]. There were significant decreases in claudin-5 protein concentration in both the aged cortex (A; 1± 0.119 vs 0.365 ± 0.071; **p<0.01; Student's *t*-test; n=6-7) and hippocampus (B; 1 ± 0.165 vs 0.443 ± 0.127; *p<0.05; Student's *t*-test; n=6-7) when compared with young animals. This age-related decrease in claudin-5 protein concentration was not replicated at the mRNA expression level in either the cortex (C; 1 ± 0.229 vs 1.478 ± 0.289; Student's *t*-test; n=7-9) or hippocampus (D; 1 ± 0.161 vs 1.237 ± 0.242; Student's *t*-test; n=7-9).

3.6.3 Occludin changes in cortex and hippocampus of young and aged animals

Occludin protein concentration and mRNA expression in cortical and hippocampal tissue was quantified by Western immunoblotting and qPCR respectively [Figure 3.8]. There were significant decreases in occludin protein concentration in both the aged cortex (A; 1 ± 0.063 vs 0.687 ± 0.069; **p<0.01; Student's *t*-test; n=8) and hippocampus (B; 1 ± 0.061 vs 0.704 ± 0.078; *p<0.05; Student's *t*-test; n=8-9) when compared with young animals. This age-related decrease in occludin protein concentration was not replicated at the mRNA expression level in either the cortex (C; 1 ± 1.888 vs 1.079 ± 0.121; Student's *t*-test; n=7-8) or hippocampus (D; 1 ± 0.081 vs 1.355 ± 0.182; Student's *t*-test; n=7-8).

3.6.4 ZO-1 changes in cortex and hippocampus of young and aged animals

ZO-1 protein concentration and mRNA expression in cortical and hippocampal tissue was quantified by Western immunoblotting and qPCR respectively [Figure 3.9]. There were no significant changes in ZO-1 protein concentration between young and aged animals in cortex (A; 1 ± 0.073 vs 1.139 ± 0.095; Student's *t*-test; n=8-9) and hippocampus (B; 1 ± 0.168 vs 1.373 ± 0.354; Student's *t*-test; n=7-8). However, there were significant increases in ZO-1 mRNA expression with age, in both the cortex (C; 1

± 0.078 vs 2.423 ± 0.012; ***p<0.001; Student's *t*-test; n=6-8) and hippocampus (D; 1 ± 0.095 vs 2.550 ± 0.250; ***p<0.001; Student's *t*-test; n=6-8).

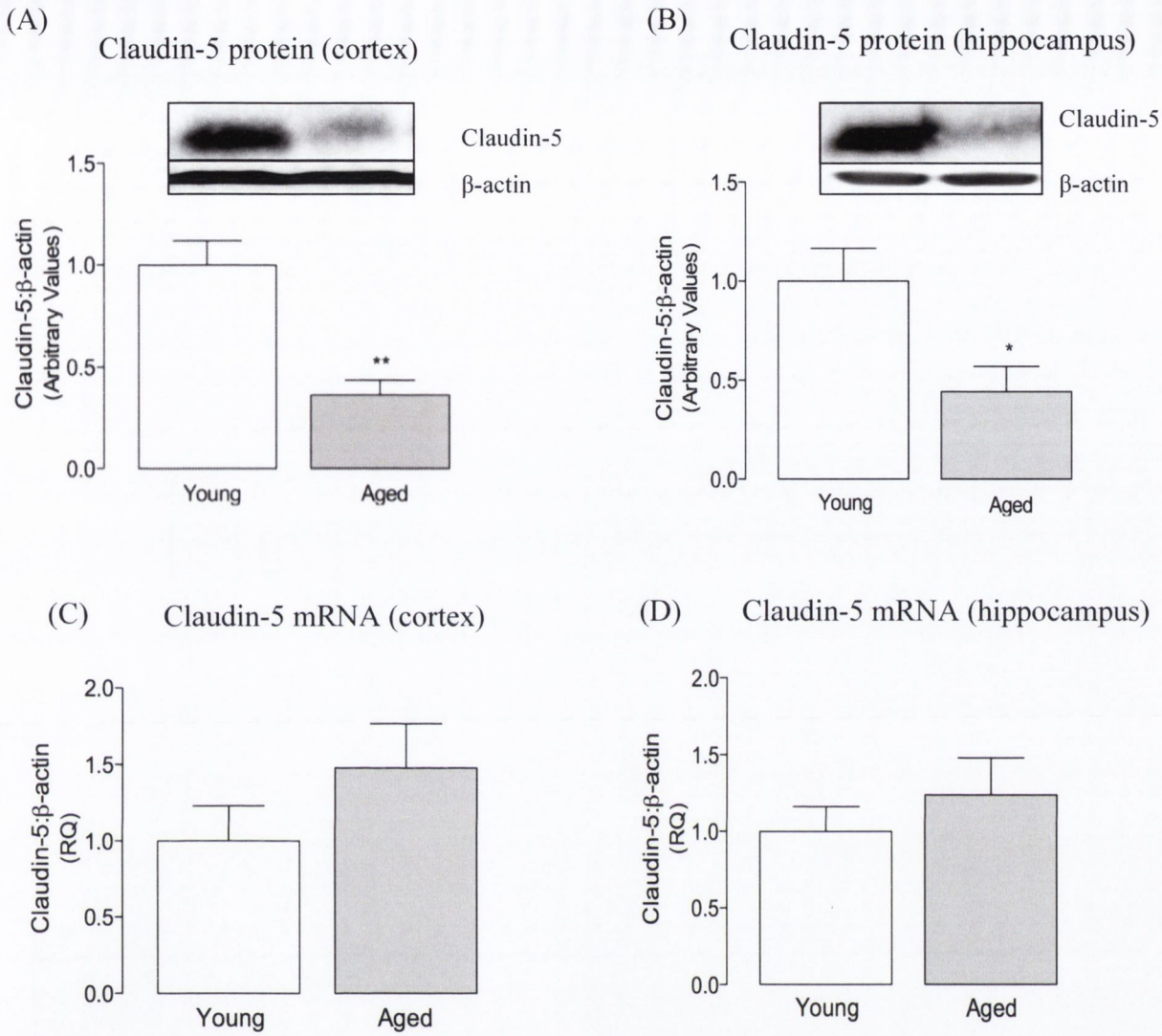

Figure 3.7: Claudin-5 protein concentration was decreased in the aged cortex and hippocampus.

There were significant decreases in the protein concentration of claudin-5 in the aged cortex (A) and hippocampus (B). mRNA expression of claudin-5 in young compared with aged animals was unchanged in both the cortex (C) and hippocampus (D). Data expressed as mean ± SEM, n=6-7; *$p<0.05$, **$p<0.01$; Student's *t*-test.

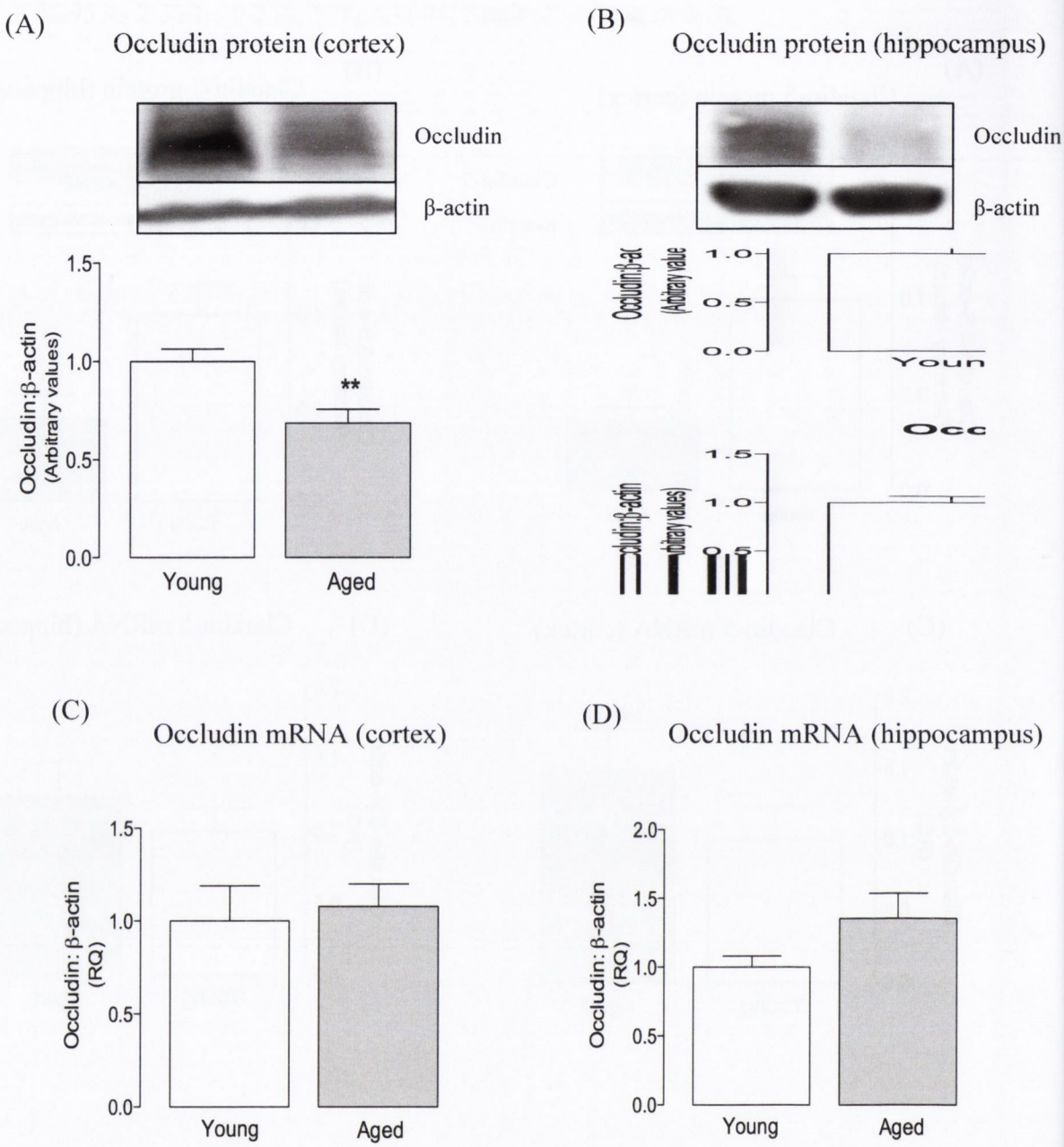

Figure 3.8: Occludin protein concentration was decreased in the aged rat cortex and hippocampus.

Occludin protein concentration was significantly decreased in the aged cortex (A) and hippocampus (B) compared with young animals. Occludin mRNA expression was not significantly altered in the aged cortex (C) or hippocampus (D). Data expressed as mean ± SEM, n=7-9; *$p<0.05$, **$p<0.01$; Student's *t*-test.

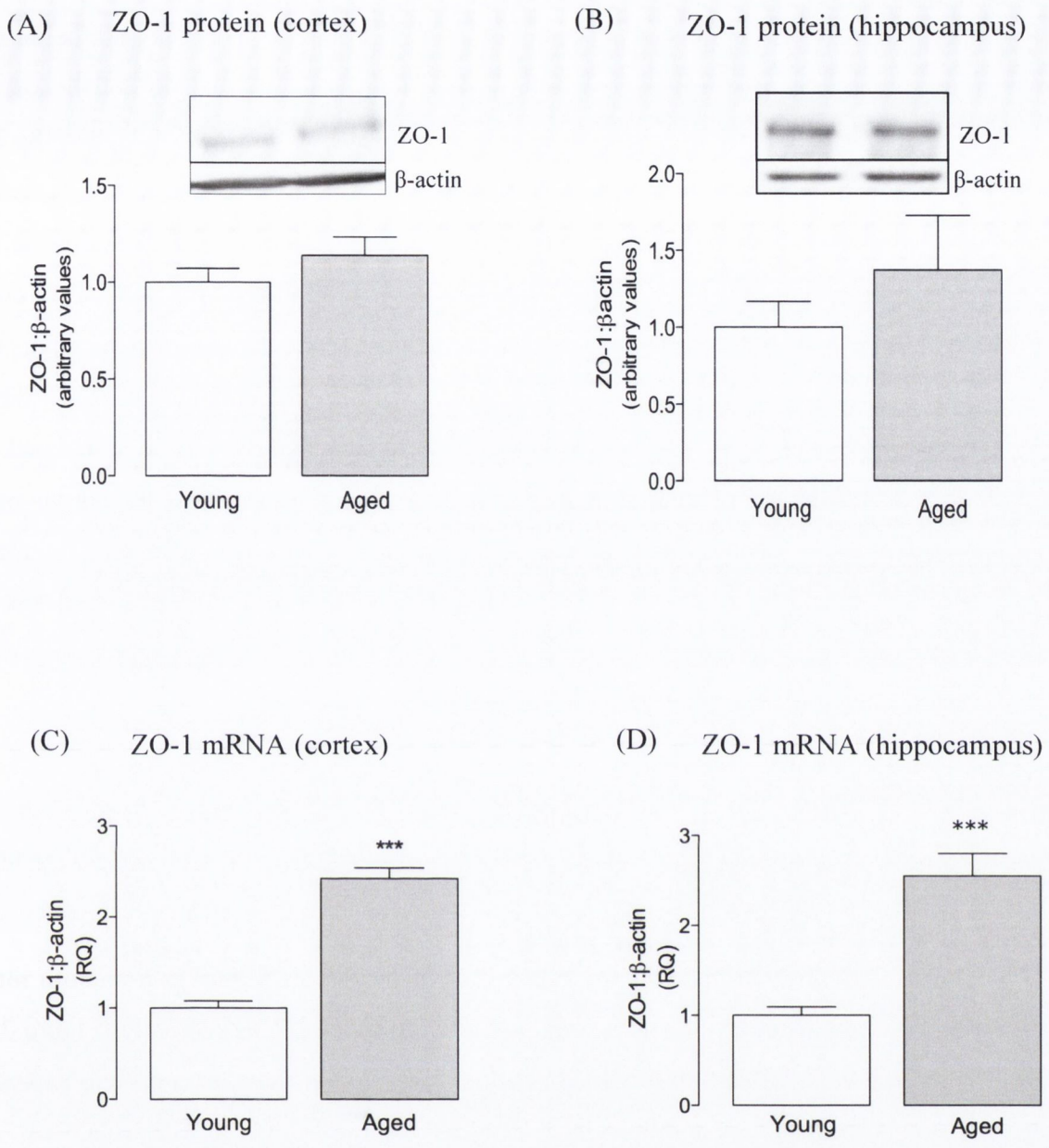

Figure 3.9: ZO-1 mRNA expression was increased in the aged cortex and hippocampus.

ZO-1 mRNA expression was significantly increased in the aged cortex (C) and hippocampus (D) compared with the young group. However, ZO-1 protein concentration was not significantly altered in the aged cortex (A) or hippocampus (B). Data expressed as mean ± SEM, n=6-9; ***$p<0.001$; Student's *t*-test.

3.7 Assessment of neurovascular unit integrity at the ageing blood-brain barrier

A number of other cell types in close anatomical proximity to brain endothelial cells, share signalling pathways with them and contribute to the establishment and maintenance of the BBB. These cells include neurons, astrocytes, pericytes, the basal lamina and the extracellular matrix; all collectively referred to as the "neurovascular unit". Endothelial cells bind to extracellular matrix proteins like laminin via their integrin receptors and are anchored in place to maintain stability and allow correct intercellular signalling (Hawkins & Davis, 2005). Pericytes are perivascular cells, encircling endothelial cells and are enclosed within the endothelial basal lamina. Disruption of the basal lamina and/or pericytes has been shown to be associated with increased BBB permeability. It was demonstrated that when the extracellular matrix was disrupted by bacterial collagenase in the rat brain, there was substantial opening of the BBB (Rosenberg *et al.*, 1993). Similarly, (Nishioku *et al.*, 2009) observed that LPS fragmented the basal lamina of cerebral vessels in mice, leading to loosening of the pericytes and causing increased BBB permeability.

3.7.1 Expression of pericyte marker, α-smooth muscle actin in cortex and hippocampus of young and aged animals

Protein concentration and mRNA expression of the pericyte marker α-smooth muscle actin was quantified by Western immunoblotting and qPCR respectively [Figure 3.10]. There was no significant difference in cortical α-smooth muscle actin protein expression between young and aged animals (A; 1 ± 0.193 vs 1.068 ± 0.140; Students *t*-test; n=7-9). Although mRNA expression of α-smooth muscle actin mRNA tended to decrease in the aged cortex, it was not statistically significant (B; 1 ± 0.077 vs 0.696 ± 0.140; Student's *t*-test; n=7-9). However, mRNA expression of α-smooth muscle actin was significantly decreased in the aged hippocampus (C; 1 ± 0.067 vs. 0.461 ± 0.017; ***$p<0.001$; Student's *t*-test; n=7-8).

3.7.2 Expression of pericyte marker, PDGFR-β in cortex and hippocampus of young and aged animals

Protein concentration and mRNA expression of the pericyte marker PDGFR-β was quantified by Western immunoblotting and qPCR respectively [Figure 3.11]. There were significant decreases in PDGFR-β protein expression in both the cortex (A; 1 ± 0.093 vs 0.604 ± 0.138; *p<0.05; Student's *t*-test; n=7) and hippocampus (B; 1 ± 0.067 vs. 0.696 ± 0.047; **p<0.01; Student's *t*-test; n=8). These changes were not replicated at the mRNA level where PDGFR-β was unchanged between young and aged animals in both the cortex (C; 1 ± 0.089 vs. 0.992 ± 0.066; Student's *t*-test; n=7-9) and hippocampus (D; 1 ± 0.054 vs 0.929 ± 0.037; Student's *t*-test; n=7).

3.7.3 Laminin changes in the young and aged rat brain

Protein concentration of the basal lamina marker laminin was quantified by Western immunoblotting [Figure 3.12]. Laminin protein concentration was significantly decreased in both the aged cortex (A; 1 ± 0.235 vs 0.4625 ± 0.082; *p<0.05; Student's *t*-test; n=5-7) and hippocampus (B; 1 ± 0.079 vs 0.763 ± 0.066; *p<0.05; Student's *t*-test; n=8-9) when compared with young animals. Micrographs representing laminin staining patterns from young (C) and aged (D) animals are shown in Figure 3.12.

3.7.4 Structural changes at the aged neurovascular unit

In order to investigate whether the basal lamina was anatomically intact and surrounding the pericytes, cryosections from young and aged animals were double immunostained for the basal lamina marker laminin and the pericyte marker α-smooth muscle actin, and assessed by confocal microscopy. Colocalisation of the two markers was indicative of an intact basal lamina ensheathing the adjacent pericytes. Micrograph A in Figure 3.13 is representative of the intact neurovascular unit observed in young animals, where colocalisation of laminin and α-smooth muscle actin was evident. Micrographs B and C represent the varying degrees of basal lamina separation from the pericytes in aged animals, particularly in the 28 month old (C). The ratio of colocalised pixels divided by the total number of pixels for a given blood vessel was used as a measure of neurovascular unit integrity. Semi-quantitative analysis of double immunostained cryosections revealed that there was a significant decrease in the degree of colocalisation between laminin and α-smooth muscle actin in the aged, compared to

the young animals (D; 1 ± 0.070 vs. 0.795 ± 0.061; *p<0.05; Student's *t*-test; n=19-28 blood vessels, from 3-4 animals per age group).

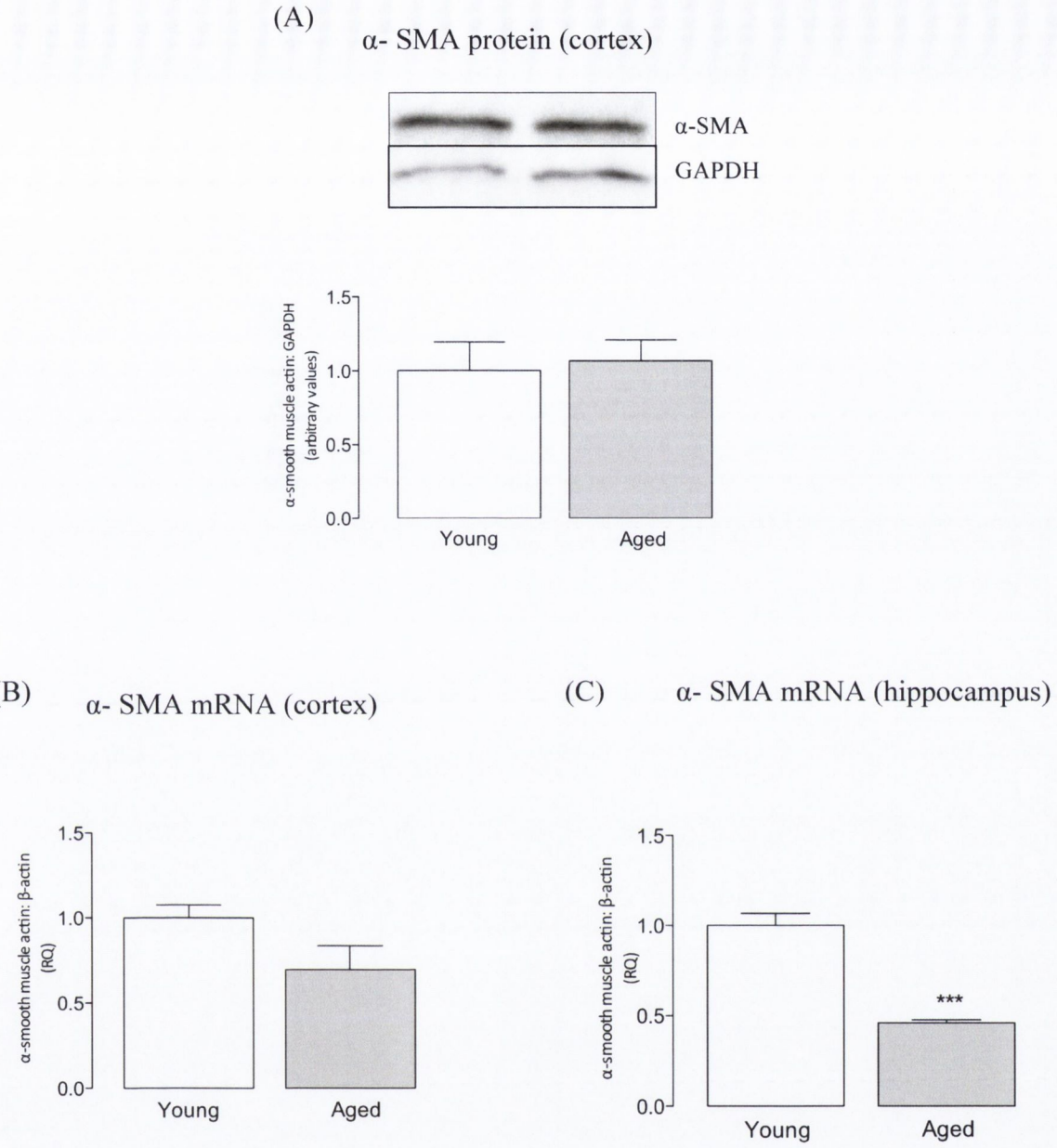

Figure 3.10: mRNA expression of the pericyte marker, α-smooth muscle actin (α-SMA) was decreased in the aged rat hippocampus.

There were significant decreases in α-SMA mRNA expression in the aged hippocampus (C) but not in the aged cortex at either protein (A) or mRNA (B) levels. Data expressed as mean ± SEM, n=7-9; ***$p<0.001$; Student's *t*-test.

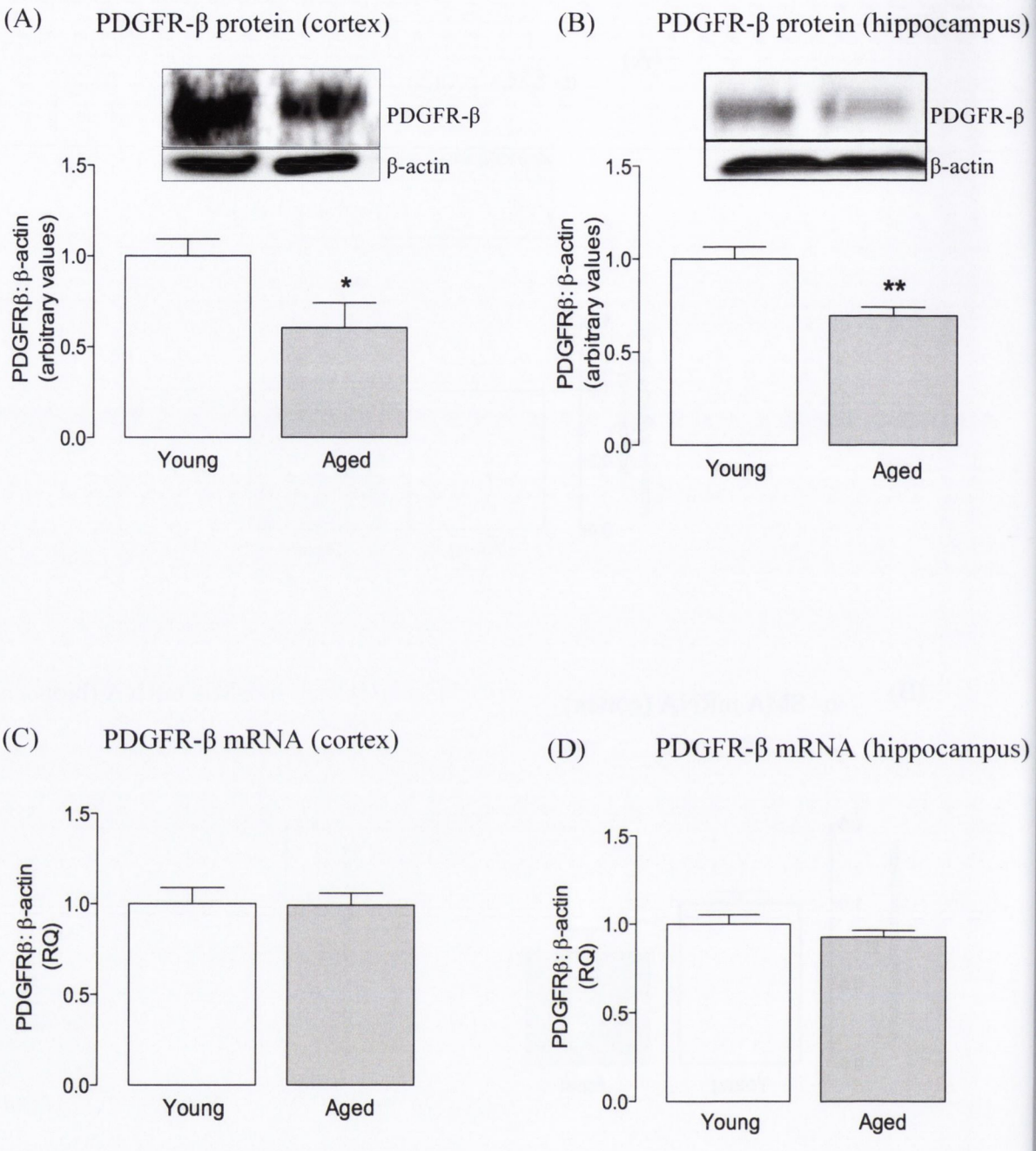

Figure 3.11: PDGFR-β protein concentration was decreased in the aged cortex and hippocampus.

PDGFR-β protein concentration was significantly decreased in both the aged cortex (A) and hippocampus (B). PDGFR-β mRNA expression was unchanged between young and aged cortex (C) and hippocampus (D). Data expressed as mean ± SEM, n=7-9; *$p<0.05$, **$p<0.01$; Student's *t*-test.

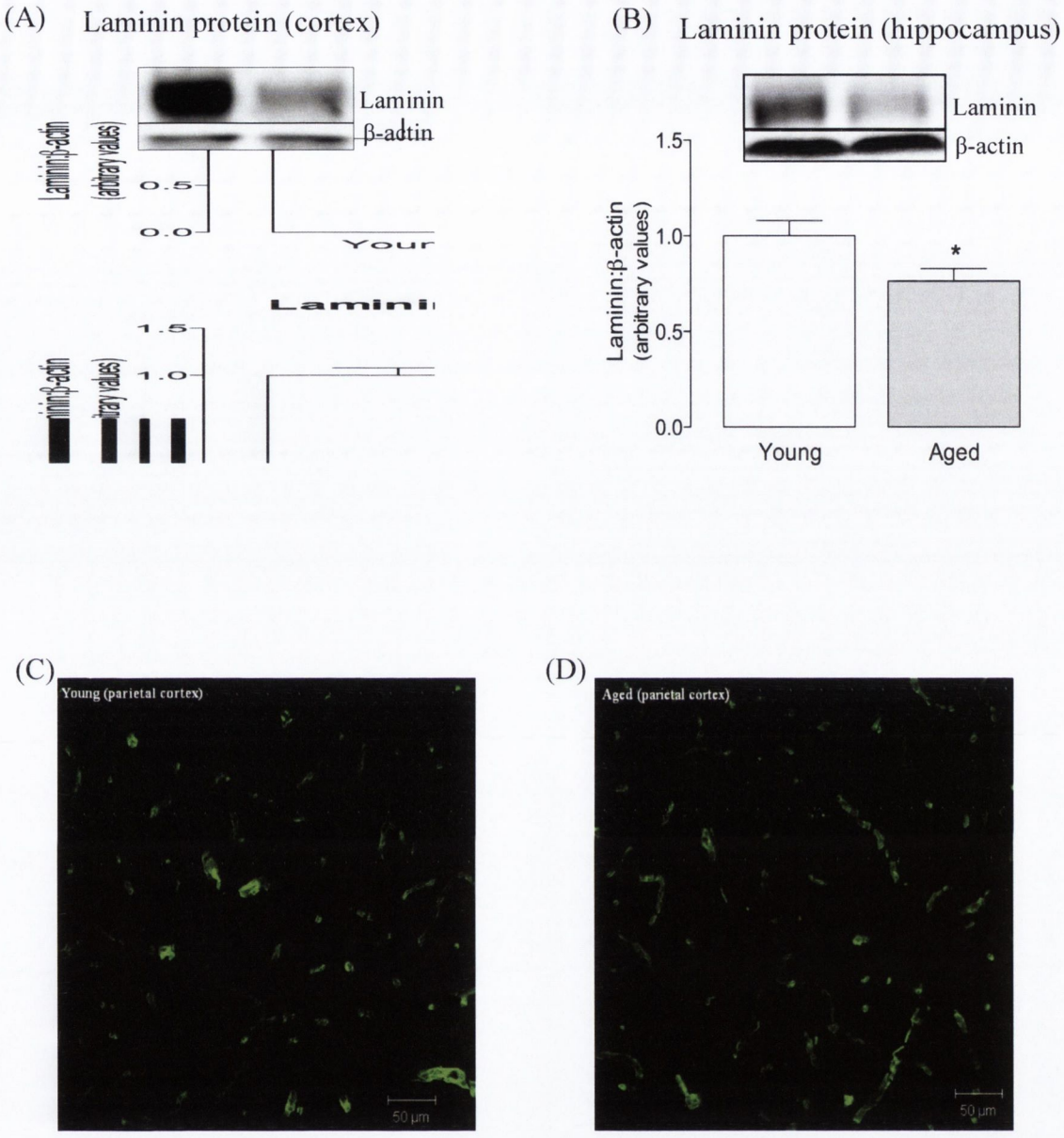

Figure 3.12: Laminin protein concentration was decreased in the aged rat cortex and hippocampus.

Laminin protein concentration was significantly decreased in both aged cortex (A) and hippocampus (B) compared with young animals. Micrographs (C) and (D) illustrate laminin staining in the young and aged cortices respectively. Data expressed as mean ± SEM, n=5-9; *$p<0.05$, Student's *t*-test.

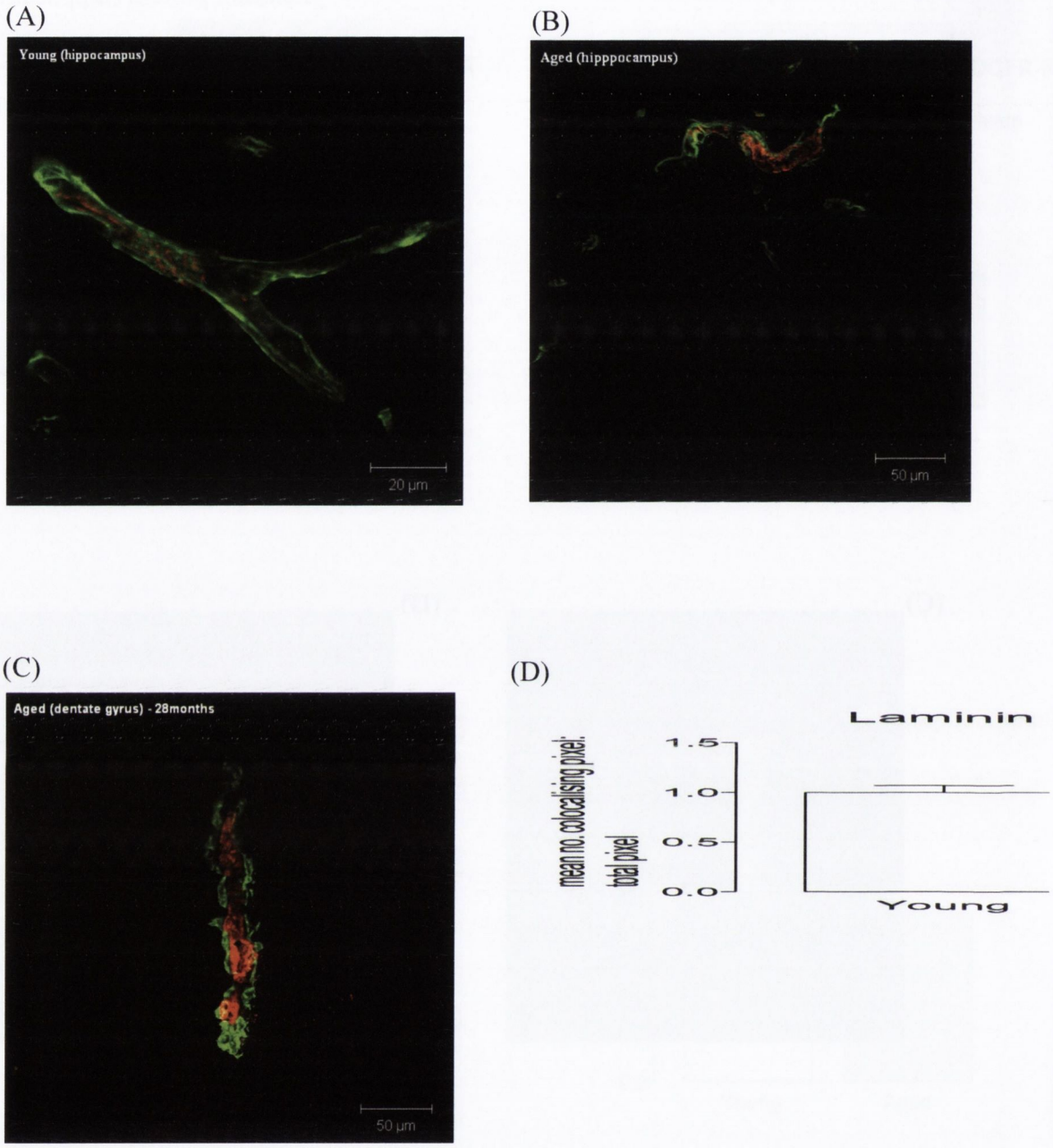

Figure 3.13: The neurovascular unit was structurally altered in the aged rat brain.

Micrograph (A) is representative of the intact neurovascular unit observed in young animals, as indicated by colocalisation of the pericytes (α-smooth muscle actin, red) by the basal lamina (laminin, green). Micrographs B and C represent the varying degrees of basal lamina separation from the enclosed pericytes in aged animals, especially in the 28 month old animal (C). Semi-quantitative analysis of micrographs revealed that there was a significant decrease in the degree of colocalisation of laminin with α-smooth muscle actin (D), indicating neurovascular unit structural changes with age. Data expressed as mean ± SEM, n=19-28 blood vessels; *$p<0.05$; Student's *t*-test.

3.8 Assessment of matrix metalloproteinase activity with age

Matrix metalloproteinase- (MMP) -2 and MMP-9 are known modulators of the basal lamina and tight junction proteins. Western immunoblotting was used to assess total MMP-9 and TIMP-1 protein concentration in young and aged cortical and hippocampal tissue. Gelatin zymography was used to assess enzymatic activity levels of MMP-2 and MMP-9 in serum from (i) young and aged rats, (ii) young, middle-aged and aged healthy human subjects and (iii) young human subjects, subjects with Alzheimer's disease and their (aged) carers.

3.8.1 MMP concentration and activity in young and aged rat serum

Total MMP-9 concentration was significantly decreased in the aged rat cortex (A; 1 ± 0.681 vs 0.755 ± 0.058; *$p<0.05$; Student's *t*-test, n=8-9), but not hippocampus (B; 1 ± 0.067 vs 0.940 ± 0.113; Student's *t*-test, n=8-9). Enzymatic activity of both MMP-2 and MMP-9 were assessed by gelatin zymography Figures 3.15 and 3.14, respectively. There was a significant increase in enzymatic activity of MMP-2 in aged compared with young rat serum (Figures 3.15 A and B; 1 ± 0.140 vs. 1.417 ± 0.113; *$p<0.05$; Student's *t*-test; n=5-8). While MMP-9 activity was lower than that of MMP-2 (serum must by 5x more concentrated to visualise MMP-9), the overall activity of MMP-9 was significantly increased in the aged serum (Figures 3.14 C and D; 1 ± 0.066 vs. 1.273 ± 0.048 **$p<0.01$; Student's *t*-test; n=5-9).

3.8.2 TIMP-1 concentration in in young and aged rat tissue and serum

TIMP-1 protein concentration in plasma from young and aged rats was assessed by ELISA. TIMP-1 protein concentration in young and aged cortex and hippocampus was assessed by Western immunoblotting [Figure 3.16]. TIMP-1 protein concentration was not altered with age in the cortex (A; 1 ± 0.099 vs 1.014 ± 0.123; Student's *t*-test; n=6) and hippocampus (B; 1 ± 0.089 vs 1.021 ± 0.096; Student's *t*-test; n=7). Similarly, there was no age-related change in TIMP-1 serum concentrations (C; 1840 ± 295.7 vs 1845 ± 221.3; Student's *t*-test; n=5-8).

3.8.3 MMP activity in serum from young and aged humans

Gelatin zymography was used to assess any age-related changes in MMP-2 and -9 activity in human serum [Figure 3.17]. MMP-2 activity could not be detected in any of the human serum samples. There were no significant differences in MMP-9 activity in serum from young, middle-aged and aged healthy subjects (A; 1 ± 0.016 vs. 1.012 ± 0.015 vs 1.011 ± 0.014; one-way ANOVA; n=4-8). However, the MMP-9 activity levels were significantly increased in serum from subjects with Alzheimer's disease and their carers, when compared to their younger counterparts (B; 1 ± 0.040 vs. 1.226 ± 0.009 vs 1.434 ± 0.027; ***$p<0.001$; one-way ANOVA, n=4-8).

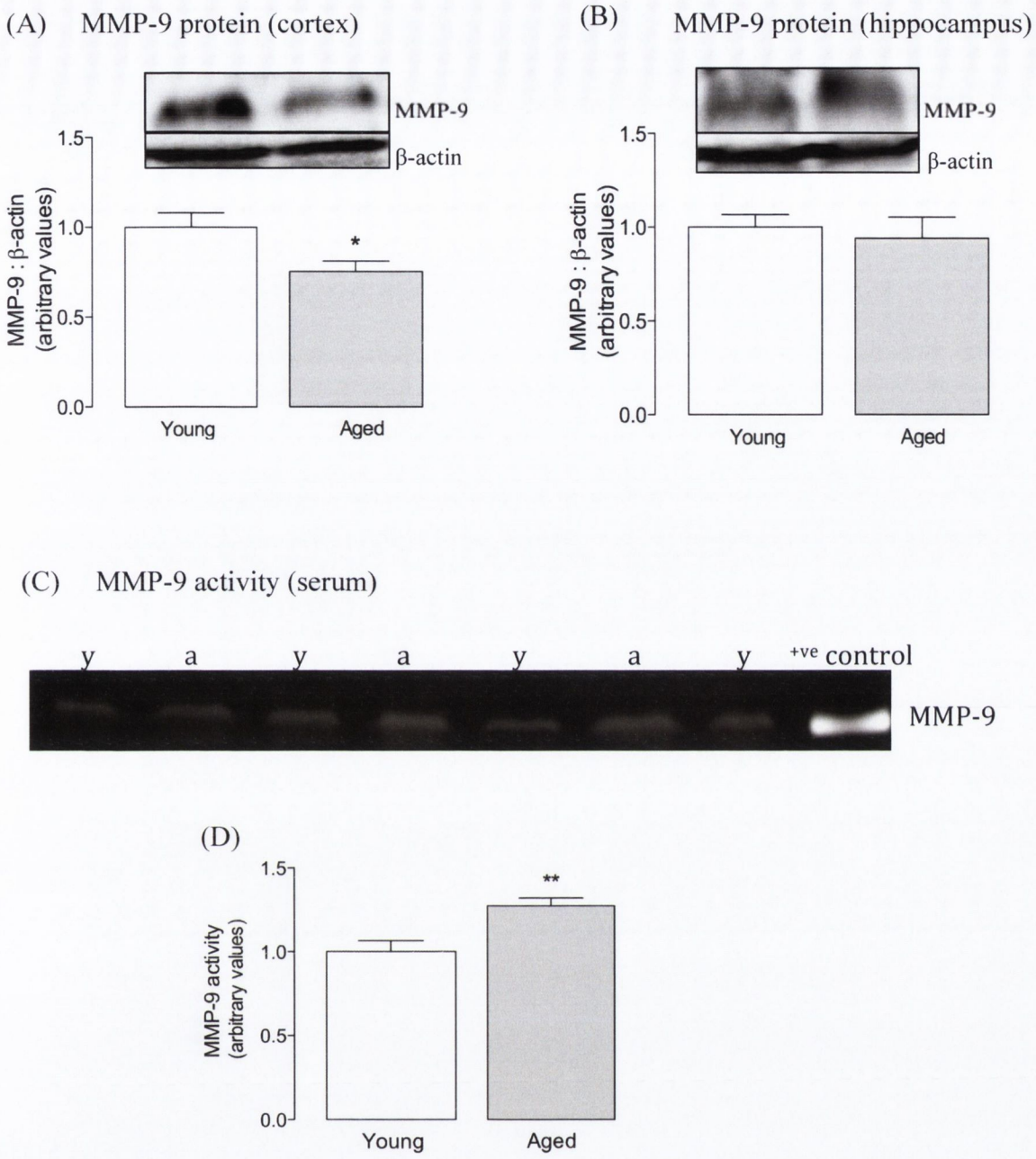

Figure 3.14: Decreased cortical MMP-9 concentration and increased serum MMP-9 activity in the aged rat.

Total MMP-9 protein concentration was significantly decreased in the aged cortex (A) but not in the aged hippocampus (B). The gelatin zymography gel (C) is representative of the enzymatic activity of MMP-9 in serum from young (y) and aged (a) rats. Quantitative analysis of the gelatin zymography gels illustrates the significant increase in MMP-9 enzymatic activity in serum from aged rats (D). Data expressed as mean ± SEM, n=5-9; *$p<0.05$, **$p<0.01$; Student's *t*-test.

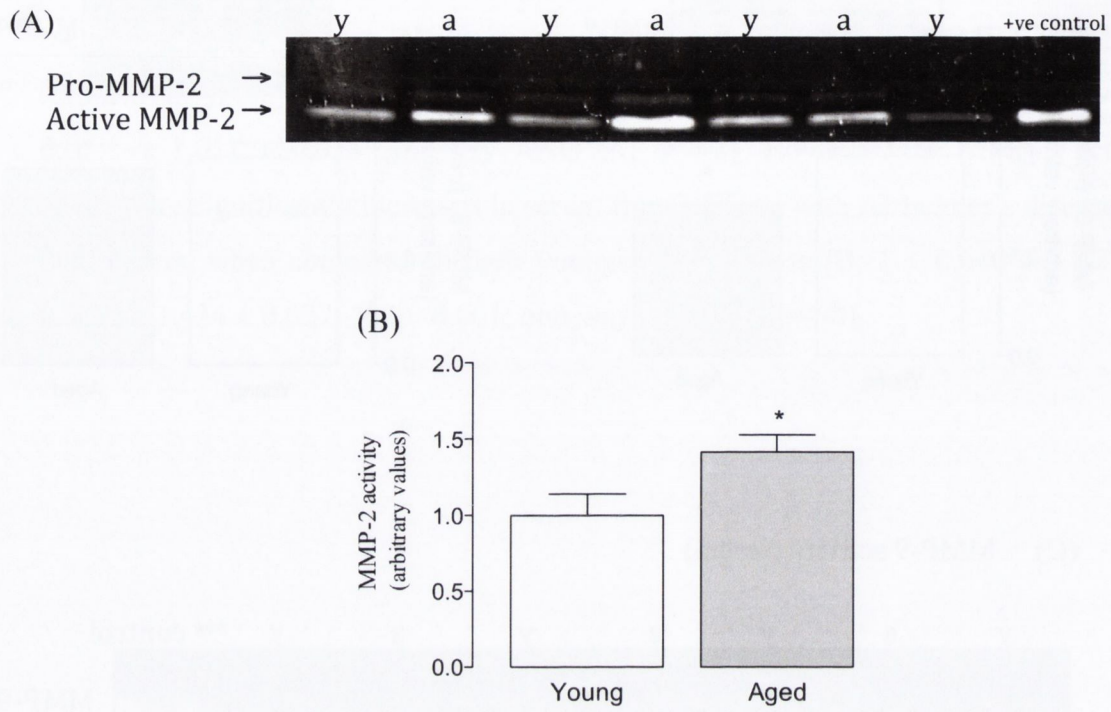

Figure 3.15: Increased serum MMP-2 activity in the aged rat.

The gelatin zymography gel (A) is representative of the enzymatic activity of MMP-2 in serum from young (y) and aged (a) rats. Quantitative analysis of the gelatin zymography gels illustrates the significant increase in MMP-2 enzymatic activity in serum from aged rats when compared to serum from young rats (B). Data expressed as mean ± SEM n=5-8; *$p<0.05$; Student's *t*-test.

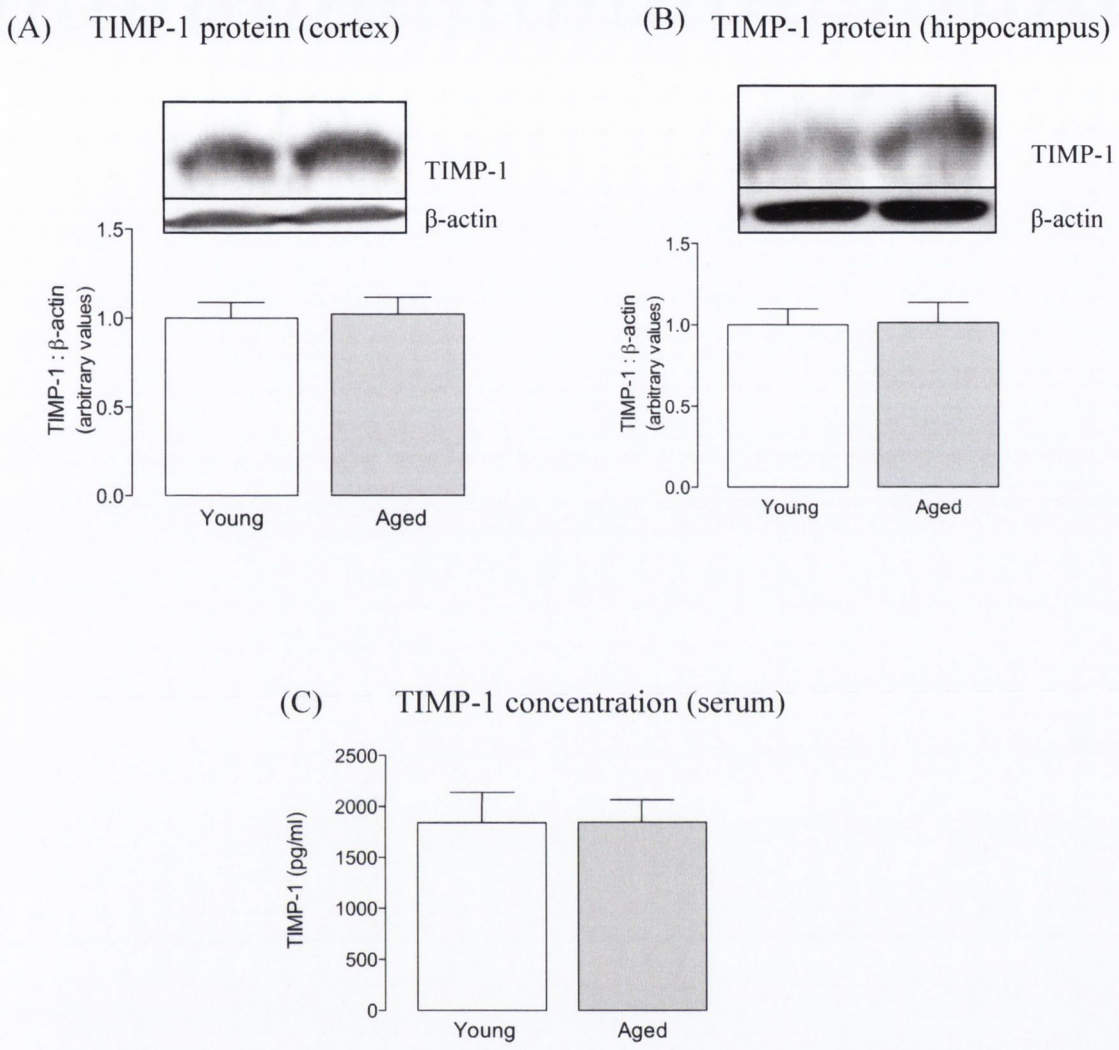

Figure 3.16: TIMP-1 protein concentration in brain tissue and TIMP-1 serum concentrations were not altered with age.

TIMP-1 protein concentration was unchanged in the aged, compared to the young cortex (A) and hippocampus (B). Similarly, the serum concentration of TIMP-1 was not significantly different in the aged, compared to the young group (C). Data expressed as mean ± SEM, n=5-8; Student's *t*-test.

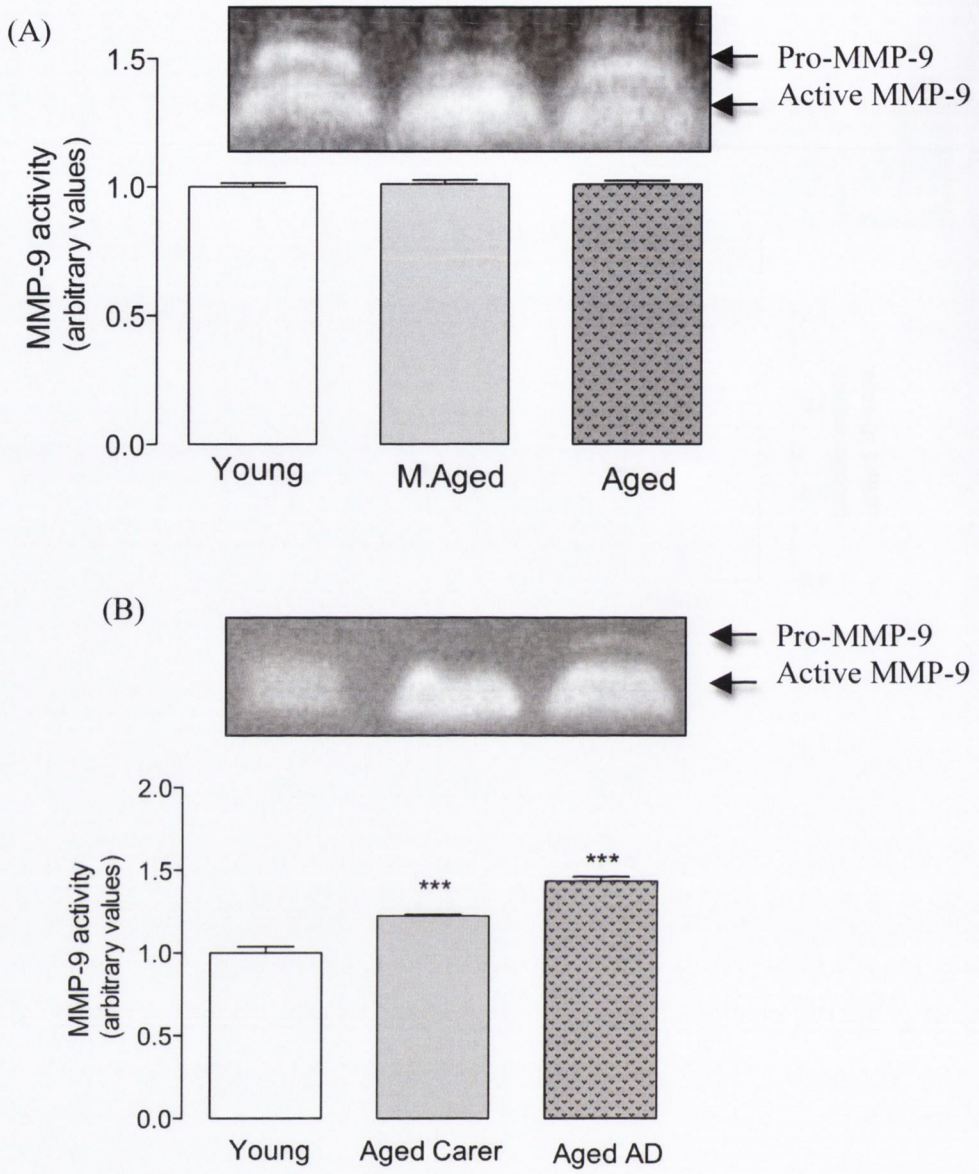

Figure 3.17: MMP-9 activity was significantly increased in serum from subjects with Alzheimer's disease and their carers.

There was no significant difference in the MMP-9 activity levels in serum from healthy young, middle-aged and aged subjects (A). However, MMP-9 enzymatic activity was significantly increased in subjects with Alzheimer's disease and their carers, when compared to serum from young subjects (B). Data expressed as mean ± SEM, n=4-8; ***$p<0.001$ versus young control; one-way ANOVA followed by Newman Keuls *post-hoc* test.

3.9 Discussion

Impairments in the structure and function of the ageing BBB may cause or exacerbate age-related neurodegeneration by facilitating the entry of potentially harmful molecules into an already fragile neural environment. With this in mind, the aims of this study were to assess the functional and structural integrity of the ageing blood-brain barrier and to assess matrix metalloproteinase activity with age.

The data from this study indicate increased BBB permeability with age, as evidenced by extravasation of (i) endogenous plasma albumin and (ii) exogenous sodium fluorescein to the brain parenchyma. The increased BBB permeability is accompanied by decreased protein expression of the tight junction (TJ) proteins claudin-5 and occludin. In addition, the age-related degradation of the protective basal lamina coupled with an age-related increase in MMP activity, known modulators of the basal lamina, provides compelling evidence for structural as well as functional BBB changes with increasing age.

To assess BBB permeability in young and aged animals, the migration of substances of varying molecular weights to the brain parenchyma was investigated. Young and aged rats were given a tail-vein injection of sodium fluorescein (376 Da; a fluorescent marker), to assess the integrity and permeability of the BBB. This molecule is too large to cross a functional BBB and should not be apparent in the brain parenchyma. Although basal background fluorescence was similar between both age groups, there was some unexpected visible fluorescence observed in micrographs from the aged controls. The appearance of these fluorescent granules in aged controls could not be attributed to sodium fluorescein and was likely due to the presence of lipofuscin, an age-related autofluorescent substance that accumulates in the lysosomes of post-mitotic cells like neurons. It is derived from phagocytosed cellular components and cannot be degraded nor exocytosed by cells (Terman & Brunk, 2004). In the aged tissue, it was possible to visualise these lipofuscin-like granules across all excitation wavelengths, a property which is characteristic of lipofuscin (Brunk & Terman, 2002) Despite the occurrence of background fluorescence in the aged samples, the mean fluorescent intensity was about 200-250 pixels, whereas the fluorescence in the sodium fluorescein injected animals ranged from 480-1750 (see Table 3.1) The autofluorescence in the aged samples was considered too little to account for the increased fluorescence in the sodium fluorescein injected group.

Of the animals that received a sodium fluorescein injection, the results show that sodium fluorescein significantly extravasated into the aged, but not young parenchyma, indicating the BBB was disrupted with age. In particular, the highest fluorescent reading was obtained in the oldest animal (28 months) in the aged group. Further support of BBB breakdown with age came from the observation that endogenous albumin expression (65 kDa), a plasma protein, was also significantly increased in the aged cortex. This can only be attributed to a disruption in the paracellular pathway of the BBB because albumin is not transported across the transcellular pathway nor is it synthesised *de novo* in the CNS (Algotsson & Winblad, 2007). Plasma levels of albumin in young and aged animals are similar, so the increased albumin concentration in the aged cortex could not be accounted for due to increased circulating levels of albumin in the aged animal, indeed if anything, one may have expected a reduction in circulating plasma albumin in the aged animals due to impaired liver function with age, however, liver function was not assessed in these animals.

Taken together, these findings provide strong evidence that BBB functionality is significantly compromised in the aged brain, as evidenced by the presence of plasma components (sodium fluorescein and albumin) in brain parenchyma of aged but not young animals. These findings are similar to those of (Pelegri *et al.*, 2007) who monitored concentrations of IgG in the brain parenchyma of senescence-accelerated mice. They observed significantly greater quantities of IgG in the brains of senescent-accelerated aged mice (12 month old) compared to age-matched senescence-resistant strains and they postulated that there was a defective BBB with increasing age. They hypothesised that the IgG traversed the BBB due to either (i) changes in the transcellular protein carriers of the capillary endothelial cells or (ii) due to changes in the tight junction proteins which would normally regulate the paracellular pathway between adjacent capillary endothelial cells. Though the study mentioned the possibility that the IgG found in brain parenchyma was due to *de novo* synthesis, this mechanism was ruled out due to the fact that all IgG found in the brain parenchyma of the mice was located in very close proximity to the blood vessels, indicating that the IgG had migrated directly from the capillaries. Bake and collegues (2009) also noted that there was significantly increased levels of IgG protein in the brains of aged Sprague-Dawley rats compared to young rats and these results were more profound in the reproductive senescent females rat brain (Bake *et al.*, 2009).

Alzheimer's disease (AD) is an age-related neurodegenerative disease and there is extensive evidence of a compromised BBB in the AD brain. Plasma proteins have been detected in brain tissue from AD patients (Ryu & McLarnon, 2009) and in cerebrospinal fluid from AD patients (Algotsson & Winblad, 2007). A systematic review of the literature assessing 31 human studies, highlighted evidence of increased BBB permeability in normal ageing, and in particular in brains from patients with AD and vascular dementia when compared with age-matched controls (Farrall & Wardlaw, 2009). It is highly plausible that BBB impairment during normal physiological ageing, as found in this research, may be a primary or secondary event contributing to the pathogenesis of BBB disturbances, a common aetiology of age-related neurodegenerative diseases.

Having established an age-related disruption of the paracellular pathway of the BBB, the integrity of the endothelial TJ proteins comprising the paracellular barrier was investigated. Claudin-5 and occludin protein concentration were significantly decreased in the hippocampus and cortex of aged animals, however mRNA expression was unchanged. This finding indicated that the TJ proteins themselves were being directly degraded, rather than decreased due to a downregulation of expression. Considering TJ proteins are the primary contributor to the BBB, their disruption is the likely cause of the age-related increase in plasma components found in the aged tissue. The TJ findings from this study are somewhat similar to results obtained by (Bake *et al.*, 2009). Having established there were age-related increases in BBB permeability, they subsequently found alterations in claudin-5, but not occludin expression in the hippocampus of both aged female humans and Sprague-Dawley rats. Immunohistochemical analysis indicated that although there was significant disruption in the localization of claudin-5 at the TJ in aged rats and humans, there were no changes in overall claudin-5 protein expression. The occludin and ZO-1 findings from our research concur with those from a study in which significant reductions in occludin protein expression but not ZO-1 were observed in aged male Fischer rats (Mooradian *et al.*, 2003). Interestingly, they too found significant increases in ZO-1 mRNA expression but not protein concentration with age. Indeed, the mRNA expression of all tight junctions in our research tended to be greater in the aged animals, though not significantly, suggesting substantial disruption is occurring to the aged TJ protein.. Such post-translational modifications have been documented when the TJ proteins have been subjected to oxidative stress

(Blasig *et al.*, 2011) and considering that oxidative stress is a feature of the aged brain (Venkateshappa *et al.*, 2012) such changes are a distinct possibility.

Interestingly, a permeability study on claudin-$5^{-/-}$ knockout mice reported increased BBB permeability to molecules up to 800Da in size in the knockout but not the claudin-$5^{+/-}$ mice (Nitta *et al.*, 2003). The authors attributed this finding to the presence of other claudin isoforms, namely claudin-12, remaining at the BBB, thus preventing the permeability of larger molecules, > 800Da, into the brain parenchyma. The aged animals in our research had decreased occludin protein expression, whereas the claudin-$5^{-/-}$ mice had similar occludin protein concentrations to the wildtype mice. It is possible that as well as the claudin-5 disruption, there are age-related disruptions in additional claudin isoforms in the aged animals from our research. These factors may be contributing to an even more pronounced disruption of the BBB and facilitating the extravasation of larger molecules e.g. albumin, in the aged animals.

In the context of AD, an extensively studied neurodegenerative condition, parallel changes in increased BBB permeability and TJ protein modification have been established. The increased BBB permeability in AD brains (Algotsson & Winblad, 2007; Ryu & McLarnon, 2009) has led to investigations into the integrity of TJ proteins at the BBB in AD patients, and animal models of AD. Incubating primary endothelial cells from rat cerebral cortex with $A\beta_{1-42}$ resulted in relocation of claudin-5 and ZO-1 to the cytoplasm, and reductions in occludin expression (Marco & Skaper, 2006). In a more recent study on an immortalized human brain endothelial cell line, $A\beta_{1-40}$ increased the paracellular permeability to a tracer of MW 70kDa, and this was attributed to the MAPK-mediated down-regulation of occludin (Tai *et al.*, 2010).

In addition to the endothelial tight junctions, components of the NVU (glia, neurons, pericytes, basal lamina) are important in maintaining and regulating the BBB, so any age-related changes in NVU components could result in disruption of the BBB (Bell & Zlokovic, 2009; Zlokovic, 2011). Because age-related changes in neurons and glia have been researched extensively (Lynch, 2010; Salminen & Ojala, 2001; Jurgens & Johnson, 2012), the status of the pericytes and basal lamina in the aged brain was investigated here. Pericytes encircle endothelial cells and experimentally knocking out pericytes, or disrupting the PDGFR-PDGFR-β signalling pathway between pericytes and endothelial cells in mice resulted in death of the animals due to vascular

haemorrhage (Armulik *et al.*, 2005). In a similar study, PDGFR-β knockout mice lack CNS pericytes and die at the embryonic stage from vascular haemorrhage (Daneman *et al.*, 2010). These studies show the importance of pericytes in vessel maintenance *in vivo*.

A comprehensive study on age-related pericyte changes showed that PDGFR-$\beta^{+/-}$ mice had substantially disrupted PDGFR-β signalling and when aged PDGFR-$\beta^{+/-}$ animals were compared to their younger wild-type counterparts (PDGFR-$\beta^{+/+}$), and it was found that the numbers of pericytes were significantly decreased (up to 60%) in the aged animals (Bell *et al.*, 2010), as measured by the number of positively stained pericytes per mm^2 of capillary stained. The decreased pericyte numbers correlated with a 20-50-fold increase in plasma molecules (IgG, plasmin, fibrin, hemosiderin and thrombin and TMR-dextran, 40kDa) in the brain parenchyma of the aged PDGFR-$\beta^{+/-}$, indicating profound BBB breakdown. Although the mice in the above study were genetically mutated, it is possible that pericytes numbers are decreased in the normal ageing brain, as evidenced by the decreased expression of PDGFR-β in this study. As PDGFR-β is responsible for recruiting pericytes to endothelial cells and stabilising the pericyte-endothelial unit (Armulik *et al.*, 2005) decreased pericyte numbers could contribute to BBB disruption. Whilst it is known from *in vitro* (Lai & Kuo, 2005; Nakagawa *et al.*, 2007) and *in vivo* (Krueger & Bechmann, 2010) studies that pericytes significantly contribute to the maintenance of BBB function, the precise molecular mechanisms are yet to be determined.

The basal lamina surrounding cerebral blood vessels and ensheathing the pericytes is also crucial to the BBB. It has been noted that LPS-injected mice develop fragmentation of the cerebral basal lamina leading to subsequent pericyte detachment from the endothelial cell wall. These structural changes were accompanied by a functional disruption in the BBB, as evidenced by the increased permeability to sodium fluorescein (Nishioku *et al.*, 2009). It was hypothesized the LPS led to a destabilization of the laminin-pericyte unit, ultimately exposing the endothelial cells expressing TJ proteins to further disruption. Immunohistochemical micrographs from our research indicate that there is a distinct fragmentation of the basal lamina with age, thereby exposing the pericytes. These changes were particularly apparent in the oldest animal of the aged cohort. The decreased co-localisation of lamina and pericytes in the aged brain would ultimately expose the normally ensheathed pericytes and endothelial cells,

facilitating further damage by circulating and parenchymal cytotoxins. Whilst the Nishioku study demonstrated that inflammation, from an exogenous source of LPS disrupted the BBB, the increased inflammation already existing in the ageing brain may be causing the changes observed in the aged Wistar rats.

The reductions in laminin expression as found in this study are somewhat paralleled in a recent study on the basal lamina from the human internal limiting membrane of the eye, another basal membrane in the nervous system (Candiello *et al.*, 2010). The authors found that despite there being a general thickening of the basal membrane with increasing age (88-yrs-old vs. 43-yrs-old), there were also changes in the biochemical composition of the lamina, particularly, a decrease in expression of laminin-1, one of the predominant laminin isoforms in the cerebral microvasculature (Palu & Liesi, 2002; Hallmann *et al.*, 2005). The authors postulated that due to the general homogeneity in basal membrane structure, similar changes with increasing age could be occurring in the other cerebral membranes, e.g. the basal lamina ensheathing cerebral blood vessels. Interestingly, depending upon the activation state of the endothelial cells different laminin isoforms are expressed; with pro-inflammatory stimuli causing a shift from the predominant laminin-8 and -1 isoforms in endothelial basal lamina to the laminin-10 isoform (Sixt *et al.*, 2001). The laminin antibody used in this study was polyclonal and picked up all laminin isoforms so in future studies, it would be interesting to assess which specific laminin isoforms are reduced with age.

The balance of matrix metalloproteinases (MMP) and tissue-inhibitors of MMP (TIMP) is responsible for maintaining basal lamina stability (Yang *et al.*, 2007). It has been postulated that MMP-mediated proteolysis of the basal lamina loosens the base on which the TJ proteins are anchored and/or proteolysis of the components of the extracellular matrix of brain capillary endothelial cells exposes the tight junction proteins, rendering them susceptible to damage (Gurney *et al.*, 2006). Interestingly, our results documented a significant increase in MMP-2 and MMP-9 plasma activity in aged rats, despite there being no changes in TIMP-1 expression or overall MMP-9 expression. This may be underlying the age-related reduction in laminin expression and NVU fragmentation seen in the aged animals. It has been shown that MMP-9 inhibitors can rescue laminin proteolyis in the brain following cerebral ischemia in mice (Gu *et al.*, 2005) and in cultured human brain endothelial cells (Haorah *et al.*, 2007).

MMP have also been documented to disrupt tight junctions directly *in vivo*; decreased claudin-5 and occludin expression was attributed to increased MMP activity in mice following an LPS injection as MMP-3 knockout mice had attenuated TJ disruption. MMP-3 is a known activator of MMP-9 on brain capillary endothelial cells (Gurney *et al.*, 2006). MMP-2 and -9 directly lead to decreased claudin-5 and occludin expression following middle cerebral artery occlusion in rats (Yang *et al.*, 2007). Both studies noted significant increases in BBB permeability as a result of the disrupted tight junctions. A number of other *in vitro* studies support the *in vivo* observations by Gurney *et al.*, 2006 and implicate MMP as capable of altering TJ protein expression (Reijerkerk *et al.*, 2006; Chen *et al.*, 2009; Lischper *et al.*, 2010). Despite the wealth of literature implicating MMP as disruptors of the BBB, very little exists in the literature with respect to changes in MMP/TIMP ratios under normal physiological ageing conditions in healthy human subjects. It is well documented that MMP activity increases where neuroinflammation features (Yong *et al.*, 2001; McColl *et al.*, 2008) which itself is a major underlying characteristic in the aged brain (Lynch & Lynch, 2002). Despite the significant increase in detecting MMP-9 activity in aged rat serum, there were no significant differences in MMP-9 activity in serum from young, middle-aged and aged healthy human subjects. This result contrasts with a study by (Bonnema *et al.*, 2007) that noted that there was decreased MMP-9 expression and increased MMP-2 expression with increasing age in serum from 77 subjects with no clinically significant cardiovascular disease.

Upregulation of MMP-2 and -9 activity has been implicated in a multitude of vascular diseases including vascular dementia and stroke, in addition to AD. Increased levels of MMP-9 activity in ischemic areas of post-mortem stroke brains have been observed with a concomitant increase in BBB permeability in those areas (Rosell *et al.*, 2008). The findings from our study indicate that there are significantly increased levels of MMP-9 in both aged carers and AD subjects when compared with young controls. These findings correlate with increased MMP-2 and -9 activity levels found in CSF and plasma of MCI and AD patients compared with control (Lorenzl *et al.*, 2003; Lim *et al.*, 2011), proteases that have been shown to disrupt the BBB (Candelario-Jalil *et al.*, 2011). In one particular study, cerebral ischemia was induced in MMP-9 knockout and wild-type mice, leading to degradation of ZO-1 protein and increased BBB permeability

to Evan's blue dye. These results were less profound in the MMP-9 knockout mice (Asahi *et al.*, 2001).

In summary, the findings from this research provide evidence for a disrupted BBB with age, both functionally as evidenced by increased permeability, and structurally, as evidenced by decreased TJ protein concentration and fragmented basal lamina. The increased activity of matrix metalloproteinases -2 and -9 in aged rat serum, possibly as a result of increasing age-related inflammation in the brain, could be a potential cause of the age-related BBB dysfunction.

Chapter 4

Does inflammation exacerbate age-related changes in the blood-brain barrier?

4.1 Introduction

The elderly human population is more susceptible to bacterial infections and this often correlates with increased mortality and is a factor contributing to other morbidities (Butcher *et al.*, 2001; Goldstein, 2010). Leukocyte extravasation to the CNS, indicating BBB disruption often occurs following systemic infection (Zhou *et al.*, 2009). It is thought that Alzheimer's disease, an age-related neurodegenerative disease is exacerbated by systemic inflammation (Sly *et al.*, 2001) as it has been reported that systemic inflammation is associated with the cognitive decline seen in AD patients (Holmes *et al.*, 2009). Many studies document the disruptive effect of LPS (a potent stimulator of systemic inflammation) on the barrier properties in a multitude of tissues; corneal epithelia (Yi *et al.*, 2000), intestinal epithelia (Sheth *et al.*, 2007) and amniotic barriers (Kobayashi *et al.*, 2010). Of particular interest to this study are the observations of the disruptive effect of LPS, on the barrier properties of the BBB *in vivo* (Xaio *et al.*, 2001; Erickson *et al.*, 2012) and brain derived endothelium *in vitro* (Wong *et al.*, 2004; Xiaolu *et al.*, 2011; Cardoso *et al.*, 2012). Chapter 3 reported the dramatic reduction in tight junction proteins at the ageing BBB, resulting in increased permeability. We set out to establish if an additional inflammatory insult could further exacerbate damage to an already fragile ageing BBB.

There is an abundance of evidence documenting increased levels of pro-inflammatory cytokines, particularly IL-1β in the aged brain (Lynch & Lynch, 2002; Lynch, 2010) an increase in inate immune genes in the aged brain (Cribbs *et al.*, 2012) and a concomitant decrease in anti-inflammatory cytokines (Ye & Johnson, 2001; Nolan *et al.*, 2005). This age-related shift towards a pro-inflammatory profile is thought to be a major factor in contributing to the normal ageing of the brain and also to the pathogenesis of age-related neurodegenerative diseases like AD (Loane *et al.*, 2009) (Blasko *et al.*, 2004; Godbout *et al.*, 2005; Lynch, 2010). Indeed, increased levels of IL-1β have been found in post-mortem brain tissue of AD and PD patients (Araujo & Lapchak, 1994; Licastro *et al.*, 2005). IL-1β is known to contribute to BBB damage in a multitude of neurodegenerative diseases including AD and PD in addition to MS and ischemic stroke (Capaldo & Nusrat, 2009), possibly due to its pathogenic effects on the cerebral vasculature (Allan & Rothwell, 2001). Despite the evidence of IL-1β being a contributor to neurodegenerative diseases, and also that it increases barrier permeability

both in the PNS (Al-Sadi *et al.*, 2010) and CNS (Xaio *et al.*, 2001), there is a dearth of literature on the precise effect that IL-1β exerts on the ageing BBB.

The aims of this chapter were:

1. To investigate the effects of systemic inflammation on the young and aged blood-brain barrier.

2. To assess the specific impact of IL-1β signalling on the aged blood-brain barrier in IL-1R1$^{-/-}$ mice and their age matched C57Bl/6 controls.

4.2 Methods

4.2.1 Tissue samples

The LPS treatment group (section 2.1.3) consisted of young (3-month) and aged (26-month) rats (Bantham & Kingman, UK) that were randomly assigned to either saline-treated (control) or LPS-treated groups (n=6 per group). Animals received an intraperitoneal injection of either sterile, nonpyrogenic isotonic saline (0.9% saline solution, B. Braun, Ireland) or LPS (100μg/kg; LPS from E. coli, Serotype R515 (Re), Alexis, Switzerland). Animals were sacrificed by decapitation 4 hours after intraperitoneal injection.

It was thought that sacrificing animals 4 hours following LPS administration might be an appropriate timepoint to observe BBB changes because based on the literature, the downstream consequences of LPS signalling e.g. release of pro-inflammatory cytokines, peaks in the 3-6 hour timeframe (Nadeau & Rivest, 1999) and *in vitro* studies have observed that LPS induced the disruption of tight junctions by 3 hours post injection (Xiaolu *et al.*, 2011), suggesting that BBB changes can occur by 4 hours.

The hippocampus, frontal cortex and striatum were dissected free from the left and right hemispheres, snap frozen in liquid nitrogen (Cryoproducts, Ireland) and stored at -80 °C for later protein analysis.

The IL-1R1$^{-/-}$ mice and corresponding C57BL/6 wildtype (WT) controls (section 2.1.2) were further divided into either young (2-month) or middle-aged (14-18-month) groups. Therefore the four experimental groups were as follows: young WT (n=5), middle-aged

WT (n=6), young IL-1R1$^{-/-}$ (n=5) and middle-aged IL-1R1$^{-/-}$ (n=7) male mice. The animals did not any undergo further intervention. Animals were sacrificed by cervical dislocation, the hippocampus was dissected free, snap frozen in liquid nitrogen (Cryoproducts, Ireland) and stored at -80 °C for later protein analysis.

4.2.2 Experimental procedures

The experimental procedures carried out in this chapter are detailed in Chapter 2 where the following techniques are further described: protein assay (section 2.3) and Western immunoblotting (section 2.7). All data is presented as mean ± SEM. Data was analysed by two-way ANOVA followed by *post-hoc* Bonferroni tests to determine significance.

4.3. The effect of LPS on tight junction protein concentration in the young and aged rat brain

Claudin-5 protein concentration was significantly decreased with age in the cortex (Figure 4.1 A; $F(1,16) = 20.28$; $p = 0.0004$) and striatum (Figure 4.1 B; $F(1,13) = 11.15$; $p = 0.0053$). ANOVA revealed a significant age x LPS effect in striatum ($F(1,13) = 4.859$; $p = 0.0461$). Bonferroni *post-hoc* test did not reveal any further significance. Claudin-5 protein concentration could not be detected in the hippocampus (Appendix 2).

Analysis of occludin in young and aged animals following LPS treatment revealed a significant age effect in the cortex (Figure 4.2 A; $F(1,16) = 53.44$; $p = <0.0001$), hippocampus (Figure 4.2 B; $F(1,12) = 6.230$; $p = 0.0281$) and striatum (Figure 4.3; $F(1,14) = 24.75$; $p = 0.0002$). Bonferroni *post-hoc* test revealed a significant decrease in occludin between saline-treated young and aged animals (***$p<0.001$) and between LPS-treated young and aged animals ($^{***}p<0.001$) in the cortex. Although there was a significant reduction of occludin with age in the hippocampus, *post-hoc* tests could not further establish where the changes lay. There was a significant decrease in occludin between young and aged saline-controls (*$p<0.05$) and between young and aged LPS-treated groups ($^{**}p<0.01$) in the striatum.

ZO-1 concentration could not be detected in brain tissue from this cohort (Appendix 3A).

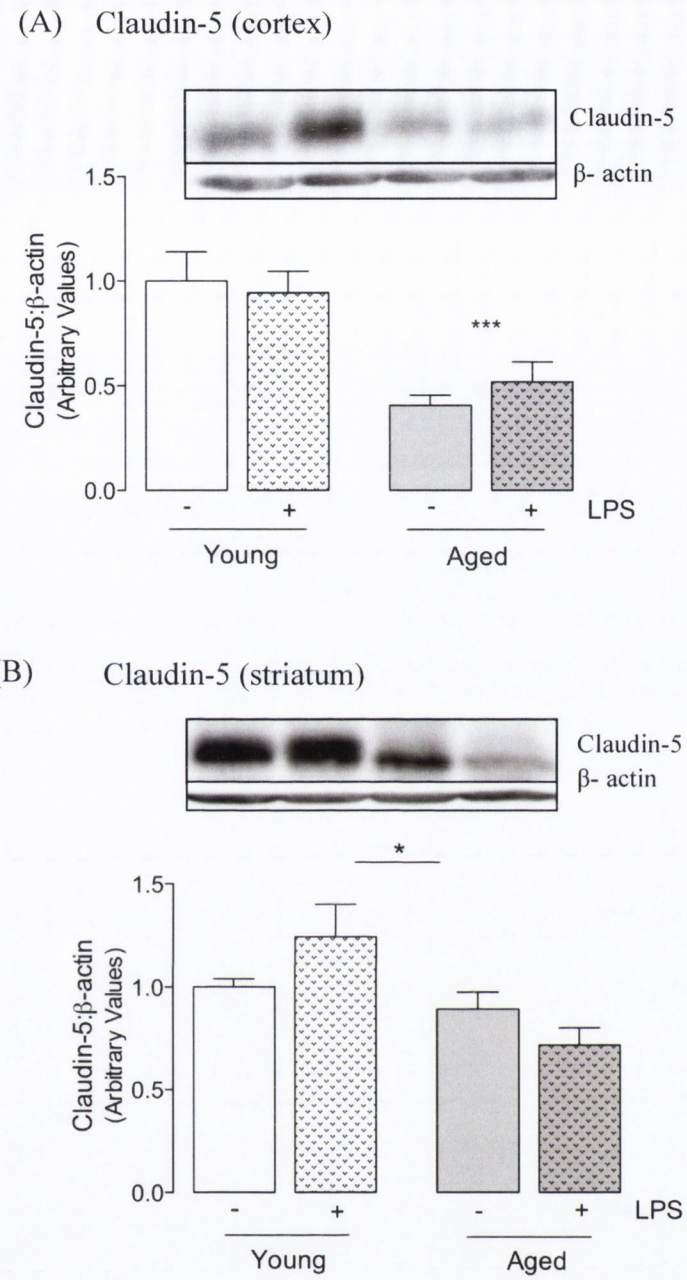

Figure 4.1: The age-related decrease in claudin-5 protein concentration in the striatum was exacerbated by LPS treatment.

There was a significant decrease in claudin-5 in both the aged rat cortex (A) and striatum (B) and LPS (100μg/kg) treatment did not enhance this effect. Data expressed as mean ± SEM, n=5-6; # # $p<0.01$ versus young rats, *** $p<0.001$ versus young rats; two-way ANOVA followed by *post-hoc* Bonferroni test.

(A) Two-way ANOVA: Age $_{effect}$ F (1,16) = 20.28; p = 0.0004, LPS $_{effect}$ F (1,16) = 0.05894; p = 0.8113, Interaction $_{effect}$ F (1,16) = 0.5465; p = 0.4704.

(B) Two-way ANOVA: Age $_{effect}$ F (1,13) = 11.15; p = 0.0053, LPS $_{effect}$ F (1,13) = 0.1279; p = 0.7263, Interaction $_{effect}$ F (1,13) = 4.859; p = 0.0461.

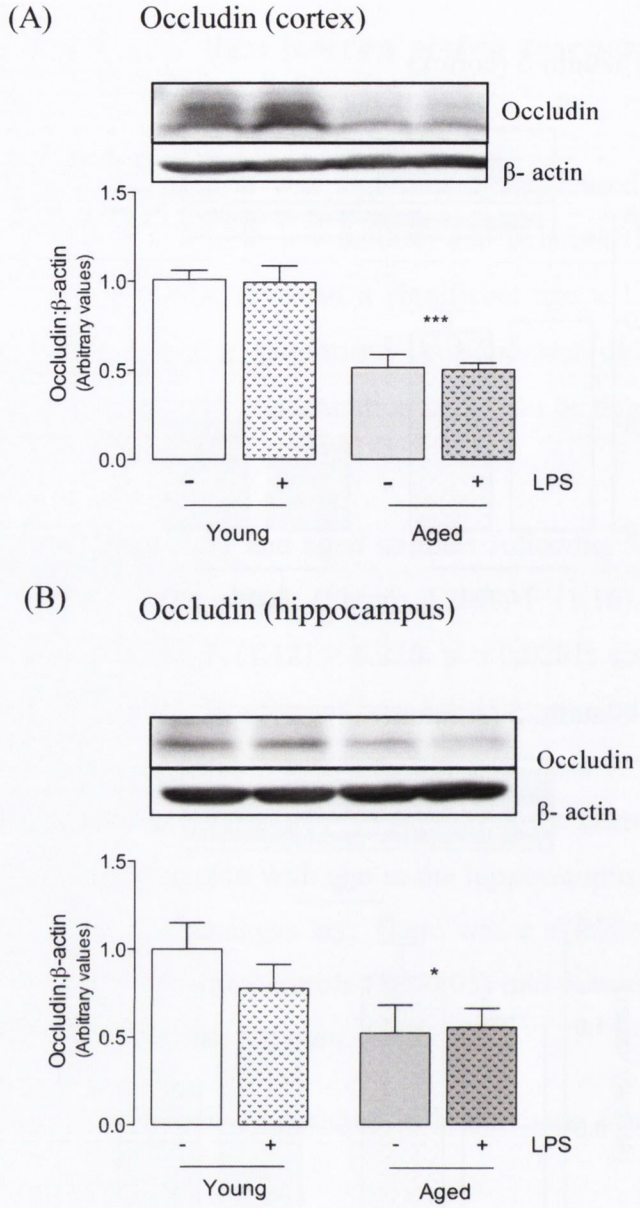

Figure 4.2: The age-related decrease in occludin protein concentration in the rat cortex and hippocampus was not exacerbated by LPS treatment.

There was a significant decrease in occludin in the aged rat cortex (A) and hippocampus (B) compared with young animals in both saline and LPS-treated groups. This result was not enhanced by LPS (100μg/kg) treatment. Data expressed as mean ± SEM, n=4-5; *** $p<0.001$ versus young animals; * $p<0.05$ versus young animals; two-way ANOVA followed by *post-hoc* Bonferroni test.

(A) Two-way ANOVA: Age $_{effect}$ $F(1,16) = 53.44$; $p = <0.0001$, LPS $_{effect}$ $F(1,16) = 0.04332$; $p = 0.8378$, Interaction $_{effect}$ $F(1,16) = 0.001632$; $p = 0.9683$.

(B) Two-way ANOVA: Age $_{effect}$ $F(1,12) = 6.230$; $p = 0.0281$, LPS $_{effect}$ $F(1,12) = 0.4600$; $p = 0.5105$, Interaction $_{effect}$ $F(1,12) = 0.8398$; $p = 0.3775$.

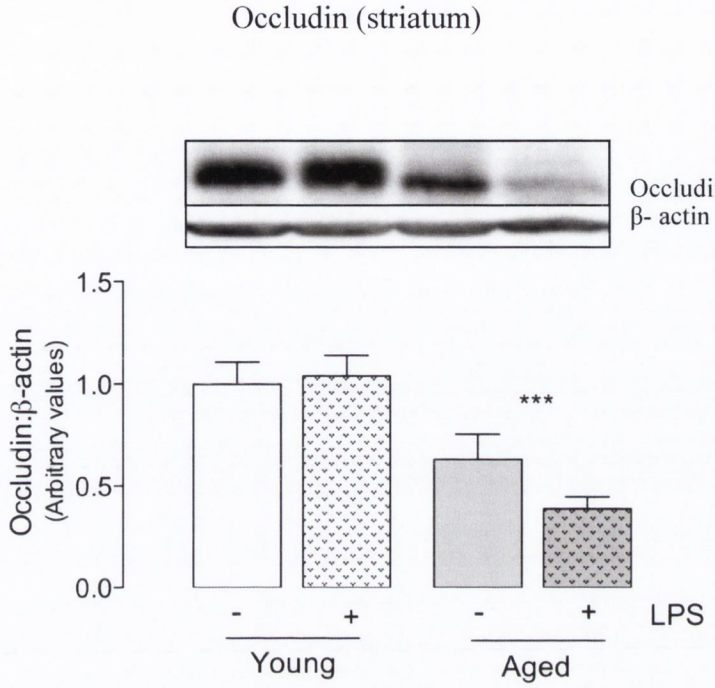

Figure 4.3: The age-related decrease in occludin protein concentration in the rat striatum was not exacerbated by LPS treatment.

There was a significant decrease in occludin in the aged rat striatum compared with both young saline- and LPS-treated groups. This result was not enhanced by LPS (100μg/kg) treatment. Data expressed as mean ± SEM, n=5; ***$p<0.001$ versus young animals; two-way ANOVA followed by *post-hoc* Bonferroni test.

Two-way ANOVA: Age $_{effect}$ $F(1,14) = 24.75$; $p = 0.0002$, LPS $_{effect}$ $F(1,14) = 0.9638$; $p = 0.3429$, Interaction $_{effect}$ $F(1,14) = 1.915$; $p = 0.1881$.

4.4 The effect of LPS on laminin and PDGFR-β protein concentration in young and aged rat brain

A significant age effect on laminin protein concentration was detected in the hippocampus (Figure 4.4 B; $F(1,17) = 24.04$; $p = 0.0001$) and striatum (Figure 4.5; $F(1,13) = 14.97$; $p = 0.0019$), though the age effect was not significant in the cortex (Figure 4.4 A; $F(1,12) = 3.968$; $p = 0.0696$). Bonferroni *post-hoc* tests revealed a significant decrease in laminin in hippocampus when saline-treated young animals were compared to saline-treated aged animals (**$p<0.01$) and also when LPS-treated young and aged animals (**$p<0.01$) were compared. Similar results were obtained following *post-hoc* tests in the striatum when either saline-treated young and aged animals (*$p<0.05$) or LPS-treated young and aged animals (*$p<0.05$), were compared. LPS did not have an effect in the cortex or the hippocampus but there was a significant LPS effect in the striatum (Figure 4.5; $F(1,13) = 8.635$; $p = 0.0115$). Although bonferroni *post-hoc* tests could not establish where this LPS effect lay but the corresponding immunoblots indicated that treatment with LPS further decreased laminin protein concentration, particularly in the aged cohort.

Analysis of PDGFR-β protein concentration revealed a significant effect of age in the cortex (Figure 4.6 A; $F(1,12) = 5.126$; $p = 0.0429$), hippocampus (Figure 4.6 B; $F(1,16) = 18.97$; $p = 0.0005$) and striatum (Figure 4.7; $F(1,15) = 5.728$; $p = 0.0302$). Bonferroni *post-hoc* tests revealed a significant decrease in PDGFR-β between saline-treated young and aged hippocampus (*$p<0.05$) and between LPS-treated young and aged hippocampus (**$p<0.01$).

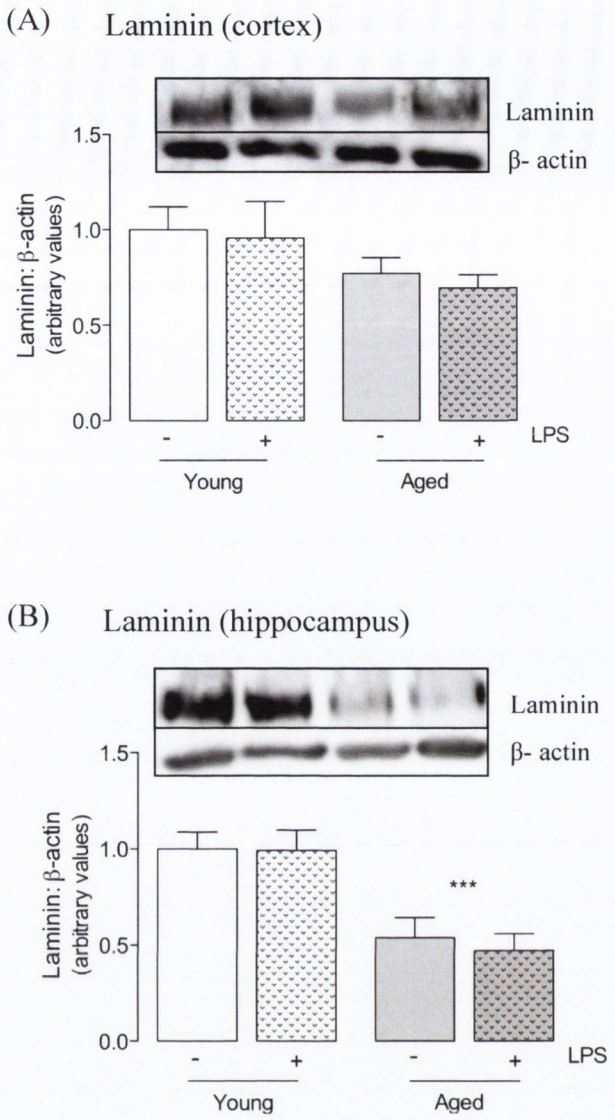

Figure 4.4: The age-related decrease in laminin protein concentration in the rat cortex and hippocampus was not exacerbated by LPS treatment.

There was a significant decrease in laminin protein concentration in hippocampus from aged, compared with young, animals in both saline- and LPS-treated groups. This effect was not enhanced by LPS (100μg/kg) treatment. While there was a decrease in laminin in the aged cortex, this change did not reach statistical significance. Data expressed as mean ± SEM, n=4-6; *** $p<0.01$ versus young animals; two-way ANOVA followed by *post-hoc* Bonferroni test.

(A) Two-way ANOVA: Age $_{effect}$ $F(1,12) = 3.968$; $p = 0.0696$, LPS $_{effect}$ $F(1,12) = 0.2394$; $p = 0.6335$, Interaction $_{effect}$ $F(1,12) = 0.01856$; $p = 0.8939$.

(B) Two-way ANOVA: Age $_{effect}$ $F(1,17) = 24.04$; $p = 0.0001$, LPS $_{effect}$ $F(1,17) = 0.1325$; $p = 0.7203$, Interaction $_{effect}$ $F(1,17) = 0.09057$; $p = 0.7671$.

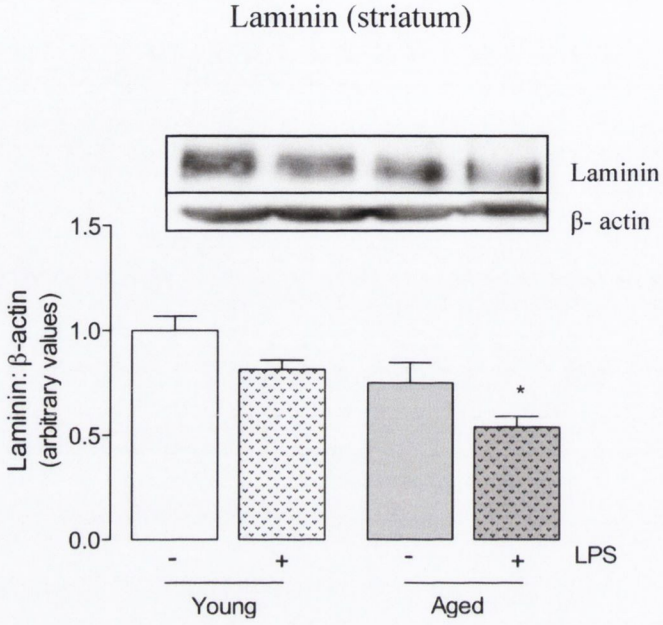

Figure 4.5: The age-related decrease in laminin protein concentration in the rat striatum was enhanced by LPS treatment.

Laminin was significantly decreased in the aged rat striatum compared with young animals. This effect was significantly enhanced with LPS (100μg/kg) treatment. Data expressed as mean ± SEM, n=4-5; * $p<0.05$ versus LPS-treated young animals; two-way ANOVA followed by *post-hoc* Bonferroni test.

Two-way ANOVA: Age $_{effect}$ $F(1,13) = 14.97$; $p = 0.0019$, LPS $_{effect}$ $F(1,13) = 8.635$; $p = 0.0115$, Interaction $_{effect}$ $F(1,13) = 0.03609$; $p = 0.8523$.

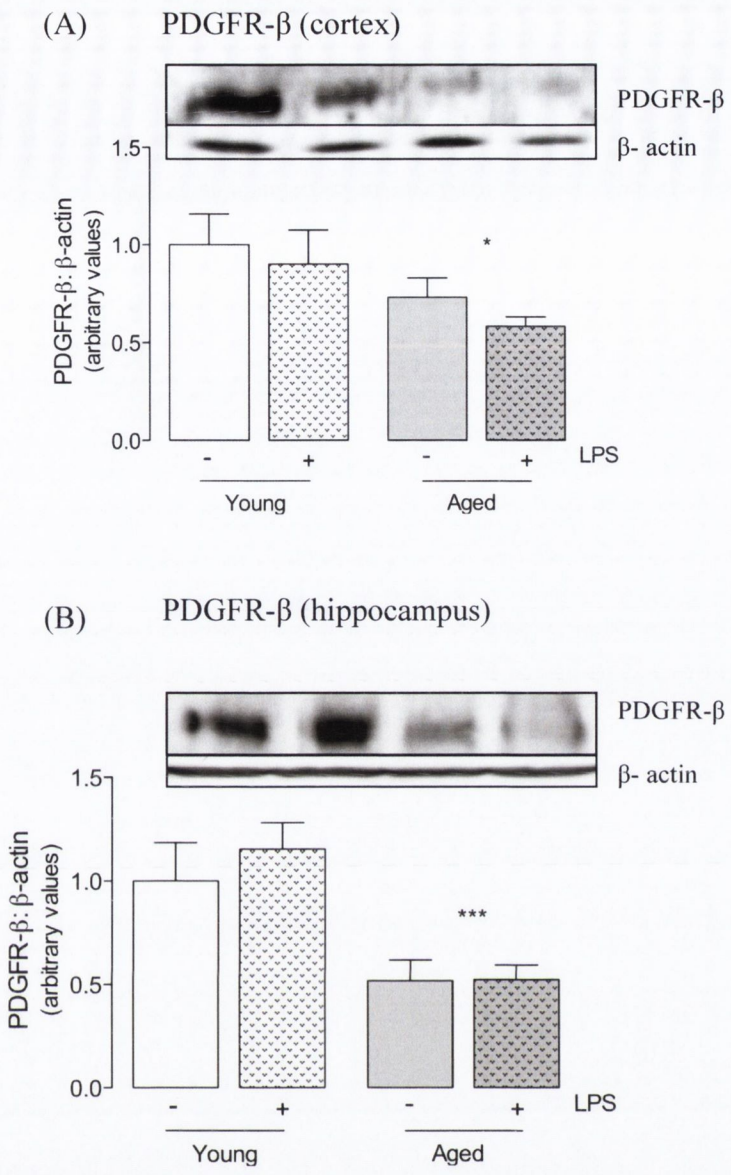

Figure 4.6: The age-related decrease in PDGFR-β protein concentration in the rat cortex and hippocampus was not exacerbated by LPS treatment.

There was a significant decrease in PDGFR-β in both the aged rat cortex (A) and hippocampus (B) compared with young animals in both saline- and LPS-treated groups. This effect was not enhanced by LPS (100μg/kg) treatment. Data expressed as mean ± SEM, n=4-5; * $p<0.05$ versus young animals, *** $p<0.001$ versus young animals; two-way ANOVA followed by *post-hoc* Bonferroni test.

(A) Two-way ANOVA: Age $_{effect}$ $F(1,12) = 5.126$; $p = 0.0429$, LPS $_{effect}$ $F(1,12) = 0.9025$; $p = 0.3609$, Interaction $_{effect}$ $F(1,12) = 0.03880$; $p = 0.8471$.

(B) Two-way ANOVA: Age $_{effect}$ $F(1,16) = 18.97$; $p = 0.0005$, LPS $_{effect}$ $F(1,16) = 0.4004$; $p = 0.5358$, Interaction $_{effect}$ $F(1,16) = 0.3377$; $p = 0.5693$.

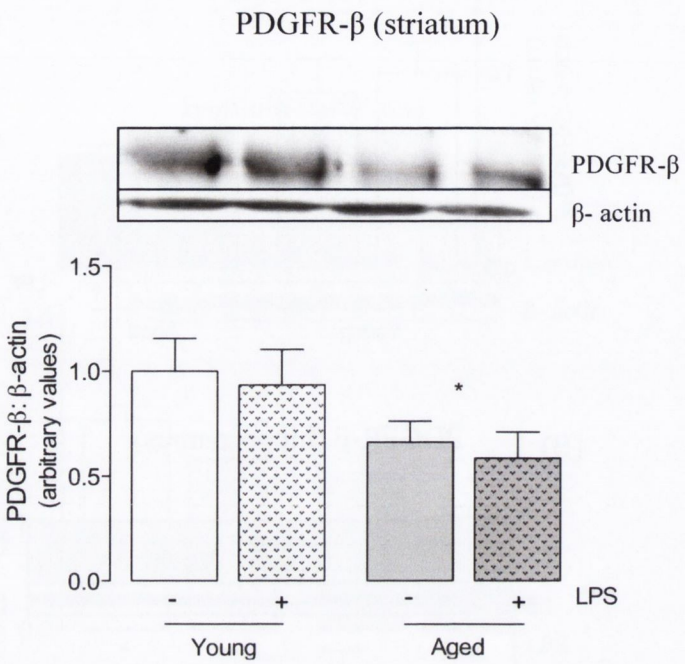

Figure 4.7: The age-related decrease in PDGFR-β protein concentration in the rat striatum was not exacerbated by LPS treatment.

PDGFR-β was significantly decreased in the aged rat striatum compared with young animals. This effect was not enhanced by LPS (100μg/kg) treatment. Data expressed as mean ± SEM, n=4-5; * $p<0.05$ versus young animals; two-way ANOVA followed by *post-hoc* Bonferroni test.

Two-way ANOVA: Age $_{effect}$ $F(1,15) = 5.728$; $p = 0.0302$, LPS $_{effect}$ $F(1,15) = 0.2426$; $p = 0.6295$, Interaction $_{effect}$ $F(1,15) = 0.001754$; $p = 0.9671$.

4.5 The effect of LPS on TLR4 protein concentration in the young and aged rat brain

As LPS signals via TLR4 we investigated whether TLR4 protein concentration was modulated by either age or LPS. Though the effect of age on TLR4 was not significant in the hippocampus (Figure 4.8 A; $F(1,18) = 3.149$; $p = 0.0929$), there was a significant age effect evident in the striatum (4.8 B; $F(1,14) = 7.809$; $p = 0.0143$). ANOVA did not detect a significant LPS effect in either tissue. TLR4 protein concentration could not be detected in samples of cortex from this cohort (see Appendix 3).

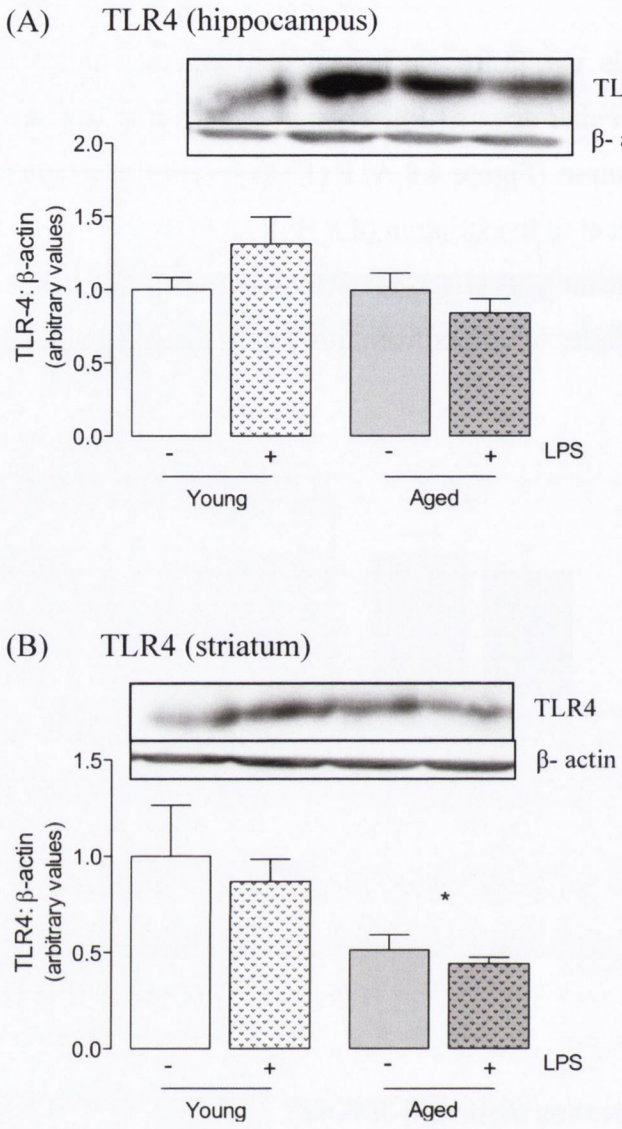

Figure 4.8: The age-related decrease in TLR4 protein concentration in the rat hippocampus and striatum was not exacerbated by LPS treatment.

There was a significant decrease in TLR4 in the aged rat striatum (B) compared with young animals in both control- and LPS-treated groups. This effect was not enhanced by LPS (100μg/kg) treatment. TLR4 was not significantly decreased in the aged hippocampus (A). Data expressed as mean ± SEM, n=5-6; * $p<0.05$ versus young groups; two-way ANOVA followed by *post-hoc* Bonferroni test.

(A) Two-way ANOVA: Age $_{effect}$ $F(1,18) = 3.149$; $p = 0.0929$, LPS $_{effect}$ $F(1,18) = 0.3264$; $p = 0.5749$, Interaction $_{effect}$ $F(1,18) = 0.3056$; $p = 0.0978$.

(B) Two-way ANOVA: Age $_{effect}$ $F(1,14) = 7.809$; $p = 0.0143$, LPS $_{effect}$ $F(1,14) = 0.03093$; $p = 0.8629$, Interaction $_{effect}$ $F(1,14) = 0.1256$; $p = 0.7284$.

4.6 PECAM protein concentration in young and middle-aged wildtype and IL-1R1$^{-/-}$ mice

It has been reported that vascular density decreases with age (Shah & Mooradian, 1997) so we set out to determine if there were any differences in endothelial numbers in wildtype and IL-1R1$^{-/-}$ mice. It was important to establish this so that any possible alterations in endothelial tight junction protein concentration were not a result of differences in endothelial numbers. The protein concentration of the abundant endothelial cell marker, PECAM, was assessed in hippocampus from young and middle-aged C57 wildtype and IL-1R1$^{-/-}$ mice. ANOVA did not reveal any effect of age (Figure 4.9; F (1,18) = 0.5466; p = 0.4692) or genotype (F (1,18) = 0.5197; p = 0.4802) on PECAM.

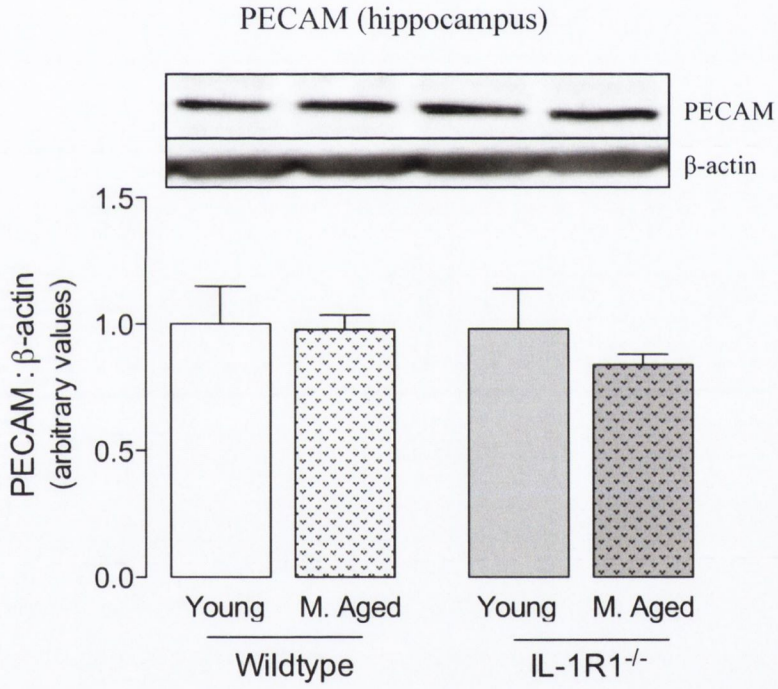

Figure 4.9: PECAM protein concentration was not altered by age or genotype.

There were no significant changes in PECAM between wildtype and IL-1R1$^{-/-}$ mice, irrespective of age. Data expressed as mean ± SEM, n=4-7; two-way ANOVA followed by *post-hoc* Bonferroni test.

Two-way ANOVA: Age $_{effect}$ F (1,18) = 0.5466; p = 0.4692, Genotype $_{effect}$ F (1,18) = 0.5197; p = 0.4802, Interaction $_{effect}$ F (1,18) = 0.2965; p = 0.5928.

4.7 Assessment of BBB permeability in young and middle-aged wildtype and IL-1R1$^{-/-}$ mice

A relative increase in the brain parenchyma of the endogenous plasma protein, albumin (65 kDa), was taken to indicate that there was increased extravasation from the vasculature to the brain and hence, increased permeability. However, ANOVA did not reveal any effect of age (Figure 4.10; F (1,18) = 0.2703; p = 0.1175) or genotype (F (1,18) = 0.001341; p = 0.9712) on albumin expression.

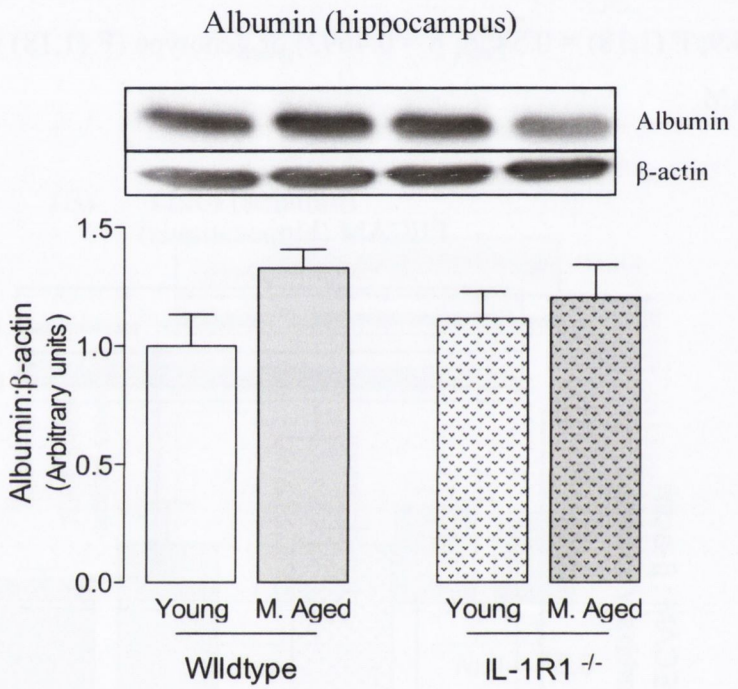

Figure 4.10: Albumin protein concentration was not altered by age or genotype.

There were no significant changes in albumin levels between wildtype and IL-1R1$^{-/-}$ mice, irrespective of age. Data expressed as mean ± SEM, n=5-7; two-way ANOVA followed by *post-hoc* Bonferroni test.

Two-way ANOVA: Age $_{effect}$ F (1,18) = 0.2703; p = 0.1175, Genotype $_{effect}$ F (1,18) = 0.001341; p = 0.9712, Interaction $_{effect}$ F (1,18) = 0.8899; p = 0.3580.

4.8 Assessment of tight junction proteins in young and middle-aged wildtype and IL-1R1$^{-/-}$ mice

Tight junction proteins are modulated by age (Chapter 3) and by pro-inflammatory cytokines e.g. IL-1β (Al-Sadi *et al.*, 2010), so tight junction protein concentration in young and middle-aged C57 wildtype and IL-1R1$^{-/-}$ mice was investigated. More specifically, claudin-5, occludin and ZO-1 protein expression was assessed in hippocampus by Western immunoblotting.

ANOVA revealed that claudin-5 expression was significantly affected by both age (Figure 4.11; $F(1,17) = 6.908$; $p = 0.0176$) and genotype ($F(1,17) = 6.144$; $p = 0.0240$) which resulted in a significant age x genotype effect ($F(1,17) = 7.461$; $p = 0.0142$). Bonferroni *post-hoc* tests further established that claudin-5 was significantly increased (**$p<0.01$) in the middle-aged but not the young IL-1R1$^{-/-}$ mice when compared with their wildtype counterparts.

Genotype had an effect on occludin protein concentration when wildtype and IL-1R1$^{-/-}$ mice were compared (Figure 4.12; $F(1,19) = 10.06$; $p = 0.0050$) though there were no significant age-related differences ($F(1,19) = 2.222$; $p = 0.1524$).

Similarly, genotype but not age also impacted on ZO-1 protein concentration (Figure 4.13; $F(1,19) = 11.78$; $p = 0.0028$ and $F(1,19) = 0.1129$; $p = 0.7405$, respectively) where ZO-1 levels were decreased in the IL-1R1$^{-/-}$ mice. This reduction was particularly apparent in the young IL-1R1$^{-/-}$ mice, as indicated by Bonferroni *post-hoc* tests (**$p<0.01$).

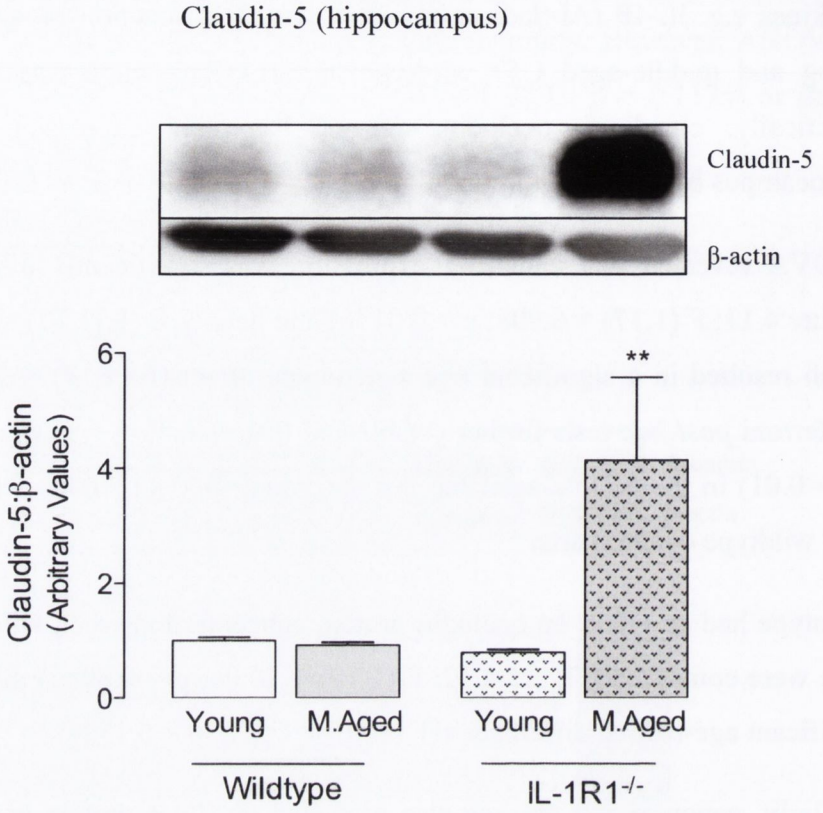

Figure 4.11: Claudin-5 protein concentration was significantly increased in middle-aged IL-1R1$^{-/-}$ mice.

Claudin-5 protein concentration was significantly increased in IL-1R1$^{-/-}$ mice compared with their wildtype counterparts. Data expressed as mean ± SEM, n=5-6; **p<0.01 versus middle-aged wildtype mice; two-way ANOVA followed by *post-hoc* Bonferroni test.

Two-way ANOVA: Age $_{effect}$ F (1,17) = 6.908; p = 0.0176, Genotype $_{effect}$ F (1,17) = 6.144; p = 0.0240, Interaction $_{effect}$ F (1,17) = 7.461; p = 0.0142.

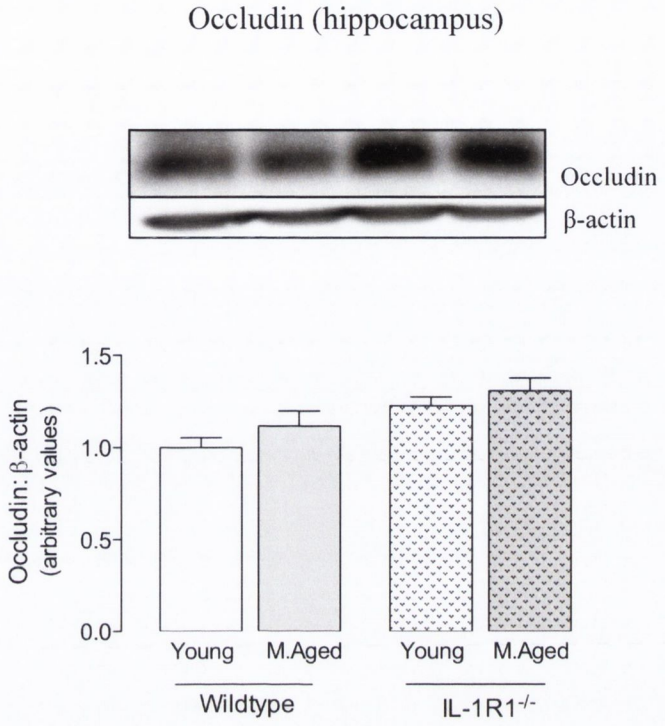

Figure 4.12: Occludin protein concentration was increased in IL-1R1$^{-/-}$ mice.

Occludin protein concentration was increased in IL-1R1$^{-/-}$ mice compared with wildtype mice, in both young and middle-aged animals. Data expressed as mean ± SEM, n=5-7; two-way ANOVA followed by *post-hoc* Bonferroni test.

Two-way ANOVA: Age $_{effect}$ F (1,19) = 2.222; p = 0.1524, Genotype $_{effect}$ F (1,19) = 10.06; p = 0.0050, Interaction $_{effect}$ F (1,19) = 0.07440; p = 0.7880.

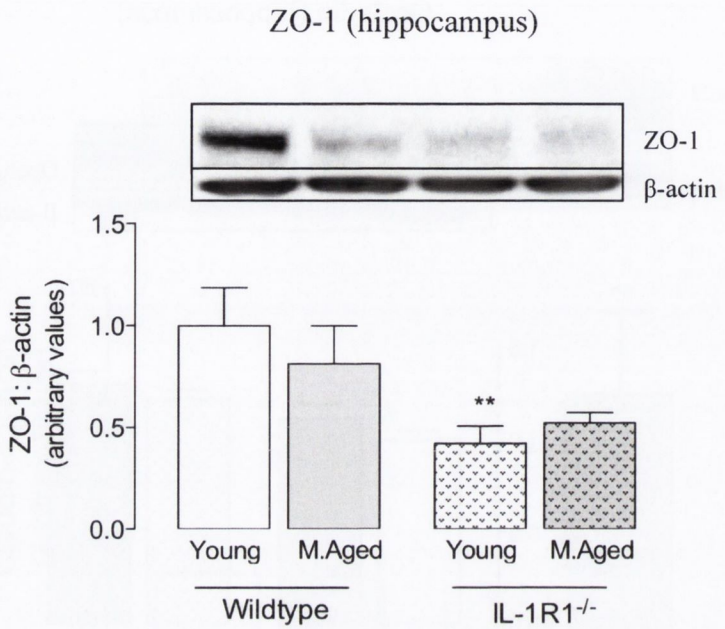

Figure 4.13: ZO-1 protein concentration was decreased in IL-1R1$^{-/-}$ mice.

ZO-1 protein concentration was significantly decreased in young IL-1R1$^{-/-}$ mice compared with wildtype animals (**p<0.01). While there was a tendency for ZO-1 to decrease in middle-aged IL-1R1$^{-/-}$ mice, it was not significant following *post-hoc* analysis. Data expressed as mean ± SEM, n=5-7; **p<0.01 versus young wildtype; two-way ANOVA followed by *post-hoc* Bonferroni test.

Two-way ANOVA: Age $_{effect}$ F (1,19) = 0.1129; p = 0.7405, Genotype $_{effect}$ F (1,19) = 11.78; p = 0.0028, Interaction $_{effect}$ F (1,19) = 1.301; p = 0.2682.

4.9 Assessment of laminin and PDGFR-β protein concentration in young and middle-aged wildtype and IL-1R1$^{-/-}$ mice

Concentration of proteins of the NVU, namely laminin and PDGFR-β, were modulated with age (Chapter 3). Here, the additional contribution of IL-1β signalling was investigated in hippocampus from young and middle-aged wildtype and IL-1R1$^{-/-}$ mice.

Laminin is a key component of the basal lamina and laminin protein concentration was decreased in IL-1R1$^{-/-}$ mice (Figure 4.14; F (1,19) = 6.545; p = 0.0192) though these changes were not altered by age (F (1,19) = 0.6652; p = 0.4248).

The pericyte marker PDGFR-β was not significantly altered by age (Figure 4.15; F (1,19) = 0.8182; p = 0.3770) or genotype (F (1,19) = 0.2898; p = 0.5966).

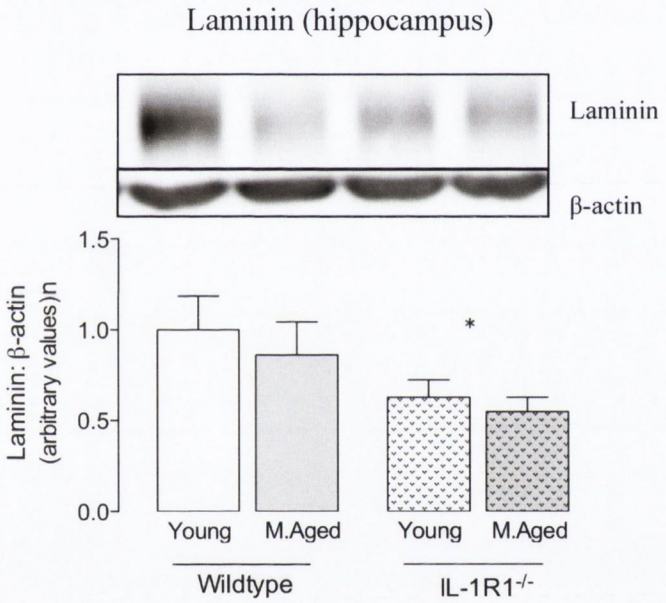

Figure 4.14: Laminin protein concentration was decreased in IL-1R1$^{-/-}$ mice.

Laminin protein concentration was significantly decreased in IL-1R1$^{-/-}$ mice compared with wildtype animals. Data expressed as mean ± SEM, n=5-7; ∗p<0.05 versus wildtype mice; two-way ANOVA followed by *post-hoc* Bonferroni test.

Two-way ANOVA: Age $_{effect}$ F (1,19) = 0.6652; p = 0.4248, Genotype $_{effect}$ F (1,19) = 6.545; p = 0.0192, Interaction $_{effect}$ F (1,19) = 0.04852; p = 0.8280.

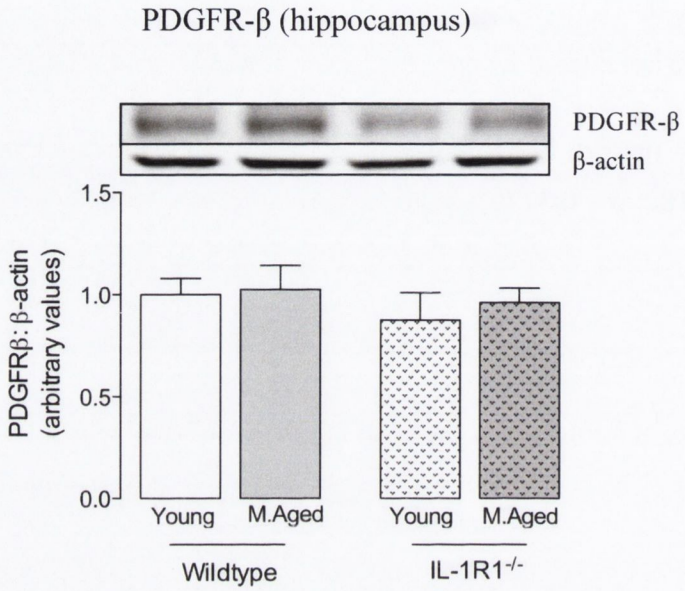

Figure 4.15: PDGFR-β protein concentration was not altered by age or genotype.

PDGFR-β protein concentration was unchanged in IL-1R1$^{-/-}$ mice compared with wildtype animals, irrespective of age. Data expressed as mean ± SEM, n=5-7; two-way ANOVA followed by *post-hoc* Bonferroni test.

Two-way ANOVA: Age $_{effect}$ F (1,19) = 0.8182; p = 0.3770, Genotype $_{effect}$ F (1,19) = 0.2898; p = 0.5966, Interaction $_{effect}$ F (1,19) = 0.08314; p = 0.7762.

4.10 Discussion

The previous chapter reported that tight junction proteins were modified with age and that there was increased BBB permeability leading to permeation of both small molecules and large plasma proteins, into the aged rat brain.

The first aim of this chapter was to investigate the effects of systemic inflammation on the young and aged BBB. The overall objective was to establish if an additional inflammatory insult, as often occurs with age, could exacerbate damage to an already fragile ageing BBB. LPS, a bacterial endotoxin, was injected systemically and used as a stimulus to trigger an inflammatory response in young and aged rats. TLR4, the receptor for LPS, is highly expressed on cerebral endothelial cells (Dauphinee & Karsan, 2006; Zhou *et al.*, 2009).

While there were age-related reductions in tight junction protein expression in this study, supporting our results presented in Chapter 3, there was no further exacerbation (in the main) by LPS.

This was quite surprising as there are many studies documenting the disruptive effects of LPS on the *in vivo* BBB (Xaio *et al.*, 2001; Erickson *et al.*, 2012) and *in vitro* models of the BBB (Xiaolu *et al.*, 2011; Cardoso *et al.*, 2012). The literature regarding the disruptive effects of LPS on barrier function is quite varied in both *in vitro* and *in vivo* experiments. Throughout the literature pertaining to BBB permeability, there are wide-ranges of LPS doses administered over varied time-courses. Thus, it is difficult to confirm the best course of LPS administration and as of yet, there is no "standard" experimental design for LPS treatment. There are a number of possibilities that could have resulted in the limited LPS disruption at the BBB observed in this study.

The ageing BBB is functionally disrupted, facilitating even the entry of plasma proteins into brain parenchyma (Chapter 3). It is possible LPS did not further disrupt tight junctions at the ageing BBB because they had reached a basal plateau. Extending this line of thought, LPS may not have affected the young BBB because the endothelial cells are still healthy and capable of withstanding an insult. This is a possibility when one considers the primary function of the cerebral endothelium is to limit disturbance to the CNS. The differential effect of LPS on claudin-5 and occludin in the striatum of young and aged rats would favour this explanation as the interaction effect, combined with the immunoblots which showed that LPS caused an increase in claudin-5 expression in the

young animals, but a reduction in the aged LPS-treated rats. It is possible that the endothelial cells of young animals retain the capacity to protect themselves when faced with a potential toxin, an attribute that is not present in the aged animal. Following this line of thought, it has been shown that comparable traumatic brain injury in young and aged C57 mice resulted in significantly greater BBB permeability and claudin-5 disruption in the aged animals, indicating reduced protective capacity of the aged cerebral endothelial cells (Lee *et al.*, 2012). In addition, it has been observed that senescent human umbilical vein endothelial cells were more susceptible to oxidative damage *in vitro* (Carlisle *et al.*, 2002). Another *in vitro* study reported that aged pulmonary endothelial cells were more susceptible to apoptosis induced following the co-incubation with a breast cancer cell line. Though both studies involve endothelial cultures, they support the idea that aged endothelial cells are more vulnerable to damage (Merkle *et al.*, 2005).

The dose of LPS administered to the animals in this study was quite low (100μg/kg) when compared with most of the literature that administers LPS by intraperitoneal injection, and perhaps was not a potent enough stimulus to modulate the tight junction proteins. However, despite this, LPS did provoke an inflammatory response in the same animals (see Appendix 4, p.212). Other *in vivo* studies that observed barrier disruption following a systemic LPS injection administered a dose of 3mg/kg (Xaio *et al.*, 2001; Jaeger *et al.*, 2009; Erickson *et al.*, 2012). A single acute injection of LPS at such a low dose may also be inadequate to disrupt the barrier as it has been shown that rats that received a single high-dose injection of LPS (1mg/kg) did not show altered BBB permeability. However animals that received a prolonged chronic stimulus (0.2mg/kg every 2 days for 10 days) displayed increased BBB permeability to plasma molecules (Stolp *et al.*, 2005). In another *in vivo* study it was noted that although a single dose of LPS (3mg/kg) caused increased BBB permeability in rats, the results were very varied. When multiple LPS injections were administered (i.p. 0, 6, 24 h) it produced a more pronounced BBB disruption and the results were less variable (Xaio *et al.*, 2001). Further support for the suggestion that a single dose of 100 μg/kg was too low is supported by Zhou *et al.*, (2009) who noted that 500 μg/kg of LPS administered intraperitoneally caused increased neutrophil adhesion to cerebral endothelial vessels though the neutrophils were still restricted from entering the brain parenchyma.

Extravasation of leukocytes into the brain parenchyma, indicating BBB disruption, was not observed until higher doses (2-10 mg/kg) of LPS were administered.

It was thought that sacrificing animals 4 hours following LPS administration might be an appropriate timepoint to observe BBB changes because based on the literature, the downstream consequences of LPS signalling e.g. release of pro-inflammatory cytokines, peaks in the 3-6 hour timeframe (Nadeau & Rivest, 1999). However, *in vitro* studies have observed that LPS induced the disruption of tight junctions by 3 hours post injection (Xiaolu *et al.*, 2011) and *in vivo* studies have noted BBB disruption at 4 hours post-injection (Zhou *et al.*, 2009), suggesting that BBB changes can occur by 4 hours. Although, in an *in vitro* model of the BBB, did not detect permeability changes in primary human brain endothelial cells until 18-24 hours post LPS treatment (Wong *et al.*, 2004).

Some *in vitro* studies have reported that although overall tight junction expression did not change following LPS treatment, there were disruptions to the subcellular localisation of claudin, occludin and ZO-1, where the proteins were internalised away from the cell membrane (Yi *et al.*, 2000; Schlegel *et al.*, 2009; Xiaolu *et al.*, 2011; Cardoso *et al.*, 2012). Tissue sections were not available in our study so in future, it would be desirable to investigate the *in situ* localisation of tight junctions with confocal microscopy.

Endothelial cells are located at the interface between the blood and the brain and therefore are the principal cells susceptible to systemic insults. That endothelial cells exposed to LPS might modulate TLR4 expression was investigated because down regulated endothelial TLR4 expression might account for the limited effect of LPS on tight junction protein expression. Downregulation of TLR4 expression could be a protective mechanism to prevent unwarranted damage to the CNS during a systemic insult and this type of response is considered an important homeostatic measure from an evolutionary perspective (Miggin & O'Neill, 2006). In healthy gut epithelia there is limited TJ disruption by LPS and this is facilitated by the LPS-induced downregulation of TLR4 and its adaptor protein MD-2 (Abreu *et al.*, 2001). This adaptive response prevents chronic inflammation and tight junction disruption which underlies inflammatory bowel disorder such as Crohn's disease and irritable bowel disease (Al-Sadi *et al.*, 2008). It was hypothesized that similar responses may occur in cerebral

endothelium in response to low-dose LPS treatment. However, results from this research indicate that TLR4 expression was not significantly altered by systemic LPS, though expression levels were decreased with age. Our study investigated TLR4 expression in whole hippocampal homogenates and one cannot rule out the possibility that there was endothelial-specific downregulation of TLR4 which might be better assessed by flow cytometry, had the tissue been available.

Laminin and PDGFR-β expression levels were decreased with age, a finding that replicated the results described in Chapter 3. LPS disrupted the basal lamina as evidenced by decreased laminin protein expression in young and aged rats. Interestingly this change was only observed in the striatum, the anatomical area that also revealed the LPS-induced reduction in claudin-5 expression. LPS-mediated disruption of the NVU has been described; mice that were administered LPS systemically (20mg/kg) significant BBB breakdown was evident with the extravasation of sodium fluorescein and plasma proteins to the brain parenchyma. These changes in BBB permeability were accompanied with significant basal lamina fragmentation that was apparent 6 hours post-LPS injection (Nishioku *et al.*, 2009).

In our study, LPS was administered at a lower dose (100μg/kg) than is often used in the literature (3mg/kg). Whilst one cannot exclusively say LPS does not have a detrimental effect on young and aged tight junction protein expression, it is clear that at low doses, the damage is limited. This would be an appropriate response to systemic insult in order to minimise unwarranted CNS disruption and is key in maintaining BBB homeostasis.

Neuroinflammation is thought to be a major factor in contributing to the normal ageing of the brain and also to the pathogenesis of age-related neurodegenerative diseases like AD (Blasko *et al.*, 2004; Godbout *et al.*, 2005; Lynch, 2010). IL-1β is known to contribute to BBB damage in a multitude of conditions including MS and stroke, in addition to neurodegenerative diseases such AD and PD (Capaldo & Nusrat, 2009), possibly by its effects on the cerebral vasculature (Allan & Rothwell, 2001). Despite the evidence of IL-1β being a contributor to neurodegenerative diseases, and that it is known to modulate barrier permeability both in the PNS and CNS, there is very little literature on the specific effects of IL-1β on the ageing BBB. The second aim of this chapter was to assess the specific impact of IL-1β signalling on the aged BBB. To

address this, assessments were made in hippocampus from young and middle-aged C57 wildtype and IL-1R1$^{-/-}$ mice.

The tight junction proteins claudin-5 and occludin were significantly increased in the IL-1R1$^{-/-}$ animals when compared with their age-matched wildtype counterparts. Interestingly, claudin-5 expression was differentially affected in the young and middle-aged IL-1R1$^{-/-}$ mice, being significantly increased in the middle-aged but not young IL-1R1$^{-/-}$. Occludin however was significantly increased in both the young and middle-aged IL-1R1$^{-/-}$. These findings suggest an inflammatory basis to the age-related BBB disruption, mediated by IL-1 signalling. A number of studies have assessed the effect of IL-1β on barrier function *in vivo*. IL-1β adenovirus induced increased BBB permeability to fibrinogen in the cortex of adult rats by about 14 days post-treatment (Argaw *et al.*, 2006) and a striatal injection of IL-1β increased BBB permeability in 3-week-old rats, though the BBB was returned to control conditions by 24 hours (Blamire *et al.*, 2000). One particular study, (Ching *et al.*, 2005) investigated the effect of IL-1β on BBB permeability in IL-1R1$^{-/-}$ mice. (Ching *et al.*, 2005) first found that intracerebroventricular injection of IL-1β caused leukocyte infiltration to the brains of wildtype but not IL-1R1$^{-/-}$ mice, though the BBB disruption was diminished by 72 hours post-injection. In a later study, the same research group created endothelial specific knockdown of the IL-1R1 in mice (eIL-1R1$^{-/-}$) and found that intracerebroventricular injection of IL-1β again caused leukocyte infiltration to brain in non-transgenic littermates of eIL-1R1$^{-/-}$ but that these BBB changes were not present in the eIL-1R1$^{-/-}$ animals (Ching *et al.*, 2007). These results confirm that IL-1β is indeed capable of dramatically disrupting BBB permeability by its direct actions on endothelial cells. It may be the case that administering IL-1β and not LPS, as an inflammatory challenge, produces more consistent results when assessing BBB permeability.

Most of the literature documents the effects of IL-1β on brain permeability following a single administration of IL-1β (permeability returning to normal within 24-72 hours post-treatment). The findings from these acute studies are not necessarily reflective of/cannot be extrapolated to the chronic neuroinflammation present in the aged brain. However, a recent study investigated the effects of chronically over-expressing IL-1β in the brains of transgenic mice (Shaftel *et al.*, 2007). The sustained IL-1β expression resulted in increased BBB permeability to leukocytes for up to one-year and may be more reflective of the sustained IL-1β expression in the aged brain. Despite the

widespread acceptance that IL-1β increases BBB permeability, few of the studies above have extended their investigations to the effects of IL-1β on the tight junction proteins, and whether the increased BBB permeability is as a direct consequence of disrupted tight junction protein expression. In the CNS, decreased TEER was observed in cultured human corneal epithelial cells following IL-1β treatment and whilst tight junction protein concentration was unchanged, the subcellular localisation of occludin and ZO-1 was disrupted (Kimura *et al.*, 2009). In the periphery, the barrier properties of Caco-2 epithelial cells were dramatically decreased following IL-1β (10ng/ml) treatment (Al-Sadi & Ma, 2007) and this was attributed to the MEKK-mediated downregulation of occludin and claudin-1 (Al-Sadi *et al.*, 2010).

There were no significant changes in ZO-1 expression in aged compared with young rats in the previous chapter. IL-1R1$^{-/-}$ significantly increased claudin-5 and occludin in the middle-aged mice, suggesting IL-1β was indeed having a negative effect on these proteins with age. Interestingly, ZO-1 expression was significantly decreased in the IL-1R1$^{-/-}$ mice, suggesting that IL-1 signalling may have a beneficial impact on this endothelial protein. These findings somewhat contradict previous studies, both *in vivo* and *in vitro*, where IL-1β either changed the subcellular localisation of ZO-1 (Kimura *et al.*, 2009), decreased ZO-1 expression (Sozen *et al.*, 2009) or had no effect at all on ZO-1 (Al-Sadi *et al.*, 2010). Despite the well-established receptors for IL-1β, IL-1R1 and IL-1RII, it has been suggested that there are additional functional IL-1 receptors in the brain. This hypothesis stems from evidence demonstrating that IL-1β can cause ischemic brain damage independently of IL-1R1 (Touzani *et al.*, 2002; Andre *et al.*, 2006). It has also been suggested that the knocking out of IL-1R1 causes a compensatory ability of IL-1RII to signal in a functional way rather than act as a decoy receptor (Touzani *et al.*, 2002). So in the context of the literature, our ZO-1 results are difficult to explain. It is possible that IL-1β is indeed still deleterious for ZO-1, reducing its expression by acting on alternate IL-1 receptors, or perhaps IL-1β is actually beneficial and disruption IL-1 signalling via the IL-1R1 is proving to be detrimental. Perhaps IL-1ra normally protects ZO-1 in the brain, and removing the IL-1R1 also negates its protective effects.

There were no significant differences in the relative expression of albumin in the brains of IL-1R1$^{-/-}$ mice, suggesting that the barrier was not functionally enhanced, despite the increased tight junction expression observed in the IL-1R$^{-/-}$ mice. These findings were

somewhat surprising as one would have expected a relative decrease in albumin levels in the knockout animals, based on the hypothesis that IL-1β causes increased BBB permeability. There were no significant increases in albumin in the middle-aged wildtype compared with young wildtype mice, though an increasing trend was apparent. There were significant age-related increases in albumin expression in the brain parenchyma in the previous chapter, so it is possible that the BBB still somewhat intact in middle-aged animals and that it is only with increasing old-age that marked BBB disruption occurs facilitating the entry of large plasma proteins. Future studies might consider assessing the extravasation of smaller compounds e.g. sodium fluorescein in the middle-aged IL-1R1$^{-/-}$ mice *or* assessing BBB permeability in an aged group of IL-1R1$^{-/-}$ mice.

After assessing the effect of IL-1 on the primary tight junctions of the BBB, the effects of IL-1 on proteins of the NVU, namely laminin and PDGFR-β, were also investigated.

PDGFR-β expression was not modulated by either age or genotype. Though there was an age-related decrease in PDGFR-β expression reported in the previous chapter suggesting potentially decreased pericyte numbers and at the very least, disrupted pericyte-endothelial signalling, this result was not apparent in middle-aged mice. This discrepancy might be because the age-related changes in the rats were only evident in old-age so the middle-aged mice were not old enough. Also it may be that there are species-specific differences in PDGFR-β expression profiles. In any case irrespective of age, the fact that PDGFR-β expression was not altered in the IL-1R1$^{-/-}$ mice would suggest that it is unlikely that IL-1β signalling directly modulates PDGFR-β expression.

In Chapter 3, laminin, the basal lamina protein was significantly decreased with age and physically fragmented and detached from pericytes. Though there was a trend of decreased laminin expression when wildtype young and middle-aged mice were compared, this result was not significant. Laminin expression was decreased in IL-1R$^{-/-}$ animals when compared with their wildtype counterparts. There is limited literature in relation to IL-1β mediated laminin disruption, although one study has shown that IL-1β decreased the laminin receptor in human umbilical vein endothelial cells, which resulted in disrupted endothelial adhesion to laminin, however they did not assess laminin glycoprotein expression (Defilippi *et al.*, 1992).

Our previous hypothesis was that it was the age-related increases in IL-1β that mediated upregulation of MMP, ultimately leading to basal lamina disruption. However, in the case of the IL-1R1$^{-/-}$ mice laminin expression was not increased as hypothesised, rather it remains reduced. It is possible that other pro-inflammatory cytokines e.g. TNF-alpha, which are also upregulated with age (though not assessed here), are activating/upregulating MMP and disrupting the basal lamina (Candelario-Jalil *et al.*, 2011).

In conclusion, this study has found that a low-dose of LPS administered systemically, does not disrupt either the young or aged BBB. This muted response highlights the plasticity of the cerebral endothelial cells and their ability to mount an appropriate response (or not) to a particular inflammatory stimulus. The pro-inflammatory cytokine, IL-1β appears to be a key molecule underlying the age-related tight junction protein disruptions, as evidenced by the increased tight junction protein concentration in IL-1R1$^{-/-}$ mice. This research provides good evidence that there is an inflammatory basis underlying the age-related BBB disruptions.

Chapter 5

Investigating the impact of inflammatory stimuli on aspects of the neurovascular unit in vitro.

5.1 Introduction

Previously we described that middle-aged IL-1R1$^{-/-}$ mice showed increased tight junction expression when compared to aged wildtype mice (Chapter 4) so further investigation into IL-1β-mediated modulation of tight junction expression was warranted. Despite the literature documenting IL-1β mediated disruption of the tight junctions *in vivo* (e.g. during subarachnoid haemorrhaging in mice (Sozen *et al.*, 2009)) or following central injections of IL-1β (Ching *et al.*, 2005) and *in vitro* (e.g. endothelial cells exposed to hypoxic conditions or IL-1β-treated epithelial cells (Al-Sadi *et al.*, 2010) the molecular signalling mechanisms underlying these effects in cerebral endothelial cells is limited. Endothelial cells express IL-1R1 and activation of this receptor leads to activation of a variety of mitogen-associated protein kinase (MAPK) signalling cascades (Pearson *et al.*, 2001). There is conflicting evidence in the literature regarding the ERK-MAPK and JNK regulation of tight junctions (Gonzalez-Mariscal *et al.*, 2008). However, the majority of studies have found that activation of the ERK-MAPK pathway disrupts tight junction protein expression, leading to barrier dysfunction. Incubation of porcine cerebral endothelial cells with an ERK inhibitor (PD98059) prevented H_2O_2-mediated disruption of ZO-1 and occludin expression (Fischer *et al.*, 2005). ERK signalling in response to a protein kinase C activator resulted in increased paracellular permeability and altered cellular distribution of ZO-1 in human corneal epithelial cells (Wang *et al.*, 2004). However, a recent study on primary mouse endothelial cell lines demonstrated that MAPK inhibitors did not affect the barrier properties (Thornton *et al.*, 2010). The consensus from the literature is that ERK signalling is capable of carrying out opposing effects on tight junction protein expression depending on the cell type under investigation and the nature of the insult elicited, see (Gonzalez-Mariscal *et al.*, 2008) for a full review of the cell types and treatment conditions.

LPS, a know disruptor of TJ as outlined in chapter 4, altered claudin-5 expression in the rat striatum but not other areas. As such, to further clarify the role of LPS in TJ modulation, we decided to treat monolayers of endothelial cells with LPS. Metalloproteinases (MMP), in addition to MAPK-mediated pathways, can disrupt tight junctions during inflammation *in vivo* (e.g. during ischaemia (Yang *et al.*, 2007)) and *in vitro* (e.g. when endothelial cells were exposed to oxidative stress (Lischper *et al.*,

2010)). Considering that we previously reported an age-related increase in MMP activity (Chapter 3) and that IL-1β is a known activator of MMP-9 via MAPK signalling (Liang *et al.*, 2007) it is highly plausible that the age-related increase in the proinflammatory cytokine IL-1β may be underlying MMP-mediated tight junction disruption.

The aims of this chapter were:

1. To investigate if IL-1β and LPS disrupted tight junction protein concentration in an endothelial cell line.
2. To establish the signalling cascade underlying IL-1β and LPS mediated tight junction disruption.
3. To investigate the impact of MMP on IL-1β mediated tight junction disruption.

5.2 Methods

5.2.1 Experimental procedures

The experimental procedures carried out in this chapter are detailed in Chapter 2 where the following techniques are further described: protein assay (section 2.3), immunohistochemistry (section 2.6), and Western immunoblotting (section 2.7), gelatin zymography (section 2.9) and ELISA (section 2.10). All data is presented as mean ± SEM. Data was analysed by one- or two-way ANOVA followed by *post-hoc* Newman-Keuls or Bonferroni tests respectively, to determine significance.

5.2.2. bEnd.3 culture

The mouse endothelial cell line, bEnd.3, was cultured as described in Chapter 2 (sections 2.11.1 – 2.11.8). As the bEnd.3 *in vitro* experiments became somewhat of a characterisation of the optimal culturing and treatment procedures, the table below gives an overview of each experiment (Table 5.1). Further detail on each experiment is included with the relevant figures throughout this chapter.

Figure(s)	Cells	Passage number	Plating density; substratum	Treatment (single dose)	Duration of treatment (hours)
Figures 5.1 A, 5.2 A-D	bEnd.3	3-4	2×10^5; poly-l-lysine	IL-1β (10ng/ml)	1, 3, 6, 12, 24
Figures 5.1 B, 5.3 A to D	bEnd.3	3-4	2×10^5; poly-l-lysine	LPS (100ng/ml)	1, 3, 6, 12, 24
Figure 5.4	bEnd.3	12-14	1×10^5; poly-l-lysine	All media removed and replaced with either fresh media (control) or fresh media containing IL-1β (10ng/ml)	6
Figure 5.5	bEnd.3	8-10	1×10^5; poly-l-lysine	IL-1β added as a 10x solution; final concentration 10ng/ml in well	3, 6
Figures 5.6, 5.7	bEnd.3	3-4	1×10^5; fibronectin	IL-1β added as a 10x solution; final concentration 10ng/ml in well	1, 6, 12, 24, 48
Figure 5.8	bEnd.3	14-17	1×10^5; fibronectin	All cells were serum-starved for 3-4 hours. Then IL-1β added as a 10x solution in serum-free or serum-containing media; final concentration 10ng/ml in well	3-4
Figures 5.9 to 5.18	Organotypic slices	Prepared fresh	3 organotypic hippocampal slices were cultured per well	IL-1β (10ng/ml) IL-1ra (250ng/ml) MMP inhibitor (ONO4817) (10 or 20μM)	1, 6 or 24

Table 5.1: Summary of the cell culturing conditions employed in all *in vitro* experiments.

5.3 The effect of inflammatory mediators IL-1β and LPS on tight junctions in bEnd.3

bEnd.3 cells (passage 3-4) were plated at a density of 2 x 10^5 cells/ml in 6-well and 24-well plates, and were cultured for 1-2 days until confluence was reached. When the endothelial cells were ready for treating, the media was removed and was replaced with fresh media containing IL-1β (10ng/ml; R&D Systems, UK) or fresh media containing LPS (100ng/ml; Alexis® Biochemical, Enzo Life Sciences, Switzerland) and incubated for 1, 3, 6, 12 or 24 hours before they were harvested. Control wells were incubated in fresh media without IL-1β or LPS.

One-way ANOVA revealed that the protein concentration of claudin-5 (*$p<0.05$), occludin (**$p<0.01$) and ZO-1 (***$p<0.001$) was significantly decreased following IL-1β treatment (10ng/ml). All tight junction proteins were maximally reduced (by up to ~75% less than untreated controls) between 3 to 6 hours following IL-1β treatment, and the protein concentration of all tight junction proteins returned to control/above control levels, by 24 hours (Figure 5.1 A). Please refer to appendix 5, for significance levels pertaining to each tight junction protein, following *post-hoc* test.

Very similar results were obtained following LPS treatment (100ng/ml) where claudin-5 (*$p<0.05$), occludin (***$p<0.001$) and ZO-1 (***$p<0.001$) protein concentration was significantly reduced (Figure 5.1 B; ANOVA). As with the IL-1β treatment, all tight junctions were reduced to their lowest levels between 3 to 6 hours of LPS treatment and apart from ZO-1, levels returned to untreated control levels by 24 hours. Please refer to appendix 6, for significance levels pertaining to each tight junction protein, following *post-hoc* test.

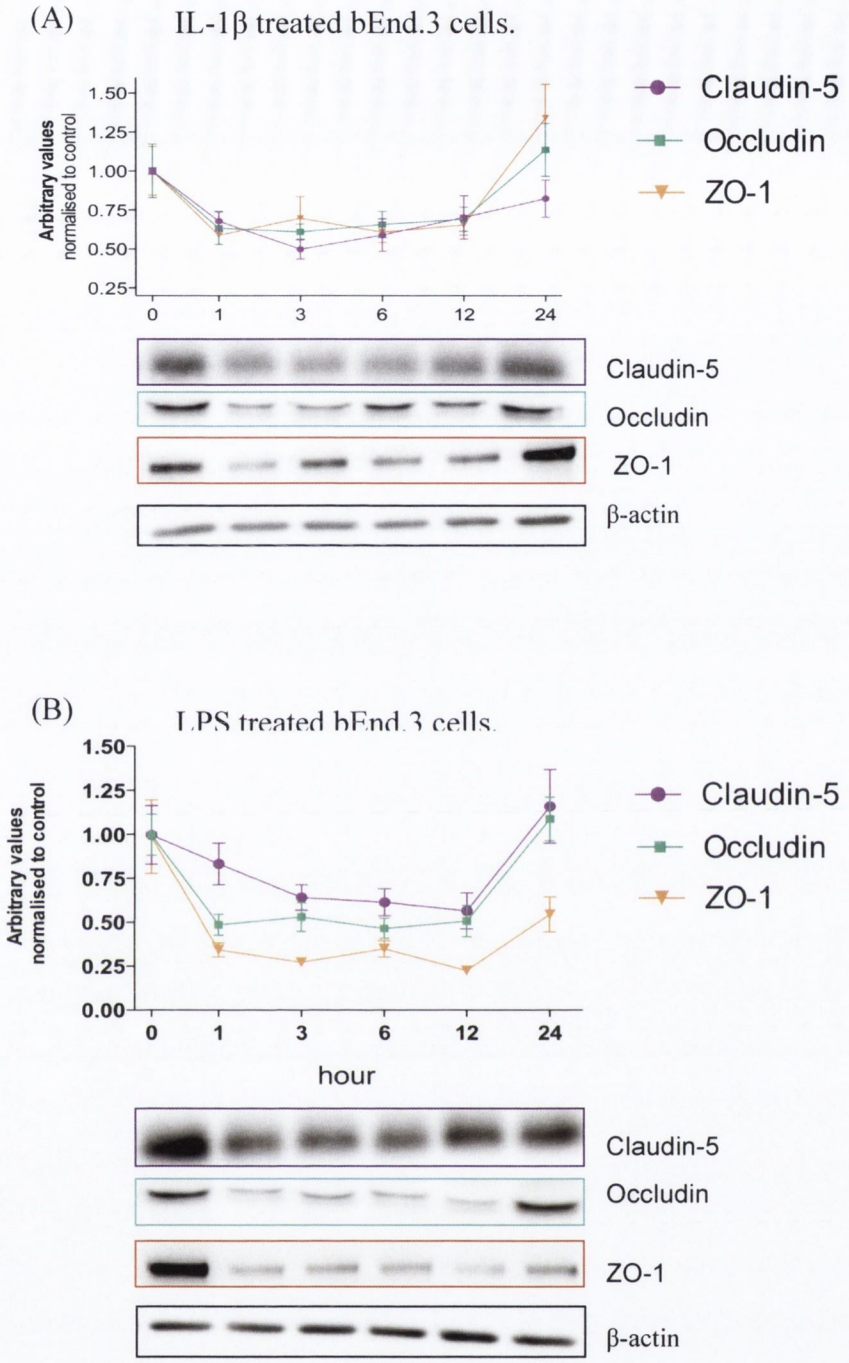

Figure 5.1: IL-1β and LPS treatment of bEnd.3 cells reduced tight junction proteins in a time-dependent manner.

A. IL-1β (10ng/ml) significantly reduced claudin-5 (*$p<0.05$), occludin (**$p<0.01$) and ZO-1 (***$p<0.001$) concentration though all tight junction concentration levels returned to untreated control levels by 24 hours. B. Similarly, LPS significantly reduced claudin-5 (*$p<0.05$), occludin (***$p<0.001$) and ZO-1 (***$p<0.001$), though all except ZO-1 concentration returned to control levels by 24 hours. Data expressed as mean ± SEM, n=6-8; one-way ANOVA followed by *post-hoc* Newman-Keuls test. See appendix 5, 6 for *post-hoc* data in relation to individual tight junction proteins.

5.4 The effect of IL-1β and LPS on protein kinases in bEnd.3

Activation (phosphorylation) of the protein kinases JNK-1, JNK2/3, ERK1 and ERK2 was assessed in bEnd.3 cells following up to 24 hours treatment with IL-1β (10ng/ml). Though there was a trend of increased phospho-JNK-1 and phospho-JNK2/3 activation following 1 hour treatment with IL-1β, these increases were not significant (Figures 5.2 A and B, respectively; ANOVA). However, phospho-ERK1 was significantly increased following treatment with IL-1β for 6 hours (Figure 5.2 C; *$p<0.05$; ANOVA) but activation levels returned to untreated control concentration levels by the 12 hour timepoint. Phospho-ERK2 protein concentration was significantly decreased from untreated control levels after 1 hour of IL-1β treatment and remained so after 3 hours (Figure 5.2 D; *$p<0.05$; ANOVA). Phospho-ERK2 protein concentration levels fluctuated; returning to untreated control levels by 6 hours before decreasing again by 12 hours (though not significantly) and returning again to untreated control levels by 24 hours.

There was a trend where LPS treatment (100ng/ml) decreased both phospho-JNK-1 and -2/3 protein concentration after 1 hour although concentration levels increased thereafter, except in the case of phosph-JNK-1 which decreased again after 24 hours; these results were not significant (Figures 5.3 A and B; ANOVA). The pattern of ERK activation mimicked somewhat the pattern of activation previous observed following IL-1β treatment (Figures 5.2 C and D compared with Figures 5.3 C and D). Phospho–ERK1 significantly decreased at 3 hours (*$p<0.05$) and 12 hours (**$p<0.01$) following LPS treatment before returning to control levels by 24 hours (Figure 5.3 C). Phospho-ERK2 was significantly decreased at 1 hour (*$p<0.05$) and 12 hours (**$p<0.01$) following LPS treatment (Figure 5.3 D). As with phospho-ERK1, phospho-ERK2 protein concentration also returned to control levels by 24 hours.

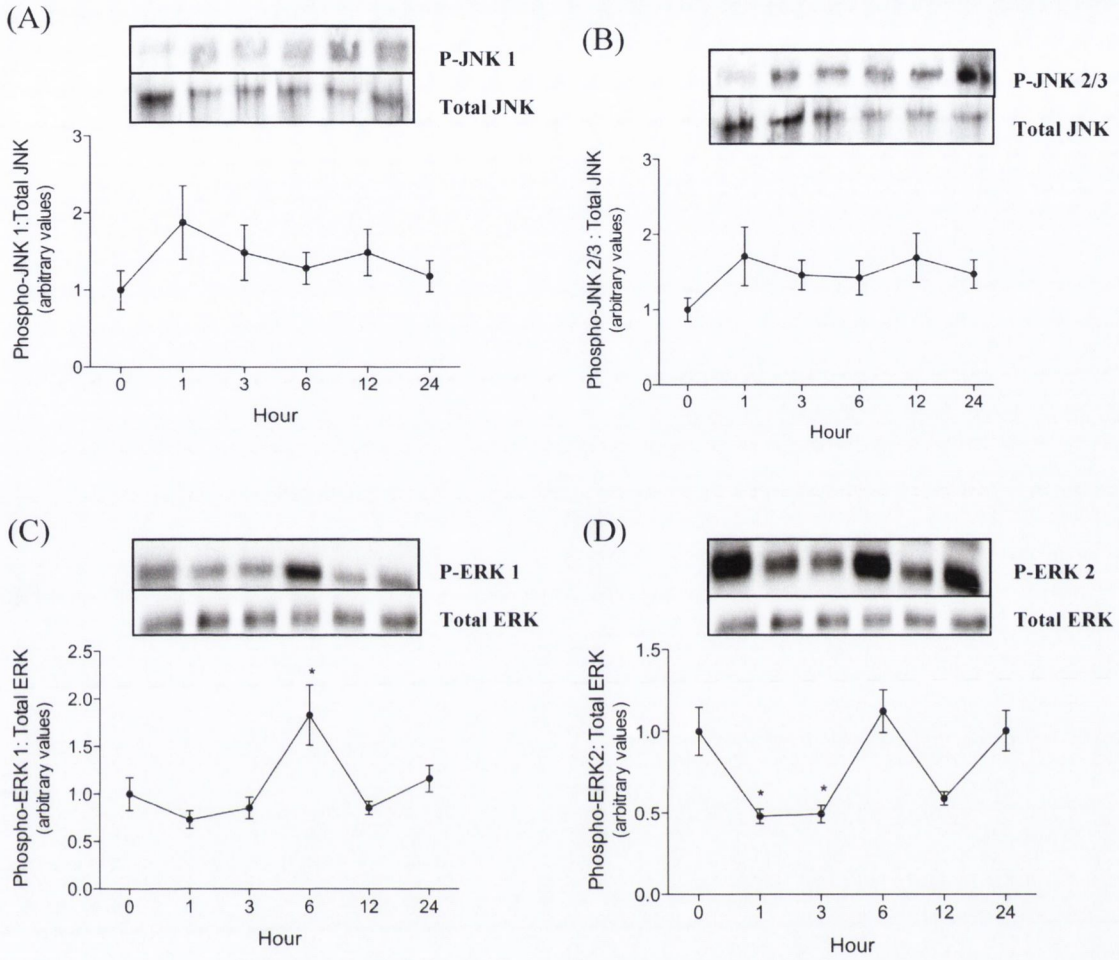

Figure 5.2: Phospho-ERK1, 2 but not phospho-JNK were altered over the course of IL-1β treated bEnd.3.

Phospho-JNK1 (A) and phospho-JNK -2/3 (B) were unchanged following IL-1β (10ng/ml) treatment. Phospho-ERK1 (C) significantly increased at 6 hours following IL-1β treatment. Phospho-ERK2 (D) significantly decreased at 3 and 6 h post-treatment. Data expressed as mean ± SEM, n=4; * $p<0.05$ versus 0 h; one-way ANOVA followed by *post-hoc* Newman-Keul test.

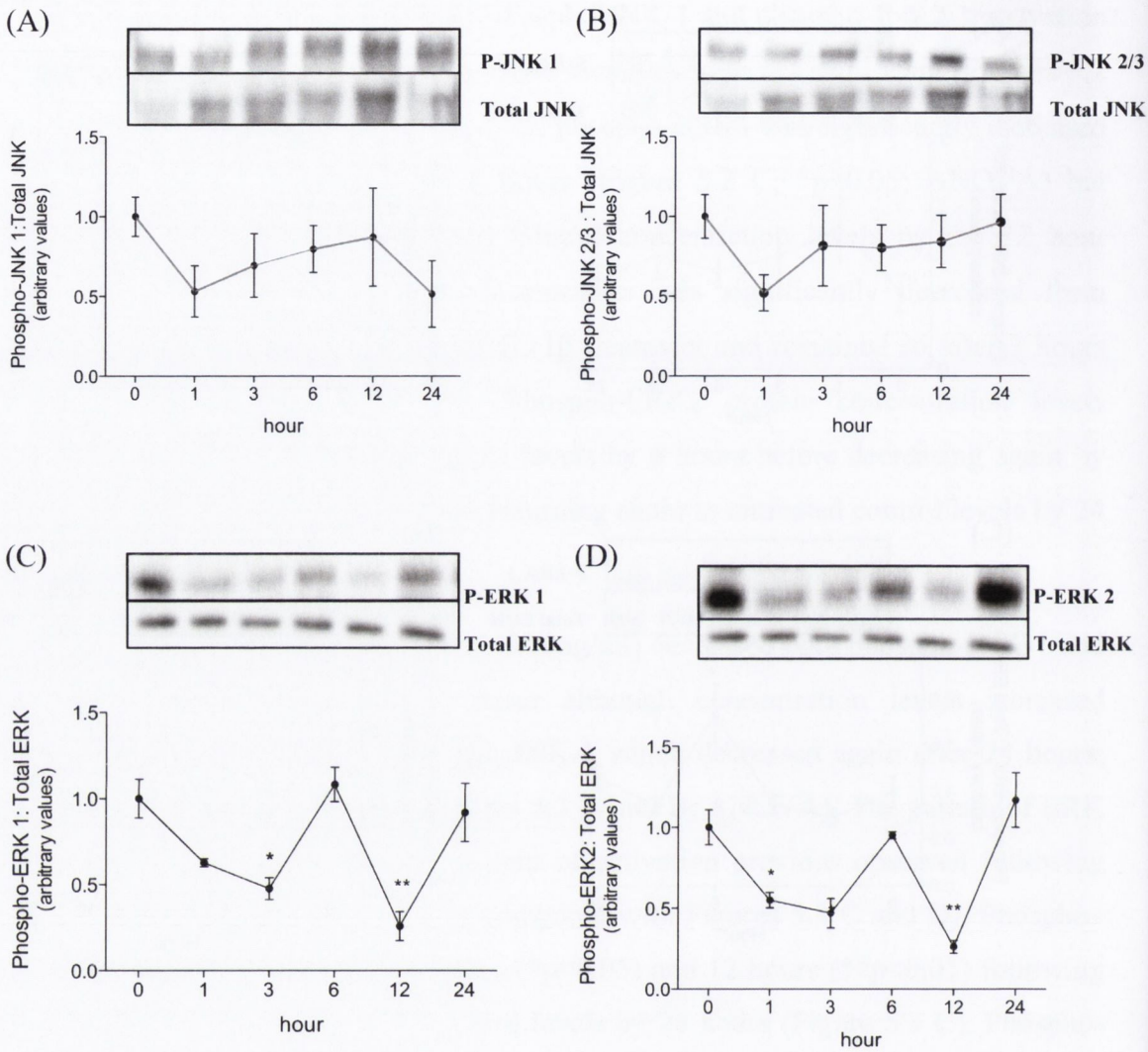

Figure 5.3: Phospho-ERK1, 2 but not phospho-JNK were altered over the course of LPS treated bEnd.3.

Phospho JNK 1 (A) and phospho JNK -2/3 (B) were unchanged following LPS (100ng/ml) treatment. Phospho-ERK1 (C) significantly decreased in bEnd.3 at 3 hours and 12 hours following LPS treatment. Phospho-ERK2 (D) significantly decreased at 1 hour and 12 hours post-treatment. Data expressed as mean ± SEM, n=4-6; * $p<0.05$ versus 0 h, ** $p<0.01$ versus 0 h;; one-way ANOVA followed by Newman-Keuls *post-hoc* test.

5.5 The effect of timing and media changes on tight junction protein expression in bEnd.3

Following the initial timecourse experiments with IL-1β and LPS which demonstrated tight junction disruption and protein kinase activation (sections 5.3 and 5.4 above), we next set out to further investigate the signalling cascades downstream of IL-1β and LPS. In particular we were interested in accessing if tight junction mRNA expression was modulated downstream of either IL-1β or LPS in the same endothelial cells.

Despite the widespread use of the bEnd.3 cell line in *in vitro* permeability experiments, a systematic characterisation of the factors that modulate their tight junctions, has not been carried out to date.

Reproducing the initial IL-1β- and LPS-mediated effects proved to be challenging and as such, the subsequent *in vitro* experiments on bEnd3 cells evolved into a characterisation of the treatment conditions that might affect results. In our initial attempt to replicate the timecourse experiments (IL-1β and LPS decrease TJ concentration), the Western immunoblotting results varied tremendously at each time point, so much so that we carried out parallel experiments with IL-1β from 2 different companies – but the cellular response to both reagents was comparable (see Appendix 8). We then set out to establish the optimal culturing parameters that would guarantee reproducible IL-1β- or LPS-mediated effects on tight junction protein expression as observed in section 5.3. Outlined in the following sections (and summarised in table 5.1) are the treatment conditions employed when treating bEnd.3 with IL-1β, and the effect the impact they had on the outcome of an experiment, particularly the effect of a media change on TJ.

5.5.1 The effect of media change when treating bEnd.3

Because the inflammatory insults IL-1β and LPS decreased claudin-5, occludin and ZO-1 protein concentration maximally following 3-6 hours exposure with either insult, we chose, in the first instance, to treat bEnd.3 cells with IL-1β for 6 hours. bEnd.3 cells (passage 12-14) were plated at a density of 1 x 10^5 cells/ml in 24-well plates, and were cultured for 1-2 days until confluence was reached. When the endothelial cells were

ready for treating, all of the media was removed and was replaced with either fresh media (control) or fresh media containing IL-1β (10ng/ml). Cells were treated 6 hours before they were harvested. There was a significant effect of time on claudin-5 protein concentration (Figure 5.4; F (1,9) = 21.75; p= 0.0016), where claudin-5 was significantly decreased after 6 hours, irrespective of treatment. The claudin-5 reduction was not further decreased by IL-1β (10ng/ml).

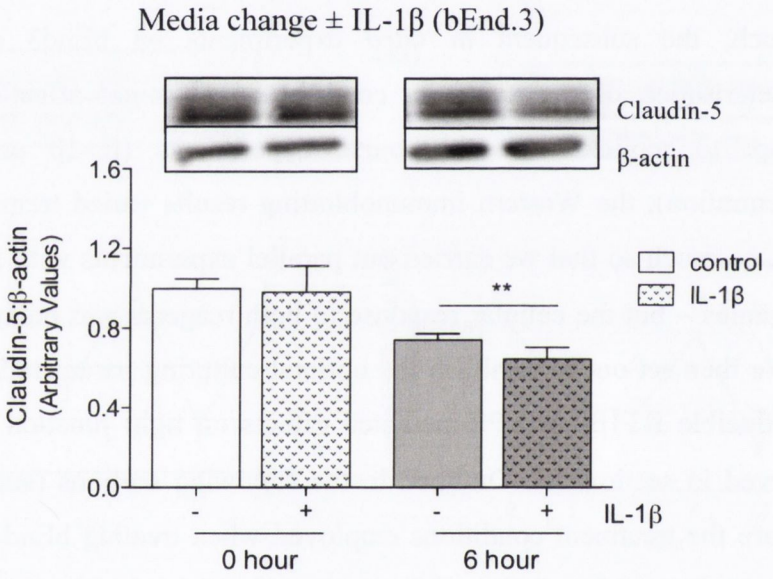

Figure 5.4: Claudin-5 protein concentration was significantly decreased after 6 hours *in vitro*, irrespective of treatment.

bEnd.3 cells were treated with either fresh media (control) or fresh media containing IL-1β, 10ng/ml) for 6 hours. Claudin-5 protein concentration was significantly decreased with time, irrespective of whether IL-1β was present or not. Data expressed as mean ± SEM, n=3-4; **p<0.01, two-way ANOVA followed by *post-hoc* Bonferroni test.

Two-way ANOVA: Time $_{effect}$ F (1,9) = 21.75; p = 0.0016, IL-1β $_{effect}$ F (1,9) = 0.5567; p = 0.4769, Interaction $_{effect}$ F (1,9) = 0.5567; p = 0.4769.

5.5.2 IL-1β-treatment of bEnd.3 cells with minimal media disruption

Because the tight junction proteins were decreased irrespective of whether or not IL-1β was present, the results indicated that the process of changing the media was enough to modulate TJ on endothelial cells.

bEnd.3 cells (passage 8-10) were plated at a density of 1 x 10^5 cells/ml in 24-well plates, and were cultured for 1-2 days until confluence was reached. When the endothelial cells were ready for treating, 50 µl media was removed from all wells and was used to make up a 10x concentration of IL-1β. To the same media was added either fresh media (control) or IL-1β which was reapplied to all wells and the final concentration of IL-1β in the 'treatment' wells was 10ng/ml, as before. Cells were treated for 3 to 6 hours before they were harvested. In the absence of a full media change, IL-1β alone did not reduce protein expression of claudin-5, occludin or ZO-1 at either 3 or 6 hours (Figure 5.5 A-D; Student's *t*-test; n= 4-6).

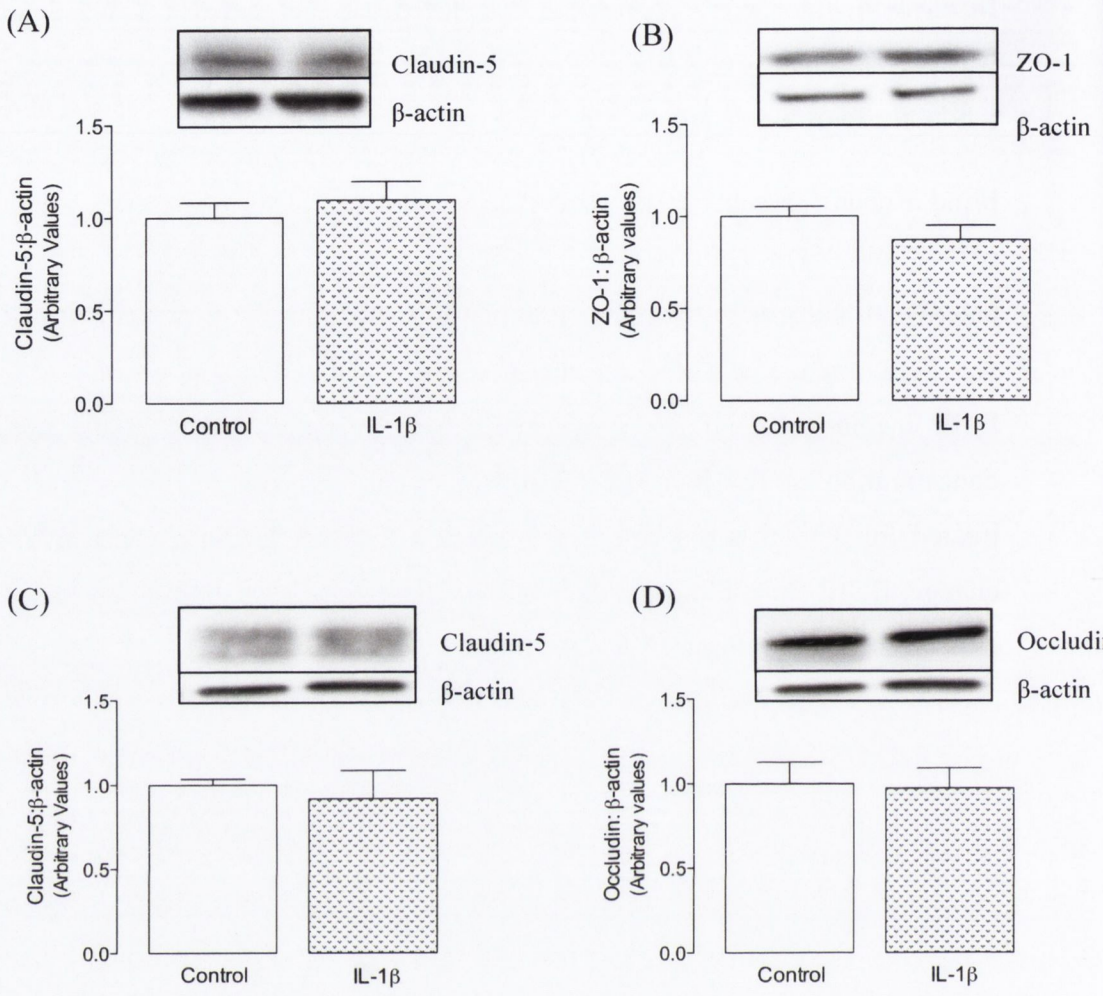

Figure 5.5: Claudin-5, occludin or ZO-1 protein concentration was not modulated following an incubation with IL-1β for either 3 or 6 hours in the absence of simultaneous media change.

bEnd.3 cells were treated with IL-1β (applied as 10x treatment; final concentration 10ng/ml) to minimise disruption associated with the media change. IL-1β did not modulate claudin-5 protein expression following either a 3 hour (A) or 6 hour (C) treatment. Similarly, ZO-1 (B) and occludin (D) expression levels were not altered by IL-1β following either a 6 hour treatment (B and D, respectively). Data expressed as mean ± SEM, n=4-6; Student's *t*-test.

5.6 The effect of IL-1β on the cellular distribution of the tight junction proteins in bEnd.3 cells

In the previous experiments, there was no overall modulation of total cellular tight junction protein concentration following incubation with IL-1β. Therefore we investigated if instead the cellular distribution of the tight junction proteins was altered over time.

Prior to plating bEnd.3 cells, 24-well plates were pre-coated with fibronectin from bovine plasma (4μg/ml in PBS, Sigma) at 37°C for a minimum of 2 hours to aid adherence of the cells to the culture flasks. The fibronectin was removed, wells were rinsed with sterile PBS and allowed to air-dry. bEnd.3 cells (passage 5-7) were plated at a density of 1 x 10^5 cells/ml in 24-well plates, and were cultured for 1-2 days until confluence was reached. When the endothelial cells were ready for treating, 50μl media was removed from all wells and was used to make up a 10x concentration of IL-1β. To the same media was added either fresh media (control) or IL-1β which was reapplied to all wells, and the final concentration of IL-1β in the 'treatment' wells was 10ng/ml, as before. Cells were treated for up to 48 hours (1, 6, 12, 24, 48 hours) before they were harvested. Then cellular homogenates were further subfractionated into membrane-rich and cytosolic-rich fractions (section 2.11.8).

On no occasion was occludin protein concentration detected in cytosolic fractions. In addition, occludin protein concentration in the membrane fraction was not altered by IL-1β treatment, irrespective of the length of time the cells were exposed to the insult (Figure 5.6).

Cytosolic protein concentration of claudin-5 were significantly increased in a time-dependant manner (Figure 5.7 A; $F(1,36) = 2.845$; $p = 0.0269$). Although *post-hoc* Bonferroni tests could not find at which timepoint these changes occurred, the corresponding immunoblots indicated that claudin-5 increased gradually over 48 hours, and this increase occurred in the presence or absence of IL-1β.

Analysis of the membrane fraction showed that claudin-5 protein concentration fluctuated significantly over time when compared to untreated controls (Figure 5.7 B; $F(1,41) = 2.601$; $p = 0.0392$). *Post-hoc* Bonferroni tests could not establish where these

changes occurred as there was a lot of variation in expression levels over the course of 48 hours.

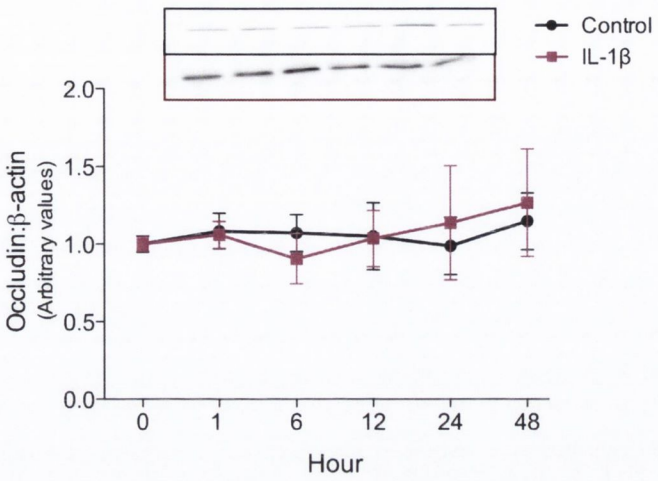

Figure 5.6: Occludin protein concentration was unchanged in the membranes of bEnd.3 cells following IL-1β treatment

IL-1β (10ng/ml) did not modulate occludin protein concentration in the membranes of bEnd.3 cells, irrespective of the incubation time. Data expressed as mean ± SEM, n=4; two-way ANOVA followed by *post-hoc* Bonferroni test.

Two-way ANOVA: Time $_{effect}$ F (1,35) = 0.3099; p = 0.9037, IL-1β $_{effect}$ F (1,35) = 0.008 ; p = 0.9274, Interaction $_{effect}$ F (1,35) = 0.1608; p = 0.5985.

(A) Cytosolic fraction

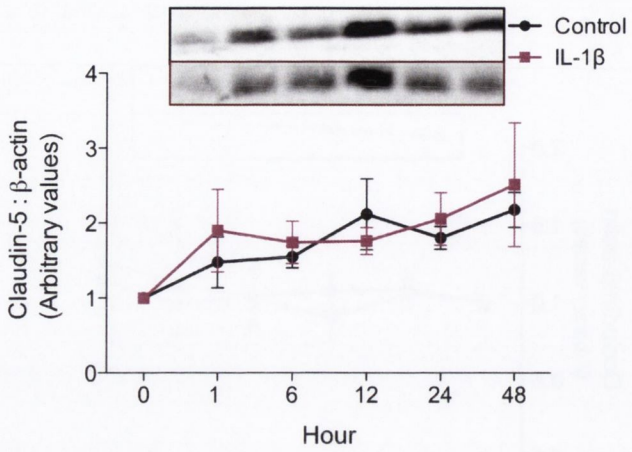

(B) Membrane fraction

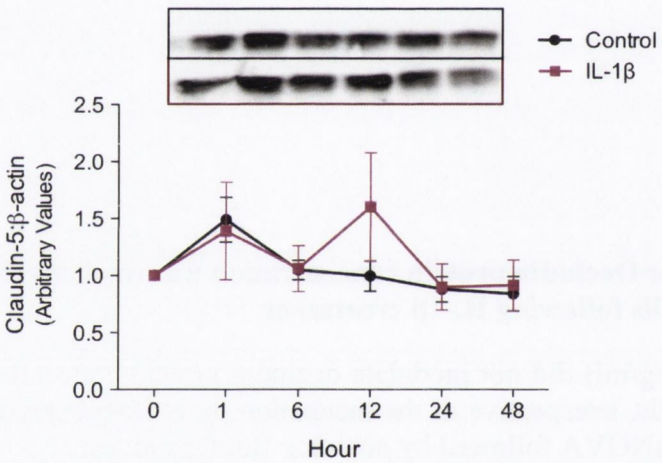

Figure 5.7: Claudin-5 protein concentration changed significantly over time in both membrane and cytosolic fractions irrespective of IL-1β treatment.

Cytosolic levels of claudin-5 increased significantly over time and up to 48 hours (A). This increase occurred irrespective of treatment and IL-1β did not further augment the changes. Claudin-5 protein concentration fluctuated over time in the membrane fraction whether or not IL-1β was present. Data expressed as mean ± SEM, n=4; two-way ANOVA followed by *post-hoc* Bonferroni test.

(A) Two-way ANOVA: Time $_{effect}$ $F(1,36) = 2.845$; $p = 0.0269$, IL-1β $_{effect}$ $F(1,36) = 0.4374$; $p = 0.5126$, Interaction $_{effect}$ $F(1,36) = 0.2901$; $p = 0.9157$.

(B) Two-way ANOVA: Time $_{effect}$ $F(1,41) = 2.601$; $p = 0.0392$, IL-1β $_{effect}$ $F(1,41) = 0.8053$; $p = 0.3748$, Interaction $_{effect}$ $F(1,41) = 0.7392$; $p = 0.5985$.

5.7 The effect of serum starving bEnd.3 in reducing variability

Serum-starving cells is routinely used *in vitro* to synchronise the growth cycles of proliferating cells by forcing cells to withdraw into the G0/G1 phase of the cell cycle where basal activity is decreased (Cooper, 2003). In an attempt to reduce variability within results from the bEnd.3 it was decided to serum starve them prior to treatment to synchronize proliferation.

Prior to plating bEnd.3 cells, 24-well plates were pre-coated with fibronectin from bovine plasma (4µg/ml in PBS, Sigma) at 37 °C for a minimum of 2 hours. The fibronectin was removed, wells were rinsed with sterile PBS and allowed to air-dry.

bEnd.3 cells (passage 14-17) were plated at a density of 1 x 10^5 cells/ml in 24-well plates, and were cultured for 1-2 days until confluence was reached. When the endothelial cells were ready for treating, all media was removed and replaced with serum-free media from 3-4 hours. IL-1β (10x) was made up in media ± serum and was applied to all treatment wells at a final concentration of 10ng/ml. Control wells contained either media ± serum. Cells were treated for 1 or 6 hours before they were harvested.

Irrespective of whether cells were treated in fresh serum-free culture media or fresh serum-free media containing IL-1β, claudin-5 protein concentration was significantly decreased over time (Figure 5.8 A; $F(1,10) = 4.498$; $p = 0.0442$). Bonferroni *post-hoc* tests did not reveal where the changes lay, but examination of the immunoblots indicated that over time, claudin-5 decreased in a time-dependant manner.

ANOVA revealed a significant time x IL-1β effect in cells treated with full-media following serum-starving (Figure 5.8 B; $F(1, 12) = 7.017$; $p = 0.0096$). Bonferroni *post-hoc* tests revealed that media alone induced a significant increase in claudin-5 protein concentration at 6 hours (**$p<0.01$) when compared to IL-1β-treated cells.

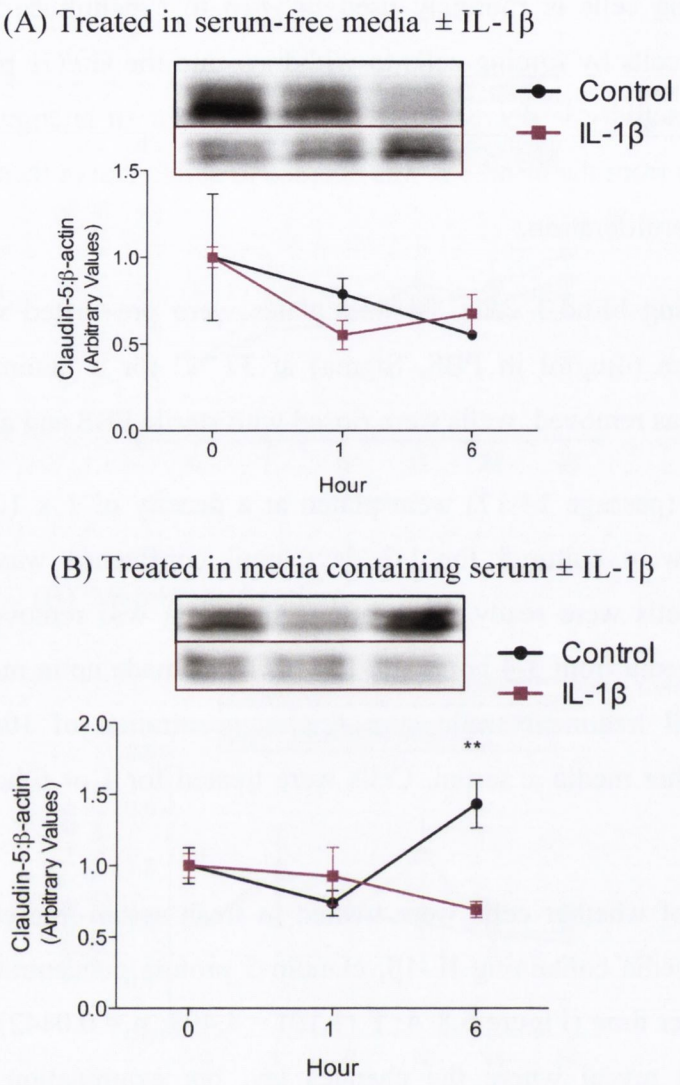

Figure 5.8: IL-1β caused continued decreases in claudin-5 protein concentration in bEnd.3.

bEnd.3 were serum starved for 3 hours prior to treatment. Cells were then either treated in fresh media (with or without IL-1β, 10ng/ml) or treated in serum free media (with or without IL-1β, 10ng/ml). Claudin-5 remained decreased following treatment in serum-free media (A), regardless of treatment. Cells that were replenished with fresh media had significantly increased protein concentration of claudin-5 at 6 hours compared with cells replenished with fresh media containing IL-1β (B). Data expressed as mean ± SEM, n=2-3; **p<0.01 versus 6 hours IL-1β; two-way ANOVA with Bonferroni *post-hoc* test.

(A) Two-way ANOVA: Time $_{effect}$ $F(1,10) = 4.498$; $p = 0.0442$, IL-1β $_{effect}$ $F(1,10) = 0.1071$; $p = 0.7310$, Interaction $_{effect}$ $F(1,10) = 0.8566$; $p = 0.4565$.

(B) Two-way ANOVA: Time $_{effect}$ $F(1,12) = 1.665$; $p = 0.2300$, IL-1β $_{effect}$ $F(1,12) = 2.971$; $p = 0.1104$, Interaction $_{effect}$ $F(1,12) = 7.017$; $p = 0.0096$.

5.8 Integrity of organotypic hippocampal slices

Though the original research plan was to further investigate the signalling pathways downstream of IL-1β and LPS, which modulated endothelial tight junction proteins, this proved challenging in the bEnd.3 cells. We also investigated signalling in another source of endothelial cells: human endothelial vascular endothelial cells (HUVEC). However, optimal growing conditions and the cell responses were inconsistent from batch-to-batch (data not shown) so further investigations were discontinued. We next decided to use organotypic hippocampal slices because they could be stably maintained in culture and contained an intact vascular network that was essential to studying endothelial tight junction proteins and other proteins of the NVU.

Organotypic hippocampal slices were harvested from postnatal day (PN) 10 mice and treated following 9-10 days *in vitro* (DIV). Micrographs A and B in Figure 5.9 illustrate the anatomical regions of the organotypic hippocampus slices. After 10 DIV, slices were examined under a dissecting microscope and only those slices that were physically intact and free from any obvious nicks or scarring, were treated (micrograph C). The rich vascular network of an organotypic hippocampal slice after 10 DIV is illustrated in micrograph D and this slice has been immunostained with laminin.

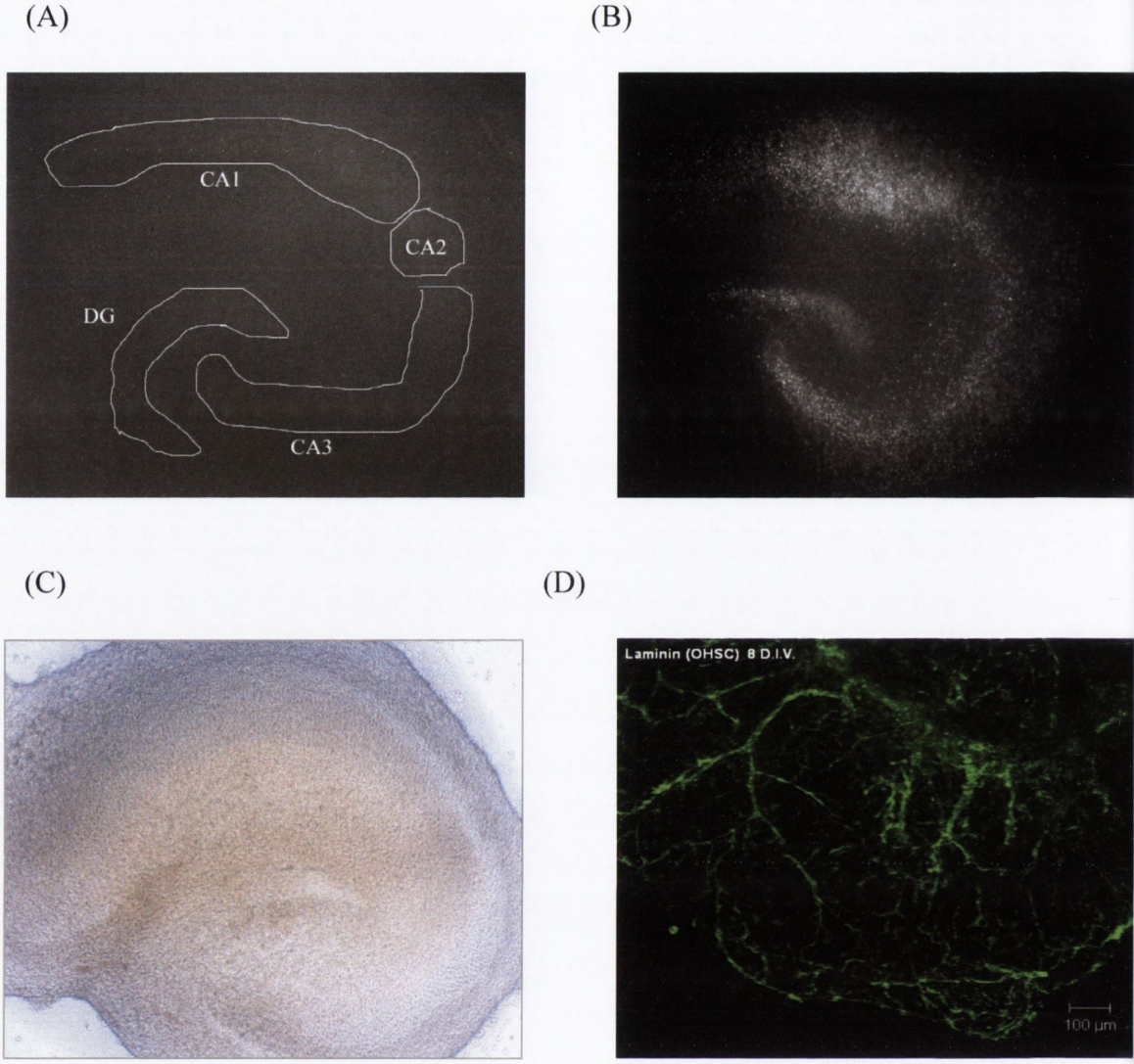

Figure 5.9: Organotypic hippocampal slices from postnatal day 10 mice.

The anatomical regions of an organotypic hippocampal slice are illustrated in micrographs A and B. Micrograph C is representative of an organotypic hippocampal slices that remained intact and free from glial scarring following 9-10 days *in vitro* (DIV). Micrograph D illustrates that vascular network at 10 DIV and has been immunostained with laminin.

5.9 IL-1β treatment decreased claudin-5 and occludin protein concentration and increased ERK1/2 activation in organotypic hippocampal slices

Organotypic hippocampal slices after 10 DIV were treated with IL-1β (10ng/ml) for 24 hours. IL-1β significantly decreased claudin-5 protein concentration (Figure 5.10 A; *$p<0.05$; Student's *t*-test; n=7-8) and occludin (B; *$p<0.05$; Student's *t*-test; n=9) when compared to untreated controls. Laminin and PDGFR-β protein concentration were not significantly modulated by IL-1β (C and D, respectively; Student's *t*-test; n=4-5). Both phospho-ERK1 (E; ***$p<0.001$; Student's *t*-test; n=5) and phospho-ERK2 (F; ***$p<0.001$; Student's *t*-test; n=5) protein concentration were significantly increased following 24 hour treatment with IL-1β (10ng/ml), when compared to untreated controls (media alone).

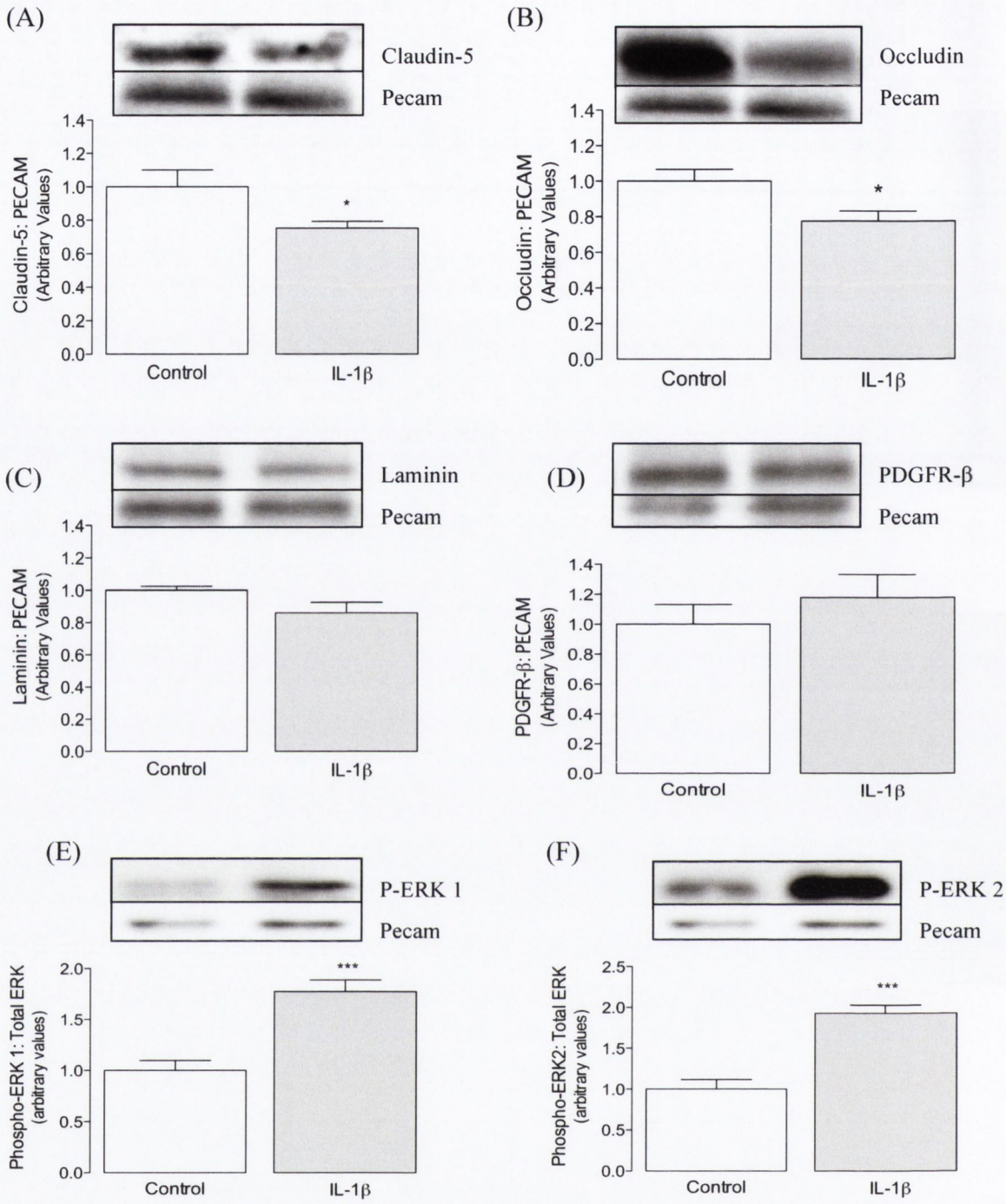

Figure 5.10: IL-1β treatment decreased tight junction protein concentration and increased ERK1/2 activity in organotypic hippocampal slices, though laminin and PDGFR-β expression was not altered.

Claudin-5 (A) and occludin (B) protein concentration were significantly decreased following IL-1β treatment (10ng/ml; 24 hours) though laminin (C) and PDGFR-β (D) protein concentration was unchanged. Both phospho-ERK1 and phospho-ERK2 (D, E) were significantly increased 24 hours post-treatment. Data expressed as mean ± SEM, n=4-9; * $p<0.05$, *** $p<0.001$ versus untreated controls; Student's *t*-test.

5.10 The effect of IL-1β on the structural integrity of the NVU in organotypic hippocampal slices

All of the micrographs in Figure 5.11 below illustrate positively immunostained organotypic hippocampal slices with laminin. The basal lamina appeared intact in slices from untreated controls (A and B) whereas the basal lamina from IL-1β-treated slices appeared more fragmented (C and D).

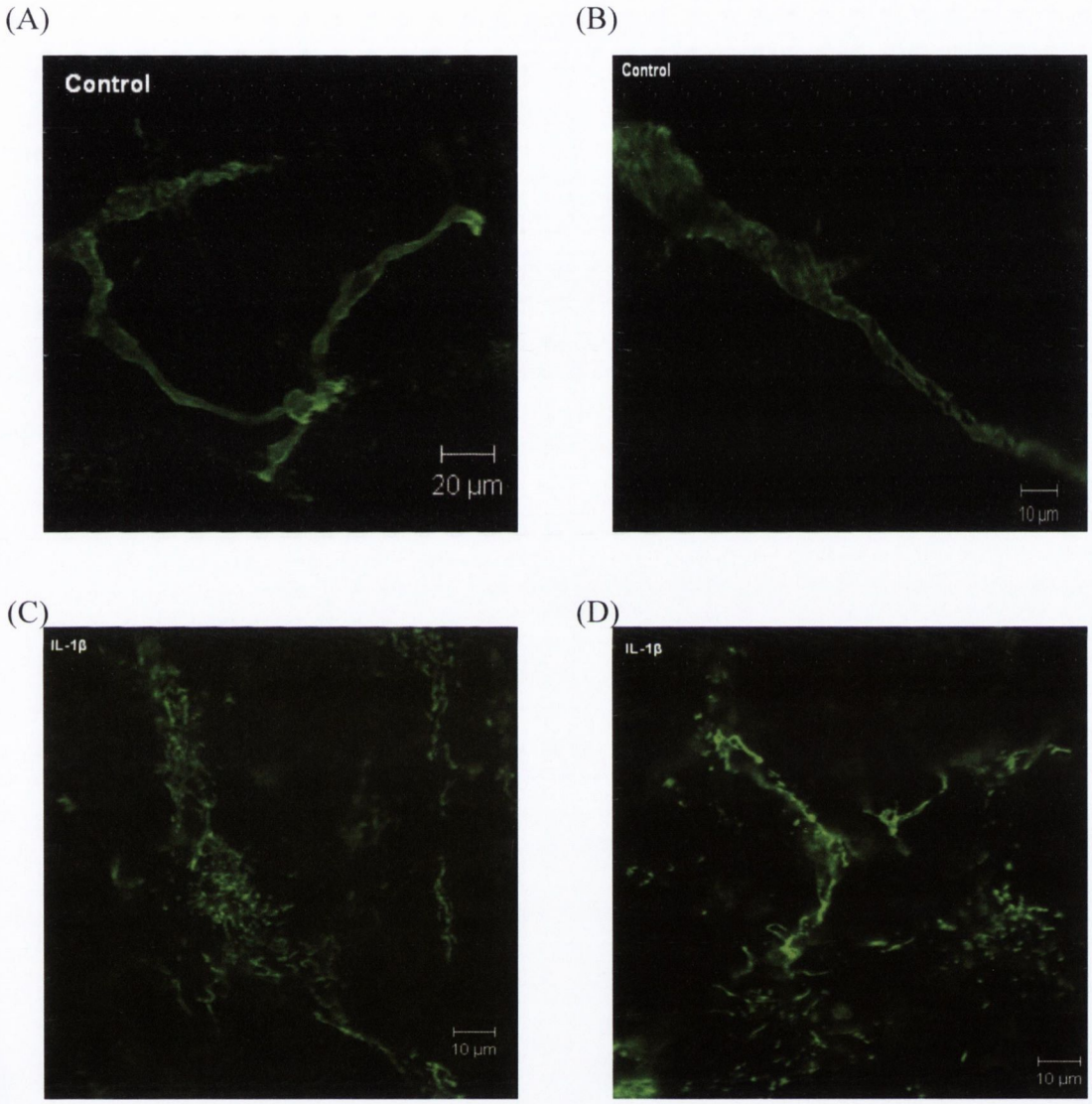

Figure 5.11: Laminin appeared fragmented in organotypic hippocampal slices following IL-1β treatment

Confocal images of organotypic hippocampal slices illustrate the fragmented nature of laminin following IL-1β treatment for 24 hours (C and D, 10ng/ml) compared to slices from untreated controls (A and B).

5.11 IL-1β treatment modulated laminin and PDGFR-β protein concentration in a time-dependant manner in organotypic hippocampal slices

Though IL-1β did not significantly alter laminin and PDGFR-β at the 24 hour timepoint as assessed by Western immunoblotting (Figure 5.10 C and D), laminin fragmentation was visible by 24 hours as assessed by confocal microscopy (Figure 5.11 C and D). Therefore we set out to investigate if these NVU proteins had been altered at an earlier timepoint when organotypic hippocampal slices were incubated with IL-1β (10ng/ml) for 1 or 6 hours.

Laminin protein concentration was significantly increased 1 hour after IL-1β treatment (Figure 5.12 A; ***$p<0.001$; ANOVA; n=3-4) and subsequently its concentration was significantly decreased (***$p<0.001$) 6 hours after IL-1β treatment. PDGFR-β was decreased 1 hour following IL-1β treatment, though this reduction was not statistically significant (Figure 5.12 B). However, by 6 hours, PDGFR-β protein concentration was significantly decreased (Figure 5.12 B; *$p<0.05$; ANOVA; n=3-4) when compared to untreated controls.

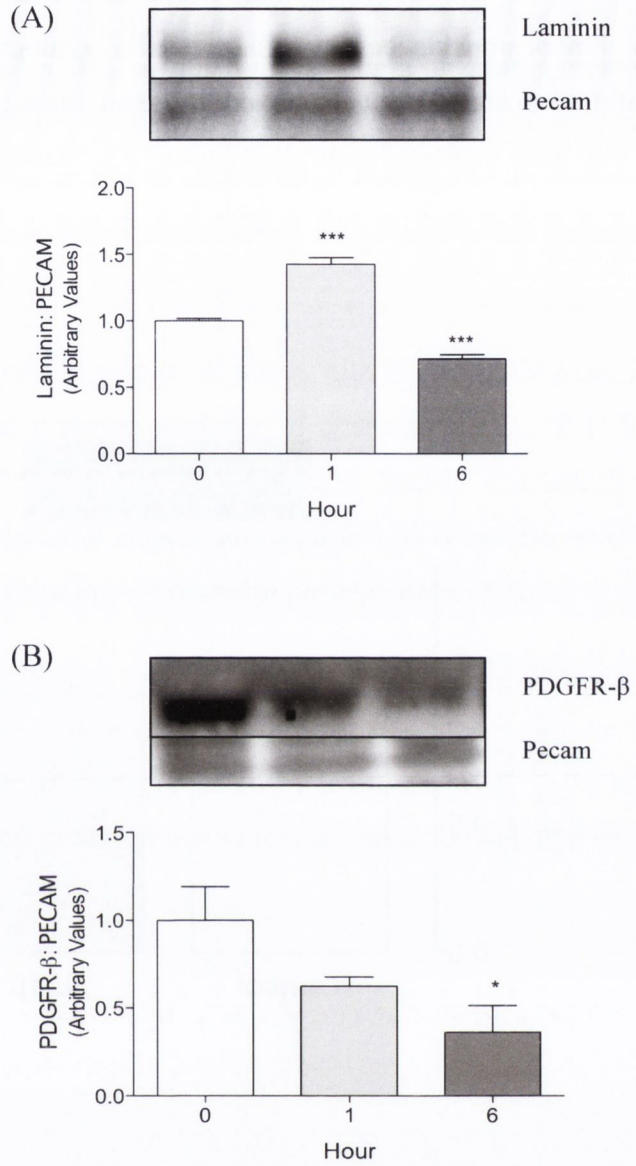

Figure 5.12: IL-1β treatment modulated laminin and PDGFR-β protein concentration in a time-dependant manner in organotypic hippocampal slices.

IL-1β treatment (10ng/ml) significantly increased laminin protein concentration after 1 hour exposure (A). Both laminin (A) and PDGFR-β were significantly decreased 6 hours post IL-1β treatment when compared to untreated controls. Data expressed as mean ± SEM, n=3-4; * $p<0.05$, *** $p<0.001$ versus control; one-way ANOVA followed by Newman-Keuls *post-hoc* test.

5.12 The effect of IL-1β on MMP activity in organotypic hippocampal slices

MMP-9, a known modulator of laminin, could not be detected in supernatants from organotypic hippocampal slices by either gelatin zymography or ELISA. However MMP-2 could be detected, though its activity level from IL-1β-treated slices was not different to that from untreated controls (Figure 5.13; Student's *t*-test; n=8).

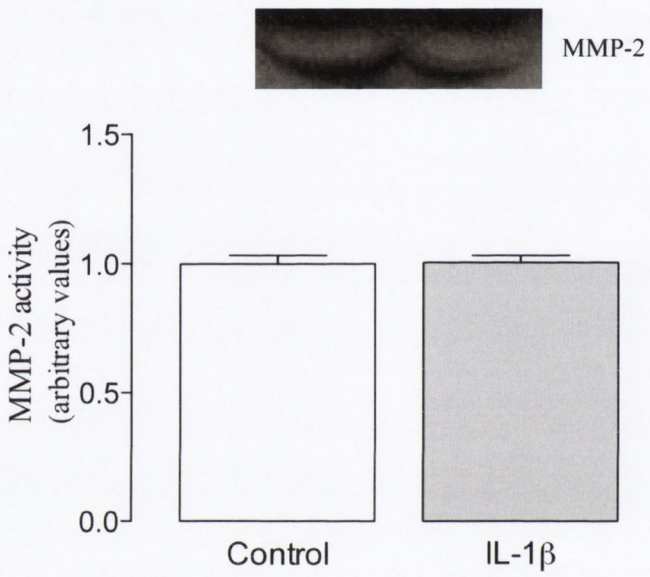

Figure 5.13: MMP-2 activity was unchanged in supernatant from untreated and IL-1β-treated organotypic hippocampal slices.

MMP-2 activity levels as assessed by gelatin zymography were not changed following IL-1β treatment (10ng/ml; 24 hours). Data expressed as mean ± SEM, n=8; Student's *t*-test.

5.13 The effect of IL-1ra in attenuating the IL-1β-mediated disruptions in tight junction proteins in organotypic hippocampal slices

In the previous chapter we demonstrated that the tight junction proteins were modulated by IL-1β (10ng/ml) when we assessed young and middle-aged, wild type and IL-1R1$^{-/-}$ knockout mice. Here we sought to extend those findings to the *in vitro* scenario where organotypic hippocampal slices were treated with IL-1β in the absence/presence of IL-1ra.

Treatment of organotypic hippocampal slices with IL-1ra (250ng/ml; 1h pre-treat, 24 h co-incubation) showed a strong tendency to attenuate the IL-1β (10ng/ml; 24 hours) mediated reductions in claudin-5 and occludin protein concentration, though these changes were not statistically significant (Figure 5.14 A and B: ANOVA; n=3-4). IL-1ra itself did not alter claudin-5 or occludin protein concentration.

Laminin protein concentration was significantly decreased following 24 hours treatment with IL-1β (10ng/ml), when compared to untreated controls (Figure 5.14 C; *$p<0.05$; n=3-4). This reduction was not prevented by treatment with IL-1ra and in fact, IL-1ra itself attenuated laminin concentration to levels similar to the IL-1β-treated group.

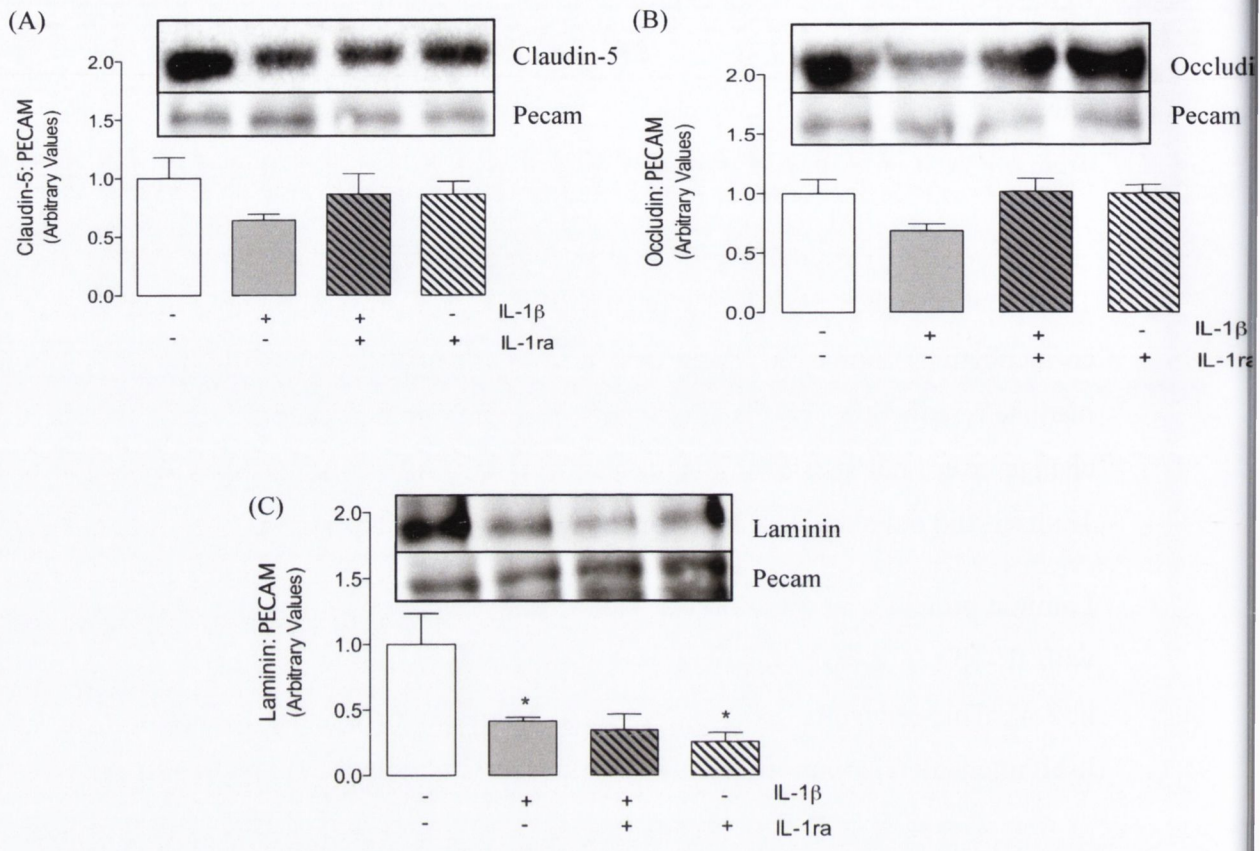

Figure 5.14: IL-1ra attenuated, though not significantly, the IL-1β-mediated reductions in claudin-5 and occludin, but not laminin.

IL-1ra pre-treatment (250ng/ml; 1 hour) of organotypic hippocampal slices prior to co-treatment with IL-1β (10ng/ml; 24 hours) did not fully attenuate the IL-1β-mediated reductions in claudin-5 (A) or occludin (B). Both IL-1β and IL-1ra significantly reduced laminin protein concentration when compared to untreated control levels (C). Data expressed as mean ± SEM, n=3-4; * $p<0.05$ versus control; two-way ANOVA followed by Bonferroni *post*-hoc test.

(A) Two-way ANOVA: IL-1β $_{effect}$ F (1,11) = 1.411; p = 0.2599, IL-1ra $_{effect}$ F (1,11) = 0.07, p = 0.7846, Interaction $_{effect}$ F (1,11) = 1.464; p = 0.2577.

(B) Two-way ANOVA: IL-1β $_{effect}$ F (1,11) = 2.341; p = 0.1542, IL-1ra $_{effect}$ F (1,11) = 2.727, p = 0.1269, Interaction $_{effect}$ F (1,11) = 2.766; p = 0.1245.

(C) Two-way ANOVA: IL-1β $_{effect}$ F (1,11) = 2.829; p = 0.1207, IL-1ra $_{effect}$ F (1,11) = 7.610, p = 0.0186, Interaction $_{effect}$ F (1,11) = 5.272; p = 0.0423.

5.14 The effect of IL-1ra in attenuating the IL-1β-mediated modulation of ERK1/2 activities in organotypic hippocampal slices

Previously, we reported an IL-1β-mediated increase in both ERK1 and ERK2 activity levels (Figure 5.10, E and F). Next we investigated if pre-treatment with IL-1ra could modulate these effects.

Although there was a tendency for IL-1β (10ng/ml; 24 hours) to increase phosphorylation of ERK1 and 2, the large variability meant these changes were not statistically significant. Therefore, it was not possible to truly evaluate the impact of IL-1ra as larger samples numbers were required (Figure 5.15 A and B; ANOVA; n=3-4).

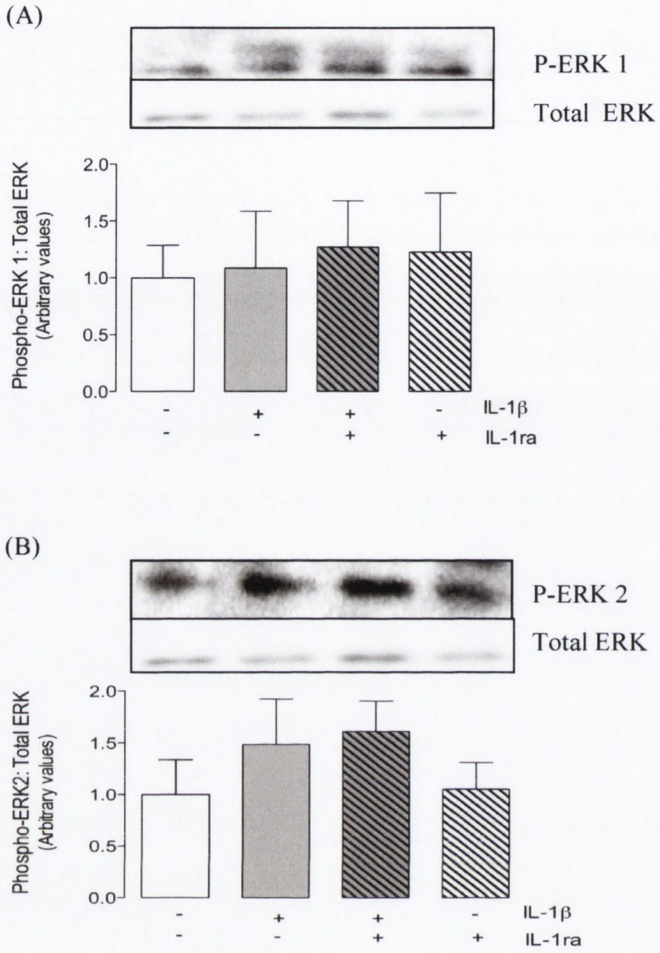

Figure 5.15: Neither IL-1β or IL-1ra modulated the phosphorylation levels of ERK1 or ERK2.

Pre-treatment of organotypic hippocampal slices with IL-1ra (250ng/ml) 1 hour prior to co-treatment of the slices with IL-1β (10ng/ml; 24 hours) did not attenuate phosphor-ERK1 (A) or phospho-ERK2 (B) levels. Data expressed as mean ± SEM, n=3-4; two-way ANOVA followed by Bonferroni *post-hoc* test.

(A) Two-way ANOVA: IL-1β $_{effect}$ F (1,8) = 0.0218; p = 0.8861, IL-1ra $_{effect}$ F (1,8) = 0.2209, p = 0.6509, Interaction $_{effect}$ F (1,8) = 0.00235; p = 0.9625.

(B) Two-way ANOVA: IL-1β $_{effect}$ F (1,8) = 2.211; p = 0.9023, IL-1ra $_{effect}$ F (1,8) = 0.06160, p = 0.811, Interaction $_{effect}$ F (1,8) = 0.01075; p = 0.920.

5.15 The effect of ONO4817, a broad scale MMP inhibitor, on laminin and PDGFR-β expression in organotypic hippocampal slices following IL-1β treatment.

Despite the fact that (i) we could not detect MMP-9 in supernatant from organotypic hippocampal slices for technical reasons and (ii) IL-1β did not induce an increase in MMP-2 activity (Figure 5.13 above), we could not rule out the possibility that MMP-9 or other MMP might be underlying the IL-1β-induced decrease in laminin and PDGFR-β protein concentration after a 6 hour treatment. Therefore, we used a broad spectrum MMP inhibitor which was more selective for MMP-2 and -9, in addition to MMP-8, -12 and -13 to assess the possible role of MMP activation following treatment with IL-1β. In the literature, this inhibitor is used at concentrations ranging from 10 to 20μM (Muraishi *et al.*, 2001), so we decided to use both concentrations in our *in vitro* experiments.

There was a trend for IL-1β (10ng/ml) to reduce PDGFR-β protein concentration but this was not statistically significant following a two-way ANOVA (Figure 5.16 A; $F(1,18) = 2.894$; $p = 0.1061$). There was an MMP inhibitor effect though this was not statistically significant (Figure 5.16 A; $F(1,18) = 3.157$, $p = 0.0668$). More specifically, when the organotypic hippocampal slices were pre-incubated with the inhibitor at a concentration of 10μM for 1 hour, followed by the 6 hour IL-1β treatment, the PDGFR-β protein concentration was similar to untreated controls. This effect was not replicated when the slices were pre-incubated with the inhibitor at 20μM. Surprisingly, the decreased PDGFR-β protein concentration following IL-1β were also observed with the inhibitor at 20μM (with or without IL-1β co-incubation).

There was no statistically significant effect of either the inhibitor or IL-1β treatment on laminin protein concentration. This was surprising given that a 6 hour IL-1β treatment had previously been shown (Figure 5.12 A)

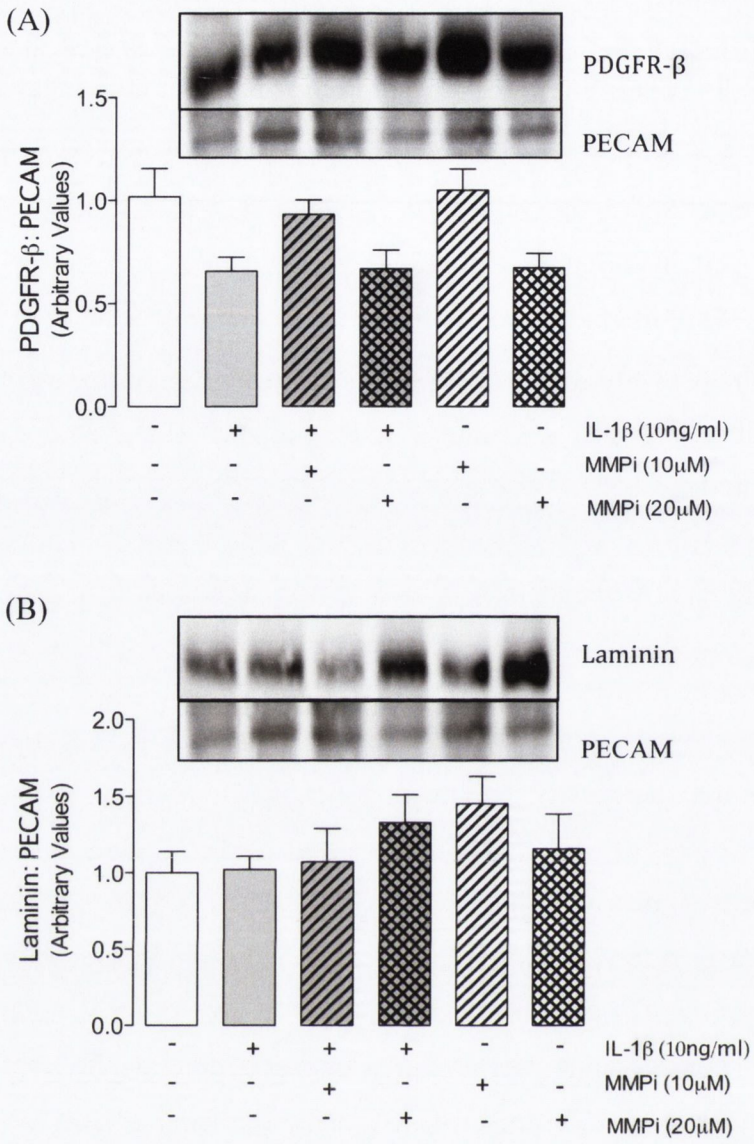

Figure 5.16: The broad spectrum MMP inhibitor differentially affected PDGFR-β and laminin protein concentration

Organotypic hippocampal slices were pre-treated with the broad spectrum MMP inhibitor, ONO4817 1 hour prior to a 6 hour treatment with IL-1β (10ng/ml). Though there was no statistical effect of either MMP inhibitor or IL-1β on either PDGFR-β or laminin protein concentration, there was a trend where the MMP inhibitor (10μM) prevented the IL-1β-induced decrease in PDGFR-β protein concentration. Data expressed as mean ± SEM, n=3-6; two-way ANOVA followed by Bonferroni *post-hoc* test.

(A) Two-way ANOVA: Inhibitor $_{effect}$ $F(1,18) = 3.157$; $p = 0.0668$, IL-1β $_{effect}$ $F(1,18) = 2.894$; $p = 0.1061$, Interaction $_{effect}$ $F(1,18) = 1.464$; $p = 0.2577$.

(B) Two-way ANOVA: Inhibitor $_{effect}$ $F(1,18) = 1.744$; $p = 0.2032$, IL-1β $_{effect}$ $F(1,18) = 2.050$; $p = 0.6561$, Interaction $_{effect}$ $F(1,18) = 1.249$; $p = 0.3105$.

5.16 The effect of ONO4817, a broad scale MMP inhibitor, on claudin-5 and occludin protein concentration in organotypic hippocampal slices following IL-1β treatment.

IL-1β (10ng/ml) treatment for 6 hours decreased claudin-5 protein concentration in organotypic hippocampal slices (significant with a student *t*-test; $p<0.05$) though the IL-1β effect was not significant by a two-way ANOVA (Figure 5.17 A; $F(1,17) = 3.054$; $p = 0.0986$). There was a significant inhibitor effect on claudin-5 (Figure 5.17 A; $F(1,17) = 7.034$, $p = 0.0059$). Bonferroni *post-hoc* tests revealed that at 20μM, the MMP inhibitor rescued claudin-5 protein concentration when compared with IL-1β-treated organotypic hippocampal slices (**$p<0.01$) but not at 10μM. In fact, incubation with just the MMP inhibitor at 10μM decreased claudin-5 protein concentration similar to IL-1β-treated levels.

Occludin protein concentration was decreased with a 6 hour IL-1β treatment, though this reduction was not significant with the two-way ANOVA (Figure 5.17 B; $F(1,18) = 2.674$; $p = 0.1194$). There was a significant effect of MMP inhibitor treatment (Figure 5.17 B; $F(1,18 = 5.206$, $p = 0.0164$). Pre-treatment with the MMP inhibitor at 10μM prevented the IL-1β-induced reduction in occludin concentration to levels that were similar to untreated controls. There was a differential effect with the MMP inhibitor at 20μM. Bonferroni *post-hoc* tests revealed that the MMP inhibitor (20μM), in the absence or presence of IL-1β, significantly decreased occludin protein concentration (*$p<0.05$).

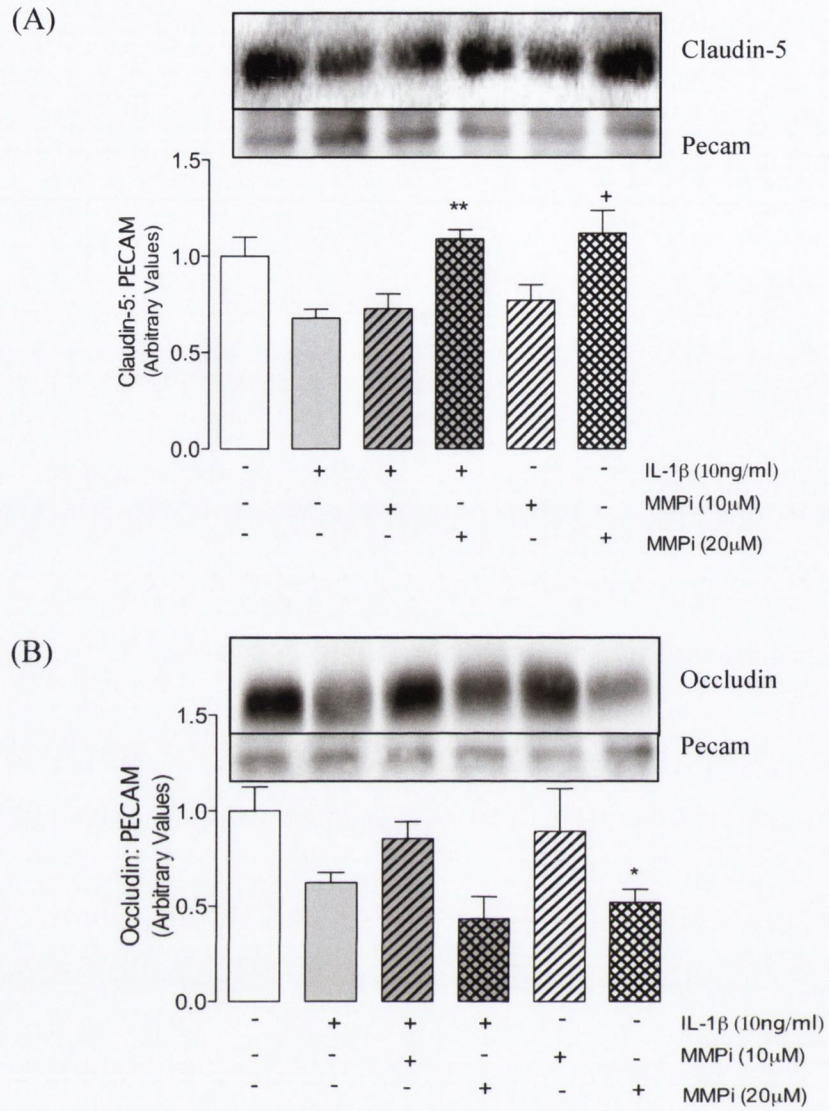

Figure 5.17: The broad spectrum MMP inhibitor differentially affected claudin-5 and occludin protein concentration.

Organotypic hippocampal slices were pre-treated with the broad spectrum MMP inhibitor, ONO4817, 1 hour prior to a 6 hour treatment with IL-1β (10ng/ml). There was an inhibitor effect on both claudin-5 and occludin protein concentration where the MMP inhibitor at 20μM was most effective at preventing the IL-1β-induced decrease in claudin-5 whereas 10μM was more effective at returning occludin protein concentration to that of the untreated controls. Data expressed as mean ± SEM, n=3-6; **$p<0.05$ versus IL-1β, + $p<0.05$ versus MMP inhibitor 10μM, *$p<0.05$ versus control; two-way ANOVA followed by Bonferroni *post-hoc* test.

(A) Two-way ANOVA: Inhibitor $_{effect}$ $F(1,17) = 7.034$; $p = 0.0059$, IL-1β $_{effect}$ $F(1,17) = 3.054$; $p = 0.0986$, Interaction $_{effect}$ $F(1,17) = 1.938$; $p = 0.1745$.

(B) Two-way ANOVA: Inhibitor $_{effect}$ $F(1,18) = 5.206$; $p = 0.0164$, IL-1β $_{effect}$ $F(1,18) = 2.674$; $p = 0.1194$, Interaction $_{effect}$ $F(1,18) = 1.333$; $p = 0.2885$.

5.17 The effect of ONO4817, a broad scale MMP inhibitor, on MMP activity in organotypic hippocampal slices following IL-1β treatment.

MMP-2 activity in supernatant from organotypic hippocampal slices was not modulated by IL-1β or by the broad spectrum MMP inhibitor at 10μM or 20μM (Figure 5.18; ANOVA; n=3). MMP-9 activity could not detected by gelatin zymography.

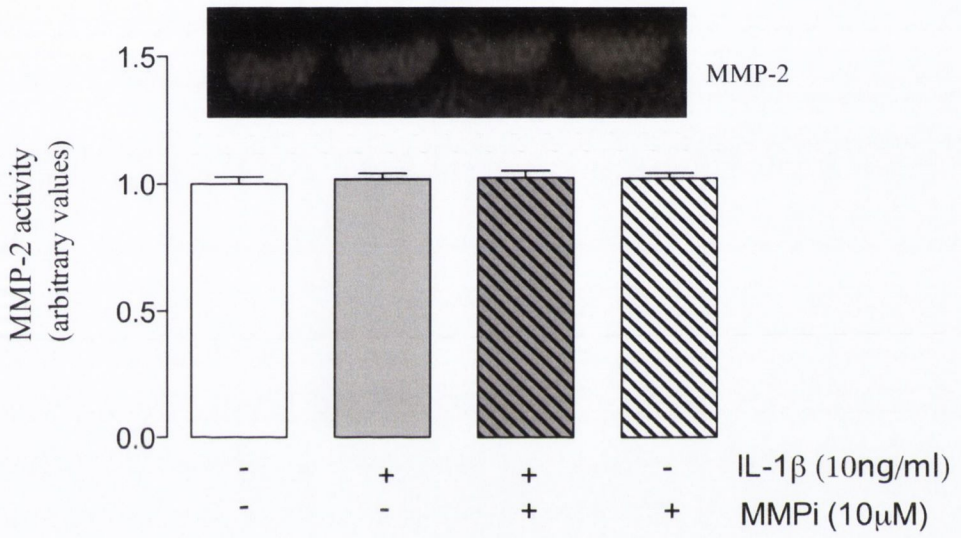

Figure 5.18: The broad spectrum MMP inhibitor did not alter MMP-2 activity at 10μM concentration.

Gelatin zymography did not reveal a significant difference in MMP-2 enzymatic activity between control and IL-1β (10ng/ml, 6 hours) treated organotypic hippocampal slices. Data expressed as mean ± SEM; n=3; one-way ANOVA followed by Newman-Keul *post-hoc* test.

5.18 Discussion

The previous chapter reported that IL-1R1$^{-/-}$ mice show increased levels of tight junction protein concentration compared to middle aged wildtype mice. Thus, the aim of this chapter was to investigate in further detail the contribution of IL-1β in mediating reduction of tight junction protein concentration, on endothelial cells. Despite the literature documenting IL-1β-mediated disruption of the BBB (Ching *et al.*, 2005; Argaw *et al.*, 2006) and disruption of tight junction concentration in the periphery (Al-Sadi *et al.*, 2010), there is limited information regarding the molecular signalling mechanisms by which this occurs, particularly in cerebral endothelial cells.

When attempting to mimic *in vitro*, the biochemical composition and functional properties of the BBB *in vivo*, most BBB models now employ a multi-cell model encompassing not only endothelial cells but also astrocytes and pericytes (Cohen-Kashi Malina *et al.*, 2009) or conditioned media from these cell types (Deli *et al.*, 2005). These multi-celled models are often used to assess BBB functionality. However because we sought to investigate, in the first instance, the IL-1β- and LPS-mediated signalling mechanisms resulting in tight junction protein concentration on endothelial cells we chose to use a monolayer of endothelial cells (bEnd.3) so as to minimise the confounding influence of other cells of the NVU i.e. to minimise the effects of their physical connections with endothelial cells, as well as their secreted signalling molecules. Then, having established the IL-1β/LPS-induced pathway(s) modulating tight junction protein expression in endothelial cells, it was the aim to extend the investigations to multi-cell models/ conditioned media from cells of the NVU, in an attempt to produce an *in vitro* environment that was more reflective of the *in vivo* BBB.

Initially, we observed that both LPS and IL-1β profoundly decreased claudin-5, occludin and ZO-1 as early as 1 hour post-treatment. The concentration levels of the tight junction proteins reduced by up to 75% of their pre-treatment level, between 3 to 6 hours post-treatment, but levels recovered by 24 hours. These results are supported by other studies in the literature documenting that both IL-1β and LPS disrupt tight junction proteins (Sozen *et al.*, 2009; Xiaolu *et al.*, 2011). Disrupted ZO-1 expression in mice following sub-arachnoid haemorrhage has been attributed to IL-1β activity and LPS (5μg/ml) decreases claudin-5, occludin and ZO-1 in bEnd.3 also leading to disrupted permeability (Xialou *et al.*, 2011).

The initial treatment procedures on bEnd.3 cells involved a standard media change, whereby all media was removed from each well and replaced with either fresh warmed-media (control wells) or fresh media containing recombinant IL-1β (treatment wells). We observed a reduction in TJ following both IL-1β and LPS treatment, a result that is supported by much of the literature. We were surprised when application of a concentrated (10x) IL-1β treatment did not disrupt claudin-5, occludin or ZO-1 from 3 to 6 hours, despite this being the timepoints at which tight junction protein expression was previously shown to be at their lowest. Therefore, we had to consider that a full media change might be sufficient to disrupt tight junction protein expression.

Having established that endothelial tight junction proteins were disrupted following an insult, either by IL-1β or media change, we investigated the molecular signalling pathways that may have been underlying such disruptions. Endothelial cells express IL-1R1 (Boraschi *et al.*, 1991) and activation of this receptor in response to stressful stimuli leads to activation of a variety of mitogen-associated protein kinase (MAPK) signalling cascades, including ERK, JNK and p38. These serine/threonine kinases are capable of regulating a multitude of cellular activities including gene expression (Pearson *et al.*, 2001). As the tight junction proteins themselves are capable of being phosphorylated (Gonzalez-Mariscal *et al.*, 2008), the MAPK might directly phosphorylate the tight junction proteins, or they may regulate transcription of tight junction proteins at the mRNA level. The literature is conflicted regarding tight junction protein phosphorylation and regulation (Gonzalez-Mariscal *et al.*, 2008) thus we have limited our discussion to the effects of MAPK specifically on brain endothelium.

Following IL-1β and LPS treatment of bEnd.3 over 24 hours, immunoblotting did not reveal any changes in p-JNK1/2 expression, indicating that the JNK-MAPK was not mediating the profound tight junction proteins reductions. In contrast, there were significant changes in bEnd.3 expression of phospho ERK1 and -2 over the timecourse. Following IL-1β treatment of bEnd.3, phospho ERK2 was significantly decreased at 1, 3 and 12 hours i.e. when tight junction proteins were at their lowest expression levels, as indicated by the immunoblots for tight junction proteins. Phospho ERK1/2 showed very similar expression patterns in the LPS-treated bEnd.3 i.e. there was a parallel decrease in both phospho ERK1/2 and tight junction protein expression. These findings indicated that phospho-ERK may be required to maintain tight junction protein

expression during inflammation. We attempted to pre-treat b.End3 cells with an ERK inhibitor (U0126) to further elucidate the role of ERK signalling, but because the cells were not responsive to IL-1β or LPS (data not shown), this set of experiments was abandoned. Although the literature is conflicted regarding ERK regulation of tight junction proteins (Gonzalez-Mariscal *et al.*, 2008), most studies have found that activation of the ERK-MAPK pathway disrupts tight junction proteins leading to barrier dysfunction. LPS-injected ethanol-drinking rats had increased BBB permeability, a result that was attributed to ERK- but not JNK-mediated reductions in occludin and ZO-1 (Singh *et al.*, 2007). An ERK inhibitor applied to porcine cerebral endothelial cells prevented H_2O_2-mediated ZO-1 and occludin disruption (Fischer *et al.*, 2005) and a study on human corneal epithelial cells showed that the cells displayed increased paracellular permeability and altered cellular distribution of ZO-1, mediated by ERK signalling (Wang *et al.*, 2004). However, a study on primary mouse endothelial and rat endothelial cell lines demonstrated that increased neutrophil migration i.e. barrier disruption of endothelial cells, was unaffected by MAP kinase inhibitors, indicating that changes in barrier function were independent of the MAPK signalling cascades (Thornton *et al.*, 2010), so this study supports our findings that ERK activation may maintain tight junction protein concentration. Having read the literature on the role of ERK, it seems that ERK is capable of carrying out opposing effects on tight junction protein expression, depending on the cell type under investigation and the nature of the insult.

The claudin-5 and occludin immunoblots in our study displayed a single band so there was no obvious evidence of phosphorylation, which would be indicated by bands of increased molecular weight. Another approach to assess tight junction protein phosphorylation would be to carry out an immunoprecipitation assay for claudin-5/occludin and also probe with an anti-serine/threonine antibody. In addition, one could pre-treat b.End3 cells with an ERK inhibitor prior to the IL-1β treatment to investigate ERK's contribution to tight junction proteins disruption.

Given the findings that IL-1β application to bEnd.3 yielded different results on TJ depending on whether there was a full media change/ minimal media disruption, we had to consider that a full media change might be sufficient to disrupt tight junction protein concentration.

This hypothesis was confirmed by subsequent experiments showing that changing the media alone, significantly decreased claudin-5 protein concentration in bEnd.3 to such an extent that additional insult with IL-1β did not further decrease claudin-5 concentration. These findings are similar to a study on Caco-2 epithelial cells, a cell line often used in barrier research. Li and colleagues (2003) found that changing the media of Caco-2 cells decreased transepithelial electrical resistance (TEER) to less than 25% of the TEER values prior to changing the media (Li *et al.*, 2003). We hypothesised that changing the 'old' media and replacing wells with fresh media caused tight junction protein disruptions possibly due to the removal of endothelial growth factors secreted by the cells themselves. However, the authors of the Caco-2 study attributed the changes in TEER to exposure of the Caco-2 to the atmosphere, because when they changed the media using a perfusion technique (gradually diluting old media with new media), TEER was not altered. It was not surprising that bEnd.3 responded in such a profound manner to changing the media, as by their very nature, endothelial cells are highly sensitive and responsive to local environmental changes.

For all subsequent experiments on the bEnd.3 it was decided to remove a small volume of media, to which IL-1β was added (10X) and this same media was returned to the cells thereby minimising exposure of the bEnd.3 cells to the atmosphere and minimising dilution/removal of endothelial-derived growth factors. Surprisingly, IL-1β administered as a 10x treatment did not decrease endothelial tight junction protein concentration. Because the protein concentration was not altered we investigated if instead, the tight junction proteins were being re-distributed within the cell from the membrane to the cytosol and *vice versa*. When we assessed both membrane and cytosolic fractions, we consistently found that cytosolic levels of claudin-5 protein concentration increased steadily in the course of 48 hours, irrespective of whether or not IL-1β was present and had doubled in relative quantity by 48 hours. We expected that the increased cytosolic concentration of the protein would correlate with a parallel decrease in membrane levels - however this was not the case. Whilst membrane concentration of endothelial claudin-5 changed over time following in the presence/absence of IL-1β, it did not decrease below the initial protein concentration levels at time zero. In fact, claudin-5 protein concentration increased by about 50%, one hour following treatment with IL-1β.

It is possible that the increased cytosolic expression of claudin-5 was not due to the internalisation of already existing claudin-5, but instead due to the expression of newly synthesised claudin-5 in the cytosol, ready to be transported to the membrane. In future, PCR for claudin-5 or inclusion of actinomycin D (an inhibitor of transcription) would clarify if the increased claudin-5 protein concentration the cytosol was indeed newly synthesised protein, rather than redistribution/internalisation of the membrane protein. Claudin-5 and occludin are regulated by the ubiquitination-proteasome system and proteasome inhibition caused increased claudin-5 concentration in the cytosol (Mandel *et al.*, 2012). Interestingly, we never detected occludin concentration in the cytosolic fraction of endothelial cells and membrane levels were not altered by treatment.

Up to this point, the data gleaned from the bEnd.3 experiments was variable and we considered that the high proliferative capacity of these cells might be altering their properties. Serum-starving cells is routinely used *in vitro* to synchronise the growth cycles of proliferating cells by forcing cells to withdraw into the G0/G1 phase of the cell cycle where basal activity is decreased (Cooper, 2003). Following serum starvation, bEnd.3 cells were treated in the either serum-free or full media. When bEnd.3 cells were treated in serum-free media, claudin-5 protein concentration decreased over time. However, when cells were treated in media containing serum, claudin-5 protein concentration in untreated controls increased (by 6 hours) beyond the starting expression levels at time zero. This was not the case when IL-1β was included in the media containing serum where claudin-5 protein concentration continued to decline over time. This finding indicated that whilst IL-1β may not disrupt bEnd.3 tight junction proteins *per se*, it did prevent recovery of an already insulted population of cells. In fact, a recent study indicated that rather than sending cells into a quiescent state, serum starving cells as a culturing technique, can itself dramatically affect cellular signalling in cells e.g. disruption of ERK-MAPK signalling (Pirkmajer & Chibalin, 2011). The authors argued that basal activity is not necessarily reduced and serum-starving procedures described in the literature are so ambiguous about the duration and degree of serum-starvation that results have to be interpreted with caution. The authors maintain that the serum-starving technique needs to be optimised specifically for the cell type being investigated (Pirkmajer & Chibalin, 2011).

Considering the volume of literature that documents the disruptive nature of IL-1β on barrier properties in various cell types, coupled with our finding that tight junction proteins were increased in IL-1R$^{-/-}$ mice, it was surprising that IL-1β did not (apart from the initial experiments) modulate tight junction protein expression in bEnd.3 monolayers. It is possible that in the absence of the NVU, the endothelial monolayers are less responsive to insult, in an attempt to maintain homeostasis and retain barrier function.

The BBB is established and maintained by continuous signalling and communication between the cerebral endothelial cells and the cells of the NVU (Abbott *et al.*, 2006). A recent study emphasised just how vital the NVU is in mediating inflammatory changes at the BBB. Chaitanya and colleagues (2011), in their very comprehensive study investigating the effects of the pro-inflammatory cytokines IL-1β, TNF-α, IFN-γ on endothelial cells, found that monolayers of either mouse or human endothelial cells did not respond to cytokines (Chaitanya *et al.*, 2011). Their results agree somewhat with ours, in that bEnd.3 cells were in the main, unresponsive to IL-1β; findings which disagree with the large body of evidence indicating that IL-1β disrupts tight junction protein concentration. Chaitanya and colleagues (2011) also acknowledged their surprise at this unexpected result. In fact, TEER decreased steadily over 7 days in their endothelial cells in the absence of an insult, and there was no further augmentation when pro-inflammatory cytokines were included. IFN-γ actually increased the TEER of endothelial monolayers and the endothelial metabolic rate was decreased which was considered to be an adaptive response to conserve energy in an effort to maintain endothelial barrier integrity. Similarly, our findings show that in response to insult, be it a media change or IL-1β treatment, membrane expression of claudin-5 consistently increased at one hour post-treatment, possibly an adaptive response to minimise barrier disruption. However, in their study, Chaitanya and colleagues (2011) found that endothelial cells, when co-cultured with cytokine-treated astrocytes, had significantly decreased TEER. This study indicated that pro-inflammatory cytokines disrupt endothelial barrier function in an indirect manner, via astrocyte signalling rather than directly via the endothelial cells themselves. This study highlighted the importance that the cumulative effect of signalling from many cell types can have on barrier function, particularly during pathological conditions.

Taking the study by Chaitanya and colleagues (2011), which highlighted the importance of the NVU in mediating cytokine disruptions on endothelial cells, and also our finding that bEnd.3 monolayers were not responsive to IL-1β, it was decided to steer away from an endothelial cell monolayer system and instead, to utilise organotypic hippocampal slice cultures to study the effects of IL-1β on tight junction proteins.

The use of organotypic slice cultures (OSC) to study BBB biology is a relatively new model. Whilst it is unlikely to be possible to study the "barrier" function of the BBB in OSC, as the *in vitro* preparation by nature severs the vessels, it may prove to be a valuable tool for investigating tight junction regulation. Although, in a recent model of the BBB, OSC were cultured on top of endothelial monolayers to address the impact of various NVU components on the barrier properties of the underlying endothelial cell monolayer (Zehendner *et al.*, 2009; Kovacs *et al.*, 2011). The advantage of using OSC to study tight junction modulation is that the vessels remain intact *in situ*, and continue to be supported both physically and biochemically by the neighbouring cells/components of the NVU. It was previously thought that capillaries needed to be perfused to maintain endothelial cell survival (Carmeliet & Storkebaum, 2002) however it has since been shown that vessels from rat cortex survived in the absence of intraluminal flow for up to 3 weeks and the authors demonstrated that the cellular and trophic environment of OSC was sufficient to maintain vessels in culture (Moser *et al.*, 2003). Brain capillaries are preserved in OSC and the tight junction proteins claudin-5, occludin and ZO-1 were preserved in OSC from neonatal mice brains (Bendfeldt *et al.*, 2007). In addition, Glut-1 and p-glycoprotein transporter proteins were not only maintained, but retained full functionality in slice cultures and the integrity of the basal lamina was also intact in OSC (Camenzind *et al.*, 2010). Our organotypic hippocampal slice cultures (OHSC) were maintained for 7-10 days *in vitro* (DIV) prior to treatment in order to give sufficient time to recover from the trauma of explantation. Though OSC have been treated after 3 DIV in some studies, we allowed the OHSC additional time to recover and for the explantation-induced inflammatory processes to subside (Huuskonen *et al.*, 2005) before we subjected the slices to further inflammatory insults in our effort to investigate the role of inflammation on tight junction protein expression.

Our results from mouse OHSC show that a 24 hour treatment of IL-1β, at physiologically relevant concentrations (10ng/ml) caused significant reductions in both

claudin-5 and occludin protein concentration. These findings were striking given that a 24 hour application of IL-1β did not disrupt tight junctions in bEnd.3 monolayers. These results highlight both the destructive effect of inflammation on tight junction proteins and also the profound influence the surrounding NVU has on the impact of inflammation on BBB integrity. Though results from Western immunoblotting did not reveal a significant decrease in laminin protein concentration following a 24 hour treatment with IL-1β, the basal lamina appeared to be fragmented in IL-1β-treated OHSC, as determined by confocal microscopy. However, when laminin or PDGFR-β expression was investigated at earlier timepoints, both proteins were significantly decreased after 6 hours treatment with IL-1β, indicating that protein concentration recovered to untreated control levels by 24 hours. Taken collectively, our findings that IL-1β disrupts tight junction proteins in OHSC and that IL-1R$^{-/-}$ mice showed increased tight junction protein concentration with age, provides compelling evidence in support of the hypothesis that neuroinflammation impacts negatively on tight junction/BBB integrity.

Our research found that in response to a 24 hour IL-1β treatment, the OHSC displayed significantly elevated levels of both phospho-ERK1 and 2. It raises the possibility that phospho-ERK mediated the tight junction protein disruptions, and whilst this conflicts the findings from our bEnd.3 data, the results from the OHSC support the main body of literature on the role of ERK phosphorylation and tight junction protein modification (Wang *et al.*, 2004; Fischer *et al.*, 2005; Singh *et al.*, 2007; Al-Sadi *et al.*, 2010).

Whilst it is highly plausible that ERK phosphorylation mediated the tight junction proteins disruptions seen in OHSC, further studies are required to confirm this. Despite the increased activity in ERK1/2 following IL-1β treatment, the cell-type(s) involved, need to be determined. In order to determine if the increased phospho-ERK expression correlated with decreased endothelial tight junction protein expression, one could (i) double-immunostain OHSC with cell-specific antibodies and antibodies to phospho-ERK and tight junction proteins or (ii) pre-treat the OHSC with an ERK inhibitor, isolate the endothelial cells from the OHSC and probe for phospho-ERK and tight junction proteins by Western immunoblotting. Immunoprecipitating claudin-5 from the OHSC followed by probing with an anti-serine/threonine antibody would indicate if phospho-ERK was directly phosphorylating claudin-5. Pre-treatment with actinomycin

D would indicate if IL-1β induced ERK activation was modulating the tight junction proteins at the mRNA level.

IL-1ra is the endogenous antagonist for the IL-1R1 and binds competitively to the receptor to prevent downstream signalling following the binding of either IL-1β or IL-1α ligands (Hannum *et al.*, 1990). Other studies where the BBB was not under investigation, reported that IL-1β (6ng/ml) increased microglial activity in OSC and this was attenuated by incubation with IL-1ra (100ng/ml) (Hailer *et al.*, 2005). Similarly, an investigation into IL-1 signalling in the context of haem-driven inflammation in OSC reported that the haem-mediated activation of the IL-1 pathway was reduced by IL-1ra (sub-cutaneous injection, 100/mg/kg) (Greenhalgh *et al.*, 2012). A very recent study demonstrated that IL-1ra (25mg/kg) administered subcutaneously following middle cerebral artery occlusion (MCAO) in male rats with co-morbities (age, corpulency), resulted in decreased BBB disruption and decreased cytokine levels in the brain (Pradillo *et al.*, 2012). IL-1β is known to exacerbate brain damage in a number of conditions including subarachnoid haemorrhage, stroke and dementia (Allan *et al.*, 2005). IL-1ra based therapies are currently being employed or investigated in inflammatory diseases where IL-1β is thought to contribute to pathology e.g. rheumatoid arthritis (Dinarello, 2011) and acute stroke (Emsley *et al.*, 2005). We found that pre-treatment of OHSC with IL-1ra attenuated the IL-1β mediated reductions in claudin-5 and occludin, which implied that IL-1ra preserved tight junction expression following treatment with IL-1β. IL-1ra tended to decrease the IL-1β-mediated increases in phospho-ERK, although those results did not reach statistical significance. In contrast to the protective role of IL-1ra on claudin-5 and occludin protein concentration, laminin protein concentration was significantly decreased following both IL-1ra and IL-1β application for 24 hours. As previously discussed, our work demonstrated that laminin expression was decreased in both young and middle-aged IL-1R1 $^{-/-}$ mice. Taken together these findings imply that the IL-1R1 signalling pathway is required to maintain laminin expression in the basal lamina. It's possible that the laminin is still decreased in the IL-1R1$^{-/-}$ mice due to MMP release from other cell types, possibly induced by cytokines other than IL-1β (Galis *et al.*, 1994).

IL-1β is a known activator of MMP-9 (Haorah *et al.*, 2007) and MMP disrupt the basal lamina and tight junction proteins themselves, contributing to increased BBB

permeability via MAPK signalling pathways (Liang *et al.*, 2007). Thus, a broad spectrum MMP inhibitor (ONO4817) was applied to OHSC to investigate if IL-1β mediated MMP activity was underlying the tight junction protein disruptions.

Claudin-5 and occludin were differentially regulated by different concentrations of the MMP inhibitor. More specifically, at 20μM the inhibitor prevented the IL-1β-induced reduction in claudin-5 protein concentration whereas at 10μM the inhibitor, even on its own, decreased claudin-5 protein concentration. The converse was true when occludin was assessed – the lower 10μM concentration was more effective at returning occludin expression following IL-1β treatment, to levels similar to the untreated control group. The finding that a broad spectrum MMP inhibitor rescued IL-1β-mediated tight junction protein reductions (albeit at different concentrations) is supported by a number of studies both *in vivo* and *in vitro*. An injection of MMP inhibitor (BB-1101) 10 minutes prior to MCAO in rats, prevented the degradation in claudin-5 and occludin which was apparent in animals that had undergone MCAO (Yang *et al.*, 2007). An MMP inhibitor (GM-6001) rescued H_2O_2-mediated occludin cleavage in primary porcine endothelial cells *in vitro* (Lischper *et al.*, 2010). Treatment of OHSC with the MMP inhibitor at 10 μM significantly rescued the IL-1β-mediated reductions in PDGFR-β. This was an interesting result, because *in vivo*, PDGFR-β protein concentration was not altered in IL-1R1$^{-/-}$ mice. Laminin protein concentration was not altered by IL-1β in this set of experiments, so it is difficult to assess the true impact that the MMP inhibitor might have. However, it appeared that at the 10μM concentration the MMP inhibitor alone increased laminin protein concentration beyond untreated control levels. It must be acknowledged that ONO4817 the MMP inhibitor used in our study is a broad spectrum inhibitor. Though it is most selective at inhibiting MMP-2 and -9 (Ki = 0.73 and 2.1 nM, respectively) it is also very selective for MMP-8, -12 and -13 and much less so for MMP-3 and -7. The IL-1β treatment may be inducing some or all of these MMP and hence explain the MMP inhibitor's ability to rescue the various proteins.

Our results did not reveal an IL-1β-mediated increase in basal MMP-2 activity, nor did application of MMP inhibitor, at any molarity or timecourse modulate basal MMP-2 expression. As gelatin zymography nor ELISA could detect MMP-9 activity, we are unable to confirm whether or not IL-1β modulated its activity, nor could we confirm that the MMP inhibitor actually inhibited its activity. These results were perplexing

given that IL-1β is a known upregulator of MMP-9 in glia (Crocker *et al.*, 2006) epithelia and endothelia (Haorah *et al.*, 2007). We were most interested in MMP-2 AND -9 in light of their increased activity in the aged rat brain and aged human serum. However, given that we were unable to measure MMP-9 activity in OHSC, MMP-9's role *in vitro* remains to be determined.

In vitro models of the BBB encompass not only endothelial cells but also astrocytes and pericytes, or at the very least, conditioned media from these cells of the NVU. It is unrealistic to expect that any endothelial cell type *in vitro*, whether cultured with or without NVU components, will display the full phenotypic and functional properties of the BBB *in vivo*. Despite our best efforts and despite the evidence from the literature (Brown *et al.*, 2007), bEnd.3 monolayers do not appear to be a suitable model for investigating tight junction proteins under inflammatory conditions. Treatment of OHSC with IL-1β significantly reduced protein concentration of claudin-5, occludin and elements of the NVU, laminin and PDGFR-β. The literature (Huuskonen *et al.*, 2005) suggests that the OHSC are more representative of the *in vivo* BBB due to intact endothelial-NVU signalling pathways and hence this *in vitro* system may be a more promising prospect for assessing altered tight junction protein concentration rather than the endothelial monolayers. IL-1β disrupted tight junction proteins of the BBB *ex vivo* in the OHSC and this may be mediated by MMP (which ones, are yet to be determined) because the broad spectrum MMP inhibitor rescued IL-1β-induced tight junction disruptions. In addition, further research is needed to establish if the alterations in tight junction protein concentration are mediated by the ERK-MAP kinase signalling cascade.

Chapter 6

General Discussion

6. General Discussion

The results presented in Chapter 3 demonstrated that the BBB was functionally and structurally disrupted in the aged rat brain. Increased BBB permeability with age was evidenced by extravasation of (i) endogenous plasma albumin and (ii) exogenous sodium fluorescein to the brain parenchyma. This increased BBB permeability was likely due to the decreased claudin-5 and occludin protein concentration, which was observed in the same rat tissue.

It is noteworthy that the research varies greatly when assessing BBB permeability. It is difficult to find a standard "young" or "old age, in addition, studies vary in their definition of "healthy" older subjects. The techniques employed to measure BBB permeability also vary; plasma IgG and albumin extravasation via immunohistochemistry and/or MRI assessment of injected tracers. That BBB permeability was modulated with age is in agreement with some human studies described in the literature. A meta-analysis study of the human literature by Farrall & Wardlaw. (2009) noted that six studies (213 young healthy versus 238 old healthy subjects) documented significant increases in BBB permeability with age, as assessed by MRI and immunohistochemistry where appropriate, though these studies did not assess changes in TJ proteins. The age-related increases in BBB permeability in human studies are further accentuated in patients with AD and vascular dementia when compared to age-matched controls (Farrall & Wardlaw, 2009). In addition, plasma components were detected in brain tissue autopsied from AD patients (Ryu & McLarnon, 2009) and in cerebrospinal fluid from AD patients (Algotsson & Winblad, 2007). The meta-analysis of the literature argues that there is a significant disruption to the ageing BBB, even more so in diseased subjects (e.g. those with dementias) but the lack of homogeneity of the results merits further research. The advantage in using the rat tissue in our study is that we correlated all the parallel findings in the same animals i.e. sodium fluorescein was administered *in vivo* and assessed in *ex vivo* tissue, along with albumin extravasation and tight junction protein concentration.

One might argue that because the young and aged animals in our study were not perfused prior to sacrificing, the sodium fluorescein and albumin observed in the rat brains may be due to those markers being retained in the blood vessels, rather than

being extravasated. However, even if this was the case, there are still significantly increased levels observed in the sodium fluorescein injected aged animals, when compared to the sodium fluorescein injected young cohort (all animals having received the exact same solution, volume and for the same duration). In addition, there were no observable differences in albumin expression in the plasma of young and aged animals, despite there being a significant increase in the cortex of aged animals. In future, it would be preferable to perfuse the animals prior to sacrificing them, although the perfusion process itself can negatively impact on the integrity of the vasculature including the issue of BBB permeability (Murakami *et al.*, 2000). Additional measurements of blood flow, perfusion and BBB permeability would also be desirable and would be achieved by MRI imaging. Smaller molecular weight gadolinium-based contrast agents could also be used (e.g. gadolinium-DTPA; molecular weight ~570Da) to detect more subtle age-related changes and might be more informative that probing for larger proteins, like albumin (65kDa), which is more indicative of extensive BBB disruption.

Though most age-associated changes in the brain accumulate subtly over time, yet we have demonstrated profound disruption to essential proteins in the brain endothelium. In future studies, it would be desirable to have a middle-aged group also, in order to better track the nature and progression of BBB disruption i.e. do the changes directly correlate with increasing age in a linear fashion, or, do these changes occur rapidly within a narrow window of time in "old" age.

Most of the research studies investigating alterations in BBB permeability *in vitro*, have done so on models mimicking pathological conditions e.g. hypoxia, brain injury, stroke (Sandoval & Witt, 2008), AD (Marco & Skaper, 2006). There has been very little research documenting the BBB changes occurring at the molecular level during normal physiological ageing – yet understanding such age-related changes at the cellular and molecular level may be invaluable in providing a reference point for when the biological mechanisms begin to go awry, predisposing the brain to further insult/pathologies. That vascular dysfunction may precede age-related neurodegeneration has been demonstrated recently in transgenic mice of different ages, with deficient pericytes (Bell *et al.*, 2010).

Our findings that the tight junction proteins claudin-5 and occludin are significantly decreased with normal physiological ageing, corresponds with two other studies in the literature. It is highly likely that the decreased tight junction protein concentration in the aged brain is responsible for the increased BBB permeability in the same animals. Despite our best efforts, we could not get access to post-mortem tissue from young and aged human subjects so as to further investigate if the same age-related changes were mirrored in aged human brains.

It is highly plausible that the BBB disruption and subsequent extravasation of substances from the circulatory system (as demonstrated in Chapter 3), might allow the entry of potential neurotoxins to the brain and/or the accumulation of potential neurotoxins within the brain (e.g. metabolites) and may exacerbate the age-related decline in cognitive function. It may be that BBB impairment (a common denominator in neurodegenerative diseases) during normal physiological ageing is a primary or secondary event, contributing to/initiating the corresponding pathogenesis of the neurodegenerative disease. It is well-established that the elderly population is more susceptible to damage from 'insults' (Goldstein, 2010) and are slower to recover from cellular injury compared with the younger population (Lee *et al.*, 2012). In addition, the elderly are more susceptible bacterial infections, and systemic inflammation is known to exacerbate age-related dementia (Cunningham, 2011) and AD (Holmes *et al.*, 2009). Considering that the aged brain is already compromised at the BBB, we thought it merited further investigation to assess if an additional inflammatory insult (LPS, albeit, at a low concentration and single-dose) to the ageing BBB would further exacerbate the age-related changes.

LPS was systemically administered to young and aged male Wistar rats to initiate an inflammatory response in the periphery, and tight junction protein expression was assessed centrally. We were surprised to find that LPS did not exert (in the main) any additional damage to the BBB, despite the wealth of literature documenting otherwise (Xiaolu *et al.*, 2011; Erickson *et al.*, 2012). However, in the striatum, LPS did cause an increase in claudin-5 expression in the young animals, and a further decrease in the protein in the aged animals. It is possible that the cerebral endothelial cells of the young animals are capable of withstanding a potential threat to the BBB, and respond accordingly by up-regulating claudin-5 expression. In stark contrast, the aged animals

showed decreased claudin-5 expression, indicating greater susceptibility to damage. Future studies on LPS-injected animals might employ MRI to investigate the effect of LPS on BBB function/permeability in order to correlate those findings with tight junction expression.

We feel that the LPS dosage (100μg/kg) may have been a factor in the reduced endothelial response to LPS in this study, as this dose was significantly less than used to disrupt the BBB in the literature (~3mg/kg). However, quantitative PCR data from these animals indicated that LPS at 100μg/kg was sufficient to significantly increase IL-1β mRNA (Dr. Thelma Cowley, see appendix 4). Whilst there was a strong tendency for LPS to increase IL-1β protein concentration, this increase was not statistically significant. Despite this, the increase may have been sufficient to exert biological effects i.e. sufficient IL-1β production to modulate striatal claudin-5 expression levels, but not sufficient to cause more widespread effects. In future studies on LPS-mediated changes, a larger LPS dose (>1mg/kg) should be administered so that the research could be better compared to the existing literature. Alternatively, it may be that the LPS dose was not the biggest issue but that the age-related reductions were already such that no further reductions were possible i.e. there are limited margins for further reductions. Ideally further investigations using cryosections from LPS-treated animals by confocal microscopy would assess if claudin-5 proteins are delocalised away from the membrane internally in the endothelial cells (rather than global protein expression being affected), a result that has been demonstrated by (Cardoso *et al.*, 2012).

Centrally, inflammation is a feature of the ageing brain (Lynch, 2010) and the neurodegenerative brain, and in the periphery inflammatory insults directly modulate tight junction expression on epithelial cells (Al-Sadi *et al.*, 2010). Such evidence led to the hypothesis that neuroinflammation might underlie the age-related BBB disruption; more specifically, that increased levels of IL-1β in the aged brain might instigate the tight junction disruptions. Hence we used tissue from young and middle-aged wildtype and IL-1R1$^{-/-}$ mice to further investigate this hypothesis.

The major finding from this research was the observation that aged IL-1R1$^{-/-}$ mice had increased tight junction protein concentration when compared with their wildtype counterparts. This exciting finding supported our hypothesis that IL-1 signalling was

playing a key role in modulating tight junction protein expression. Due to the unavailability of IL-1R1$^{-/-}$ mice, we could not make assessments in older animals or investigate BBB functioning with MRI – all desirable outcomes to be investigated in future studies.

The fact that tight junction mRNA expression remained relatively unchanged in our young and aged rats, despite the dramatic reductions in tight junction protein concentration, indicated that considerable disruption is occurring to the TJ proteins themselves in the aged brain. Hence the reason that *in vitro* experiments were initiated - to further explore the molecular mechanisms by which IL-1β might be exerting its effect on tight junction protein concentration.

The use of a monolayer of bEnd.3 cells (an immortalised cell line derived from brain capillaries in mouse cortex) was thought to be a promising approach based on very good evidence from the literature that these cells were a good *in vitro* representation of endothelial cells *in vivo* (e.g. (Brown *et al.*, 2007)). Also, by using a monolayer of endothelial cells, we could omit any other cell-cell signalling from neighbouring cells of the NVU. Having established the mechanisms at play within endothelial cells, the intention was to extend the findings from endothelial-only experiments to co-cultures, thereby providing a better *in vitro* representation of how cells interact *in vivo* and in the presence of IL-1β. However, the results from the bEnd.3 experiments as a whole were disappointing. The cells proved to be hyper-sensitive to media disturbances and plating density, making reproducible results difficult i.e. cells did not respond in a consistent way to an insult. In an attempt to reduce variability, we serum starved the cells, and in doing so, we observed that IL-1β treatment following serum starvation, prevented the time-dependent recovery of claudin-5 protein concentration, indicating that IL-1β did exert some negative effect on tight junctions. Even with these results in mind, more reproducible and consistent results were achieved when organotypic hippocampal slice cultures were used where IL-1β significantly reduced claudin-5, occludin and laminin protein concentration. Although statistically, IL-1ra did not significantly rescue the IL-1β-mediated reductions, there was a trend towards recovery, indicating that IL-1β was central in mediating these results (rather than media changes, plating conditions etc. which induced variability in the bEnd.3 experiments). The lack of statistical significance was probably due to the low power of the experiments (large error bars and

low N numbers) and in most cases statistical significance fell just outside the accepted level of $p<0.05$. We feel that future studies with greater sample sizes would ameliorate this problem and further consolidate our findings.

In addition to BBB tight junction disturbance, we also observed disruption to components of the NVU with increased age. Laminin, a glycoprotein with a key role in maintaining structural stability of blood vessels, was significantly fragmented in the aged rat brain, exposing the underlying pericytes. Unveiling the pericytes leaves them vulnerable to damage from molecules on the abluminal (brain) side of the vessels. Indeed, we noticed a reduction in PDGFR-β in the aged rat brain, and as PDGFR-β is responsible for recruiting pericytes to endothelial cells (Armulik *et al.*, 2005) a loss of the receptor could result in decreased pericyte numbers and contribute to BBB disruption (Bell *et al.*, 2010). Also, in the LPS-injected rats, LPS disrupted the basal lamina as evidenced by decreased laminin protein concentration in both the young and aged rats. Interestingly this change was only observed in the striatum, the anatomical area that also displayed the LPS-induced reduction in claudin-5 expression and such changes corroborate with those of other groups (Nishioku *et al.*, 2009).

Previously, we had found that both MMP-2 and MMP-9, known disrupters of the BBB were increased in plasma from both aged rat and human samples, in agreement with a recent study (Lee *et al.*, 2012). MMP disrupt the BBB by their action directly on tight junctions (Asahi *et al.*, 2001) and degradation of the extracellular matrix, including the lamina proteins (Yang *et al.*, 2007). IL-1β is a known activator of MMP-9 (Liang *et al.*, 2007) so it is highly plausible that the increase in IL-1β with age, contributes to the increased MMP-2 and -9 detected in aged plasma, which in turn leads to the disruption of the tight junctions and the surrounding neurovascular unit. Unfortunately, due to the lack of tissue, we were not able to assess MMP expression or activity in IL-1R1$^{-/-}$ mice. In future, it would be interesting to see if there was a decrease in MMP activity in the aged knockout animals, which would provide support in favour of our hypothesis.

We attempted to elucidate the IL-1β/MMP signalling interplay using organotypic hippocampal slice cultures. We could not detect MMP-9 activity and we did not find increased MMP-2 activity in the slices following IL-1β treatment, so we cannot conclusively say if MMP activity was (or not) following IL-1β treatmnent. It may have

been more fruitful to detect MMP expression from the homogenate rather than the supernatant. The application of a broad scale MMP inhibitor rescued IL-1β mediated tight junction disruptions, although this was a dose-dependent effect depending on the tight junction investigated. These findings strongly indicate that IL-1β, mediates its effect on tight junctions partially through its activation of MMP. As already discussed, we could not detect MMP-9 expression, thus, in future studies, it would be ideal to repeat these investigations with a more sensitive kit to assess MMP-9 activity levels and, to apply a specific MMP-9 inhibitor to IL-1β treated slices and investigate if this too rescued the tight junctions.

Despite the varied bEnd.3 findings, we did observe that phospho-ERK, but not JNK MAPK levels fluctuated when tight junction protein concentration was at its lowest, indicating that in the same cells, that regulation of tight junction expression is partially mediated by the ERK-MAPK pathway. In addition, the organotypic slices displayed significant increases in phospho-ERK expression following IL-1β treatment and tight junction reduction, further supporting the hypothesis that IL-1β was mediating its disruptive effects through the ERK-MAPK pathway. It has been shown that IL-1β can increase MMP-9 activity via signalling along the MAPK pathway (Liang *et al.*, 2007). In order to confirm this result in our experiments, application of an ERK inhibitor to organotypic slices would be required.

In summary our findings provide evidence of a structurally and functionally disrupted BBB with age, mediated in part by the increase in inflammation that accompanies age. The pro-inflammatory cytokine, IL-1β mediates the tight junction disruption, as evidenced by the increased tight junction expression in aged IL-1R1$^{-/-}$ mice. We hypothesise that the IL-1β-mediated tight junction disruption is partially facilitated by its action on MMP, via signalling through the ERK-MAPK pathway. The age-related BBB disruption would facilitate the entry of potential neurotoxins into the brain, probably exacerbating neuronal damage in an already fragile tissue and conceivably contributing to the decline in cognitive function apparent with increasing age.

Chapter 7

Future Directions

Future directions.

The results from this research have yielded some interesting findings in relation to the ageing blood-brain barrier and has highlighted possible future research avenues;

i. An in depth study on young, middle-aged and aged IL-1R1$^{-/-}$ mice is warranted

    a. Ideally, one would set up behavioural experiments with the animals to document their cognitive capacity during the ageing process and identify the correlations, if any, between an impaired BBB and their cognition, specifically learning and memory.

    b. One could use MRI to assess BBB function in these animals and assess BBB permeability with a range of molecular weight tracers, from relatively small sodium fluorescein (376 Da) to gadolinium (559- > 1000 Da) and the larger FITC-Dextran markers (10-40 kDa), to assess the degree of BBB disruption.

    c. One could assess MMP activity in brain and serum from these animals, and administer recombinant MMP to investigate the role that MMP plays in disrupting tight junction expression in the presence or absence of the IL-1R1 receptor.

    d. One could culture organotypic hippocampal slices from IL-1R1$^{-/-}$ mice and treat with recombinant IL-1β to understand if IL-1β-mediated effects were still possible (it has been hypothesised that there are alternative IL-1 receptors; Touzani *et al.* (2002)).

ii. One could assess BBB function real-time using MRI across a wider range of ages (young, middle-aged and aged animals) and anatomical areas (to corroborate the sodium fluorescein extravasation as assessed by confocal microscopy).

    a. These animals could also be treated in the presence or absence of a larger dose of LPS (3mg/kg) to investigate the functional changes, if any, to the BBB as a result of systemic inflammation

b. Use of confocal microscopy to look at subcellular location of tight junctions in cryosections from LPS-injected animals, rather than just total protein concentration.

c. Considering that markers of pericytes and basal lamina were decreased with age (PDGFR-β, laminin) to further investigate endothelial- pericyte specific signalling (PDGF- PDGFRβ) and endothelial- basal lamina signalling e.g. the effect on integrin receptors between endothelial cells and laminin.

iii. One could take IL-1β treated organotypic hippocampal slices and treat with specific MMP inhibitors to investigate if IL-1β mediates its disruptive effects through the activation of specific MMP.

a. In addition, one could apply MAPK inhibitors (ERK, JNK, p38) to the slices to ascertain if it was this signalling pathway through which IL-1β is acting.

iv. An investigation into pericyte-endothelial communication, and how they signal together to influence TJ in the presence or absence of an inflammatory insult (IL-1β) is warranted. One could utilise co-culture systems or at the very least, pericyte conditioned media.

v. It would be interesting to get access to human brain tissue and assess the TJ protein concentration with age and also assess BBB functionality with age via MRI, to assess if the findings of this research are reflective of the human BBB.

Ideally in any future studies, it would be preferable to conduct a large scale animal experiment so both behavioural and molecular changes are investigated in relation to the ageing BBB. A wider range of ages may give a better indication of when the functional BBB changes are first seen. When addressing changes to the BBB at a molecular level, it would be preferable to assess BBB functionality using MRI before using a range of techniques including; immunohistochemistry (subcellular location of TJ), Western immunoblotting (protein concentration of TJ) and PCR (mRNA expression of TJ) to assess structural changes occurring at the TJ.

Chapter 8

References

Abbott NJ, Patabendige AA, Dolman DE, Yusof SR & Begley DJ. (2010). Structure and function of the blood-brain barrier. *Neurobiol Dis* **37,** 13-25.

Abbott NJ, Ronnback L & Hansson E. (2006). Astrocyte-endothelial interactions at the blood-brain barrier. *Nat Rev Neurosci* **7,** 41-53.

Abreu MT, Vora P, Faure E, Thomas LS, Arnold ET & Arditi M. (2001). Decreased expression of Toll-like receptor-4 and MD-2 correlates with intestinal epithelial cell protection against dysregulated proinflammatory gene expression in response to bacterial lipopolysaccharide. *J Immunol* **167,** 1609-1616.

Al-Sadi R, Ye D, Dokladny K & Ma TY. (2008). Mechanism of IL-1beta-induced increase in intestinal epithelial tight junction permeability. *J Immunol* **180,** 5653-5661.

Al-Sadi R, Ye D, Said HM & Ma TY. (2010). IL-1beta-induced increase in intestinal epithelial tight junction permeability is mediated by MEKK-1 activation of canonical NF-kappaB pathway. *Am J Pathol* **177,** 2310-2322.

Al-Sadi RM & Ma TY. (2007). IL-1beta causes an increase in intestinal epithelial tight junction permeability. *J Immunol* **178,** 4641-4649.

Alanne MH, Pummi K, Heape AM, Grenman R, Peltonen J & Peltonen S. (2009). Tight junction proteins in human Schwann cell autotypic junctions. *J Histochem Cytochem* **57,** 523-529.

Algotsson A & Winblad B. (2007). The integrity of the blood-brain barrier in Alzheimer's disease. *Acta Neurol Scand* **115,** 403-408.

Allan SM & Rothwell NJ. (2001). Cytokines and acute neurodegeneration. *Nat Rev Neurosci* **2,** 734-744.

Allan SM, Tyrrell PJ & Rothwell NJ. (2005). Interleukin-1 and neuronal injury. *Nat Rev Immunol* **5,** 629-640.

Anderton BH. (2002). Ageing of the brain. *Mech Ageing Dev* **123,** 811-817.

Ando-Akatsuka Y, Saitou M, Hirase T, Kishi M, Sakakibara A, Itoh M, Yonemura S, Furuse M & Tsukita S. (1996). Interspecies diversity of the occludin

sequence: cDNA cloning of human, mouse, dog, and rat-kangaroo homologues. *J Cell Biol* **133,** 43-47.

Andre R, Moggs JG, Kimber I, Rothwell NJ & Pinteaux E. (2006). Gene regulation by IL-1beta independent of IL-1R1 in the mouse brain. *Glia* **53,** 477-483.

Araujo DM & Lapchak PA. (1994). Induction of immune system mediators in the hippocampal formation in Alzheimer's and Parkinson's diseases: selective effects on specific interleukins and interleukin receptors. *Neuroscience* **61,** 745-754.

Argaw AT, Zhang Y, Snyder BJ, Zhao ML, Kopp N, Lee SC, Raine CS, Brosnan CF & John GR. (2006). IL-1beta regulates blood-brain barrier permeability via reactivation of the hypoxia-angiogenesis program. *J Immunol* **177,** 5574-5584.

Armulik A, Abramsson A & Betsholtz C. (2005). Endothelial/pericyte interactions. *Circ Res* **97,** 512-523.

Asahi M, Wang X, Mori T, Sumii T, Jung JC, Moskowitz MA, Fini ME & Lo EH. (2001). Effects of matrix metalloproteinase-9 gene knock-out on the proteolysis of blood-brain barrier and white matter components after cerebral ischemia. *J Neurosci* **21,** 7724-7732.

Aumailley M, Bruckner-Tuderman L, Carter WG, Deutzmann R, Edgar D, Ekblom P, Engel J, Engvall E, Hohenester E, Jones JC, Kleinman HK, Marinkovich MP, Martin GR, Mayer U, Meneguzzi G, Miner JH, Miyazaki K, Patarroyo M, Paulsson M, Quaranta V, Sanes JR, Sasaki T, Sekiguchi K, Sorokin LM, Talts JF, Tryggvason K, Uitto J, Virtanen I, von der Mark K, Wewer UM, Yamada Y & Yurchenco PD. (2005). A simplified laminin nomenclature. *Matrix Biol* **24,** 326-332.

Bake S, Friedman JA & Sohrabji F. (2009). Reproductive age-related changes in the blood brain barrier: expression of IgG and tight junction proteins. *Microvasc Res* **78,** 413-424.

Balabanov R & Dore-Duffy P. (1998). Role of the CNS microvascular pericyte in the blood-brain barrier. *J Neurosci Res* **53,** 637-644.

Balda MS & Matter K. (2008). Tight junctions at a glance. *J Cell Sci* **121,** 3677-3682.

Balda MS, Whitney JA, Flores C, Gonzalez S, Cereijido M & Matter K. (1996). Functional dissociation of paracellular permeability and transepithelial electrical resistance and disruption of the apical-basolateral intramembrane diffusion barrier by expression of a mutant tight junction membrane protein. *J Cell Biol* **134,** 1031-1049.

Basu A, Krady JK & Levison SW. (2004). Interleukin-1: a master regulator of neuroinflammation. *J Neurosci Res* **78,** 151-156.

Basu A, Krady JK, O'Malley M, Styren SD, DeKosky ST & Levison SW. (2002). The type 1 interleukin-1 receptor is essential for the efficient activation of microglia and the induction of multiple proinflammatory mediators in response to brain injury. *J Neurosci* **22,** 6071-6082.

Becher B, Prat A & Antel JP. (2000). Brain-immune connection: immuno-regulatory properties of CNS-resident cells. *Glia* **29,** 293-304.

Beck K, Hunter I & Engel J. (1990). Structure and function of laminin: anatomy of a multidomain glycoprotein. *FASEB J* **4,** 148-160.

Beckman KB & Ames BN. (1998). The free radical theory of aging matures. *Physiol Rev* **78,** 547-581.

Bell RD, Winkler EA, Sagare AP, Singh I, LaRue B, Deane R & Zlokovic BV. (2010). Pericytes control key neurovascular functions and neuronal phenotype in the adult brain and during brain aging. *Neuron* **68,** 409-427.

Bell RD & Zlokovic BV. (2009). Neurovascular mechanisms and blood-brain barrier disorder in Alzheimer's disease. *Acta Neuropathol* **118,** 103-113.

Bendfeldt K, Radojevic V, Kapfhammer J & Nitsch C. (2007). Basic fibroblast growth factor modulates density of blood vessels and preserves tight junctions in organotypic cortical cultures of mice: a new in vitro model of the blood-brain barrier. *J Neurosci* **27,** 3260-3267.

Bergers G & Song S. (2005). The role of pericytes in blood-vessel formation and maintenance. *Neuro Oncol* **7,** 452-464.

Bernacki J, Dobrowolska A, Nierwinska K & Malecki A. (2008). Physiology and pharmacological role of the blood-brain barrier. *Pharmacol Rep* **60,** 600-622.

Bhat R & Steinman L. (2009). Innate and adaptive autoimmunity directed to the central nervous system. *Neuron* **64,** 123-132.

Blamire AM, Anthony DC, Rajagopalan B, Sibson NR, Perry VH & Styles P. (2000). Interleukin-1beta -induced changes in blood-brain barrier permeability, apparent diffusion coefficient, and cerebral blood volume in the rat brain: a magnetic resonance study. *J Neurosci* **20,** 8153-8159.

Blasig IE, Bellmann C, Cording J, Del Vecchio G, Zwanziger D, Huber O & Haseloff RF. (2011). Occludin protein family: oxidative stress and reducing conditions. *Antioxid Redox Signal* **15,** 1195-1219.

Blasko I, Stampfer-Kountchev M, Robatscher P, Veerhuis R, Eikelenboom P & Grubeck-Loebenstein B. (2004). How chronic inflammation can affect the brain and support the development of Alzheimer's disease in old age: the role of microglia and astrocytes. *Aging Cell* **3,** 169-176.

Bluthe RM, Laye S, Michaud B, Combe C, Dantzer R & Parnet P. (2000). Role of interleukin-1 beta and tumor necrosis factor alpha in lipopolysaccharide-induced sickness behaviour: a study with interleukin-one type one receptor-deficient mice. *Eur J Neurosci* **12** (12), 4447-4456.

Bonnema DD, Webb CS, Pennington WR, Stroud RE, Leonardi AE, Clark LL, McClure CD, Finklea L, Spinale FG & Zile MR. (2007). Effects of age on plasma matrix metalloproteinases (MMPs) and tissue inhibitor of metalloproteinases (TIMPs). *J Card Fail* **13,** 530-540.

Boraschi D, Rambaldi A, Sica A, Ghiara P, Colotta F, Wang JM, de Rossi M, Zoia C, Remuzzi G, Bussolino F & et al. (1991). Endothelial cells express the interleukin-1 receptor type I. *Blood* **78,** 1262-1267.

Bowie AG. (2007). Translational mini-review series on Toll-like receptors: recent advances in understanding the role of Toll-like receptors in anti-viral immunity. *Clin Exp Immunol* **147,** 217-226.

Brew K, Dinakarpandian D & Nagase H. (2000). Tissue inhibitors of metalloproteinases: evolution, structure and function. *Biochim Biophys Acta* **1477,** 267-283.

Brinckerhoff CE & Matrisian LM. (2002). Matrix metalloproteinases: a tail of a frog that became a prince. *Nat Rev Mol Cell Biol* **3,** 207-214.

Brown RC, Morris AP & O'Neil RG. (2007). Tight junction protein expression and barrier properties of immortalized mouse brain microvessel endothelial cells. *Brain Res* **1130,** 17-30.

Brunk UT & Terman A. (2002). Lipofuscin: mechanisms of age-related accumulation and influence on cell function. *Free Radic Biol Med* **33,** 611-619.

Butcher SK, Chahal H, Nayak L, Sinclair A, Henriquez NV, Sapey E, O'Mahony D & Lord JM. (2001). Senescence in innate immune responses: reduced neutrophil phagocytic capacity and CD16 expression in elderly humans. *J Leukoc Biol* **70,** 881-886.

Butt AM, Jones HC & Abbott NJ. (1990). Electrical resistance across the blood-brain barrier in anaesthetized rats: a developmental study. *J Physiol* **429,** 47-62.

Camenzind RS, Chip S, Gutmann H, Kapfhammer JP, Nitsch C & Bendfeldt K. (2010). Preservation of transendothelial glucose transporter 1 and P-glycoprotein transporters in a cortical slice culture model of the blood-brain barrier. *Neuroscience* **170,** 361-371.

Candelario-Jalil E, Thompson J, Taheri S, Grossetete M, Adair JC, Edmonds E, Prestopnik J, Wills J & Rosenberg GA. (2011). Matrix metalloproteinases are associated with increased blood-brain barrier opening in vascular cognitive impairment. *Stroke* **42,** 1345-1350.

Candelario-Jalil E, Yang Y & Rosenberg GA. (2009). Diverse roles of matrix metalloproteinases and tissue inhibitors of metalloproteinases in neuroinflammation and cerebral ischemia. *Neuroscience* **158,** 983-994.

Candiello J, Cole GJ & Halfter W. (2010). Age-dependent changes in the structure, composition and biophysical properties of a human basement membrane. *Matrix Biol* **29,** 402-410.

Capaldo CT & Nusrat A. (2009). Cytokine regulation of tight junctions. *Biochim Biophys Acta* **1788,** 864-871.

Cardoso FL, Brites D & Brito MA. (2010). Looking at the blood-brain barrier: molecular anatomy and possible investigation approaches. *Brain Res Rev* **64,** 328-363.

Cardoso FL, Kittel A, Veszelka S, Palmela I, Toth A, Brites D, Deli MA & Brito MA. (2012). Exposure to lipopolysaccharide and/or unconjugated bilirubin impair the integrity and function of brain microvascular endothelial cells. *PLoS One* **7,** e35919.

Carlisle R, Rhoads CA, Aw TY & Harrison L. (2002). Endothelial cells maintain a reduced redox environment even as mitochondrial function declines. *Am J Physiol Cell Physiol* **283,** C1675-1686.

Carmeliet P & Storkebaum E. (2002). Vascular and neuronal effects of VEGF in the nervous system: implications for neurological disorders. *Semin Cell Dev Biol* **13,** 39-53.

Chaitanya GV, Cromer WE, Wells SR, Jennings MH, Couraud PO, Romero IA, Weksler B, Erdreich-Epstein A, Mathis JM, Minagar A & Alexander JS. (2011). Gliovascular and cytokine interactions modulate brain endothelial barrier in vitro. *J Neuroinflammation* **8,** 162.

Chen F, Ohashi N, Li W, Eckman C & Nguyen JH. (2009). Disruptions of occludin and claudin-5 in brain endothelial cells in vitro and in brains of mice with acute liver failure. *Hepatology* **50,** 1914-1923.

Ching S, He L, Lai W & Quan N. (2005). IL-1 type I receptor plays a key role in mediating the recruitment of leukocytes into the central nervous system. *Brain Behav Immun* **19,** 127-137.

Ching S, Zhang H, Belevych N, He L, Lai W, Pu XA, Jaeger LB, Chen Q & Quan N. (2007). Endothelial-specific knockdown of interleukin-1 (IL-1) type 1 receptor differentially alters CNS responses to IL-1 depending on its route of administration. *J Neurosci* **27,** 10476-10486.

Cohen-Kashi Malina K, Cooper I & Teichberg VI. (2009). Closing the gap between the in-vivo and in-vitro blood-brain barrier tightness. *Brain Res* **1284,** 12-21.

Colton CA. (2009). Heterogeneity of microglial activation in the innate immune response in the brain. *J Neuroimmune Pharmacol* **4,** 399-418.

Cooper S. (2003). Reappraisal of serum starvation, the restriction point, G0, and G1 phase arrest points. *FASEB J* **17,** 333-340.

Cribbs DH, Berchtold NC, Perreau V, Coleman PD, Rogers J, Tenner AJ & Cotman CW. (2012). Extensive innate immune gene activation accompanies brain aging, increasing vulnerability to cognitive decline and neurodegeneration: a microarray study. *J Neuroinflammation* **9,** 179.

Crocker SJ, Milner R, Pham-Mitchell N & Campbell IL. (2006). Cell and agonist-specific regulation of genes for matrix metalloproteinases and their tissue inhibitors by primary glial cells. *J Neurochem* **98,** 812-823.

Cross TG, Scheel-Toellner D, Henriquez NV, Deacon E, Salmon M & Lord JM. (2000). Serine/threonine protein kinases and apoptosis. *Exp Cell Res* **256,** 34-41.

Cunningham C. (2011). Systemic inflammation and delirium: important co-factors in the progression of dementia. *Biochem Soc Trans* **39,** 945-953.

Dallas S, Miller DS & Bendayan R. (2006). Multidrug resistance-associated proteins: expression and function in the central nervous system. *Pharmacol Rev* **58,** 140-161.

Daneman R, Zhou L, Kebede AA & Barres BA. (2010). Pericytes are required for blood-brain barrier integrity during embryogenesis. *Nature* **468,** 562-566.

Dauphinee SM & Karsan A. (2006). Lipopolysaccharide signaling in endothelial cells. *Lab Invest* **86,** 9-22.

de Vries HE, Kuiper J, de Boer AG, Van Berkel TJ & Breimer DD. (1997). The blood-brain barrier in neuroinflammatory diseases. *Pharmacol Rev* **49,** 143-155.

Defilippi P, Silengo L & Tarone G. (1992). Alpha 6.beta 1 integrin (laminin receptor) is down-regulated by tumor necrosis factor alpha and interleukin-1 beta in human endothelial cells. *J Biol Chem* **267,** 18303-18307.

Deli MA. (2009). Potential use of tight junction modulators to reversibly open membranous barriers and improve drug delivery. *Biochim Biophys Acta* **1788,** 892-910.

Deli MA, Abraham CS, Kataoka Y & Niwa M. (2005). Permeability studies on in vitro blood-brain barrier models: physiology, pathology, and pharmacology. *Cell Mol Neurobiol* **25,** 59-127.

Dickstein DL, Kabaso D, Rocher AB, Luebke JI, Wearne SL & Hof PR. (2007). Changes in the structural complexity of the aged brain. *Aging Cell* **6,** 275-284.

Dinarello CA. (1998). Interleukin-1 beta, interleukin-18, and the interleukin-1 beta converting enzyme. *Ann N Y Acad Sci* **856,** 1-11.

Dinarello CA. (2011). Interleukin-1 in the pathogenesis and treatment of inflammatory diseases. *Blood* **117,** 3720-3732.

Durbeej M. (2010). Laminins. *Cell Tissue Res* **339,** 259-268.

Emsley HC, Smith CJ, Georgiou RF, Vail A, Hopkins SJ, Rothwell NJ & Tyrrell PJ. (2005). A randomised phase II study of interleukin-1 receptor antagonist in acute stroke patients. *J Neurol Neurosurg Psychiatry* **76,** 1366-1372.

Erickson MA, Hartvigson PE, Morofuji Y, Owen JB, Butterfield DA & Banks WA. (2012). Lipopolysaccharide impairs amyloid beta efflux from brain: altered vascular sequestration, cerebrospinal fluid reabsorption, peripheral clearance and transporter function at the blood-brain barrier. *J Neuroinflammation* **9,** 150.

Fanning AS, Jameson BJ, Jesaitis LA & Anderson JM. (1998). The tight junction protein ZO-1 establishes a link between the transmembrane protein occludin and the actin cytoskeleton. *J Biol Chem* **273,** 29745-29753.

Farkas E & Luiten PG. (2001). Cerebral microvascular pathology in aging and Alzheimer's disease. *Prog Neurobiol* **64,** 575-611.

Farrall AJ & Wardlaw JM. (2009). Blood-brain barrier: ageing and microvascular disease--systematic review and meta-analysis. *Neurobiol Aging* **30,** 337-352.

Feldman GJ, Mullin JM & Ryan MP. (2005). Occludin: structure, function and regulation. *Adv Drug Deliv Rev* **57,** 883-917.

Fischer S, Wiesnet M, Renz D & Schaper W. (2005). H_2O_2 induces paracellular permeability of porcine brain-derived microvascular endothelial cells by activation of the p44/42 MAP kinase pathway. *Eur J Cell Biol* **84,** 687-697.

Floyd RA, West M & Hensley K. (2001). Oxidative biochemical markers; clues to understanding aging in long-lived species. *Exp Gerontol* **36,** 619-640.

Forster C. (2008). Tight junctions and the modulation of barrier function in disease. *Histochem Cell Biol* **130,** 55-70.

Furuse M, Hirase T, Itoh M, Nagafuchi A, Yonemura S & Tsukita S. (1993). Occludin: a novel integral membrane protein localizing at tight junctions. *J Cell Biol* **123,** 1777-1788.

Furuse M, Sasaki H, Fujimoto K & Tsukita S. (1998). A single gene product, claudin-1 or -2, reconstitutes tight junction strands and recruits occludin in fibroblasts. *J Cell Biol* **143,** 391-401.

Gaillard PJ, de Boer AB & Breimer DD. (2003). Pharmacological investigations on lipopolysaccharide-induced permeability changes in the blood-brain barrier in vitro. *Microvasc Res* **65,** 24-31.

Galis Z, Muszynski M, Sukhova G, Simon-Morrissey E, & Libby p. (1994). Increased expression of matrix metalloproteinases and matrix degrading activity in vulnerable regions of human atherosclerotic plaques. J Clin Invest **94**(6): 2493-2503.

Gelinas DS, Lambermon MH & McLaurin J. (2005). Ciglitazone increases basal cytokine expression in the central nervous system of adult rats. *Brain Res* **1034,** 139-146.

Glaccum MB, Stocking KL, Charrier K, Smith JL, WIllis CR, Maliszewski C, Livingston DJ, Peschon JJ & Morrissey PJ. (1997). Phenotypic and functional characterisation of mice that lack the type I receptor for IL-11. *J Imunnol* **159** (7), 3364-3371.

Godbout JP, Chen J, Abraham J, Richwine AF, Berg BM, Kelley KW & Johnson RW. (2005). Exaggerated neuroinflammation and sickness behavior in aged mice following activation of the peripheral innate immune system. *FASEB J* **19,** 1329-1331.

Goldstein DR. (2010). Aging, imbalanced inflammation and viral infection. *Virulence* **1,** 295-298.

Gonzalez-Mariscal L, Tapia R & Chamorro D. (2008). Crosstalk of tight junction components with signaling pathways. *Biochim Biophys Acta* **1778,** 729-756.

Granowitz EV, Vannier E, Poutsiaka DD & Dinarello CA. (1992). Effect of interleukin-1 (IL-1) blockade on cytokine synthesis: II. IL-1 receptor antagonist inhibits lipopolysaccharide-induced cytokine synthesis by human monocytes. *Blood* **79,** 2364-2369.

Greenfeder SA, Varnell T, Powers G, Lombard-Gillooly K, Shuster D, McIntyre KW, Ryan DE, Levin W, Madison V & Ju G. (1995). Insertion of a structural domain of interleukin (IL)-1 beta confers agonist activity to the IL-1 receptor antagonist. Implications for IL-1 bioactivity. *J Biol Chem* **270,** 22460-22466.

Greenhalgh AD, Brough D, Robinson EM, Girard S, Rothwell NJ & Allan SM. (2012). Interleukin-1 receptor antagonist is beneficial after subarachnoid haemorrhage in rat by blocking haem-driven inflammatory pathology. *Dis Model Mech* **5**(6), 823-833.

Gu Z, Cui J, Brown S, Fridman R, Mobashery S, Strongin AY & Lipton SA. (2005). A highly specific inhibitor of matrix metalloproteinase-9 rescues laminin from proteolysis and neurons from apoptosis in transient focal cerebral ischemia. *J Neurosci* **25,** 6401-6408.

Guillemin GJ & Brew BJ. (2004). Microglia, macrophages, perivascular macrophages, and pericytes: a review of function and identification. *J Leukoc Biol* **75,** 388-397.

Gurney KJ, Estrada EY & Rosenberg GA. (2006). Blood-brain barrier disruption by stromelysin-1 facilitates neutrophil infiltration in neuroinflammation. *Neurobiol Dis* **23,** 87-96.

Hailer NP, Vogt C, Korf HW & Dehghani F. (2005). Interleukin-1beta exacerbates and interleukin-1 receptor antagonist attenuates neuronal injury and microglial activation after excitotoxic damage in organotypic hippocampal slice cultures. *Eur J Neurosci* **21,** 2347-2360.

Hallmann R, Horn N, Selg M, Wendler O, Pausch F & Sorokin LM. (2005). Expression and function of laminins in the embryonic and mature vasculature. *Physiol Rev* **85,** 979-1000.

Hannum CH, Wilcox CJ, Arend WP, Joslin FG, Dripps DJ, Heimdal PL, Armes LG, Sommer A, Eisenberg SP & Thompson RC. (1990). Interleukin-1 receptor antagonist activity of a human interleukin-1 inhibitor. *Nature* **343,** 336-340.

Haorah J, Ramirez SH, Schall K, Smith D, Pandya R & Persidsky Y. (2007). Oxidative stress activates protein tyrosine kinase and matrix metalloproteinases leading to blood-brain barrier dysfunction. *J Neurochem* **101,** 566-576.

Harman D. (1956). Aging: a theory based on free radical and radiation chemistry. *J Gerontol* **11,** 298-300.

Hawkins BT & Davis TP. (2005). The blood-brain barrier/neurovascular unit in health and disease. *Pharmacol Rev* **57,** 173-185.

Hennessy EJ, Parker AE & O'Neill LA. (2010). Targeting Toll-like receptors: emerging therapeutics? *Nat Rev Drug Discov* **9,** 293-307.

Hirschi KK & D'Amore PA. (1996). Pericytes in the microvasculature. *Cardiovasc Res* **32,** 687-698.

Holgate ST. (2007). The epithelium takes centre stage in asthma and atopic dermatitis. *Trends Immunol* **28,** 248-251.

Holmes C, Cunningham C, Zotova E, Woolford J, Dean C, Kerr S, Culliford D & Perry VH. (2009). Systemic inflammation and disease progression in Alzheimer disease. *Neurology* **73,** 768-774.

Hori S, Ohtsuki S, Hosoya K, Nakashima E & Terasaki T. (2004). A pericyte-derived angiopoietin-1 multimeric complex induces occludin gene expression in brain capillary endothelial cells through Tie-2 activation in vitro. *J Neurochem* **89,** 503-513.

Huuskonen J, Suuronen T, Miettinen R, van Groen T & Salminen A. (2005). A refined in vitro model to study inflammatory responses in organotypic membrane culture of postnatal rat hippocampal slices. *J Neuroinflammation* **2,** 25.

Is M, Comunoglu NU, Comunoglu C, Eren B, Ekici ID & Ozkan F. (2008). Age-related changes in the rat hippocampus. *J Clin Neurosci* **15,** 568-574.

Jaeger LB, Dohgu S, Sultana R, Lynch JL, Owen JB, Erickson MA, Shah GN, Price TO, Fleegal-Demotta MA, Butterfield DA & Banks WA. (2009). Lipopolysaccharide alters the blood-brain barrier transport of amyloid beta

protein: a mechanism for inflammation in the progression of Alzheimer's disease. *Brain Behav Immun* **23,** 507-517.

Jurgens, H. A. and R. W. Johnson (2012). Dysregulated neuronal-microglial cross-talk during aging, stress and inflammation. Exp Neurol **233**(1): 40-48.

Karin M & Ben-Neriah Y. (2000). Phosphorylation meets ubiquitination: the control of NF-[kappa]B activity. *Annu Rev Immunol* **18,** 621-663.

Kimura K, Teranishi S & Nishida T. (2009). Interleukin-1beta-induced disruption of barrier function in cultured human corneal epithelial cells. *Invest Ophthalmol Vis Sci* **50,** 597-603.

Kitajewski J. (2011). Endothelial laminins underlie the tip cell microenvironment. *EMBO Rep* **12,** 1087-1088.

Kobayashi K, Miwa H & Yasui M. (2010). Inflammatory mediators weaken the amniotic membrane barrier through disruption of tight junctions. *J Physiol* **588,** 4859-4869.

Kovacs R, Papageorgiou I & Heinemann U. (2011). Slice cultures as a model to study neurovascular coupling and blood brain barrier in vitro. *Cardiovasc Psychiatry Neurol* **2011,** 646958.

Kozler P & Pokorny J. (2003). Altered blood-brain barrier permeability and its effect on the distribution of Evans blue and sodium fluorescein in the rat brain applied by intracarotid injection. *Physiol Res* **52,** 607-614.

Krueger M & Bechmann I. (2010). CNS pericytes: concepts, misconceptions, and a way out. *Glia* **58,** 1-10.

Lai CH & Kuo KH. (2005). The critical component to establish in vitro BBB model: Pericyte. *Brain Res Brain Res Rev* **50,** 258-265.

Lee CK, Weindruch R & Prolla TA. (2000). Gene-expression profile of the ageing brain in mice. *Nat Genet* **25,** 294-297.

Lee P, Kim J, Williams R, Sandhir R, Gregory E, Brooks WM & Berman NE. (2012). Effects of aging on blood brain barrier and matrix metalloproteases following controlled cortical impact in mice. *Exp Neurol* **234,** 50-61.

Li N, DeMarco VG, West CM & Neu J. (2003). Glutamine supports recovery from loss of transepithelial resistance and increase of permeability induced by media change in Caco-2 cells. *J Nutr Biochem* **14,** 401-408.

Liang KC, Lee CW, Lin WN, Lin CC, Wu CB, Luo SF & Yang CM. (2007). Interleukin-1beta induces MMP-9 expression via p42/p44 MAPK, p38 MAPK, JNK, and nuclear factor-kappaB signaling pathways in human tracheal smooth muscle cells. *J Cell Physiol* **211,** 759-770.

Licastro F, Candore G, Lio D, Porcellini E, Colonna-Romano G, Franceschi C & Caruso C. (2005). Innate immunity and inflammation in ageing: a key for understanding age-related diseases. *Immun Ageing* **2,** 8.

Lim NK, Villemagne VL, Soon CP, Laughton KM, Rowe CC, McLean CA, Masters CL, Evin G & Li QX. (2011). Investigation of matrix metalloproteinases, MMP-2 and MMP-9, in plasma reveals a decrease of MMP-2 in Alzheimer's disease. *J Alzheimers Dis* **26,** 779-786.

Lin MT & Beal MF. (2006). Mitochondrial dysfunction and oxidative stress in neurodegenerative diseases. *Nature* **443,** 787-795.

Lischper M, Beuck S, Thanabalasundaram G, Pieper C & Galla HJ. (2010). Metalloproteinase mediated occludin cleavage in the cerebral microcapillary endothelium under pathological conditions. *Brain Res* **1326,** 114-127.

Liu X, Tu M, Kelly RS, Chen C & Smith BJ. (2004). Development of a computational approach to predict blood-brain barrier permeability. *Drug Metab Dispos* **32,** 132-139.

Lo EH, Wang X, & Cuzner ML. (2002). Extracellular proteolysis in brain injury and inflammation: role for plasminogen activators and matrix metalloproteinases. *J Neurosci Res* **69,** 1-9.

Loane DJ, Deighan BF, Clarke RM, Griffin RJ, Lynch AM & Lynch MA. (2009). Interleukin-4 mediates the neuroprotective effects of rosiglitazone in the aged brain. *Neurobiol Aging* **30,** 920-931.

Lorenzl S, De Pasquale G, Segal AZ & Beal MF. (2003). Dysregulation of the levels of matrix metalloproteinases and tissue inhibitors of matrix metalloproteinases in the early phase of cerebral ischemia. *Stroke* **34,** e37-38; author reply e37-38.

Lynch AM & Lynch MA. (2002). The age-related increase in IL-1 type I receptor in rat hippocampus is coupled with an increase in caspase-3 activation. *Eur J Neurosci* **15,** 1779-1788.

Lynch MA. (2008). The risky business of ageing. *Brain Behav Immun* **22,** 299-300.

Lynch MA. (2010). Age-related neuroinflammatory changes negatively impact on neuronal function. *Front Aging Neurosci* **1,** 6.

Mandel I, Paperna T, Volkowich A, Merhav M, Glass-Marmor L & Miller A. (2012). The ubiquitin-proteasome pathway regulates claudin 5 degradation. *J Cell Biochem* **113,** 2415-2423.

Marco S & Skaper SD. (2006). Amyloid beta-peptide1-42 alters tight junction protein distribution and expression in brain microvessel endothelial cells. *Neurosci Lett* **401,** 219-224.

Mark KS & Davis TP. (2002). Cerebral microvascular changes in permeability and tight junctions induced by hypoxia-reoxygenation. *Am J Physiol Heart Circ Physiol* **282,** H1485-1494.

McColl BW, Rothwell NJ & Allan SM. (2008). Systemic inflammation alters the kinetics of cerebrovascular tight junction disruption after experimental stroke in mice. *J Neurosci* **28,** 9451-9462.

Medina C & Radomski. (2006). Role of matrix metalloproteinases in intestinal inflammation. J *Pharm Exp Ther* **318** (3), 933-938.

Medzhitov R & Janeway C, Jr. (2000). Innate immunity. *N Engl J Med* **343,** 338-344.

Merkle CJ, Torres BJ, Baruch JM, Stevens K, Munoz C, Schaeffer RC, Jr. & Montgomery DW. (2005). In vitro age-related responses of endothelial cells to breast cancer cell addition. *Cancer Detect Prev* **29,** 518-527.

Miggin SM & O'Neill LA. (2006). New insights into the regulation of TLR signaling. *J Leukoc Biol* **80,** 220-226.

Mooradian AD, Haas MJ & Chehade JM. (2003). Age-related changes in rat cerebral occludin and zonula occludens-1 (ZO-1). *Mech Ageing Dev* **124,** 143-146.

Morita K, Sasaki H, Furuse M & Tsukita S. (1999). Endothelial claudin: claudin-5/TMVCF constitutes tight junction strands in endothelial cells. *J Cell Biol* **147,** 185-194.

Moser KV, Schmidt-Kastner R, Hinterhuber H & Humpel C. (2003). Brain capillaries and cholinergic neurons persist in organotypic brain slices in the absence of blood flow. *Eur J Neurosci* **18,** 85-94.

Muraishi, Y, Mitani N, Fuse H & Saiki I. (2001). Effect of a matrix metalloproteinase inhibitor (ONO-4817) on lung metastasis of murine renal cell carcinoma. *Anticancer Res* **21(6A)**, 3845-3852.

Murakami H, Takenaga H, Matsuo H, Ohtani H & Sawada Y. (2000). Comparison of blood-brain barrier permeability in mice and rats using in situ brain perfusion technique. *Am J Physiol* **279**, 1022-1028.

Murray CL, Skelly DT & Cunningham C. (2011). Exacerbation of CNS inflammation and neurodegeneration by systemic LPS treatment is independent of circulating IL-1beta and IL-6. *J Neuroinflammation* **8,** 50.

Nadeau S & Rivest S. (1999). Regulation of the gene encoding tumor necrosis factor alpha (TNF-alpha) in the rat brain and pituitary in response in different models of systemic immune challenge. *J Neuropathol Exp Neurol* **58,** 61-77.

Nakagawa S, Deli MA, Nakao S, Honda M, Hayashi K, Nakaoke R, Kataoka Y & Niwa M. (2007). Pericytes from brain microvessels strengthen the barrier integrity in primary cultures of rat brain endothelial cells. *Cell Mol Neurobiol* **27,** 687-694.

Nathan C. (2002). Points of control in inflammation. *Nature* **420,** 846-852.

Nishioku T, Dohgu S, Takata F, Eto T, Ishikawa N, Kodama KB, Nakagawa S, Yamauchi A & Kataoka Y. (2009). Detachment of brain pericytes from the basal lamina is involved in disruption of the blood-brain barrier caused by lipopolysaccharide-induced sepsis in mice. *Cell Mol Neurobiol* **29,** 309-316.

Nitta T, Hata M, Gotoh S, Seo Y, Sasaki H, Hashimoto N, Furuse M & Tsukita S. (2003). Size-selective loosening of the blood-brain barrier in claudin-5-deficient mice. *J Cell Biol* **161,** 653-660.

Nolan Y, Maher FO, Martin DS, Clarke RM, Brady MT, Bolton AE, Mills KH & Lynch MA. (2005). Role of interleukin-4 in regulation of age-related inflammatory changes in the hippocampus. *J Biol Chem* **280,** 9354-9362.

O'Neill LA, Bryant CE & Doyle SL. (2009). Therapeutic targeting of Toll-like receptors for infectious and inflammatory diseases and cancer. *Pharmacol Rev* **61,** 177-197.

O'Neill LA & Dinarello CA. (2000). The IL-1 receptor/toll-like receptor superfamily: crucial receptors for inflammation and host defense. *Immunol Today* **21,** 206-209.

O'Neill LA & Greene C. (1998). Signal transduction pathways activated by the IL-1 receptor family: ancient signaling machinery in mammals, insects, and plants. *J Leukoc Biol* **63,** 650-657.

Ojala J, Alafuzoff I, Herukka SK, van Groen T, Tanila H & Pirttila T. (2009). Expression of interleukin-18 is increased in the brains of Alzheimer's disease patients. *Neurobiol Aging* **30,** 198-209.

Palu E & Liesi P. (2002). Differential distribution of laminins in Alzheimer disease and normal human brain tissue. *J Neurosci Res* **69,** 243-256.

Pardridge WM. (2007). Blood-brain barrier delivery. *Drug Discov Today* **12,** 54-61.

Paris L, Tonutti L, Vannini C & Bazzoni G. (2008). Structural organization of the tight junctions. *Biochim Biophys Acta* **1778,** 646-659.

Pearson G, Robinson F, Beers Gibson T, Xu BE, Karandikar M, Berman K & Cobb MH. (2001). Mitogen-activated protein (MAP) kinase pathways: regulation and physiological functions. *Endocr Rev* **22,** 153-183.

Pelegri C, Canudas AM, del Valle J, Casadesus G, Smith MA, Camins A, Pallas M & Vilaplana J. (2007). Increased permeability of blood-brain barrier on the hippocampus of a murine model of senescence. *Mech Ageing Dev* **128,** 522-528.

Peppiatt CM, Howarth C, Mobbs P & Attwell D. (2006). Bidirectional control of CNS capillary diameter by pericytes. *Nature* **443,** 700-704.

Pirkmajer S & Chibalin AV. (2011). Serum starvation: caveat emptor. *Am J Physiol Cell Physiol* **301,** C272-279.

Pradillo JM, Denes A, Greenhalgh AD, Boutin H, Drake C, McColl BW, Barton E, Proctor SD, Russell JC, Rothwell NJ & Allan SM. (2012). Delayed administration of interleukin-1 receptor antagonist reduces ischemic brain damage and inflammation in comorbid rats. *J Cereb Blood Flow Metab.*

Prolla TA. (2002). DNA microarray analysis of the aging brain. *Chem Senses* **27,** 299-306.

Reijerkerk A, Kooij G, van der Pol SM, Khazen S, Dijkstra CD & de Vries HE. (2006). Diapedesis of monocytes is associated with MMP-mediated occludin disappearance in brain endothelial cells. *FASEB J* **20,** 2550-2552.

Rosell A, Cuadrado E, Ortega-Aznar A, Hernandez-Guillamon M, Lo EH & Montaner J. (2008). MMP-9-positive neutrophil infiltration is associated to blood-brain barrier breakdown and basal lamina type IV collagen degradation during hemorrhagic transformation after human ischemic stroke. *Stroke* **39,** 1121-1126.

Rosenberg GA. (2002). Matrix metalloproteinases in neuroinflammation. *Glia* **39,** 279-291.

Rosenberg GA, Estrada E, Kelley RO & Kornfeld M. (1993). Bacterial collagenase disrupts extracellular matrix and opens blood-brain barrier in rat. *Neurosci Lett* **160,** 117-119.

Rucker HK, Wynder HJ & Thomas WE. (2000). Cellular mechanisms of CNS pericytes. *Brain Res Bull* **51,** 363-369.

Ryu JK & McLarnon JG. (2009). A leaky blood-brain barrier, fibrinogen infiltration and microglial reactivity in inflamed Alzheimer's disease brain. *J Cell Mol Med* **13,** 2911-2925.

Saitou M, Fujimoto K, Doi Y, Itoh M, Fujimoto T, Furuse M, Takano H, Noda T & Tsukita S. (1998). Occludin-deficient embryonic stem cells can differentiate into polarized epithelial cells bearing tight junctions. *J Cell Biol* **141,** 397-408.

Saitou M, Furuse M, Sasaki H, Schulzke JD, Fromm M, Takano H, Noda T & Tsukita S. (2000). Complex phenotype of mice lacking occludin, a component of tight junction strands. *Mol Biol Cell* **11,** 4131-4142.

Salminen A, Ojala J, Kaarniranta K, Haapasalo A, Hiltunen M & Soininen H. (2011). Astrocytes in the aging brain express characteristics of senescence-associated secretory phenotype. Eur J Neurosci **34**(1): 3-11.

Sandoval KE & Witt KA. (2008). Blood-brain barrier tight junction permeability and ischemic stroke. *Neurobiol Dis* **32,** 200-219.

Schlegel N, Baumer Y, Drenckhahn D & Waschke J. (2009). Lipopolysaccharide-induced endothelial barrier breakdown is cyclic adenosine monophosphate dependent in vivo and in vitro. *Crit Care Med* **37,** 1735-1743.

Schneeberger EE & Lynch RD. (2004). The tight junction: a multifunctional complex. *Am J Physiol Cell Physiol* **286,** C1213-1228.

Shaftel SS, Griffin WT & O'Bannion MK. (2008). The role of IL-1 in neuroinflammation and Alzheimer's disease: an evolving perspective. *J neuroinflamm* **5** (7).

Shaftel SS, Carlson TJ, Olschowka JA, Kyrkanides S, Matousek SB & O'Banion MK. (2007). Chronic interleukin-1beta expression in mouse brain leads to leukocyte infiltration and neutrophil-independent blood brain barrier permeability without overt neurodegeneration. *J Neurosci* **27,** 9301-9309.

Shah GN & Mooradian AD. (1997). Age-related changes in the blood-brain barrier. *Exp Gerontol* **32,** 501-519.

Shepro D & Morel NM. (1993). Pericyte physiology. *FASEB J* **7,** 1031-1038.

Sheth P, Delos Santos N, Seth A, LaRusso NF & Rao RK. (2007). Lipopolysaccharide disrupts tight junctions in cholangiocyte monolayers by a c-Src-, TLR4-, and LBP-dependent mechanism. *Am J Physiol Gastrointest Liver Physiol* **293,** G308-318.

Shimizu F, Sano Y, Maeda T, Abe MA, Nakayama H, Takahashi R, Ueda M, Ohtsuki S, Terasaki T, Obinata M & Kanda T. (2008). Peripheral nerve pericytes originating from the blood-nerve barrier expresses tight junctional molecules and transporters as barrier-forming cells. *J Cell Physiol* **217,** 388-399.

Shiraga M, yano S, Yamamoto A, Ogawa H, Goto H, Miki T, Miki K, Zhang H & Sone S. (2002). Organ heterogeneity of host-derived matrix metalloproteinase expression and its involvement in multiple-organ metastasis by lung cancer cell lines. *Cancer Res* **62** (20, 5967-5973.

Sims DE. (1991). Recent advances in pericyte biology--implications for health and disease. *Can J Cardiol* **7,** 431-443.

Singh AK, Jiang Y, Gupta S & Benlhabib E. (2007). Effects of chronic ethanol drinking on the blood brain barrier and ensuing neuronal toxicity in alcohol-preferring rats subjected to intraperitoneal LPS injection. *Alcohol Alcohol* **42,** 385-399.

Sixt M, Engelhardt B, Pausch F, Hallmann R, Wendler O & Sorokin LM. (2001). Endothelial cell laminin isoforms, laminins 8 and 10, play decisive roles in T cell recruitment across the blood-brain barrier in experimental autoimmune encephalomyelitis. *J Cell Biol* **153,** 933-946.

Sly LM, Krzesicki RF, Brashler JR, Buhl AE, McKinley DD, Carter DB & Chin JE. (2001). Endogenous brain cytokine mRNA and inflammatory responses to lipopolysaccharide are elevated in the Tg2576 transgenic mouse model of Alzheimer's disease. *Brain Res Bull* **56,** 581-588.

Sozen T, Tsuchiyama R, Hasegawa Y, Suzuki H, Jadhav V, Nishizawa S & Zhang JH. (2009). Role of interleukin-1beta in early brain injury after subarachnoid hemorrhage in mice. *Stroke* **40,** 2519-2525.

Stanimirovic D & Satoh K. (2000). Inflammatory mediators of cerebral endothelium: a role in ischemic brain inflammation. *Brain Pathol* **10,** 113-126.

Steinman L. (2008). Nuanced roles of cytokines in three major human brain disorders. *J Clin Invest* **118,** 3557-3563.

Sternlicht MD & Werb Z. (2001). How matrix metalloproteinases regulate cell behavior. *Annu Rev Cell Dev Biol* **17,** 463-516.

Stevenson BR, Siliciano JD, Mooseker MS & Goodenough DA. (1986). Identification of ZO-1: a high molecular weight polypeptide associated with the tight

junction (zonula occludens) in a variety of epithelia. *J Cell Biol* **103,** 755-766.

Stolp HB, Dziegielewska KM, Ek CJ, Potter AM & Saunders NR. (2005). Long-term changes in blood-brain barrier permeability and white matter following prolonged systemic inflammation in early development in the rat. *Eur J Neurosci* **22,** 2805-2816.

Szelenyi J. (2001). Cytokines and the central nervous system. *Brain Res Bull* **54,** 329-338.

Tai LM, Holloway KA, Male DK, Loughlin AJ & Romero IA. (2010). Amyloid-beta-induced occludin down-regulation and increased permeability in human brain endothelial cells is mediated by MAPK activation. *J Cell Mol Med* **14,** 1101-1112.

Takeda K & Akira S. (2005). Toll-like receptors in innate immunity. *Int Immunol* **17,** 1-14.

Takeuchi O, Takeda K, Hoshino K, Adachi O, Ogawa T & Akira S. (2000). Cellular responses to bacterial cell wall components are mediated through MyD88-dependent signaling cascades. *Int Immunol* **12,** 113-117.

Terman A & Brunk UT. (2004). Lipofuscin. *Int J Biochem Cell Biol* **36,** 1400-1404.

Thornton P, McColl BW, Cooper L, Rothwell NJ & Allan SM. (2010). Interleukin-1 drives cerebrovascular inflammation via MAP kinase-independent pathways. *Curr Neurovasc Res* **7,** 330-340.

Touzani O, Boutin H, LeFeuvre R, Parker L, Miller A, Luheshi G & Rothwell N. (2002). Interleukin-1 influences ischemic brain damage in the mouse independently of the interleukin-1 type I receptor. *J Neurosci* **22,** 38-43.

Tsukita S, Furuse M & Itoh M. (2001). Multifunctional strands in tight junctions. *Nat Rev Mol Cell Biol* **2,** 285-293.

Tunkel AR & Scheld WM. (1993). Pathogenesis and pathophysiology of bacterial meningitis. *Annu Rev Med* **44,** 103-120.

Turksen K & Troy TC. (2004). Barriers built on claudins. *J Cell Sci* **117,** 2435-2447.

Ueno M, Sakamoto H, Kanenishi K, Onodera M, Akiguchi I & Hosokawa M. (2001). Ultrastructural and permeability features of microvessels in the hippocampus, cerebellum and pons of senescence-accelerated mice (SAM). *Neurobiol Aging* **22,** 469-478.

Venkateshappa C, Harish G, Mythri RB, Mahadevan A, Bharath MM & Shankar SK. (2012). Increased oxidative damage and decreased antioxidant function in aging human substantia nigra compared to striatum: implications for Parkinson's disease. *Neurochem Res* **37,** 358-369.

Verbeek MM, de Waal RM, Schipper JJ & Van Nostrand WE. (1997). Rapid degeneration of cultured human brain pericytes by amyloid beta protein. *J Neurochem* **68,** 1135-1141.

Vitkovic L, Konsman JP, Bockaert J, Dantzer R, Homburger V & Jacque C. (2000). Cytokine signals propagate through the brain. *Mol Psychiatry* **5,** 604-615.

Vorbrodt AW & Dobrogowska DH. (2004). Molecular anatomy of interendothelial junctions in human blood-brain barrier microvessels. *Folia Histochem Cytobiol* **42,** 67-75.

Wang Y, Zhang J, Yi XJ & Yu FS. (2004). Activation of ERK1/2 MAP kinase pathway induces tight junction disruption in human corneal epithelial cells. *Exp Eye Res* **78,** 125-136.

Weiss N, Miller F, Cazaubon S & Couraud PO. (2009). The blood-brain barrier in brain homeostasis and neurological diseases. *Biochim Biophys Acta* **1788,** 842-857.

Wolburg H & Lippoldt A. (2002). Tight junctions of the blood-brain barrier: development, composition and regulation. *Vascul Pharmacol* **38,** 323-337.

Wong D, Dorovini-Zis K & Vincent SR. (2004). Cytokines, nitric oxide, and cGMP modulate the permeability of an in vitro model of the human blood-brain barrier. *Exp Neurol* **190,** 446-455.

Xaio H, Banks WA, Niehoff ML & Morley JE. (2001). Effect of LPS on the permeability of the blood-brain barrier to insulin. *Brain Res* **896,** 36-42.

Xiaolu D, Jing P, Fang H, Lifen Y, Liwen W, Ciliu Z & Fei Y. (2011). Role of p115RhoGEF in lipopolysaccharide-induced mouse brain microvascular endothelial barrier dysfunction. *Brain Res* **1387,** 1-7.

Yang Y, Estrada EY, Thompson JF, Liu W & Rosenberg GA. (2007). Matrix metalloproteinase-mediated disruption of tight junction proteins in cerebral vessels is reversed by synthetic matrix metalloproteinase inhibitor in focal ischemia in rat. *J Cereb Blood Flow Metab* **27,** 697-709.

Ye SM & Johnson RW. (2001). An age-related decline in interleukin-10 may contribute to the increased expression of interleukin-6 in brain of aged mice. *Neuroimmunomodulation* **9,** 183-192.

Yi X, Wang Y & Yu FS. (2000). Corneal epithelial tight junctions and their response to lipopolysaccharide challenge. *Invest Ophthalmol Vis Sci* **41,** 4093-4100.

Yong VW, Power C, Forsyth P & Edwards DR. (2001). Metalloproteinases in biology and pathology of the nervous system. *Nat Rev Neurosci* **2,** 502-511.

Yoshioka M, Yokoyama N, Masuda K, Honna T, Hinode D, Nakamura R, Rouabhia M, Mayrand D & Grenier D. (2003). Effect of hydroxamic-acid based matirx metalloproteinase inhibitors on human gingival cells and porphyromonas gingivalis. *J Peridontol* **74** (8), 1219-1224.

Yurchenco PD & Schittny JC. (1990). Molecular architecture of basement membranes. *FASEB J* **4,** 1577-1590.

Zehendner CM, Luhmann HJ & Kuhlmann CR. (2009). Studying the neurovascular unit: an improved blood-brain barrier model. *J Cereb Blood Flow Metab* **29,** 1879-1884.

Zhou H, Andonegui G, Wong CH & Kubes P. (2009). Role of endothelial TLR4 for neutrophil recruitment into central nervous system microvessels in systemic inflammation. *J Immunol* **183,** 5244-5250.

Zlokovic BV. (2008). The blood-brain barrier in health and chronic neurodegenerative disorders. *Neuron* **57,** 178-201.

Zlokovic BV. (2011). Neurovascular pathways to neurodegeneration in Alzheimer's disease and other disorders. *Nat Rev Neurosci* **12,** 723-738.

Appendix

(A)

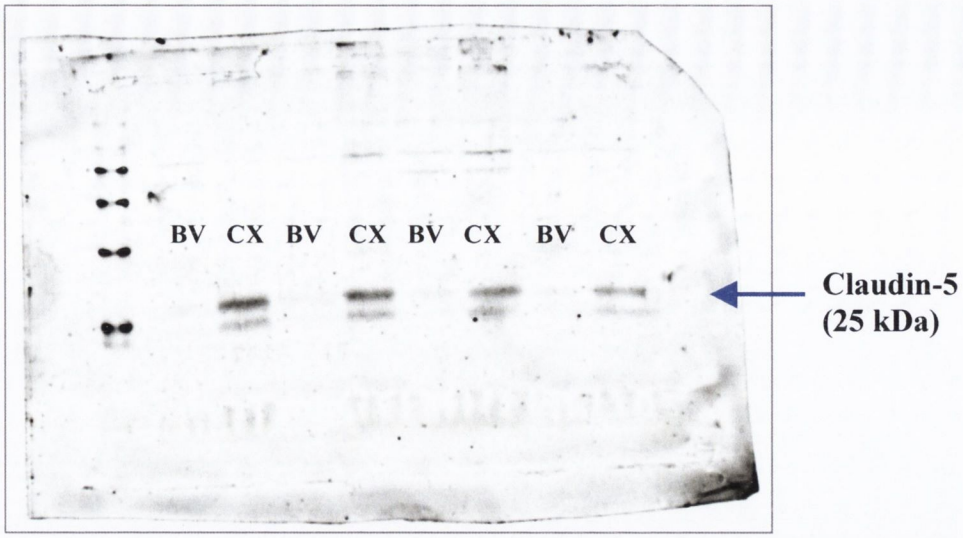

(B)

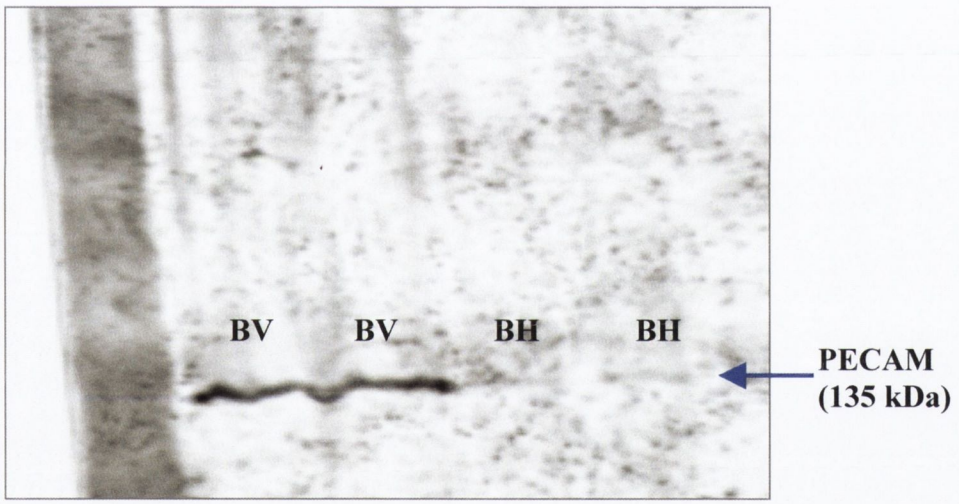

Appendix 1: Representative western immunoblots following capillary separation. Claudin-5 and PECAM are exclusively located on brain endothelial cells and were used as markers to positively identify capillary-enriched fractions post capillary separation from brain homogenate. Though the technique was repeated several times, claudin-5 consistently appeared in the cortical (CX) rather than capillary fraction (BV) following the capillary separation technique in frozen cortical tissue from Wistar rats (A). In contrast, using the same capillary separation technique on fresh whole mouse brain from C57/Bl6 mice, PECAM was localized to the capillary fraction (BV) but not the brain homogenate (BH) fraction, indicating satisfactory capillary separation (B).

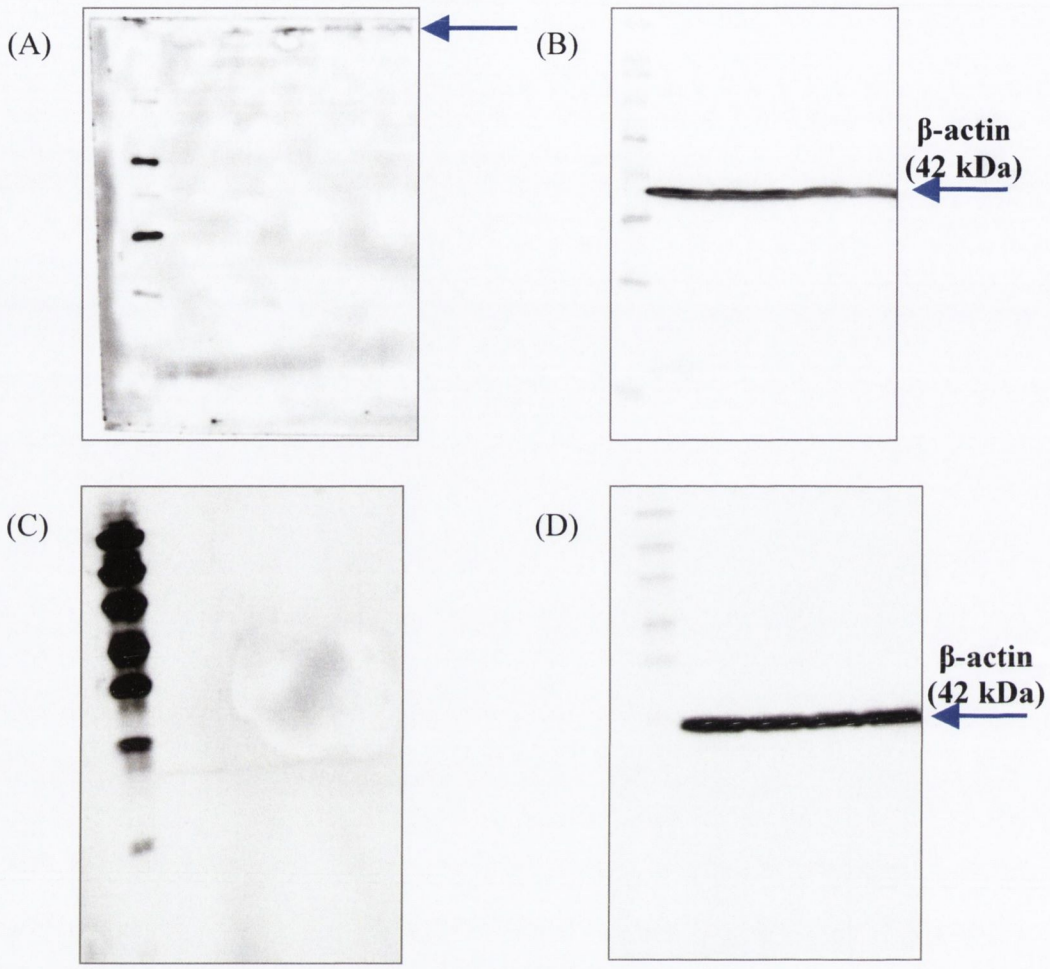

Appendix 2. Claudin-5 expression in hippocampus from saline- and LPS (100µg/kg)-treated young and aged Wistar rats.

Claudin-5 expression was not evident at the predicted molecular weight (25 kDa) in hippocampal homogenate containing sample buffer (5% β-mercaptoethanol) despite probing with the primary antibody at a concentration of 1:200. Instead an unexpected band appeared at the uppermost portion of the SDS gel (A, arrow). The same immunoblot was stripped and re-probed for β-actin which appeared at the correct molecular weight (B). Claudin-5 expression was still absent, even after increasing the β-mercaptoethanol content to 15% (C), though the same immunoblot could still be probed for β-actin (D).

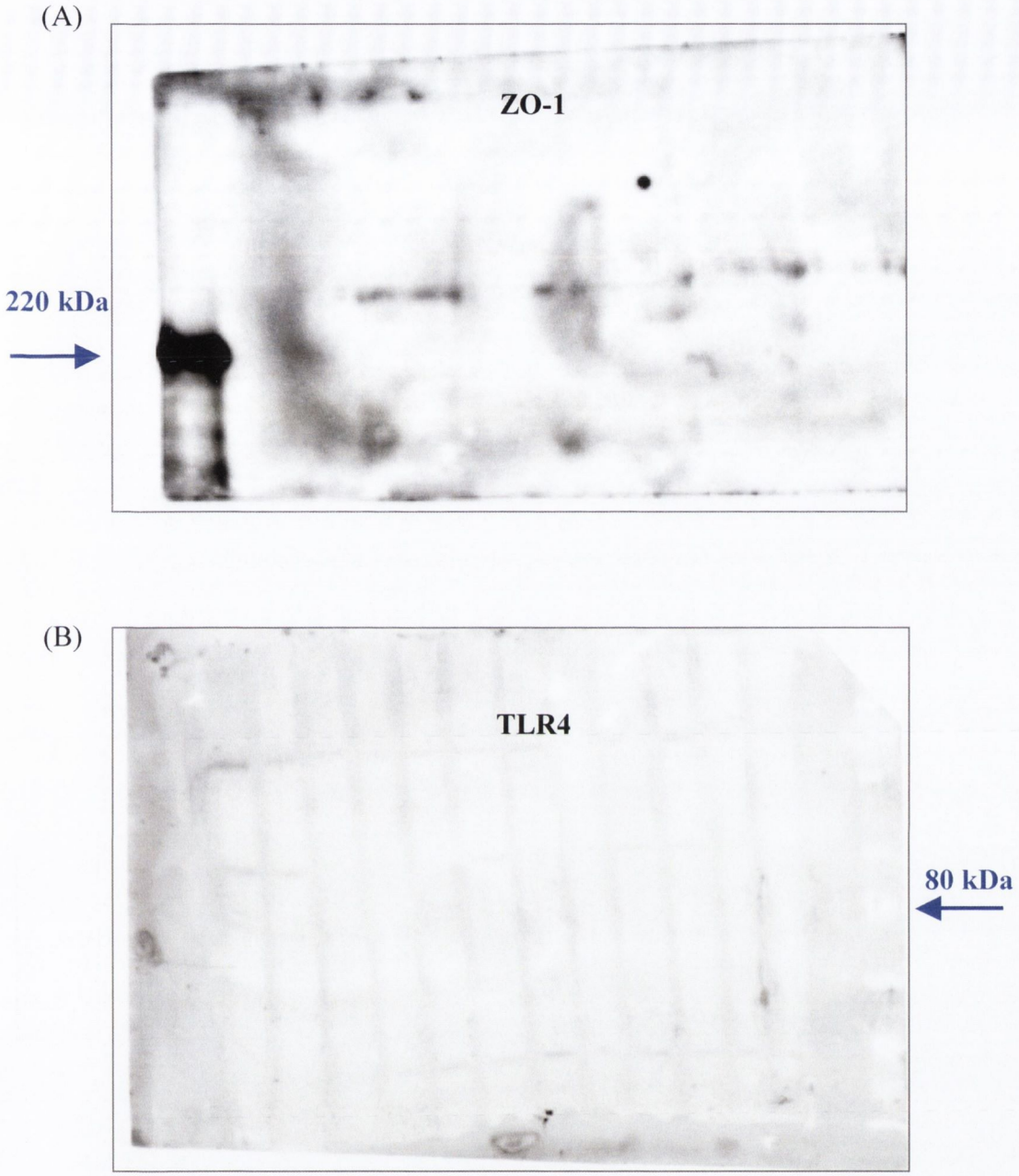

Appendix 3. ZO-1 and TLR-4 expression in hippocampus from saline- and LPS (100µg/kg)-treated young and aged Wistar rats.

Though sample buffer containing 10% β-mercaptoethanol was used in addition to incubating with the primary antibody at 1:200 for up to 24 hours, ZO-1 expression was still not analyzable (A). The representative immunoblot from rat cortex in A, is representative of similar immunoblots obtained on hippocampal and striatal samples. Similarly, positive bands for TLR4 were not observed at the predicted molecular weight (80 kDa) in cortical homogenates (B).

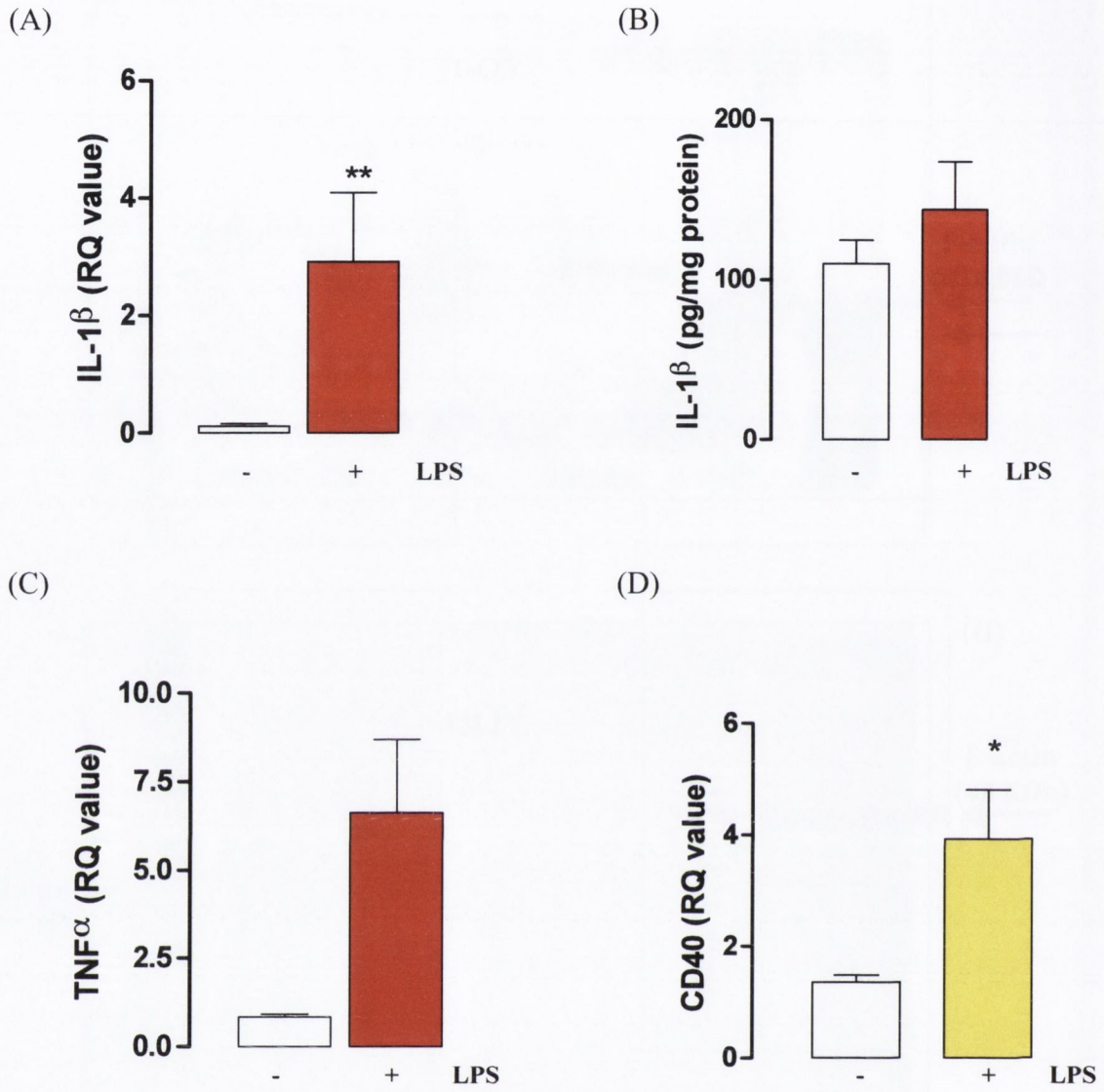

Appendix 4. Effect of LPS (100μg/kg) in hippocampus of young Wistar rats.

Though LPS did not alter tight junction protein expression (Chapter 4), administration of LPS did provoke an inflammatory response in the hippocampus in the same young Wistar rats, particularly at the mRNA level. LPS induced a significant increase in mRNA expression of IL-1β (A) and CD40 (D) though the apparent increase did not reach statistical significance for TNFα (C). In addition, an LPS-induced trend was apparent for IL-1β concentration at the protein level, though this increase was not significant (B). Data expressed as mean ±SEM; *$p<0.05$, **$p<0.01$; Student's *t*-test. Data courtesy of Dr. Thelma Cowley.

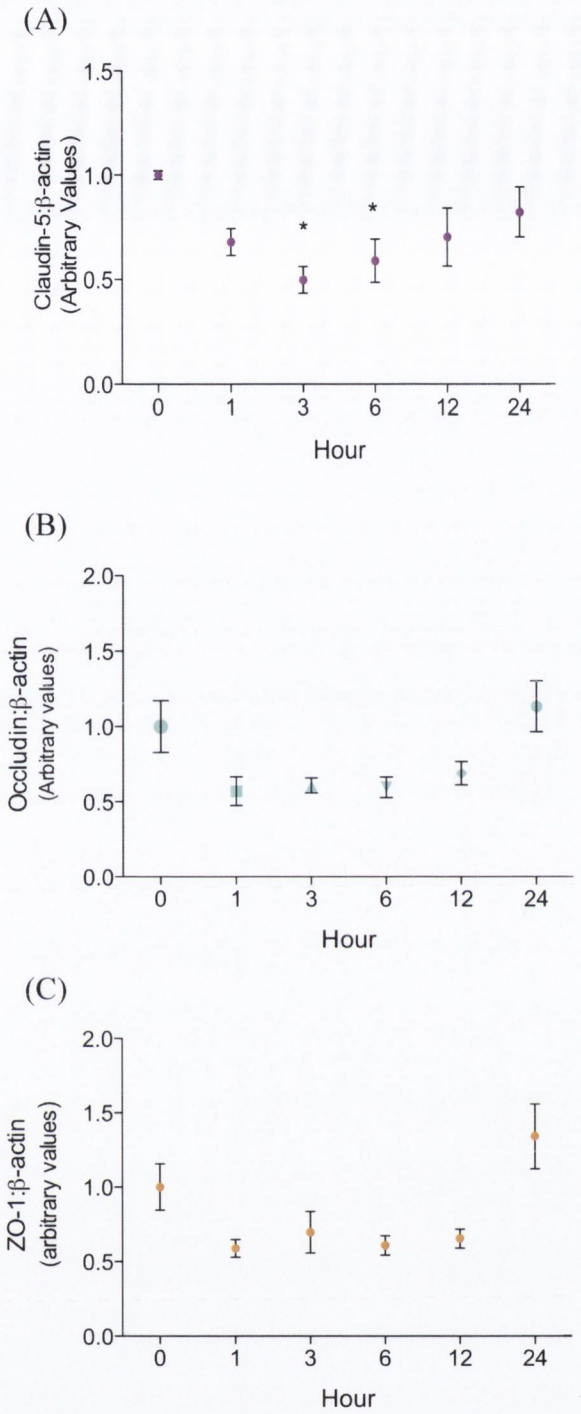

Appendix 5: IL-1β treatment (10ng/ml) of bEnd.3 cells, modulated tight junction expression in a time-dependant manner.

IL-1β significantly disrupted claudin-5 ($p<0.05$), occludin ($p<0.01$) and ZO-1 ($p<0.001$) expression levels in bEnd.3 cells in the course of a 24-hour period. Data expressed as mean ± SEM, n=6-8; *$p<0.05$ versus 0 hour timepoint; one-way ANOVA followed by Newman-Keul *post-hoc* test.

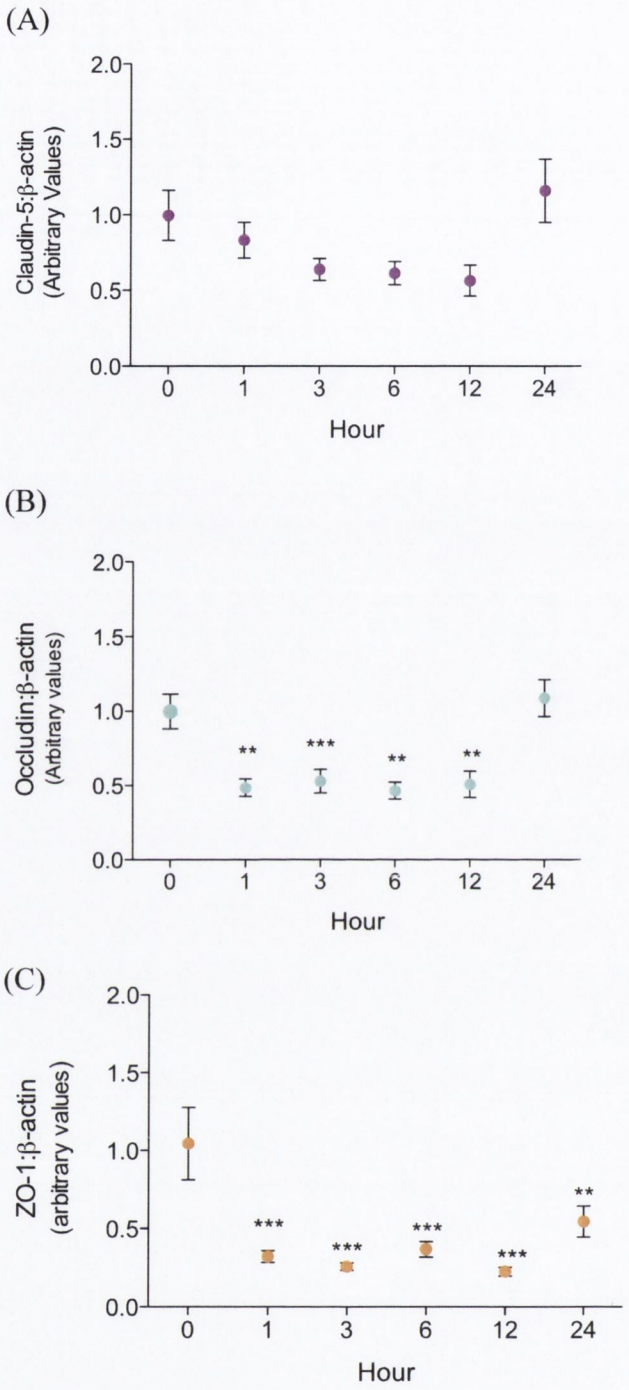

Appendix 6: LPS treatment (100ng/ml) of bEnd.3 cells, modulated tight junction expression in a time-dependant manner.

LPS significantly disrupted claudin-5 ($p<0.05$), occludin ($p<0.001$) and ZO-1 ($p<0.001$) expression levels in bEnd.3 cells in the course of a 24-hour period. Data expressed as mean ± SEM, n=6-8; *$p<0.05$, **$p<0.01$ and ***$p<0.001$ versus 0 hour timepoint; one-way ANOVA followed by Newman-Keul *post-hoc* test.

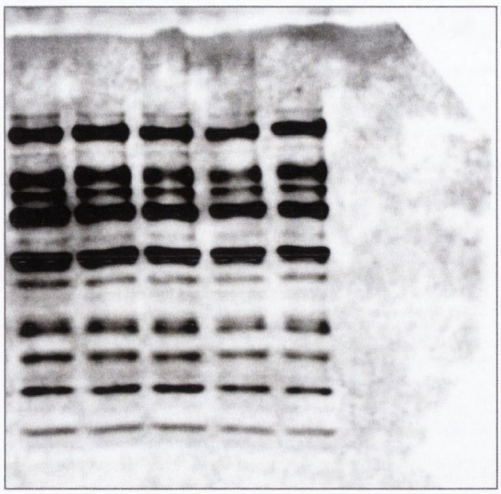

Appendix 7. IL-1R1 expression in bEnd.3.

Despite reducing the primary antibody concentration to 1:2500 and following the manufacturer's protocol, IL-1R1 expression in bEnd.3 (predicted MW 90-135 kDA) was not specific enough to quantify by densitometry due to the large quantity of non-specific bands. The immunoblot shown above is representative of the results obtained after western immunoblotting with IL-1R1.

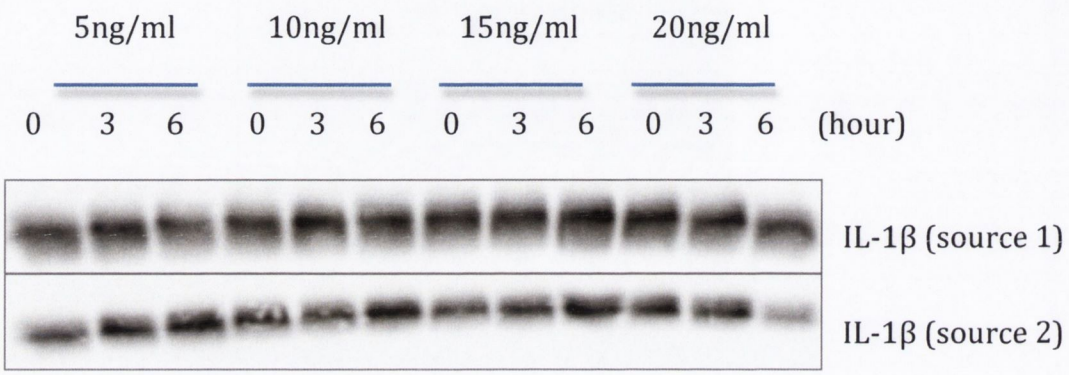

Appendix 8. The effect of IL-1β from two companies on claudin-5 expression.

Because bEnd.3 cells were not responding to IL-1β (10ng/ml) treatments in a consistent manner, we compared claudin-5 expression following treatment with IL-1β at a range of concentrations from two different sources. The blots above demonstrate that claudin-5 expression was variable in bEnd.3 cells, irrespective of the type of IL-1β used.

Appendix 9: Materials

Animal husbandry

C57Bl/6 mice	BioResources Unit, TCD.
Male Wistar rats	BioResources Unit, TCD.
Male Wistar rats	B&K Universal Limited, UK
C57BL/6 and IL-1R1$^{-/-}$ male mice	Jackson Labs, USA maintained by the laboratory group of Prof. Kingston Mills, School of Biochemistry and Immunology, TCD.

Assay kits

Pierce BCA Protein Assay Kit	ThermoFisher Scientific
IL-1β ELISA (rat)	R&D Systems, UK.
Pro-MMP9 ELISA (mouse)	R&D Systems, UK.
Pro-TIMP1 ELISA (rat)	R&D Systems, UK.

General laboratory chemicals

2-propanol	Sigma-Aldrich, Inc.
Acrylamide	Sigma-Aldrich, Inc.
Ammonium persulfate (APS)	Sigma-Aldrich, Inc.
Bovine serum albumin (BSA)	Sigma-Aldrich, Inc.
Bromophenol blue	Sigma-Aldrich, Inc.
Coomassie Blue	Sigma-Aldrich, Inc.
Dextran (MW 70kDa)	Sigma-Aldrich, Inc.
Dispase	Sigma-Aldrich, Inc.
Disodium hydrogen orthophosphate (Na_2HPO_4)	Sigma-Aldrich, Inc.
Gelatin	Sigma-Aldrich, Inc.
Glycerol	Sigma-Aldrich, Inc.
Glycine	Sigma-Aldrich, Inc.

HEPES	Sigma-Aldrich, Inc.
Hydrochloric acid (HCl)	VWR Int., Ireland
Isofluorane	Schering-Plough
Liquid Nitrogen (N_2)	Cryoproducts, IE.
Methanol	Hazardous Materials, TCD.
Marvel non-fat milk	Local supermarket
N,N,N',N'-Tetramethylethylene-diamine (TEMED)	Sigma-Aldrich, Inc.
N' N' Bis Acrylamide	Sigma-Aldrich, Inc.
Paraformaldehyde	Sigma-Aldrich, Inc
Phosphatase inhibitor cocktail I & II	Sigma-Aldrich, Inc.
Potassium chloride (KCl)	Merck, UK
Propofol	ScheringPlough,
Protease inhibitor cocktail	Sigma-Aldrich, Inc.
Saline (0.9%)	B. Braun, IE.
Sodium chloride (NaCl)	Sigma-Aldrich, Inc.
Sodium dodecyl sulfate (SDS) 99%	Sigma-Aldrich, Inc.
Sodium fluorescein (NaF)	Sigma-Aldrich, Inc.
Sodium hydroxide (NaOH)	Sigma-Aldrich, Inc.
Sodium phosphate dibasic (Na_2HPO_4)	Sigma-Aldrich, Inc.
Sodium phosphate monobasic monohydrate (NaH_2PO_4)	Sigma-Aldrich, Inc.
Tris-HCl	Sigma-Aldrich, Inc.
Triton X-100	Sigma-Aldrich, Inc.
Trizma-Base	Sigma-Aldrich, Inc.
Tween-20	Sigma-Aldrich, Inc.
β-Mercaptoethanol	Sigma-Aldrich, Inc.
Urethane	Sigma-Aldrich, Inc

Pharmacological regents

IL-1β (recombinant mouse, 401-ML)	R&D Systems, UK.
IL-1ra (recombinant mouse, 480-RM)	R&D Systems, UK.
LPS	Alexis, ENZO, Switz.
ONO4817 (Broad spectrum MMP inhibitor)	Tocris, UK.

Immunohistochemical reagents

Primary antibodies	See Table 1.1.
Secondary antibodies (AlexaFluor)	Invitrogen, UK.
Cork discs	R.A.Lamb, UK.
DAPI nuclears stain	Vector Laboratories, UK.
Hoescht stain (33342)	Invitrogen, UK.
Microscope slides	Ramboldi, Cyprus.
PAP pen	Dako, UK.
OCT mounting media	TissueTek, Sakura, USA.

Western blotting reagents

Primary antibodies	See Table 1.3.
Secondary antibodies	Jackson ImmunoResearch Laboratories, Inc., USA.
Immobilon Western Chemiluminescent HRP Substrate	Millipore, USA.
MagicMark protein standards	Invitrogen, UK.
Nitrocellulose membranes	Whatman, Germany.
Re-blot plus strong solution (×10)	Chemicon, UK.
Ponceau-S	Sigma-Aldrich, Inc.
Precision Plus Protein™ dual colour standards	Bio-Rad Laboratories Inc.

PCR Reagents

High Capacity cDNA Reverse Transcription Kit	Applied Biosystems, Pty Ltd.
Nuclease-free H_20	Sigma-Aldrich, Inc.
Specific target primers/probes (see Table 1.4)	Applied Biosystems, Pty Ltd.
TaqMan® Gene Expression Assay Kit	Applied Biosystems, Pty Ltd.
TaqMan® Universal PCR Master Mix	Applied Biosystems, Pty Ltd.
Total RNA Isolation Kit	Macherey-Nagel

Culture reagents

b.End3 cell line	ATCC, USA.
DMEM (media)	Gibco, UK.
EBSS (buffer)	Gibco, UK.
Fetal bovine serum	Gibco, UK.
Fetal horse serum	Gibco, UK.
Fibronectin	Sigma-Aldrich, Inc.
GlutaMax	Gibco, UK.
MEM (media)	Gibco, UK.
PBS (sterile)	Gibco, UK.
Penicillin	Gibco, UK.
Streptomycin	Gibco, UK.
Trypsin-EDTA	Invitrogen, UK.

Laboratory Ware

Filter paper	Whatman, USA
Microtest 96 well plate (flat bottom)	Sarstedt, Inc.
Microtubes (0.5ml)	Sarstedt, Inc.
Microtubes (1.5ml)	Sarstedt, Inc.
Optical 96-well reaction plate	Applied Biosystems, Pty Ltd.
Optical adhesive cover for PCR	Applied Biosystems, Pty Ltd.
Pipette tips	Sarstedt, Inc.
Corning HTS Transwell 24-well permeable supports (Inserts for culture plates)	Sigma-Aldrich, Inc.
Culture flasks (T25, T75, T175)	Sigma-Aldrich, Inc.

General solutions

Phosphate buffered saline (PBS)

NaCl 137mM:	8g
KCl 2.7mM:	0.2g
Na_2HPO_4 8.1mM:	1.15g
KH_2PO_4 1.15mM:	0.2g
dH_2O:	1L
pH 7.3	

Lysis buffer (1X stock, pH7.4, without inhibitors of proteinase/phosphatase activity)

10mM Tris-HCl:	0.158g
50mM NaCl:	0.292g
10mM $Na_4P_2O_7$:	0.446g
50mM NaF:	0.210g
dH_2O:	100ml
pH7.4	
IgePal:	1ml

Lysis buffer plus inhibitors

1X stock lysis buffer:	10ml
Proteinase inhibitor cocktail I:	100µl
Proteinase inhibitor cocktail II:	100µl
Phosphatase inhibitor cocktail:	100µl

Phosphate buffers

0.2M monobasic sodium phosphate buffer stock:

15.6g $Na_2HPO_4.2H_20$/500ml d.H_20

0.2M dibasic sodium phosphate buffer stock

53.65g $Na_2HPO_4.7H_20$/1L d.H_20

0.1M sodium phosphate buffer (pH=7)

117ml 0.2M monobasic sodium phosphate stock +

183ml 0.2M dibasic sodium phosphate stock +

300ml d.H_20

Western Blotting solutions

4X SPA buffer for separating gel (1.5M Tris/SDS 0.2%/ pH8.8)

Tris Base:	90.8g
SDS:	1g
d.H_20	500ml

pH 8.8 (HCl)

Stacking buffer for stacking gel (0.5M Tris/ SDS 0.4%/ pH6.8)

Tris Base:	15.13g
SDS:	1g
d.H_2O:	250ml
Bromophenol blue:	pinch

pH 6.8 (HCl)

10X Electrode Running buffer (25mM Tris/ 192mM glycine/ SDS 0.1%)

Tris Base:	30g
Glycine:	144g
SDS:	10g
d.H_20:	1L

10X Transfer Buffer (25mM Tris/ 192mM glycine/ 20% v/v Methanol)

Tris Base:	30g
Glyine:	144g
dH_2O:	1L

Add 20% methanol when making 1X preparation.

10% APS

APS:	1g
dH_2O:	10ml

Recipe for separating tris-glycine gel (western blotting)				
(1x tris-glycine gel)	**7%**	**10%**	**12%**	**15%**
30% Acrylamide	2.3 ml	3.3 ml	4 ml	5 ml
d.H_2O	5.1 ml	4.1 ml	3.4 ml	2.4 ml
4X SPA buffer	2.5 ml	2.5 ml	2.5 ml	2.5 ml
10% APS	100 µl	100 µl	100 µl	100 µl
Temed	5 µl	5 µl	5 µl	5 µl

Recipe for 4%stacking gel (western blotting)	
30% acrylamide	1.3 ml
d.H_2O	6.1 ml
Stacking buffer	2.5 ml
10% APS	50 µl
Temed	5µ l

Immunohistochemistry solutions

Phosphate buffered saline (PBS)

NaCl 137mM: 8g

KCl 2.7mM: 0.2g

Na_2HPO_4 8.1mM: 1.15g

KH_2PO_4 1.15mM: 0.2g

dH_2O: 1L

pH 7.3

4% BSA

BSA 4g

PBS 100ml

Blocking buffer

Serum:	1ml
4% BSA:	9ml

(Serum corresponds to species secondary antibody is raised in).

Antibody diluent

Serum:	1ml
PBS:	99ml

(Serum corresponds to species secondary antibody is raised in).

PHEM wash buffer

25mM HEPES sodium salt:	6.51g
10mM EGTA:	3.8g
60mM PIPES:	18.14g
2mM $MgCl_2$:	0.41g
dH_2O:	1L

(PIPES will only go into solution when exactly pH 6.9 is reached by adding concentrated (3M) NaOH). Stir until solution is clear.

4% Paraformaldehyde

Paraformaldehyde:	4g
PBS:	96ml

Heat to 60°C to dissolve paraformaldehyde, cool and add 5 drops conc NaOH, pH the solution and make up to the final volume.

Subbing solution for glass slides

Gelatine:	0.5% w/v
Chromalum:	0.05: w/v

dH_20-

Heat to 60°C, cool, coat slides for 10min and leave overnight to dry at room temperature.

Zymography Solutions

Separating gel buffer (1.5M Tris/ pH 8.8)

Tris Base: 18.15g

dH_2O: 100ml

pH 8.8 (HCl)

Stacking gel buffer (0.5M Tris/ SDS 0.4%/ pH 6.8)

Tris Base: 6.05g

SDS: 0.4g

dH_2O: 100ml

pH 6.8 (HCl)

Zymography digestion buffer (2M Tris/ pH 7.4)

Tris Base: 12.1g

dH_2O: 50ml

pH 7.4 (HCl)

10% APS

APS: 1g

dH_2O: 10ml

Gelatin solution (20mg/ml containing 1% SDS)

Porcine gelatin: 2g

dH_2O: 100ml

Heat til near boiling followed by cooling. Repeat 2-3 times.

Add 1g SDS

Sample loading buffer (see 2.14.12 above)

10X Electrode Running buffer (25mM Tris/ 192mM glycine/ SDS 0.1%)

Tris Base:	30g
Glycine:	144g
SDS:	10g
d.H_20:	1L

2.5% Triton-X buffer

Triton-X-100:	12.5ml
dH_2O:	500ml

Zymography incubation buffer (2M Tris/ pH 7.4)

Tris HCl:	25ml
NaCl:	9g
$CaCl_2$:	0.74g
NaN_3:	0.5g
dH_2O:	1L

Zymography staining solution

Methanol:	125ml
Acetic Acid:	50ml
Coomassie Blue:	0.125g
dH_2O:	325ml

Zymography de-staining solution

Methanol:	40ml
Acetic acid:	80ml
dH_2O:	880ml

Zymography separating gel (8%)

30% acrylamide:	2ml
1.5M Tris HCl pH8.8:	1.875ml
dH_2O:	2.875ml

Gelatin (20mg/ml/1%SDS):	750µl
10%APS:	25µl
Temed:	5µl

Zymography stacking gel

30% acrylamide:	325 µl
0.5M Tris HCl pH6.8:	625µl
dH_2O:	1.5ml
10%APS:	12.5µl
Temed:	2.5µl

2.14.17 Culture solutions

1X PBS

Dulbecco's 10X PBS:	5ml
Autoclaved $d.H_2O$:	45ml

Cell freezing media

DMEM culture media:	25ml
FBS:	20ml
DMSO:	5ml

Media for culturing endothelial cells

DMEM culture media (500ml) supplemented with;

Penicillin:	100µl/ml
Streptomycin:	100µl/ml
FBS:	20% w/v
GlutaMAX:	100µl/ml

Organotypic slicing medium:

EBSS: 487.5ml

1M HEPES in EBSS: 12.5ml

Organotypic culture medium: 100ml

MEM (GlutaMax, +Earle's+25mM HEPES): 50 ml

EBSS + Glucose (50 ml EBSS, 6.5g of Glucose aliquotted and stored at –20°C): 5ml

EBSS: 18 ml

Penicillin and Streptomycin: 1ml

Horse serum: 25 ml